Diagnostic Testing for Improved Load Rating of Reinforced Concrete Slab Bridges

by

Loyl Clyde Bussell, B.S.

Thesis

Presented to the Faculty of the Graduate School of

The University of Texas at Austin

in Partial Fulfillment

of the Requirements

for the Degree of

Master of Science in Engineering

The University of Texas at Austin

May 1997

Diagnostic Testing for Improved Load Rating of Reinforced Concrete Slab Bridges

Approved by
Supervising Committee:

Sharon L. Wood

Joseph A. Yura

To my wife, Melinda and my son, Jacob

Acknowledgments

I would like to thank Dr. Sharon Wood for her patience, understanding and encouragement throughout the entirety of this research. She provided the positive inspiration in order for me to complete this thesis in a timely manner. Thanks also to Dr. Joseph Yura and Dr. Karl Frank for their insight and assistance.

I would also like to thank David Jauregui and Pete Schonwetter for their continual support, not only for the project but for graduate school in general. Thanks also to David McIlrath, Blanca Velazquez, Nicole Garcia and Norm Grady, who provided the assistance to perform the testing in a timely manner. A special thanks to Robbie Barnes who answered many questions and provided both materials and equipment.

I would also like to thank the staff at Ferguson Laboratory for their help during this project. A special thanks to Wayne Fontenot and Mike Bell for answering numerous questions.

I am deeply indebted to the Texas Department of Transportation for the opportunity to participate in the Masters program. Thanks to Wayne Clendennen, Mike Lynch, Keith Ramsey, Joe Starkey and Mark Wallace for their help in providing me with the necessary information and assistance to complete my research. Thanks to Roger El-Khoury, Marilyn Dell and Robert Cuellar for their assistance throughout the entire program.

Finally, I offer special thanks to my wife, Melinda and my son, Jacob for their patience and understanding during the many late nights necessary to complete this research.

April 7, 1997

Diagnostic Testing for Improved Load Rating of Reinforced Concrete Slab Bridges

Loyl Clyde Bussell, M.S.E.

The University of Texas at Austin, 1997

Supervisor: Sharon L. Wood

There are a large number of reinforced concrete slab bridges in Texas that were constructed in the 1950s and 1960s. Although most of these bridges were designed for less than the current legal load, they are still in service and performing adequately. Currently the bridges in Texas are load rated based on a procedure similar to the original design procedure. These procedures are very conservative and result in low load ratings for slab bridges. In order to take advantage of this inherent conservatism, a method of determining a better estimate of the capacity of these bridges is needed.

This study addresses the possibility of load testing reinforced concrete slab bridges in order to verify that there is adequate capacity to increase the allowable loads. A typical slab bridge was field tested. The test procedures are discussed, and the measured results are presented and evaluated.

Table of Contents

List of Tables

List of Figures

Chapter 1. INTRODUCTION

1.1 BRIDGE LOAD TESTING FOR ~~BRIDGE~~ LOAD RATING

1.1.1 BackgroundHistory

LBridge load testing has been used for a number of years to better understand bridge behavior and to determine a more realistic the load capacity of afor the bridge than can be obtained through standard analysis. Bridges are load rated based on a given truck loading to determine the safe load capacity for that particular truck configuration. An example of this is a typical dump truck with a given axle spacing would be used to load rate a bridge. The resulting load rating would only apply for this specific type of truck. These ratings are in most cases based on the procedure outlined in the AASHTO Manual for Condition Evaluation of Bridges (AASHTO Manual) [1]. An example of this type of load rating is shown in Appendix A. Bridges may also be load rated usingbased on finite element analysismodeling. This method of analysisrating will usually give a more realistic load capacityrating becausesince the bridge is analyzed as a three dimensional structure. The results from the above rating methods along with load testing will usuallyshould provide the best estimate of load capacity.

Researchers, state agencies and private firms have all used load testing in some manner to better understand the behavior of bridges under typical truck loadings. These tests have attempted to determine load capacity, impact factors, load distribution, fatigue stresses, dynamic behavior and other specific types of behavior desiredneeded. Bridges are known to have a greater load capacity than

they were designed ~~for~~. This increase in capacity is partly due to the conservative assumptions used in bridge design. Load testing for determining bridge capacity has met with limited success. Steel girder bridge tests usually have successful results. This success is due to the fact that steel girders are easy to instrument and the behavior of steel girders is more predictable than concrete. Concrete bridges have proved to be the most difficult to test. This is due partly to the difficulty in getting accurate strain measurements in the field and then understanding the resulting data. ~~These bridges include concrete tee beam, flat slab and prestressed concrete girder bridges.~~ Determining the capacity of these types of bridges in a timely manner is difficult because of the behavior of the material~~the numerous unknowns with each bridge~~. Normal reinforced concrete cracks under service load and this cracking can make obtaining accurate surface strain data difficult. As mentioned above concrete bridges normally have greater strength than is shown by analysis. This strength may be due to higher than expected ~~M~~material~~Concrete~~ strength, load distribution~~, section properties~~, and ~~steel reinforcement strength and~~ bearing restraint~~prestress forces are just a few of the unknowns~~. In order to use the additional capacity of these bridges, this increase in capacity must be explained and shown that it will be available for the maximum loading. Because of the difficulty in obtaining good data, the majority of test~~sing~~ performed on these types of bridges are proof test~~sing~~. This type of testing will be discussed in more detail below.

1.1.2 Types of Testing

There are two types of non-destructive testing methods used in bridge load testing. These types are diagnostic testing and proof testing. Diagnostic testing involves applying a known load and measuring the effects of this load on various components[1]. These measurements are then ~~used to~~ compared to the ~~actual and~~ theoretical responses of the bridge. From these comparisons a better estimate of the actual capacity of the bridge can be determined. Diagnostic testing usually uses a loading vehicle that weighs less than the estimated capacity. Because of this it is very important to understand where the increase in capacity comes from and to insure that this additional determined strength will be available for the maximum anticipated ~~estimated~~ load.

Proof testing involves loading a bridge incrementally until a predetermined load is reached or nonlinear behavior is observed[1]. The desired load limit is determined by the legal load limit or a specified permit truck. The bridge must be monitored closely throughout the loading process to determine if nonlinear behavior occurs. This type of testing will determine directly the safe~~maximum~~ amount of load the bridge is capable of supporting.

1.2 LITERATURE REVIEW

An extensive literature search was performed to~~o~~ determine the~~o~~ current status of bridge load testing, in particular slab bridge testing. S~~There were s~~everal articles were found where detailed testing and analysis had been performed on slab bridges. Following is a brief description of the appropriate articles.

A series of articles was written by Azizinamini, et al. [2, 3, 4] that discussed the testing of slab bridges. These tests were performed on a series of continuous span slab bridges. Both service load tests and ultimate load tests were performed. The article mentions the reserve strength in most slab bridges due to the conservative rating methods outlined by the AASHTO Manual [1]. The article does not discuss bridges with structural rail or The University of Illinois Engineering Experiment Station Bulletin No. 346 (Illinois Bulletin 346) [5] method of moment distribution.

Another series of articles was written by Aktan, et al. [6], Miller, et al. [7], Hrinko, et al. [8] and Huria, et al. [9]. These article discussed the instrumentation, analysis, nondestructive testing and destructive testing of a series of slab bridges. The bridges tested were again continuous slab bridges and did not have structural curbs.

The original research performed that the TxDOT design procedure is based on is the Illinois Bulletin 346 [5]. This article discusses previous research performed on edge stiffened slabs and uses this research to develop a simplified design method to utilize curbs and edge beams as structural members. The design method uses empirical coefficients based on tests to distribute the moment to the slab and curbs.

A report was written by TxDOT based on tests performed to verify the methods suggested by researchers at The University of Illinois [10]. The designers at TxDOT in conjunction with researchers at The University of Texas tested a full scale bridge to verify the design stresses based on the Illinois Bulletin

346 [5]. The results from the TxDOT test will be compared with the test performed for this thesis.

A complete guide for load testing has been written by Lichtenstein [11]. This guide outlines the procedures for performing bridge load tests. In the guide, Lichtenstein recommends proof testing for all concrete bridges. Although the guide covers a wide range of bridge testing equipment and methods, there is no specific section covering slab bridges.

Although the above articles were insightful, none dealt with load testing of slab bridges with structural curbs. There were two articles of particular interest. The Illinois Bulletin 346 [5] which was used in the design of slab bridges in Texas since the 1950's and the TxDOT departmental research report [10] on the testing of a slab bridge. These two articles provided great insight on the design and behavior of slab bridges with structural curbs.

In addition to the literature search a nationwide survey was performed to determine if other states had developed~~were using~~ a bridge load testing program. Of the fifty states Alabama, Florida and Michigan currently have bridge load testing programs and Alaska is starting a program.

1.3 TEXAS' NEEDS FOR TESTING SLAB BRIDGES

1.3.1 Background

Concrete slab bridges are one of the earliest types of bridges in Texas. These types of bridges are not very economical because of the short span length but perform better hydraulically than the standard box culvert. They were used extensively during the building of the~~Texas'~~ Farm to Market Road system in

Texas [12]. There are approximately 2,700 slab bridges on state maintained highways. The bridges wereare initially designed according to American Association of State Highway and Transportation Officials (AASHTO) specifications [13] and AASHTO distribution factors. ~~Slab bridges in Texas were initially designed using standard AASHTO distribution factors.~~ This design method was changed in the 1950's after the University of Illinois published an improved design method in the Illinois Bulletin 346 [5].

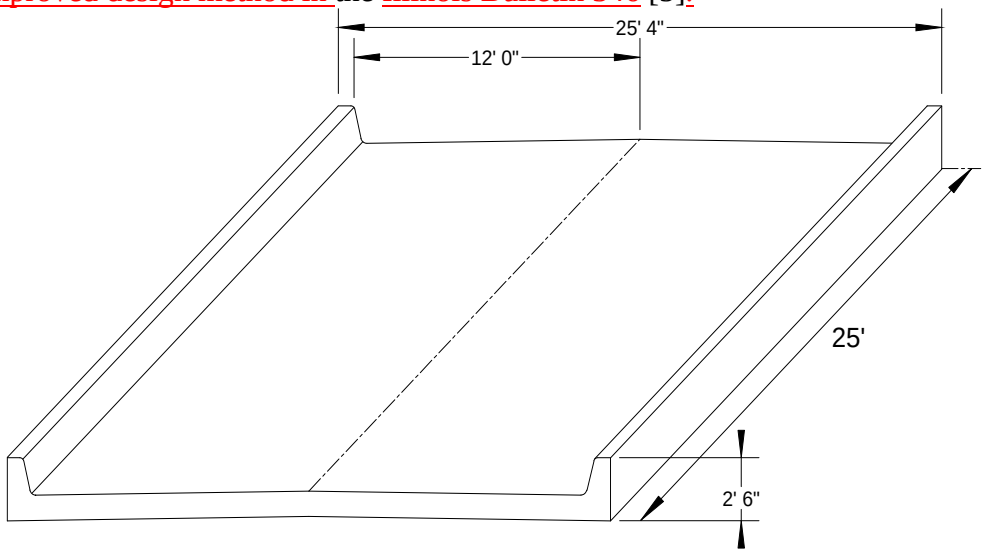

Figure 1.1 Typical Slab Bridge designed based on Illinois Bulletin 346.

The method proposed by researchers at thethe University of Illinois involved using the integral curbs as a load carrying members. T~~Illinois Bulletin 346 outlined t~~he ~~entire~~ procedure to determine the moment distributed to the curbs and to the slab is outlined in the Illinois Bulletin 346 [5]. This new design technique resulted in thinner slabs for ~~Texas'~~ slab bridges in Texas. For the typical slab bridge with a span of 25 feet the slab thickness decreased from 18

inches to 12 inches. The bridges were designed for H10 or H15 truck loadings. These trucks weigh 10 tons and 15 tons respectively. The bridges were designed and built both as normal and skewed with. The skews were typically of 15°, 30° and 45°.°. Standard plan sheets were developed and used for the different types of slab bridges.

1.3.2 Summary of Current Slab Bridges

The Texas Department of Transportation maintains a bridge database that contains information about all bridges in Texas [14]. This database was used to determine the number, age, rating and general condition of the state's slab bridges. Table 1.1 summarizes the design loads for slab bridges. The current design load for slab bridges is an HS20 design vehicle. A small number of bridges were designed with loads other than the typical design trucks. The AASHTO Manual [1] gives details on the configuration of the HS20 design truck.

Table 1.1: Summary of Design Loads for Slab Bridges (ref. 14)

Design Load	Number of Bridges
H 10	264
H 15	1226
H 20	825
HS 20	255
Other	128

Table 1.1: Summary of Design Loads for Slab Bridges (ref. 5)

The database also contains information about the condition and ratings of these bridges. There are 273 slab bridges that are structurally deficient. Structurally deficient bridges are in poor condition structurally or have inadequate

waterways. These bridges would not be candidates for load testing because of their poor structural condition.

As part of the FHWA's requirements for bridge management, bridges are load rated based on the definitions outlined in the AASHTO Manual [1]. Each bridge has an operating rating and an inventory rating. The operating rating is the maximum permissible load that can safely cross the bridge. The inventory rating represents the heaviest loads that may safely use the bridge for an indefinite period of time [1]. Table 1.2 summarizes the ratings and operating status of the existing slab bridges in Texas. TxDOT currently load posts a bridge if the operating rating of the bridge is less than the legal load, i.e. HS20. A small number of the bridges are classified as other, these bridges are posted for reasons other than load restrictions.

Table 1.2: Summary of Load Rating and Operating Status of Slab Bridges (ref.14)

Range of Load Rating	Number of Bridges	Classification		
		Posted	Open	Other
Operating Rating < H20	13	13		
Operating Rating < HS20	566	373	185	8
Inventory Rating < H20 and Operating Rating > H20	23	23		
Inventory Rating < HS20 and Operating Rating > HS20	1269	1222	19	28
Inventory Rating > HS20	828		828	

Approximately 80% of the slab bridges in Texas were built before 1960. Based on the year built approximately 1500 slab bridges were designed using the AASHTO method of load distribution and 1200 bridges were designed based on the method of load distribution utilizing the curb as a structural member [5].

1.3.3 Testing Needs for Slab Bridges in Texas

Slab bridges make up a considerable portion of the state's bridges. These bridges have been designed using different methods and several different design loads. The majority of the bridges have been in service more than thirty years ~~old~~ and were not designed for the current legal truck loads. As shown in Table 1.2 the majority of these bridges are not posted, but there are a large number with an inventory rating less than H20 or HS20. The legal load in Texas is considered equivalent to an HS20. Based on this information these bridges with inventory ratings less than HS20 are being used on a regular basis by legal trucks that exceed the inventory rating. This problem will only worsen as the legal load is increased to accommodate heavier trucks. A number of slab bridges may require posting if the legal load is increased. TxDOT needs a testing method to determine if these bridges will be overstressed by the legal loads and to determine if bridges that are load posted should be open to legal loads.

In addition to these needs many of the slab bridges require widening. Currently the bridges are eligible for widening if the load rating is H20 or greater. If the rating requirement is not met then the bridges are replaced. TxDOT could use the testing program to field test the bridges that have ratings less than H20 to determine if they could be widened rather than replaced.

1.4 OBJECTIVES AND SCOPE OF RESEARCH

The objectives of this thesis are to determine if testing slab bridges is feasible, and if so, determine the instrumentation required and the methods necessary to obtain satisfactory results. Diagnostic testing is the preferred method

of testing for TxDOT because special loading vehicles are not required and therefore this type of testing will be examined in this thesis. These objectives will ~~better~~ help the research project meet its goals in providing TxDOT with a load testing program.

This thesis will discuss the methods of analysis used for load rating a slab bridge and determine a load rating for the test bridge. The load test procedures and results will be covered in detail and an evaluation of the results will be performed to determine the validity of the data. Future research needs for slab bridges will be discussed in the conclusion.

Chapter 1. INTRODUCTION

There are a large number of bridges in Texas that were designed for less than the current legal load. Texas law states that bridges with load ratings less than the legal load must be load posted. The load posting of certain bridges may eliminate a direct trucking route and cause considerable economic impact on the trucking industry. There are two solutions to remedy this problem. The first solution is to replace the bridges, which gets very expensive when considering the entire state. The second solution is to take advantage of the inherent conservatism in design and increase the allowable loads. In order to increase the allowable load, a method of assuring that there is adequate reserve capacity is necessary.

This thesis addresses the possibility of load testing reinforced concrete slab bridges in order to verify there is adequate reserve capacity to increase the allowable loads. A typical 40-year-old slab bridge was chosen for load testing. The test procedures are discussed, the measured results presented and an evaluation of the data is performed in the following chapters.

1.1 BRIDGE LOAD TESTING FOR ~~BRIDGE~~ LOAD RATING

1.1.1 Background~~History~~

L~~Bridge l~~oad testing has been used for a number of years to better understand bridge behavior and to determine a more realistic ~~the~~ load capacity ~~of a~~for the bridge than can be obtained through standard design procedures. Bridges are load rated based on a given truck configuration to determine the safe load capacity for that particular truck. For example, a typical dump truck with a given

axle spacing could be used to load rate a bridge. The resulting load rating would apply for this specific truck configuration only.

Ratings are in most cases based on the procedure outlined in the AASHTO Manual for Condition Evaluation of Bridges (AASHTO Manual) [1]. ~~An example of this type of load rating is shown in Appendix A.~~ Assumptions made during the design, such as load distribution, are also used in this rating procedure. Bridges may also be load rated using~~based on~~ finite element analysis~~modeling~~. This method of analysis~~rating~~ will usually give a more realistic load ~~capacity~~rating because~~since~~ the bridge is analyzed as a complete three-dimensional structure, rather than a two-dimensional girder.

During the past 50 years, researchers, state departments of transportation and consulting firms have used load testing in some manner to better understand the behavior of bridges under typical truck loadings. These tests have attempted to determine the capacity of bridges and to quantify aspects of behavior such as, impact factors, load distribution, and ~~fatigue stresses,~~ dynamic behavior~~desired~~~~needed~~. Bridges are known to have a greater load capacity than the design load~~ for~~. This increase in capacity is partly due to the conservative assumptions used in bridge design.

Load testing for determining bridge capacity has met with limited success. Tests of steel girder bridges have usually led to reliable results. This success is due to the fact that steel girders are easy to instrument and the behavior of steel girders is easily modeled using simple analytical tools. Concrete bridges have proved to be more difficult to test. This is due partly to the difficulty in getting accurate strain measurements in the field. Reinforced concrete members crack

under service load and this cracking can make obtaining accurate surface strain data difficult. ~~These bridges include concrete tee beam, flat slab and prestressed concrete girder bridges.~~ Determining the capacity of typical concrete bridges in a timely manner is complicated due to the nonlinear behavior of the material at service load levels~~the numerous unknowns with each bridge~~.

As mentioned previously, reinforced concrete bridges typically have greater strength than assumed during design. This strength may be due to higher than expected ~~M~~material~~Concrete~~ strength, load distribution~~, section properties~~, and ~~steel reinforcement strength and~~ bearing restraint~~prestress forces are just a few of the unknowns~~. In order to use the additional measured capacity of these bridges, this increase in strength must be documented and shown that it will be available for the maximum loading.

1.1.2 Types of Testing

There are two types of nondestructive testing methods used in bridge load testing: diagnostic testing and proof testing. Diagnostic testing involves applying a known load and measuring the effects of this load on various components [1]. These measurements are then ~~used to~~ compared with the ~~actual and~~ theoretical responses of the bridge. From these comparisons, a better estimate of the actual capacity of the bridge can be determined. Diagnostic tests are usually performed with a loading vehicle that weighs less than the estimated capacity of the bridge. Therefore, it is very important to identify the sources of the increase in capacity and to insure that this additional strength will be available at the maximum anticipated ~~estimated~~ load.

Proof testing involves loading a bridge with increasingly larger loads until a predetermined load is reached or nonlinear behavior is observed [1]. The desired load limit is determined by the legal load limit or a specified permit truck. The bridge must be monitored closely throughout the loading process to determine if nonlinear behavior occurs. This type of testing will determine directly the safe~~maximum~~ load the bridge is capable of supporting. Because of the difficulty in obtaining reliable data, the majority of test~~s~~~~ing~~ performed on reinforced concrete bridges are proof test~~s~~~~ing~~.

1.2 LITERATURE REVIEW

An extensive literature search was performed to~~o~~ determine the~~o~~ current status of bridge load testing, in particular slab bridge testing. S~~There were s~~everal articles were found where detailed testing and analysis had been performed on slab bridges. Following is a brief description of the appropriate articles.

A series of papers was written by Azizinamini, et al. [2, 3, 4] that discussed the testing of slab bridges. These tests were performed on a series of continuous span slab bridges in Nebraska. Both service load tests and ultimate load tests were performed. The researchers conclude that the reserve strength in most slab bridges is due to the conservative rating methods outlined by the AASHTO Manual [1].

Another series of articles was written by researchers at the University of Cincinnati [6, 7, 8, 9]. These articles discussed the instrumentation, analysis, nondestructive testing and destructive testing of a series of slab bridges in Ohio.

The bridges tested were again continuous slab bridges and did not have structural curbs.

Research performed at the University of Illinois in the 1950s forms the basis for the TxDOT design procedure. The University of Illinois Engineering Experiment Station Bulletin 346 [5] discusses the results of previous research performed on edge stiffened slabs and develops a simplified design method to utilize curbs and edge beams as structural members. The design method uses empirical coefficients which are verified using the measured data, to distribute the moment to the slab and curbs.

A report was written by TxDOT based on tests performed to verify the methods suggested by researchers at the University of Illinois [10]. The designers at TxDOT, in conjunction with researchers at the University of Texas, tested a full scale slab bridge in Chandler, Texas to verify the design stresses based on the Illinois Bulletin 346 [5].

A comprehensive guide for load testing bridges has been written by Lichtenstein [11]. This guide outlines the procedures for performing bridge load tests and recommends proof testing for all concrete bridges. The guide does not address slab bridges explicitly, however.

In addition to the literature search, a nationwide survey was performed to determine if other states had developed~~were using~~ a bridge load testing program. Of the fifty states Alabama, Florida and Michigan currently have bridge load testing programs and Alaska is starting a program.

1.3 THE NEED FOR TESTING SLAB BRIDGES IN TEXAS

1.3.1 Background

Concrete slab bridges are one of the earliest types of bridges in Texas. These bridges are not very economical because of the short span length but provide better hydraulic characteristics than the standard box culvert. They were used extensively during the building of the~~Texas'~~ Farm to Market Road system in Texas [12]. There are approximately 2,700 slab bridges on state maintained highways. The bridges were~~are~~ initially designed according to American Association of State Highway and Transportation Officials (AASHTO) specifications [13] and AASHTO distribution factors were used. ~~Slab bridges in Texas were initially designed using standard AASHTO distribution factors.~~ This design method was changed in the late 1950s after the improved design method discussed in the Illinois Bulletin 346 [5] was published.

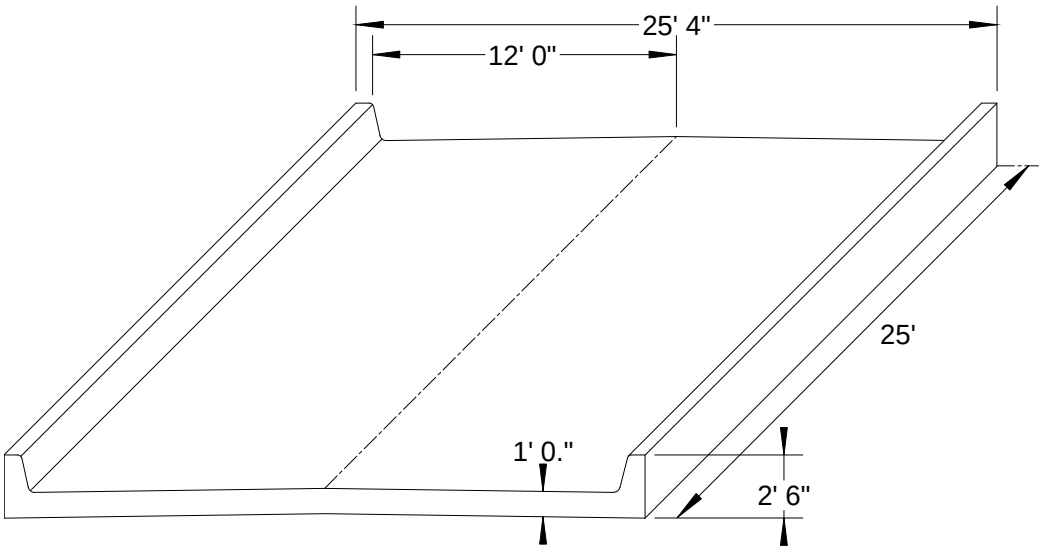

Figure 1.1 Typical Slab Bridge designed based on Illinois Bulletin 346 [5].

The method proposed by researchers at thethe University of Illinois involved using the integral curbs as a load carrying members. This new design technique resulted in thinner slabs for ~~Texas'~~ slab bridges in Texas. For the typical slab bridge with a span of 25 feet the slab thickness decreased from 18 inches to 12 inches. The bridges were designed for H10 or H15 truck loadings. These trucks weigh 10 tons and 15 tons respectively. The bridges were designed and built with both normal and skewed spans with. ~~The~~ typical skews of 15°, 30° and 45°.~~°. Standard plan sheets were developed and used for the different types of slab bridges.~~

1.3.2 Summary of Current Slab Bridges

The Texas Department of Transportation maintains a bridge database that contains information about all bridges in Texas [14]. This database was used to determine the number, age, rating and general condition of slab bridges throughout the state. Table 1.1 summarizes the design loads for slab bridges. The current design load for slab bridges is an HS20 design vehicle. A small number of bridges were designed with loads other than the typical design trucks.

Table 1.1 Summary of Design Loads for Slab Bridges [14].

Design Load	Number of Bridges
H 10	265
H 15	1226
H 20	825
HS 20	255
Other	128

~~Table 1.1: Summary of Design Loads for Slab Bridges (ref. 5)~~

Of the nearly 2700 slab bridges identified in the database, 273 are considered to be structurally deficient, which means the bridges are in poor condition or have inadequate waterways. These bridges would not be candidates for load testing because of their poor structural condition.

As part of the FHWA's requirements for bridge management, bridges are load rated based on the definitions outlined in the AASHTO Manual [1]. Each bridge has an operating rating and an inventory rating. The operating rating is the maximum permissible load that can safely cross the bridge. The inventory rating represents the heaviest load that may safely use the bridge for an indefinite period of time [1]. Table 1.2 summarizes the ratings and operating status of the existing slab bridges in Texas. TxDOT currently load posts a bridge if the operating rating of the bridge is less than the legal load, i.e. HS20. A small number of the bridges are classified as other, these bridges are posted for reasons other than load restrictions.

Table 1.2 Summary of Load Rating and Operating Status of Slab Bridges [14].

Range of Load Rating	Number of Bridges	Classification		
		Posted	Open	Other
Operating Rating < H20	13	13		
Operating Rating < HS20	566	373	185	8
Inventory Rating < H20 and Operating Rating > H20	23	23		
Inventory Rating < HS20 and Operating Rating > HS20	1269	1222	19	28
Inventory Rating > HS20	828		828	

Approximately 80% of the slab bridges in Texas were built before 1960. Based on the year built, approximately 1500 slab bridges were designed using the

AASHTO method of load distribution and 1200 bridges were designed based on the method of load distribution utilizing the curb as a structural member [5].

1.3.3 Testing Needs for Slab Bridges in Texas

Slab bridges make up a considerable portion of the state's bridges. These bridges have been designed using different methods and several different design loads. The majority of the bridges have been in service more than thirty years ~~old~~ and were not designed for the current legal truck loads. As shown in Table 1.2 the majority of these bridges are not posted, but there are a large number with an inventory rating less than H20 or HS20. The legal load in Texas is considered equivalent to an HS20. Based on this information these bridges with inventory ratings less than HS20 are being used on a regular basis by legal trucks that exceed the inventory rating. This problem will only worsen as the legal load is increased to accommodate heavier trucks. A number of slab bridges may require posting if the legal load is increased. TxDOT needs a testing method to determine if these bridges will be overstressed by the legal loads and to determine if bridges that are load posted should be open to legal loads.

In addition to these needs many of the slab bridges require widening. Currently the bridges are eligible for widening if the load rating is H20 or greater. If the rating requirement is not met then the bridges are replaced. TxDOT could use the testing program to field test the bridges that have ratings less than H20 to determine if they could be widened rather than replaced.

1.4 OBJECTIVES AND SCOPE OF RESEARCH

The objectives of this thesis are to determine if testing slab bridges is feasible, and if so, determine the instrumentation required and the methods necessary to obtain satisfactory results. Diagnostic testing is the preferred method of testing for TxDOT because special loading vehicles are not required and therefore this type of testing will be examined in this thesis. These objectives will ~~better~~ help the research project meet its goals in providing TxDOT with a load testing program.

This thesis will discuss the methods used in load testing a reinforced concrete slab bridge. A description of the test bridge and the initial load rating are discussed in Chapter 2. The test procedure used to load test the bridge will be discussed in Chapter 3. The test data from the load test is presented in Chapter 4. An evaluation of the test results is discussed in Chapter 5. A comparison of this test and the previous TxDOT slab bridge test is presented in Chapter 6. The adjustment of the initial load ratings based on the test results is shown in Chapter 7. A complete discussion of recommended testing procedures and future research needs are presented in Chapter 8. Appendix A contains a detailed description of the testing methods and the instrumentation used. Appendices B through G contain the complete test results in graphical form. The strain measured on the surface of the concrete are evaluated in Appendix H.

Chapter 2. BRIDGE ANALYSIS AND LOAD RATING

2.1 BRIDGE SELECTION

2.1.1 Type

The bridge type selected for testing was a reinforced concrete slab bridge that utilized the curbs as structural members. The bridge is located on FM 1100 over Willow Creek. This location is approximately 15 miles east of Austin off of US 290. The bridge is 25 feet 4 inches in width with a clear roadway width of 23 feet 3 inches. The span length is 25 feet and there is no skew. Figure 2.1 is an elevation view of bridge taken from the north. Figure 2.2 shows the structural details of this bridge type [10].

Figure 2.1 Elevation View of the Slab Bridge Tested.

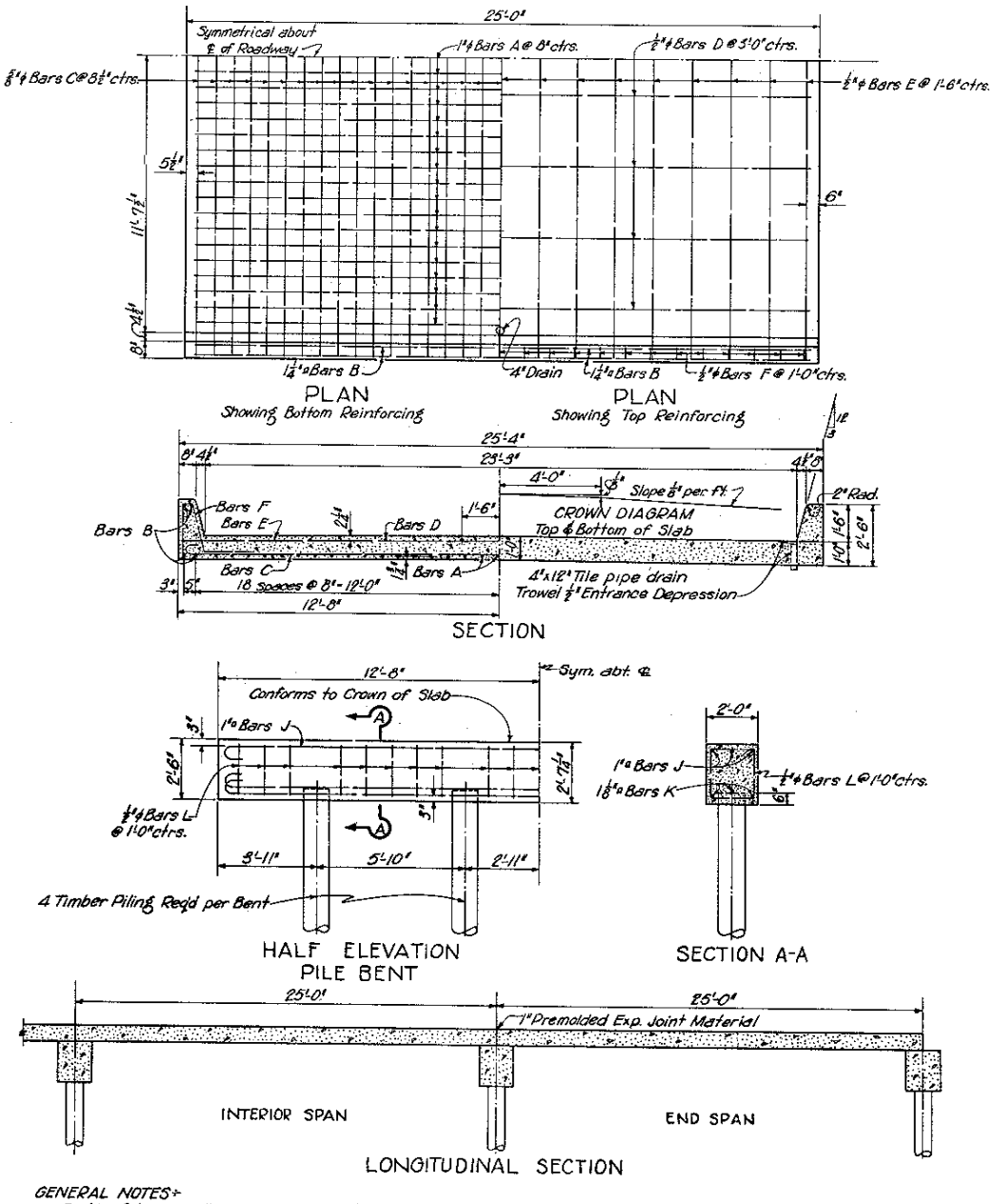

Figure 2.2 Structural Details of Slab Bridge. [10]

2.1.2 Location

The location for this bridge test was chosen because of the easy access to the underside of the bridge and the low traffic volume on FM 1100. The first span of the bridge was tested allowing access from the concrete riprap. The height from the underside of the slab at midspan and the riprap was approximately 5 feet. This was an ideal height for installation of the instrumentation.

The traffic volume for the road was very low. The approximate average daily traffic was 400 vehicles per day. During testing there were approximately ten to fifteen minutes between each passing vehicle.

2.2 SLAB SPAN BRIDGE

2.2.1 Description

The bridge was built in 1955 and designed according to AASHTO specifications [13] and the University of Illinois Engineering Experiment Station Bulletin 346 [5]. The bridge was designed for two H15 Trucks. These trucks have a 14 foot axle spacing with the front axle weighing 6 kips and the rear axle weighing 24 kips. The bridge was designed with class A concrete (f'c = 3000 psi) and Grade 40 reinforcing steel (fy = 40,000 psi). The bridge was designed by the working stress method.

Figures 2.2 and 2.3 show details of the reinforcing steel layout. The concrete cover is 1.75 inches to center of the reinforcing bar. The curbs on this bridge were retrofitted with a steel rail that is anchored into the top of the curb. This additional rail can be seen in Figure 2.1.

The bridge was in good condition. There was minor cracking of the underside of the slab. The cracking was concentrated at center line and midspan. Based on the inspection performed in April 1994, the deck, superstructure and substructure rated a 6 out of a possible 9.

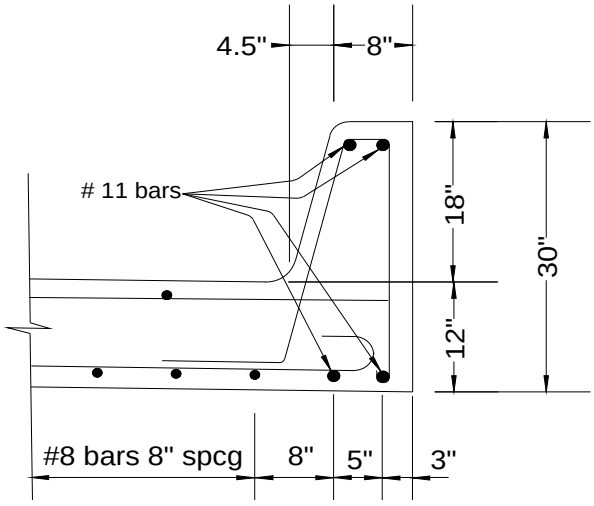

Figure 2.3 Structural Details of Curb.

2.2.2 Summary of Moment Distribution for Slab Bridges with Curbs

As discussed earlier, research was performed at the University of Illinois to establish a simplified design method to better distribute the live load and dead load moments in the slab and curb [5]. The method uses the total moment based on statics plus a fractional increase to account for the shift in the distribution when the load is on one side of the bridge [5]. The procedure uses empirical equations based on earlier research to obtain the fraction of moment resisted by the curbs [16]. The remaining moment is distributed across the width of the slab. This results in the design moment for the slab being based on an average moment

rather than the localized maximum moment. The curb is assumed to act compositely with an effective width of the slab equal to 4 times the depth of the slab. The design equations are summarized below [5]:

$$M_{curb} = C_1 \cdot \frac{Pa}{4} + C_2 \cdot \frac{pba^2}{8} + C_3 \cdot \frac{qa^2}{8} \tag{2.1}$$

$$M_{slab} = \left(m - 1.5 \cdot C_1\right) \cdot \frac{Pa}{4b} + \left(1 - 2 \cdot C_2\right) \cdot \frac{pa^2}{8} + \left(1 - C_3\right) \cdot \frac{qa^2}{4b} \tag{2.2}$$

where:

M_{curb} = Moment in the curb (kip-ft)

M_{slab} = Average moment in the slab per unit width (kip-ft/ft)

P = Magnitude of one rear wheel load including impact (kips)

a = Span length of the bridge (ft)

p = Load per unit area between inside faces of curbs (kips/ft^2)

b = Width of the roadway between inside faces of curbs (ft)

q = Load per unit length along curb (kips/ft)

m = Number of wheel loads on bridge.

The empirical coefficients C_1 , C_2 , C_3 are derived below [5]. These equations were derived based on earlier analysis of slab bridges utilizing plate theory [20].

$$C_1 = \left(\frac{12}{2.5 + G}\right) \cdot \frac{4 - (v/a)}{4 + 28 \cdot (v/a)} \tag{2.3}$$

$$C_2 = \frac{0.5 \cdot (a/b)}{0.47 \cdot G + \sqrt[3]{1.15 + (a/b)^3}} \tag{2.4}$$

$$C_3 = \frac{\sqrt[3]{1.15 + (a/b)^3}}{0.47 \cdot G + \sqrt[3]{1.15 + (a/b)^3}} \tag{2.5}$$

where:

$$G = \frac{a \cdot h^3}{12 \cdot I}$$

h = Overall depth of slab (in.)

I = Moment of inertia of the gross section of the curb only (in.^{4})

v = Axle width, center to center of truck tires (ft)

For design and load rating, the moment equations for the slab and the curb must be broken down into components corresponding to live load and dead load. The necessary equations are shown below [5]:

$$(M_{slab})_{LL} = (4 - 1.5 \cdot C_1) \cdot \frac{Pa}{4b} \tag{2.6}$$

$$(M_{slab})_{DL} = (1 - 2 \cdot C_2) \cdot \frac{pa^2}{8} + (1 - C_3) \cdot \frac{qa^2}{4b} \tag{2.7}$$

$$(M_{curb})_{LL} = C_1 \cdot \frac{Pa}{4} + 4h \cdot (M_{slab})_{LL} \tag{2.8}$$

$$\left(M_{curb}\right)_{DL} = C_2 \cdot \frac{pba^2}{8} + C_3 \cdot \frac{qa^2}{8} + 4h \cdot (M_{slab})_{DL} \qquad (2.9)$$

2.2.3 Load Rating of Test Bridge

The load rating procedure outlined in this section follows the load factor method shown in the AASHTO Manual [1]. The basic equation used for load rating a bridge is [1]:

$$RF = \frac{C - A_1 \cdot D}{A_2 \cdot L \cdot (1 + I)} \qquad (2.10)$$

where:

RF = Rating factor based on the rating vehicle used

C = Capacity of the member

A_1 = Factor for dead loads (1.3 for both inventory and operating rating)

D = Dead load effect on the member

A_2 = Factor for live load (2.17 for inventory rating and 1.3 for operating rating)

L = Live load effect on the member

I = Impact factor.

For a slab bridge with structural curbs, both the slab and the curbs must be rated to determine which controls the load rating. The capacities are based upon the appropriate sections of the AASHTO Design Specifications [13]. The rating vehicle used for this procedure is an HS20 truck. This truck is a typical design

truck with an axle spacing of 14 feet and front and rear axle weights of 8 kips and 32 kips. An additional axle is spaced at 14 feet from the rear axle and weighs 32 kips.

The bridge was rated as a 24-foot simple-span bridge. The actual span length was 25 feet with a 1 foot deduction for bearing length. The design compressive strength of the concrete was 3000 psi. However, a concrete compressive strength of 5000 psi was used for rating. The calculated capacities for both strengths are shown below. This increase in concrete strength was verified by a Schmidt Hammer test described in section 3.4.3.

The dead load moments listed below include the weight of a one-half inch asphalt overlay which was measured in the field. The dead load and live load effects are based on the moment distribution method outlined above. The capacities and moments are as follows:

C_{slab} = 34.6 kip-ft/ft (f'c = 5000 psi)

C_{slab} = 33.5 kip-ft/ft (f'c = 3000 psi)

C_{curb} = 602.4 kip-ft (f'c = 5000 psi)

C_{curb} = 579.5.4 kip-ft (f'c = 3000 psi)

D_{slab} = 6.4 kip-ft/ft

D_{curb} = 101.8 kip-ft

L_{slab} = 10.6 kip-ft/ft

L_{curb} = 135.2 kip-ft

I = 1.3

Based on the values utilizing an f'c of 5000 psi, the rating factors for the slab and curb calculated using Eq. 2.10 are:

Inventory RF_{slab} = 0.88

Inventory RF_{curb} = 1.23

Operating RF_{slab} = 1.47

Operating RF_{curb} = 2.06

The slab controls the rating factor at both inventory and operating levels. To determine the actual load rating, the rating factor is multiplied by the weight of the front two axles of the truck that was used to determine the live load effects. Combining the slab rating factors and an HS20 rating vehicle, the operating and inventory ratings are as follows:

Inventory Rating = HS17.6

Operating Rating = HS29.4

According to current TxDOT policy, this bridge would not require posting because the operating rating is greater than HS20. However, the bridge would require inspections more frequently than the normal two year interval because the inventory rating is less than HS20.

Chapter 3. TEST PROCEDURE

3.1 GENERAL

This chapter gives an overview of the instrumentation used for testing, the instrumentation installation, and a discussion of problems encountered with the instruments. The loading procedures and the actual test procedures are also briefly covered. A detailed description of the instrumentation and procedures is presented in Appendix A.

3.2 INSTRUMENTATION

3.2.1 Strain and Deflection Measurement

A total of 23 instruments were used to monitor the response of the slab bridge. All instruments were positioned at midspan of the bridge. The instruments may be divided into four groups: (a) strain gages attached to the surface of the reinforcing bars within the slab, (b) strain gages attached to the surface of the concrete, (c) strain transducers attached to the bottom surface of the slab , and (d) displacement transducers.

The strain gages were attached to the concrete in three locations: (a) the top and sides of the curb, (b) the top surface of the slab, and (c) the bottom surface of the slab. The displacement transducers monitored the vertical deflection of the slab.

Strain was measured using both electrical resistance strain gages and mechanical strain transducers. The strain gages were standard 120-ohm strain

gages with a 6-mm gage length for measuring the strain in the reinforcing bars and a 60-mm gage length for measuring the strain in concrete. Strain gage completion boxes were used to complete the full wheatstone bridge for the quarter bridge circuits..

Deflection was measured using string potentiometers. These devices were attached to the bottom of the slab and the wire was anchored to the concrete riprap. This arrangement provided a method of measuring the relative displacement between the concrete riprap and the bottom of the slab. Figure 3.1 shows a string potentiometer (A), a mechanical strain transducer (B) and a strain gage (C) attached to the surface of the concrete.

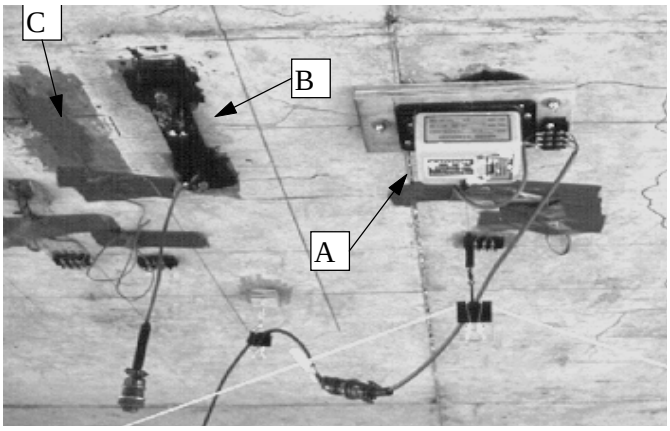

Figure 3.1 Instrumentation in Place on Bottom of Slab, (A)String Potentiometer, (B) Strain Transducer, and (C) strain gage.

The data acquisition system used was developed for TxDOT as a part of a previous research project [17]. The system was modified slightly in order to sample data at a rate required for moving loads. The data acquisition system was capable of recording 7 channels at a sample rate of 16 Hz. The data acquisition

system, the required 12 volt batteries and the mechanical strain transducers are shown in Figure 3.2.

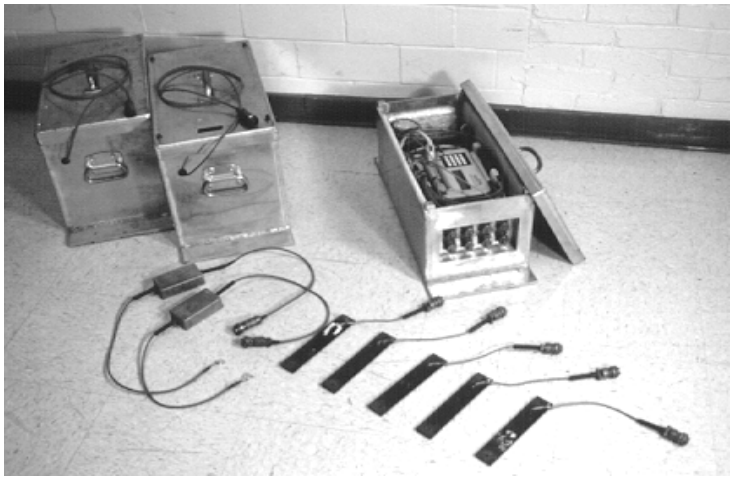

Figure 3.2 Data acquisition system and strain transducers used in test.

3.2.2 Placement and Installation of Instrumentation

The locations for the instruments were chosen based on the need to compare the data with the results of previous tests [10] and to gather adequate data to better understand the behavior of the slab bridge. Details on the placement of the various types of instrumentation are discussed in Appendix A.

Before installation of the instrumentation, the bottom of the slab was marked off in 6 in. x 6 in. grids. This grid aided in locating and marking the existing cracks in the slab. Figure 3.3 shows the crack pattern on the bottom surface of the slab at the time of testing. Because the cracked section controls during analysis, an effort was made to place the gages as close to visible cracks as possible.

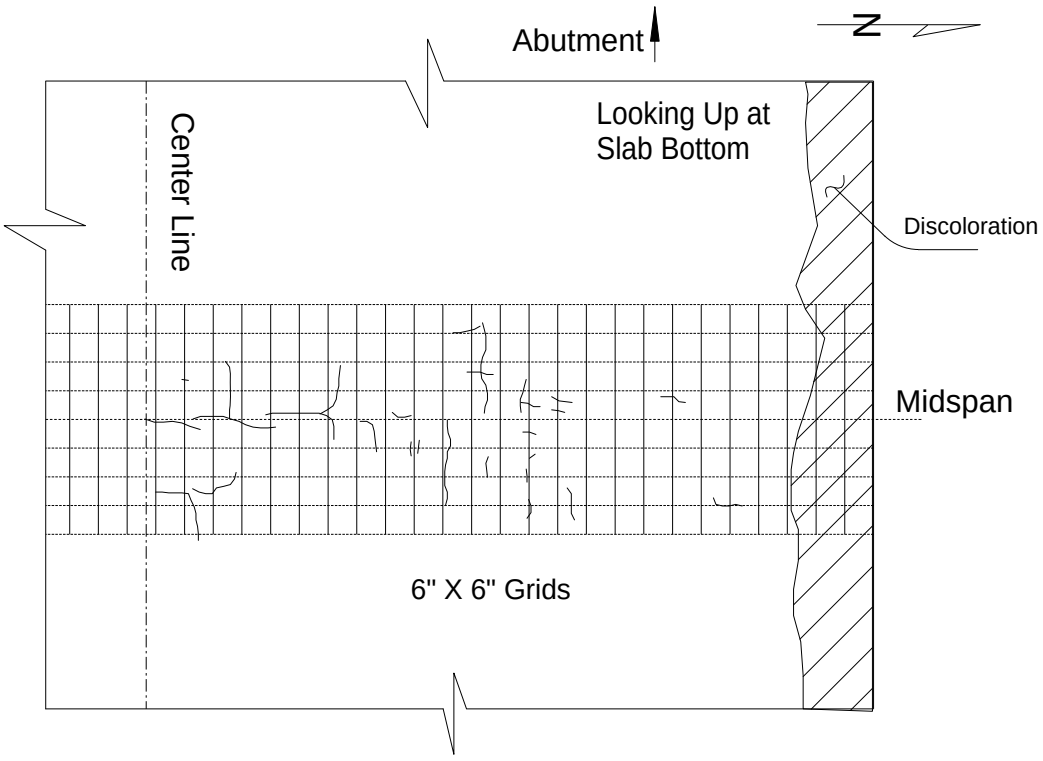

Figure 3.3 Crack Pattern on the underside of the Slab.

The installation of each type of instrument required a different technique. The reinforcing steel gages required exposing a section of rebar at midspan and preparing the rebar for gage installation. A hole of approximately 6 in. in diameter was broken out of the concrete to access the rebar. The preparation of the rebar involved grinding, sanding and cleaning. Figure 3.4 shows the grinding process while Figure 3.5 shows a rebar ready for application of a gage.

Figure 3.4 Grinding the rebar in preparation for strain gage installation.

Figure 3.5 Reinforcing steel prepared for strain gage installation.

Once the reinforcing steel was prepared, the gage was installed according to manufacturer's instructions which are outlined in Appendix A. After installation, the gage was protected by applying a coating of white acrylic and

then a layer of gray silicone sealant. The leads were then attached to a terminal block and the gage was tested to insure that it was functioning. A completed rebar gage is shown in Figure 3.6.

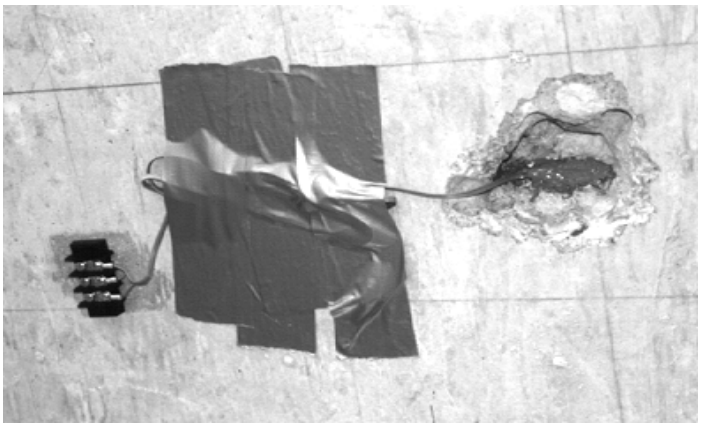

Figure 3.6 Reinforcing steel strain gage ready for testing..

The top of the slab required special preparation before the concrete strain gages could be installed. A hole approximately 6 in. by 6 in. was chiseled in the asphalt overlay. The exposed concrete surface was then thoroughly cleaned with acetone to remove all asphalt residue. During this process traffic control was required. A shallow groove was also chiseled from the gage location to the edge of the pavement. This groove provided protection for the wire leads.

Concrete strain gages require a slightly different method of installation. The concrete surface was prepared by sanding and cleaning. A thin layer of two part epoxy was then applied to the area where the gage was to be installed to provide a smooth surface. The epoxy was allowed to cure and then sanded and cleaned. The gage was then installed using a special two part epoxy for concrete strain gages. The epoxy must cure while being clamped with slight pressure.

Figures 3.7 and 3.8 show the concrete gage applied and the clamping apparatus used. The gage was then waterproofed using the same method as the reinforcing steel gages. The leads are then attached to a terminal block and then tested to verify proper operation.

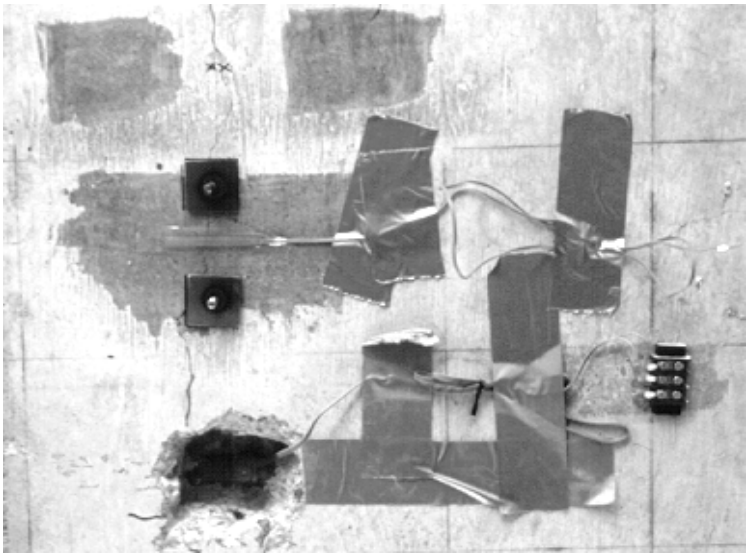

Figure 3.7 Concrete strain gage ready for clamping..

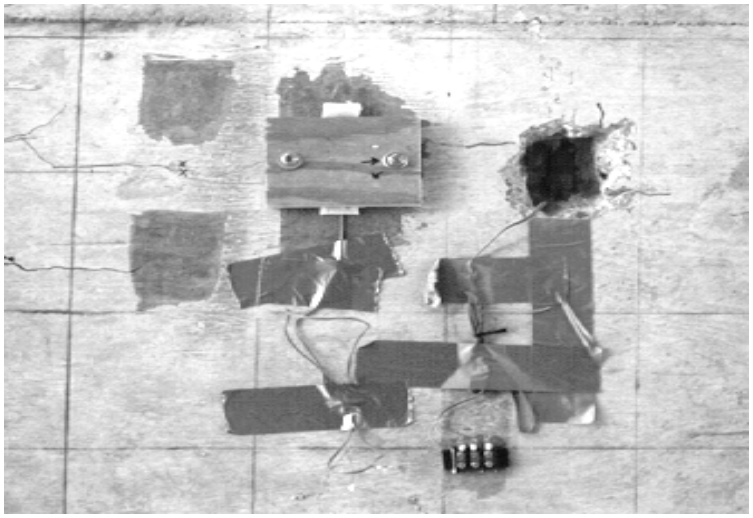

Figure 3.8 Concrete strain gage clamped with clamping apparatus.

The gages on the top of the slab required additional protection from traffic. After gage installation, the hole in the asphalt was filled with mortar sand. The sand provided the needed protection from the impact of the tires. The wire leads for these gages had to be lengthened to extend across the traffic lane.

The strain transducers were installed by attaching mounting tabs to the concrete surface and then bolting the transducers to these tabs. The string potentiometers were attached to the slab by anchor bolts. The wires were attached to eye bolts that were anchored into the concrete riprap. A strain transducer and a string potentiometer are shown in Figure 3.1.

3.2.3 Problems with Installation

Several problems were encountered during installation of the instrumentation. Problems related to weather and traffic being the two worst. The temperatures during instrumentation were generally cool, ranging from approximately 40° F to 60° F. These temperatures caused the epoxy to require an extended curing time. Ideally the epoxy can be applied in the morning and it will be fully cured by afternoon. This allows for strain gage installation to be performed in one day. The cool temperatures required an overnight curing time for the epoxy.

Although traffic was low for this bridge, it was still enough to be a problem during installation of the strain gages on the top of the slab. Traffic control was required to keep traffic off of the gages until they could be properly installed, clamped and protected.

Other problems were typical with field installation of strain gages. In one case a strain gage did not adhere to the reinforcing steel. In another case the lead wires broke off the gage, requiring removal and installation of another gage.

Despite these problems, the installation was relatively easy, although time consuming. This extensive instrumentation was not intended nor recommended for a typical bridge testing program. Recommended instrumentation for typical tests of concrete slab bridges is discussed in Chapter 6.

3.2 LOADING

The loading vehicle was acquired from the TxDOT maintenance office in Taylor, TX. The truck was a standard 10 cubic yard dump truck as shown in Figure 3.9. The truck was loaded with roadway base material and weighed approximately 49,000 pounds. The truck was driven across the bridge at both a crawl speed, approximately 5 miles per hour, and at 30 miles per hour depending on the test. The 30 mph pass was an attempt to measure impact. Because of the limited sampling rate of the data acquisition system, adequate data could not be obtained for this test.

In order to compare the results from this test with those obtained during previous load tests [10], the truck was driven across the bridge in four transverse positions. In the first location, the right front wheel of the truck was two feet from the inside face of the north curb. In the fourth location, the left front wheel was approximately three feet from the inside face of the south curb. The truck was closer to the center line of the bridge in the remaining two positions.

The truck crossed the bridge in the same position twice in order to evaluate the repeatability of the measured data.

Figure 3.9 Test Truck provided by TxDOT.

3.3 TEST

3.3.1 Test Plan

Development of a detailed test plan is one of the most important parts of a successful load test. As discussed previously, 23 instruments were used to monitor the response of the bridge, however, the data acquisition system was limited to recording the response of only 7 instruments at any time. In addition, four truck locations and two vehicle speeds were used during testing. Therefore, the test plan was essential to minimize the duration of the load test and to ensure that all desired information was collected.

The load test was divided into five series, as documented in Table A.1. Combinations of instruments were used in each series. In three of the series, the

truck crossed the bridge in all four locations. Only two locations were used in remaining two series.

3.3.2 Test Procedure

Each test series required connecting the appropriate gages for that series. The gages were then checked with the data acquisition system software to insure they were operational. The truck was then driven across the bridge in the appropriate location. An electronic marking device was used to mark the longitudinal truck position in the data. The device was triggered by a member of the testing team when the front axle crossed a designated location. Data were downloaded from the data acquisition system while the truck backed up into position for the next run. This procedure was repeated until testing was complete. There was a slight delay between each test series to connect the appropriate gages. This delay ranged from 10 to 15 minutes. Figure 3.10 shows the test in progress.

Figure 3.10 Load test in progress.

The test was completed in approximately five hours. The test preparation on the day of the test required two hours, the actual testing was two hours and the disassembly and packing of equipment required approximately one hour.

3.3.3 Traffic Control

Traffic control was accomplished by two flag persons. As stated above the traffic volume was low for this road. During actual testing the traffic was stopped. Between tests the traffic was flagged through the test site. There was minimal impact on traffic during the test.

3.3.4 Problems

The test was accomplished with few problems. The test proceeded rather quickly, but the entire test could have been performed in less than half the time if a data acquisition system capable of monitoring all the gages had been available.

The gages on the top of the slab were protected by a layer of sand in addition to the normal protection mentioned above. This worked well except when the truck tire passed directly over the gage. The pressure from the tire caused the gage to behave erratically and the resulting data were unusable.

As discussed, traffic control was not critical for this test but if traffic volumes were higher this could become a major problem. Increased traffic would drastically slow down the testing.

In summary testing problems were few but this was mainly due to the remote testing site. If tests are to be performed in areas with high traffic a data acquisition system with more capacity is needed. In addition an improved method of traffic control will be needed.

Chapter 3. TEST PROCEDURE

3.1 GENERAL

This chapter gives an overview of the instrumentation used for testing, the instrumentation installation, and a discussion of problems encountered with the instruments. The loading procedures and the actual test procedures are also briefly covered. A detailed description of the instrumentation and procedures is presented in Appendix A.

3.2 INSTRUMENTATION

3.2.1 Strain and Deflection Measurement

A total of 23 instruments were used to monitor the response of the slab bridge. All instruments were positioned at midspan of the bridge. The instruments may be divided into four groups: (a) strain gages attached to the surface of the reinforcing bars within the slab, (b) strain gages attached to the surface of the concrete, (c) strain transducers attached to the bottom surface of the slab , and (d) displacement transducers.

The strain gages were attached to the concrete in three locations: (a) the top and sides of the curb, (b) the top surface of the slab, and (c) the bottom surface of the slab. The displacement transducers monitored the vertical deflection of the slab.

Strain was measured using both electrical resistance strain gages and mechanical strain transducers. The strain gages were standard 120-ohm strain

gages with a 6-mm gage length for measuring the strain in the reinforcing bars and a 60-mm gage length for measuring the strain in concrete. Strain gage completion boxes were used to complete the full wheatstone bridge for the quarter bridge circuits. The mechanical strain transducers were used to measure surface in the concrete and had a gage length of 7 inches.

Deflection was measured using string potentiometers. These devices were attached to the bottom of the slab and the wire was anchored to the concrete riprap. This arrangement provided a method of measuring the relative displacement between the concrete riprap and the bottom of the slab. Figure 3.1 shows a string potentiometer (A), a mechanical strain transducer (B) and a strain gage (C) attached to the surface of the concrete.

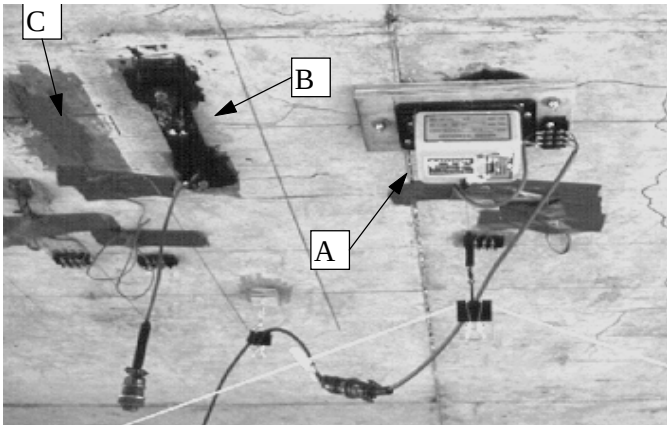

Figure 3.1 Instrumentation in Place on Bottom of Slab, (A)String Potentiometer, (B) Strain Transducer, and (C) strain gage.

The data acquisition system used was developed for TxDOT as a part of a previous research project [17]. The system was modified slightly in order to sample data at a rate required for moving loads. The data acquisition system was

capable of recording 7 channels at a rate of 16 Hz. The data acquisition system, the required 12 volt batteries and the mechanical strain transducers are shown in Figure 3.2.

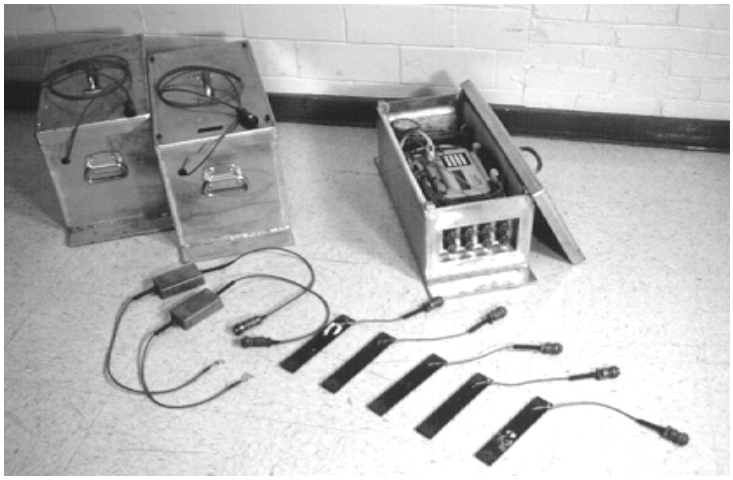

Figure 3.2 Data acquisition system and strain transducers used in test.

3.2.2 Placement and Installation of Instrumentation

The locations for the instruments were chosen based on the need to compare the data with the results of previous tests [10] and to gather adequate data to better understand the behavior of the slab bridge. Details on the placement of the various types of instrumentation are discussed in Appendix A.

Before installation of the instrumentation, the bottom of the slab was marked off in 6 in. x 6 in. grids. This grid aided in locating and marking the existing cracks in the slab. Figure 3.3 shows the crack pattern on the bottom surface of the slab at the time of testing. Because the cracked section controls

during analysis, an effort was made to place the gages as close to visible cracks as possible.

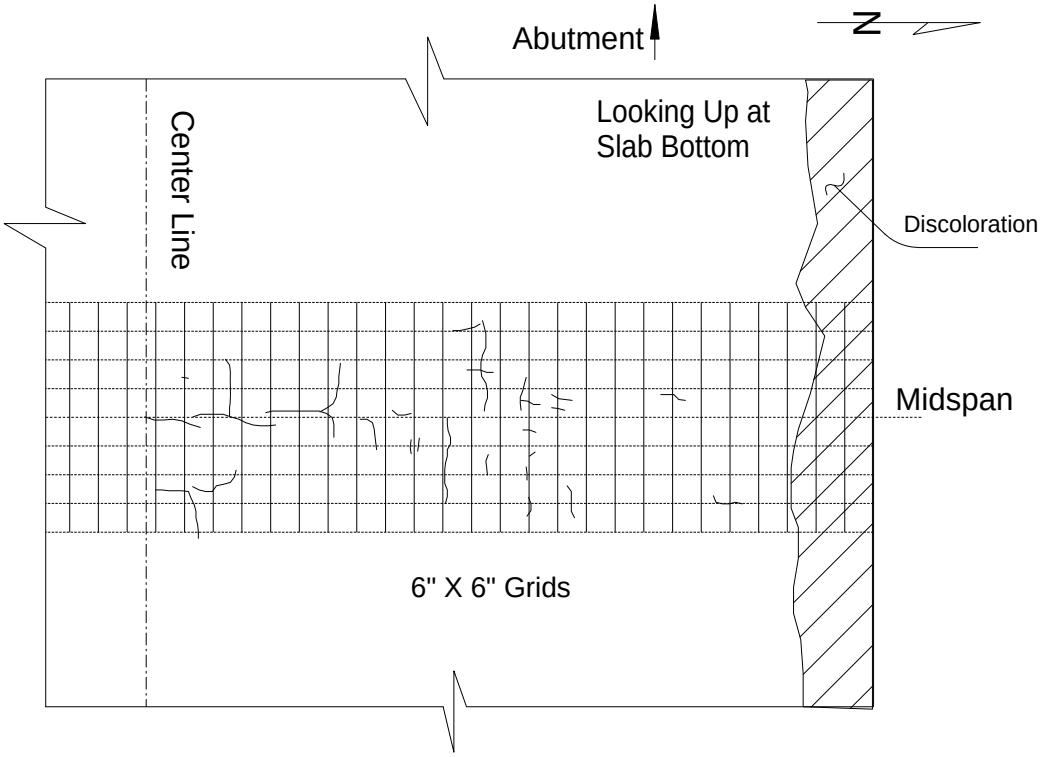

Figure 3.3 Crack Pattern on the underside of the Slab.

The installation of each type of instrument required a different technique. The reinforcing bar gages required exposing a section of rebar at midspan and preparing the rebar for gage installation. A hole of approximately 6 in. in diameter was broken out of the concrete to access the rebar. The preparation of the rebar involved grinding, sanding and cleaning. Figure 3.4 shows the grinding process while Figure 3.5 shows a rebar ready for gage installation.

Figure 3.4 Grinding the rebar in preparation for strain gage installation.

Figure 3.5 Reinforcing bar prepared for strain gage installation.

Once the reinforcing bar was prepared, the gage was installed according to manufacturer's instructions which are outlined in Appendix A. After installation, the gage was protected by applying a coating of white acrylic and then a layer of

gray silicone sealant. The leads were then attached to a terminal block and the gage was tested to insure that it was functioning. A completed rebar gage is shown in Figure 3.6.

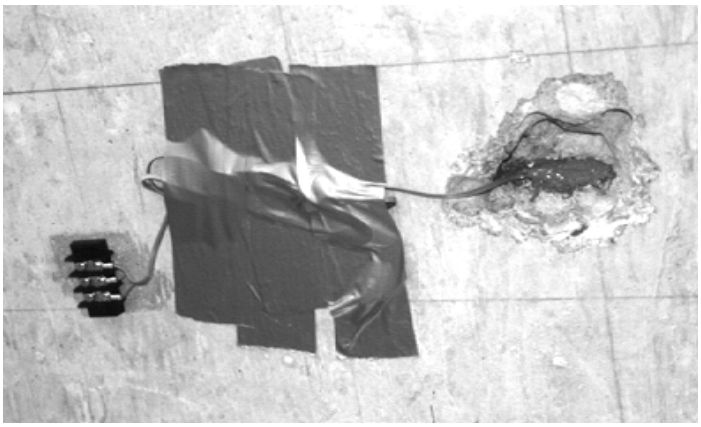

Figure 3.6 Reinforcing bar strain gage ready for testing.

The top of the slab required special preparation before the concrete strain gages could be installed. A hole approximately 6 in. by 6 in. was chiseled in the asphalt overlay. The exposed concrete surface was then thoroughly cleaned with acetone to remove all asphalt residue. During this process traffic control was required. A shallow groove was also chiseled from the gage location to the edge of the pavement. This groove provided protection for the wire leads.

Concrete strain gages require a slightly different method of installation. The concrete surface was prepared by sanding and cleaning. A thin layer of two part epoxy was then applied to the area where the gage was to be installed to provide a smooth surface. The epoxy was allowed to cure and then sanded and cleaned. The gage was then installed using a special two part epoxy for concrete strain gages. The epoxy must cure while being clamped with slight pressure.

Figures 3.7 and 3.8 show the concrete gage applied and the clamping apparatus used. The gage was then waterproofed using the same method as the reinforcing steel gages. The leads were then attached to a terminal block and then tested to verify proper operation.

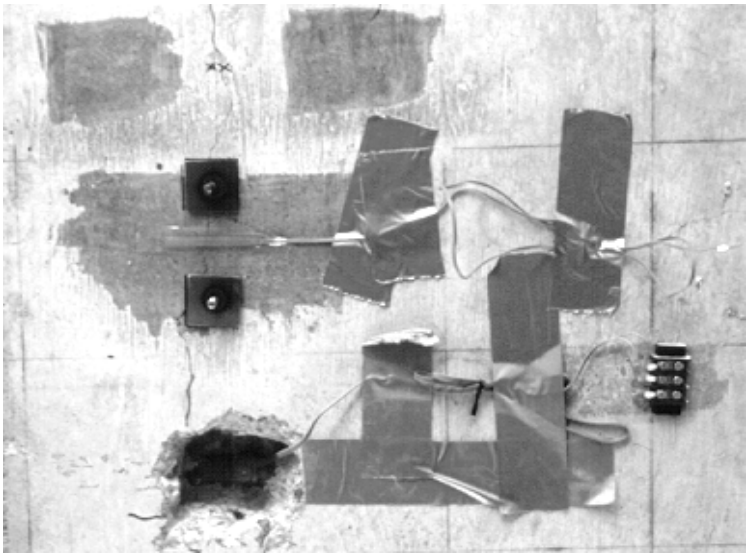

Figure 3.7 Concrete strain gage ready for clamping.

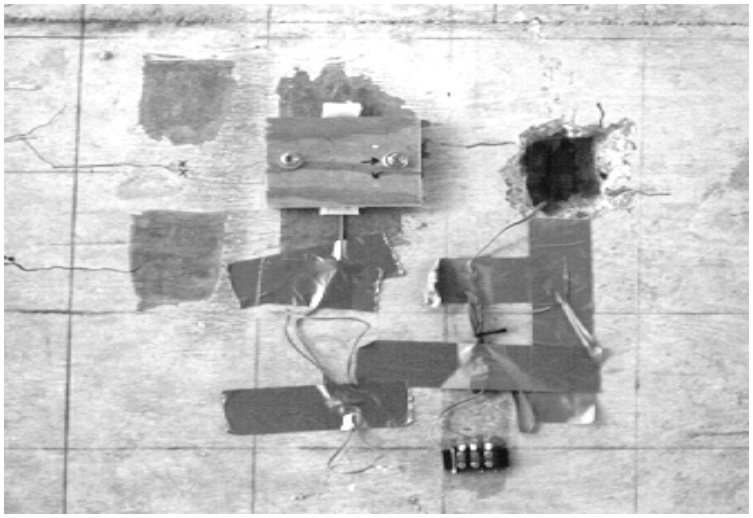

Figure 3.8 Concrete strain gage clamped with clamping apparatus.

The gages on the top of the slab required additional protection from traffic. After gage installation, the hole in the asphalt was filled with mortar sand. The sand provided the needed protection from the impact of the tires. The wire leads for these gages were lengthened to extend across the traffic lane. The terminal blocks for these gages were attached to the top of the curb.

The strain transducers were installed by attaching mounting tabs to the concrete surface and then bolting the transducers to these tabs. The string potentiometers were attached to the slab by anchor bolts. The wires were attached to eye bolts that were anchored into the concrete riprap. A strain transducer and a string potentiometer are shown in Figure 3.1.

3.2.3 Problems with Installation

Several problems were encountered during installation of the instrumentation. Problems related to weather and traffic being the two worst. The temperatures during instrumentation were generally cool, ranging from approximately 40° F to 60° F. These temperatures caused the epoxy to require an extended curing time. Ideally the epoxy can be applied in the morning and it will be fully cured by afternoon. This allows for strain gage installation to be performed in one day. The cool temperatures required an overnight curing time for the epoxy.

Although traffic was low for this bridge, it was still enough to be a problem during installation of the strain gages on the top of the slab. Traffic control was required to keep traffic off of the gages until they could be properly installed, clamped and protected.

Other problems were typical with field installation of strain gages. In one case a strain gage did not adhere to the reinforcing steel. In another case the lead wires broke off the gage, requiring removal and installation of another gage.

Despite these problems, the installation was relatively easy, although time consuming. This extensive instrumentation was not intended nor recommended for a typical bridge testing program. Recommended instrumentation for typical tests of concrete slab bridges is discussed in Chapter 8.

3.3 LOADING

The loading vehicle was acquired from the TxDOT maintenance office in Taylor, TX. The truck was a standard 10 cubic yard dump truck as shown in Figure 3.9. The truck was loaded with roadway base material and weighed approximately 49,000 pounds. The truck was driven across the bridge at both a crawl speed, approximately 5 miles per hour, and at 30 miles per hour depending on the test. The 30 mph pass was an attempt to measure impact. Because of the limited sampling rate of the data acquisition system, adequate data could not be obtained for this test.

In order to compare the results from this test with those obtained during previous load tests [10], the truck was driven across the bridge in four transverse positions. In the first location, the right front wheel of the truck was two feet from the inside face of the north curb. In the fourth location, the left front wheel was approximately three feet from the inside face of the south curb. The truck was closer to the center line of the bridge in the remaining two positions.

The truck crossed the bridge in the same position twice in order to evaluate the repeatability of the measured data.

Figure 3.9 Test Truck provided by TxDOT.

3.4 TEST

3.4.1 Test Plan

Development of a detailed test plan is one of the most important parts of a successful load test. As discussed previously, 23 instruments were used to monitor the response of the bridge, however, the data acquisition system was limited to recording the response of only 7 instruments at any time. In addition, four truck locations and two vehicle speeds were used during testing. Therefore, the test plan was essential to minimize the duration of the load test and to ensure that all desired information was collected.

The load test was divided into five series, as documented in Table A.1. Combinations of instruments were used in each series. In three of the series, the

truck crossed the bridge in all four locations. Only two locations were used in remaining two series.

3.4.2 Test Procedure

Each test series required connecting the appropriate gages for that series. The gages were then checked with the data acquisition system software to insure they were operational. The truck was then driven across the bridge in the appropriate location. An electronic marking device was used to mark the longitudinal truck position in the data. The device was triggered by a member of the testing team when the front axle crossed a designated location. Data were downloaded from the data acquisition system while the truck backed up into position for the next run. This procedure was repeated until testing was complete. There was a slight delay between each test series to connect the appropriate gages. This delay ranged from 10 to 15 minutes. Figure 3.10 shows the test in progress.

Figure 3.10 Load test in progress.

The test was completed in approximately five hours. The test preparation on the day of the test required two hours, the actual testing was two hours and the disassembly and packing of equipment required approximately one hour.

3.4.3 Schimdt Hammer Test

A Schimdt Hammer was used to determine the compressive strength of the concrete. Based on previous research [19] and the TxDOT slab bridge test [10], it was presumed the actual concrete compressive strength was greater than the design compressive strength. The tests were performed at three locations on the bridge, (a) the outside face of the curb, (b) the inside face of the curb and (c) the bottom of the slab. The tests were performed according to the manufacturer's instructions. The results of this test are shown in Table 3.1.

The Schmidt Hammer is very dependent on the location of the test. When using the instrument, careful choice of the test location should be made. The instrument is sensitive to cracks, form marks, spalls or any other surface defect. If a test is performed on any of these defects, inaccurate estimates of the concrete strength will be obtained. The Schmidt Hammer does not have the accuracy for determining exact concrete strengths, but for determining the strength within approximately 1000 psi it was adequate.

Because of the inherent variability of the Schmidt Hammer results, a conservative assumption of concrete compressive strength was made for use in analyzing this bridge. The value used was based on the mean of the test results less approximately two standard deviations. This resulted in an f'c of 5000 psi.

Table 3.1 Schmidt Hammer Results, psi.

Outside Curb	Bottom Slab	Inside Curb
5800	8500	8500
8500	7800	5500
6000	8000	5700
8500	8500	8500
6500	8200	6200
6200	8200	7000
8500	8500	6800
6000	8500	7300
6200	8200	7300
5700	8500	5800
Mean	7300 psi	
Std Dev	1200 psi	

3.4.4 Traffic Control

Traffic control was accomplished by two flag persons. As stated above the traffic volume was low for this road. During actual testing the traffic was stopped. Between tests the traffic was flagged through the test site. There was minimal impact on traffic during the test.

3.4.5 Problems

The test was accomplished with few problems. The test proceeded rather quickly, but the entire test could have been performed in less than half the time if a data acquisition system capable of monitoring all the gages had been available.

The gages on the top of the slab were protected by a layer of sand in addition to the normal protection mentioned above. This worked well except when the truck tire passed directly over the gage. The pressure from the tire caused the gage to behave erratically and the resulting data were unusable.

As discussed, traffic control was not critical for this test but if traffic volumes were higher this could become a major problem. Increased traffic would drastically slow down the testing.

In summary testing problems were few but this was mainly due to the remote testing site. If tests are to be performed in areas with high traffic a data acquisition system with more capacity is needed. In addition an improved method of traffic control will be needed.

Chapter 4. TEST RESULTS

4.1 PRESENTATION OF RESULTS

The entire set of test data for all test series are presented in Appendices B-G. Each test series, truck location and pass number are identified and graphed.

4.1.1 Method of Reduction

The strain gage setup was based on the quarter wheatstone bridge circuit. The raw data was in the form of voltage in (E_I)and millivoltage out (E_O). The formula used to convert the data to microstrain was as follows:

$$\mu\varepsilon = \frac{4000}{G_F} \cdot \frac{E_O}{E_I}$$

where:

$\mu\varepsilon$ = microstrain

G_F = Gage Factor

The strain transducer data was in the same form as the strain gage data although the transducers contained a full wheatstone bridge circuit. The data was converted to microstrain by the following formula:

$$\mu\varepsilon = \frac{1}{G_F} \cdot \frac{E_O}{E_I}$$

The string pot data was converted to inches of deflection by a similar formula:

$$\Delta = \frac{1}{G_F} \cdot \frac{E_O}{E_I}$$

4.2 STRAIN RESULTS

4.2.1 Variability of Instrumentation

The ability of the strain gages to provide accurate data is not only a function of the error in the gage but also the error in the truck location from pass to pass. Assuming proper installation the strain gage error is a known value for that particular gage. Therefore the error in truck location can be quantified. Because of the number of test series and the number of gages, only strain gage RB5 (see Appendix A for location) has enough data points to determine error in the truck location from pass to pass. Table 4.1 shows the data points, average strain values and standard deviation for each location and pass.

Table 4.1 Strain values and statistical data for strain gage RB5.

		Test Series (Readings in Microstrain)							
Location	Pass	1	3	3A	4	5	Mean	Standard Deviation	Coefficient of Variation
1	1	49.25	48.50	47.74	46.60	45.68			
1	2	51.91	50.01	45.84	50.77	47.94	48.42	2.08	4.30%
2	1	43.19	41.30	45.46	40.54	42.28			
2	2	44.71	42.06	44.71	42.06	43.04	42.93	1.60	3.74%
3	1	20.46			20.46	19.63			
3	2	20.08			19.70	19.63	19.99	0.40	1.99%
4	1	15.15			15.15	14.72			
4	2	15.53			15.53	14.72	15.14	0.36	2.40%

Based on the strain gage data the gages have an accuracy of ±1 microstrain. From the data in Table 4.1 the range due to the truck location error and the strain gage error is ±2 microstrain with an error of 5%. As a result of this analysis it is shown that the inaccuracies of the truck location have minimal effects on the strain output, therefore having the truck follow lines marked on the deck is an acceptable method of loading.

4.2.2 Comparison of Strain Transducers and Strain Gages

Both strain transducer T1 and strain gage F1 were placed on the tension surface of the slab (See Appendix A for location). These gages both spanned across the same crack in the bottom of the slab. Figure 4.1 shows the strain comparison of these two gages. The large difference between the two strain readings is due to the fact that the strain is an average strain and the transducer has more than twice the gage length of the strain gage. The shift in maximum value is due to the varying speed of the truck between the two tests and is not pertinent to this discussion.

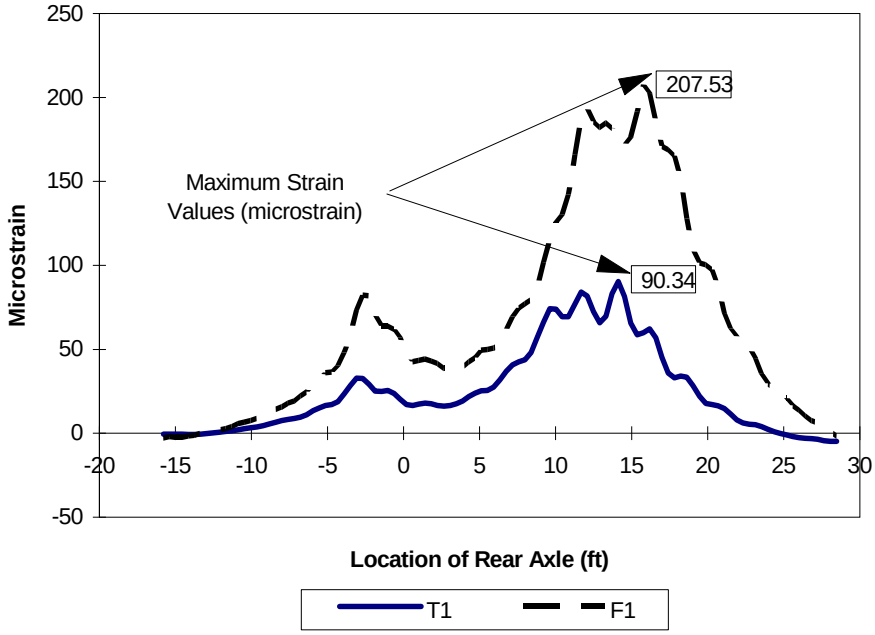

Figure 4.1 Comparison of Strain for Transducers and Strain Gages.

By taking the strain values and multiplying by the gage lengths, a change in length can be determined. As shown in Table 4.2 the difference in the measured deformations is within an average difference of 18%. The lesser values of deformation of the strain gage are expected because of the shorter gage length.

Table 4.2 Comparison of Strain Transducers and Strain Gages.

Location	Pass	T1	T1 deformation	F1	F1 deformation	% Difference
		με	μ inches	με	μ inches	Deformation
1	1	85.49	598.41	207.53	489.77	18.16%
1	2	90.34	632.39	220.98	521.51	17.53%
2	1	101.25	708.74	257.49	607.67	14.26%
2	2	109.91	769.34	257.87	608.58	20.90%
				Average % Difference		17.71%

Although the difference in deformation is 18%, the difference in gage length is 66%. This shows that the majority of the deformation occurred at the crack. This confirms that regardless of the type of gage used, the cracks in a cracked section must be crossed with the gage. Further discussion of methods to utilize this data will be covered in Chapter 5.

4.2.3 Distribution of Strain

Figures 4.2 and 4.3 show the distribution of strain in the longitudinal reinforcing steel. The strain values for truck locations 1 and 2 are superimposed to give values for comparisons with previous tests [10]. These comparisons will be shown in Chapter 5. As shown in Figures 4.2 and 4.3 the strains near center line are considerably greater than the other strains. This difference may be due to the fact that the two strain gages nearest to center line (RB1 and RB2) were in a cracked section. There were visible crack observed in these areas.

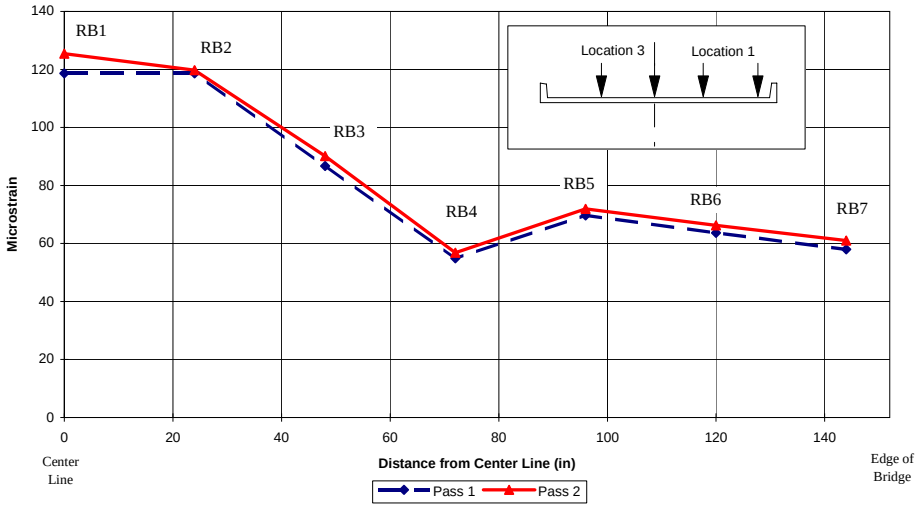

Figure 4.2 Strain Distribution in longitudinal reinforcing bars for Truck Locations 1&3.

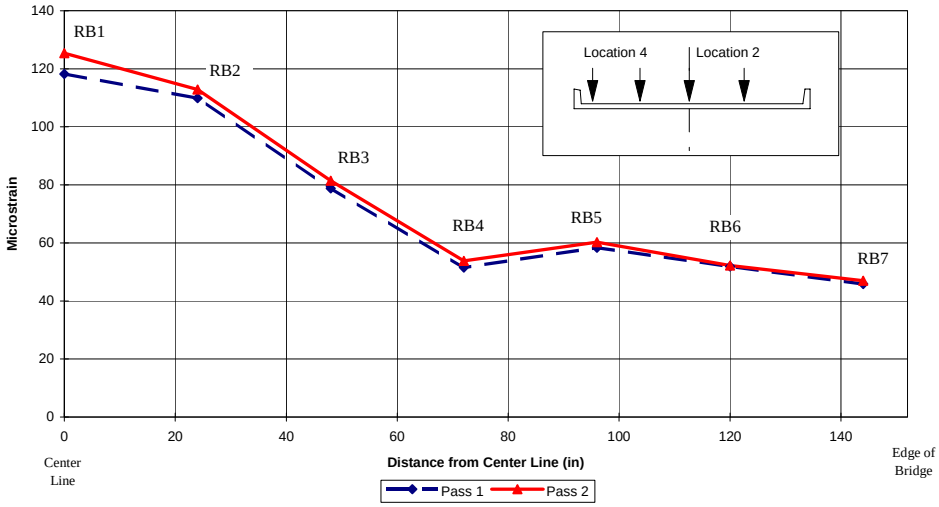

Figure 4.3 Strain Distribution in Longitudinal Reinforcing Bars for Truck Locations 2&4.

Figures 4.4 and 4.5 show the strain distribution in both the concrete on top of the slab, and the corresponding tension reinforcing steel beneath the gage. In Figure 4.4 the concrete gage in the center of the lane (C2) is showing unusually high strain values. This behavior was due to the fact that rear wheel of the truck ran over the gage.

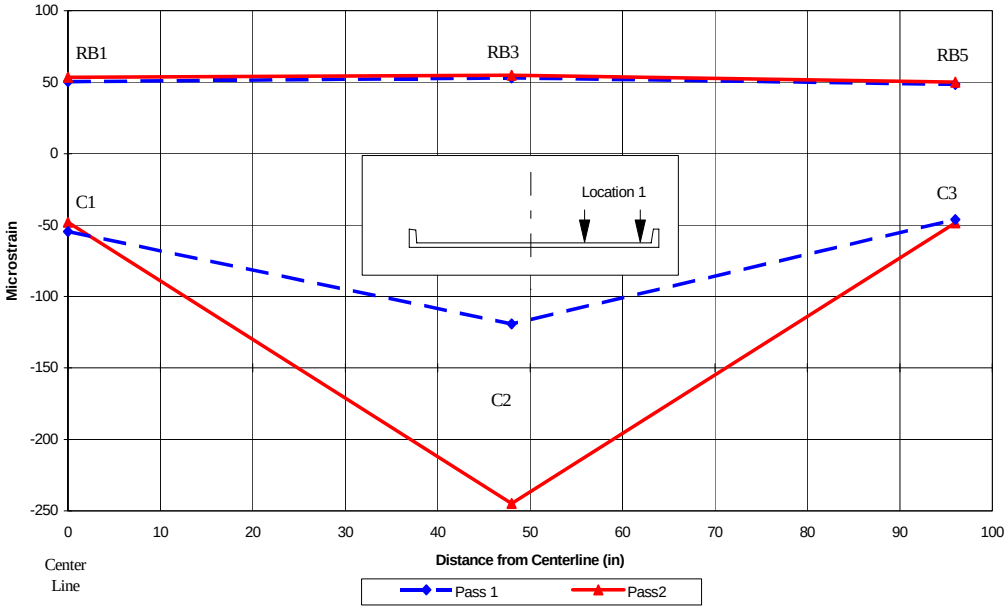

Figure 4.4 Strain Distribution across Top of Slab and Corresponding Rebar.

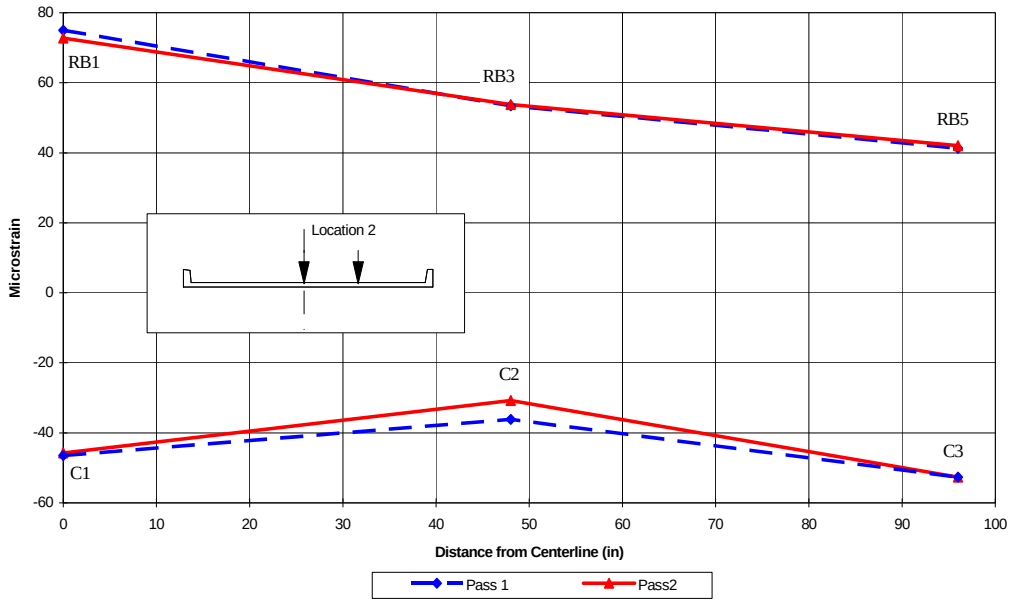

Figure 4.5 Strain Distribution across Top of Slab and Corresponding Rebar.

4.2.4 Problems with Gages

The strain gages placed on the rebar performed well throughout the test. As discussed above the variability in the reinforcing steel strain data was due to the inaccuracies of the instrumentation itself and the transverse location of the truck.

The concrete strain gages performed well except the gages placed on the top of the slab. These gages tended to have considerably more noise than the other gages. This was likely due to the longer lead wires required to extend across the lane. These gages also had problems when the truck wheel passed over the gage location. The pressure of the wheel caused the gage to give erratic

results. An example of the noisy and erratic behavior of a gage is shown in Figure 4.6. This was a later test series where a wheel had passed over the gage.

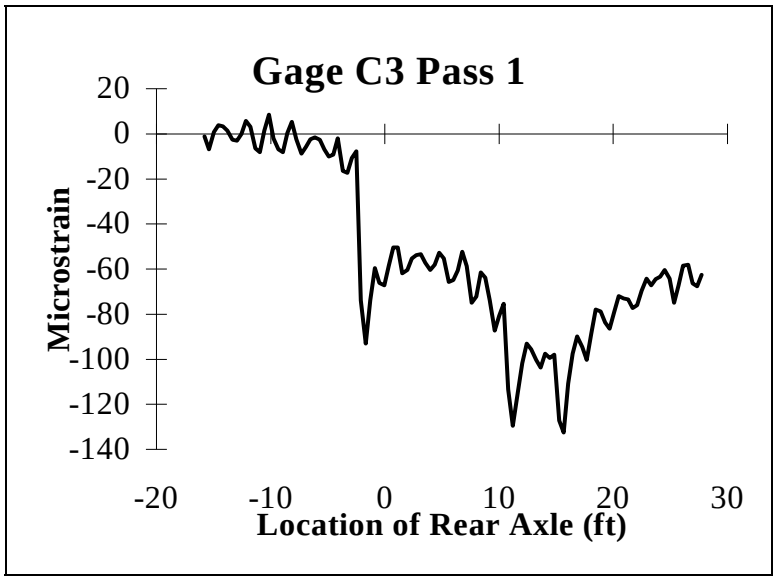

Figure 4.6 Erratic Behavior of a Concrete Gage on Top of Slab.

4.3 DEFLECTION

4.3.1 Lateral Distribution of Deflection

The deflection varied laterally across the bridge as shown in Figures 4.6 and 4.7. The data from the tests for location 1 and location 3 were superimposed to compare with previous tests. This comparison will be shown in Chapter 5. The process was also performed on the data from location 2 and location 4.

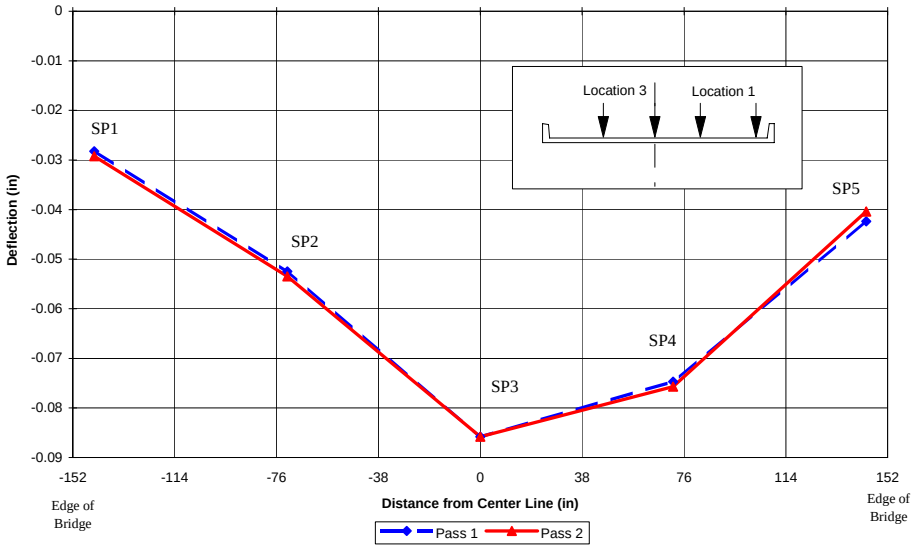

Figure 4.6 Deflection across bridge with Truck at Locations 1 & 3.

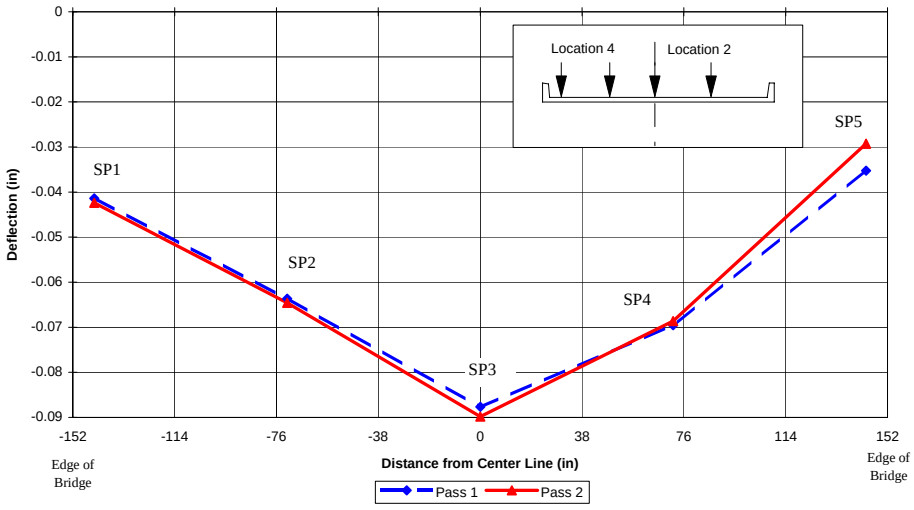

Figure 4.7 Deflection across bridge with Truck at Locations 2 & 4.

4.3.2 Problems with Gages

There were no apparent problems with the string pots while taking data. Several methods of anchoring the wire were attempted but only the approach with the wire attached straight down to the anchor worked. This limitation may prove to be a problem where the ground is not accessible below the gage.

Chapter 4. TEST RESULTS

The measured data are discussed in this chapter. The data are divided into five groups, depending on the instrument used. Measured strains in the reinforcing bars are discussed in section 4.1, strains measured on the surface of the concrete using strain gages are discussed in section 4.2, strains measured on the surface of the concrete using strain transducers are discussed in section 4.3, vertical deflections of the slab are discussed in section 4.4, and non-destructive tests to evaluate concrete compressive strength are discussed in section 4.5. The data are evaluated in Chapter 5 and compared with the results of previous investigations in Chapter 6.

4.1 MEASURED STRAIN IN REINFORCING BARS

Strain gages were placed on the reinforcing bars as discussed in Chapter 3. Appendix B contains the entire set of test results for the reinforcing bars. The data are identified by test series, truck location and pass number. An index to the tests is provided in Table A.1.

An example of the strain data recorded during the first test series for truck location 1, pass 1 is shown in Figure 4.1. The plots show the general trend of the truck influence on the reinforcing bar strains. The first peak in the strain data is the influence of the front axle passing over the gage locations at midspan. The second set of peaks is due to the influence of the tandem axle as it passes over the gage locations.

The gages near the centerline of the bridge recorded considerably higher strain values than the gages close to the curb. The gage on the curb, RB7, does not have the sharp peaks due to the axles crossing midspan. This behavior of the curb is consistent for all truck locations.

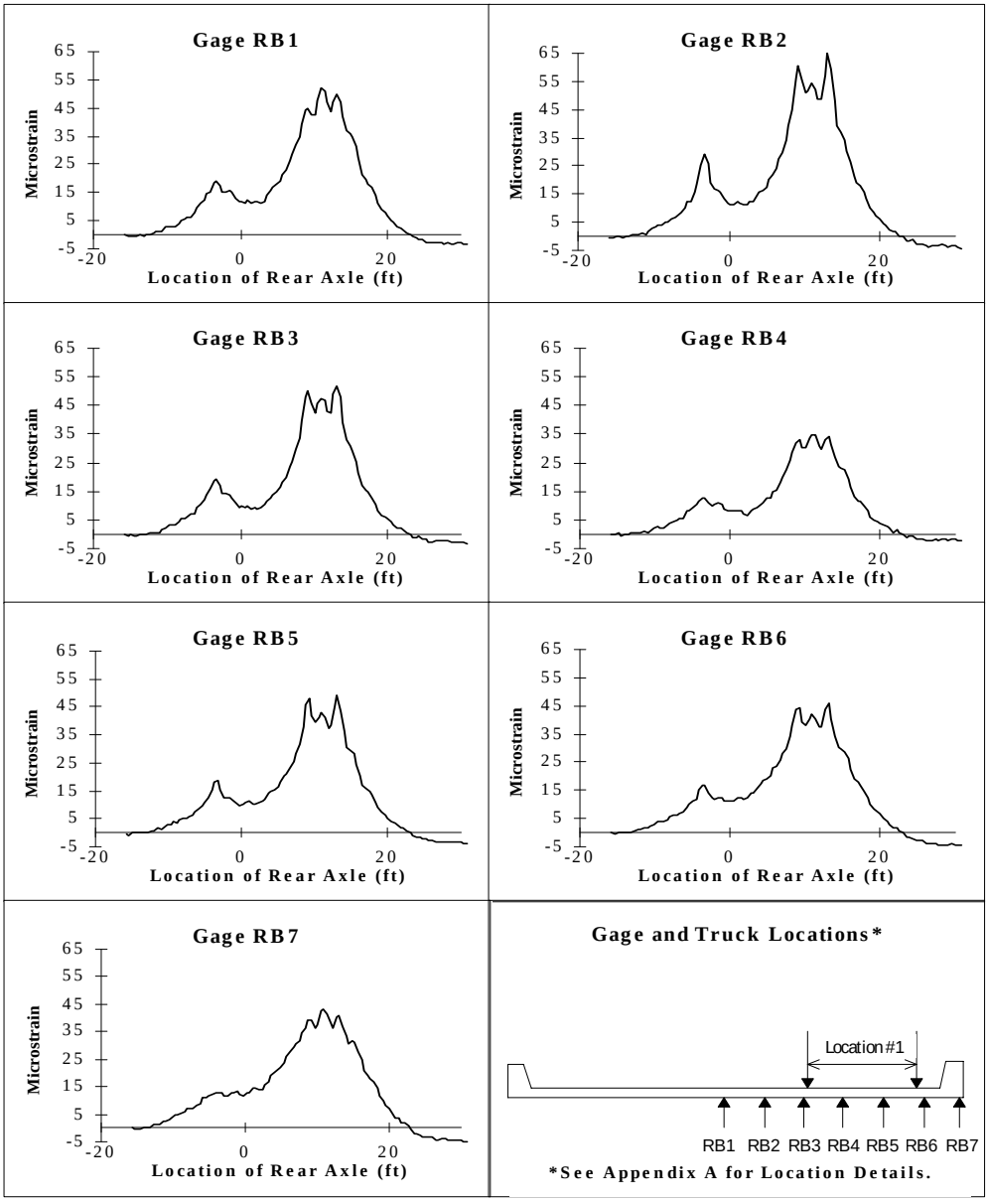

Figure 4.1 Strain Data for Test Series 1, Location 1, Pass 1.

Profiles of maximum strain for the four truck locations are shown in Figure 4.2. Reinforcing bar strains measured at the center line of the bridge exceeded the reinforcing bar strains measured at the curb for all truck locations. Note that gage RB4 seems consistently lower than the adjacent gages and may not be working properly.

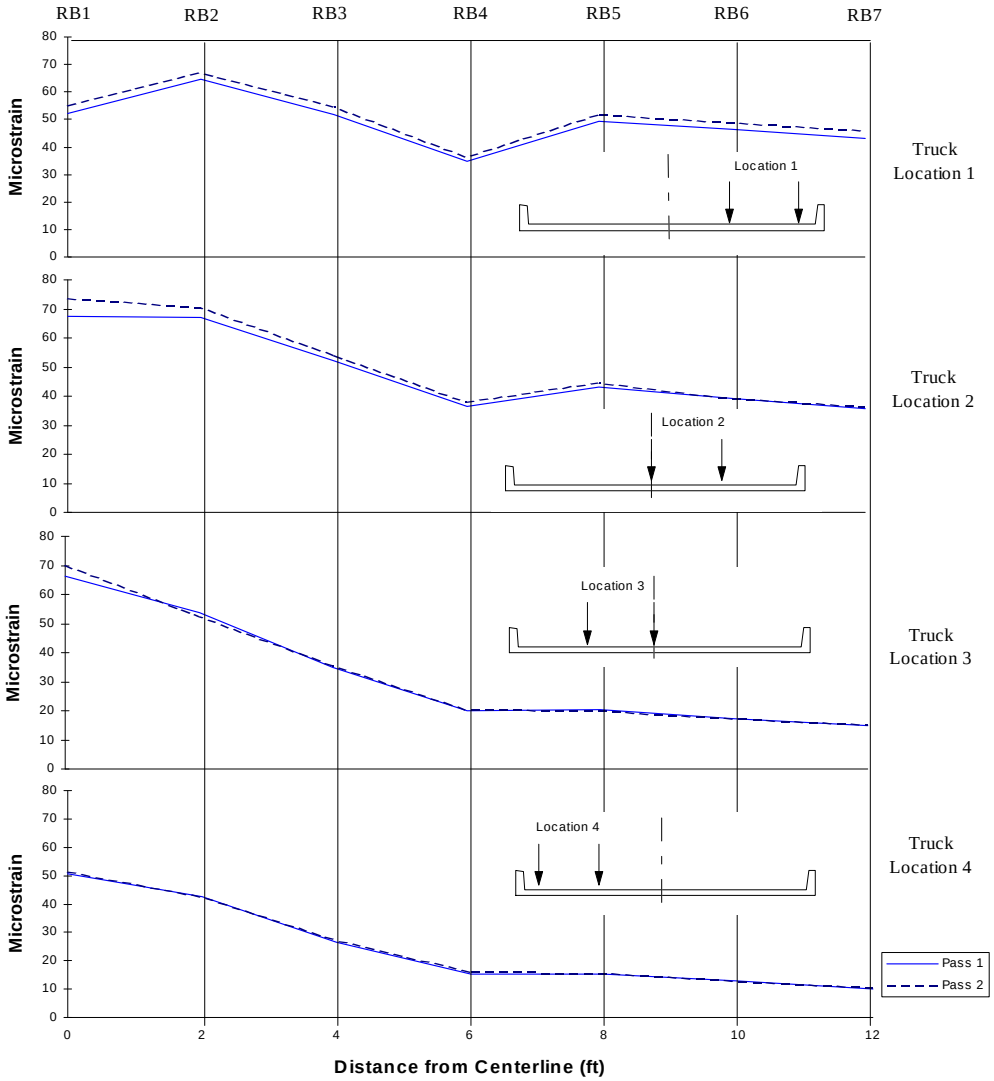

Figure 4.2 Strain Profiles based on Truck Location.

Table 4.1 summarizes the maximum reinforcing bar strain values obtained for each test. These values were used to determine the sensitivity of the strain readings to truck location.

Table 4.1 Maximum Measured Strain Values for Reinforcing Bars, microstrain.

Test Series	Truck Location	Pass	Gage #						
			RB1	RB2	RB3	RB4	RB5	RB6	RB7
1	1	1	52	65	52	35	49	46	43
	1	2	55	67	55	36	52	49	46
	2	1	67	67	52	36	43	39	36
	2	2	74	70	54	38	45	39	36
	3	1	66	54	35	20	20	17	15
	3	2	70	53	36	20	20	17	15
	4	1	51	43	27	15	15	13	10
	4	2	52	42	27	16	16	13	11
2	1	1	52	64	54	35			
	1	2	54	67	57	36			
	2	1	69	65	51	34			
	2	2	74	67	53	37			
3	1	1	50		53		48		
	1	2	53		55		50		
	2	1	75		53		41		
	2	2	73		54		42		
4	1	1					47		43
	1	2					51		43
	2	1					41		33
	2	2					42		35
	3	1					20		15
	3	2					20		14
	4	1					15		11
	4	2					16		12
5	1	1					46		
	1	2					48		
	2	1					42		
	2	2					43		
	3	1					20		
	3	2					20		
	4	1					15		
	4	2					15		

Figure 4.3 shows a plot of strain values comparing pass 1 to pass 2 for each reinforcing bar gage. The data lie within a ±10% range which indicates the strain readings are not very sensitive to exact truck location. The second pass of the truck can be driven within 8 to 12 in. of the transverse location of the first pass. This method of loading appears sufficiently accurate based on Figure 4.3.

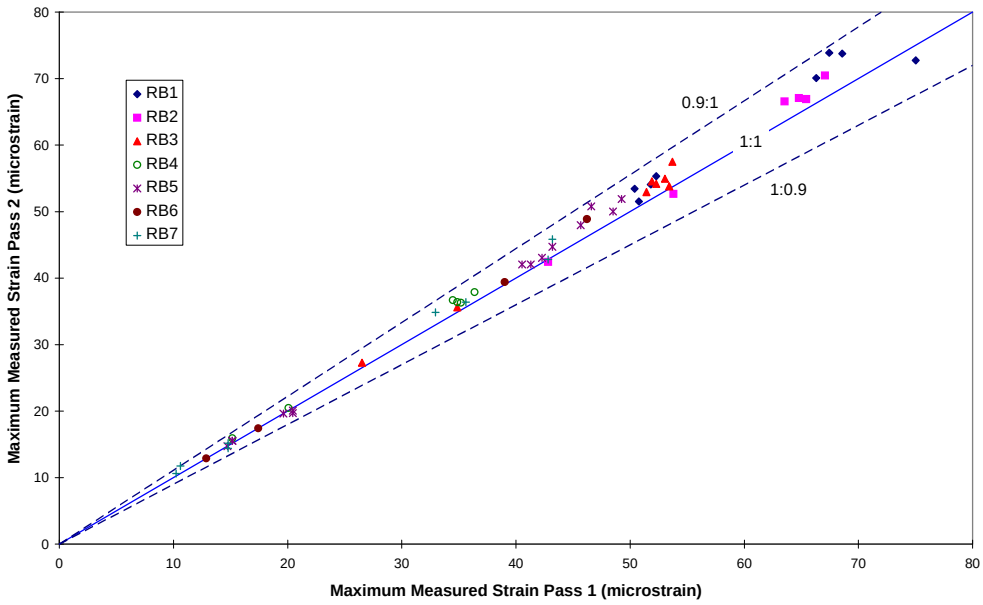

Figure 4.3 Comparison of Maximum Strain values for Pass 1 and Pass 2.

The systematic error in the data acquisition system could be quantified by evaluating the data recorded before the truck reached the bridge, which provided information on fluctuation of strain readings due to noise in the system. Based on this data, the gages have a sensitivity of ±1 microstrain.

The reinforcing bar gages performed well throughout the test. Only gage RB4 appears to be giving unusual results. Further testing after the replacement of gage RB4 would verify its behavior.

4.2 MEASURED STRAIN ON CONCRETE SURFACE USING WIRE GAGES

Concrete strains were measured using wire strain gages at three locations on the bridge cross section: (a) the curb, (b) the top of the slab, and (c) the bottom of the slab.

4.2.1 Curb Strains

A typical sample of the strain data from the curb is shown in Figure 4.4. The gages are measuring compressive strains for the entire loading history. The peak in the response due to the front axle of the truck crossing midspan is not as pronounced in the curb data as the tensile strain data recorded in the slab. Appendix F contains the entire set of data for these gages.

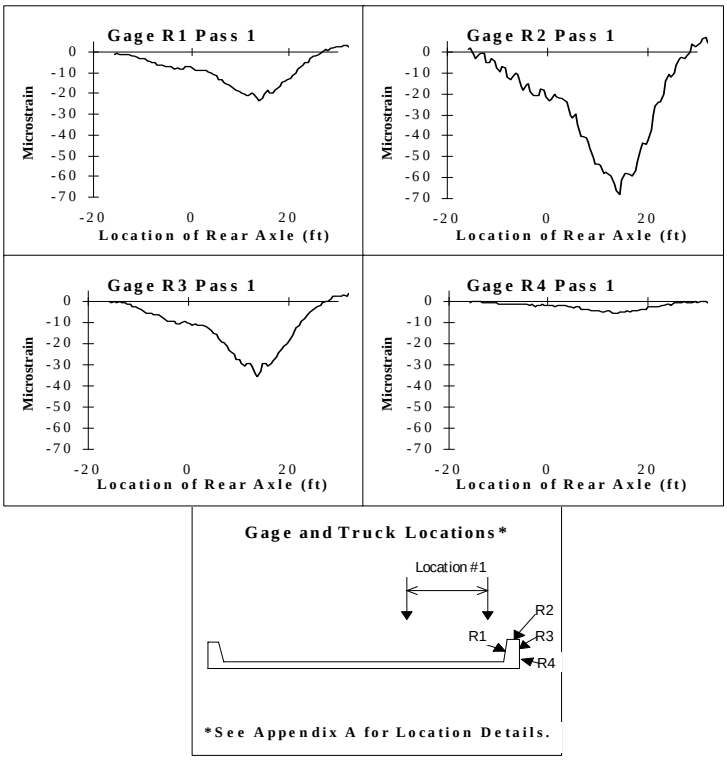

Figure 4.4 Strain Data for Test Series 4, Location 1, Pass 1.

The data from the four strain gages mounted to the surface of the curb and from the reinforcing bar within the curb were also used to plot strain gradients within the curb. Figure 4.5 and Figure 4.6 show the strain gradients based on the four truck locations. Also plotted with the strain gradients are best fit lines based on the data. From observing these plots the gages appear to be performing adequately.

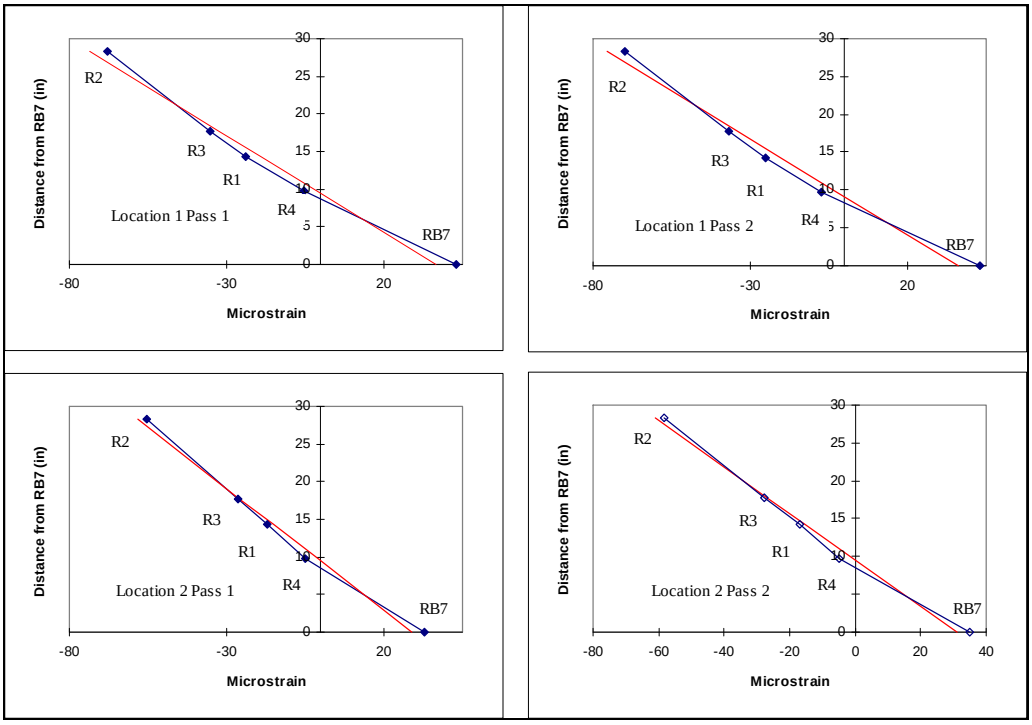

Figure 4.5 Strain Gradient for Curb, Locations 1 and 2.

Based on the linear strain behavior shown in Figures 4.5 and 4.6 only the top gage on the curb is required for future tests.

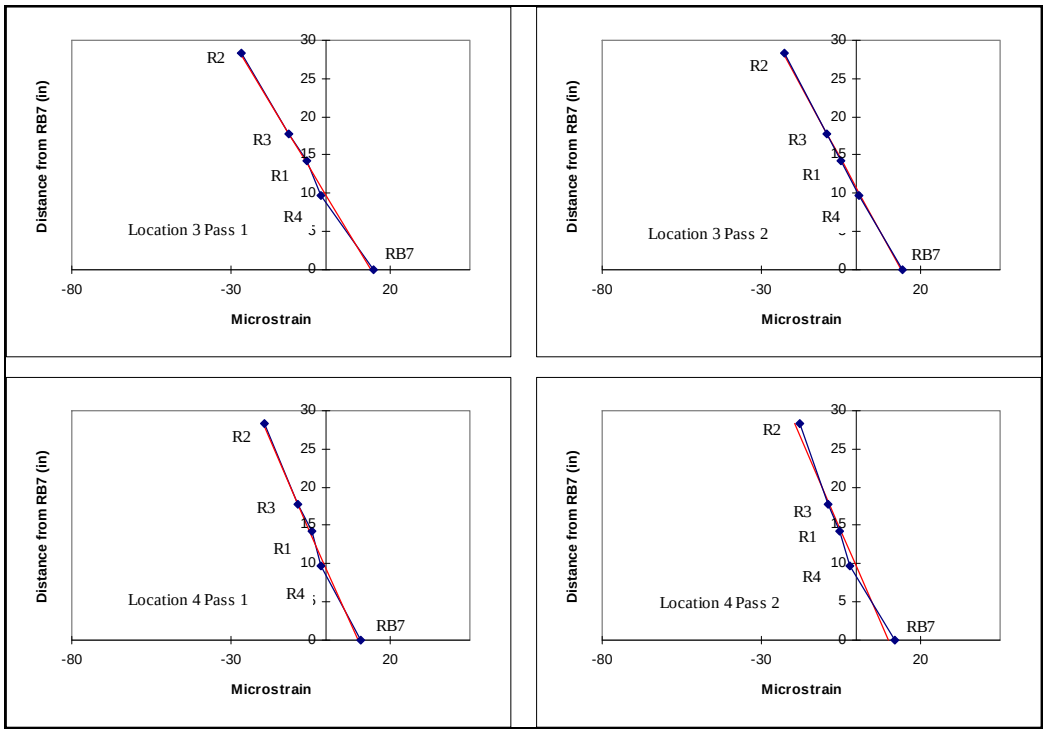

Figure 4.6 Strain Gradient for Curb, Locations 3 and 4.

The maximum strains for the curb gages are shown in Table 4.2. The strain values for R4 are relatively small, indicating that it is located slightly above the neutral axis. Figure 4.7 shows a comparison of maximum strains measured during pass 1 and pass 2. There is considerable scatter in the data for these gages as compared with the reinforcing bar gages, especially at low strain levels. However, for measured strains above 20 microstrain, the peak values recorded during pass 1 and pass 2 tended to be within ±10%. These gages were analyzed for sensitivity based on the data before loading. The wire strain gages mounted on the surface of the concrete curb have a sensitivity of ±2 microstrain.

Table 4.2 Maximum Measured Strain Values for the Curb Gages, microstrain.

Test Series	Truck Location	Pass	Gage #			
			R1	R2	R3	R4
4	1	1	-24	-68	-35	-5
	1	2	-25	-70	-37	-7
	2	1	-17	-55	-27	-5
	2	2	-17	-58	-28	-5
	3	1	-6	-27	-12	-2
	3	2	-5	-23	-10	1
	4	1	-5	-20	-9	-2
	4	2	-5	-18	-9	-2

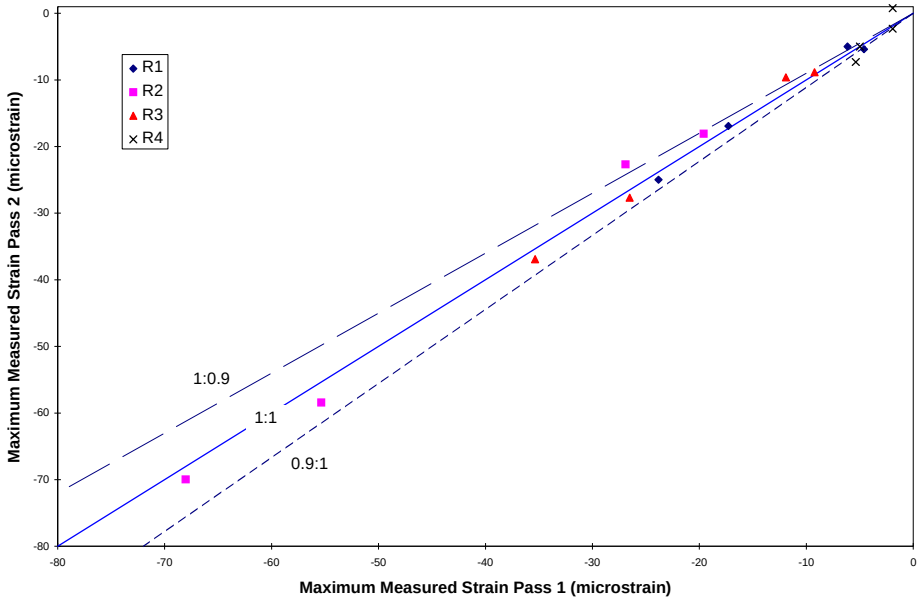

Figure 4.7 Comparison of Maximum Curb Strains for Pass 1 and Pass 2.

4.2.2 Top of Slab Strains

Wire strain gages were applied to the top of the slab in order to determine the behavior of the slab and locate the neutral axis. These gages were not only

the most difficult to install, but were the least reliable of the gages used in this series of tests. Figure 4.8 shows the general behavior of the slab strain during testing. As shown in the figure, the gages appear to have considerable noise and variation.

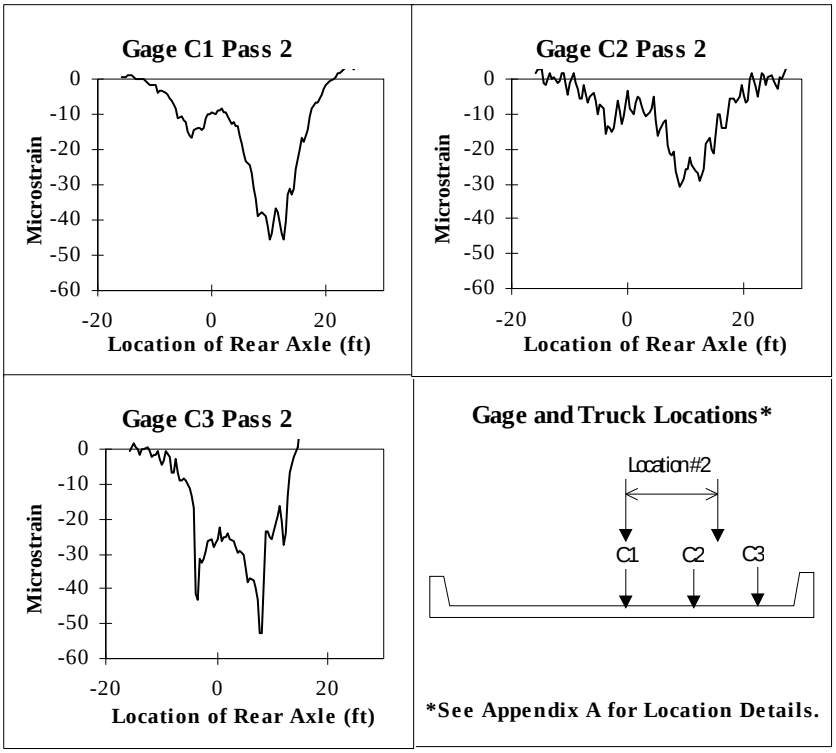

Figure 4.8 Strain Data for Test Series 3, Location 2, Pass 2.

The maximum strain readings for the gages are shown in Table 4.3. Several of the truck passes caused the gages to give unreliable data. The gage readings would jump from 10 microstrain to 200 microstrain as the tire crossed the gage. These readings were not used in Figure 4.9. Appendix D contains plots of all the data from the test.

Table 4.3 Maximum Measured Strain Values for the Top of Slab, microstrain.

Test Series	Truck Location	Pass	Gage #		
			C1	C2	C3
3	1	1	-55	*	-46
	1	2	-48	*	-48
	2	1	-47	-36	-60
	2	2	-46	-31	-53
4	1	1			-40
	1	2			-42
	2	1			*
	2	2			*
	3	1			*
	3	2			*
	4	1			-45
	4	2			-41
5	1	1			-46
	1	2			-39
	2	1			-47
	2	2			-46
	3	1			*
	3	2			*
	4	1			-43
	4	2			-39

* The data were unreliable for these locations and passes.

Figure 4.9 shows the repeatability of the top of slab gages. There is considerable scatter of the data for these gages as was expected. The top of the

slab gages had a sensitivity of ±5 microstrain. This sensitivity is based on analyzing the data before the bridge is loaded.

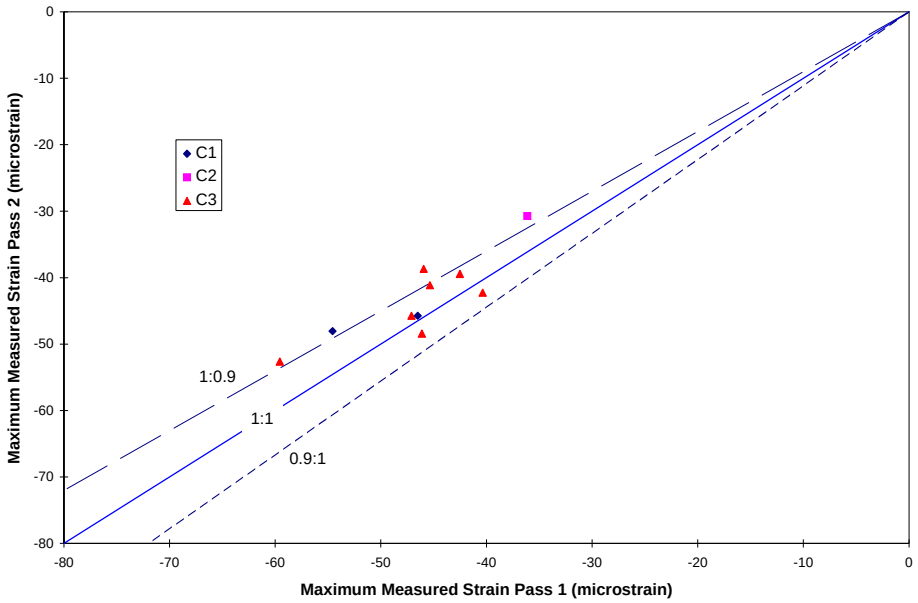

Figure 4.9 Comparison of Maximum Strain Values for the Top of Slab Gages.

The sensitivity and overall performance of these gages was much less than the other wire strain gages. The lack of reliability is likely due to the longer lead wires required to extend across the pavement. In addition to the problem with sensitivity, the gages would malfunction when the truck wheel passed over the gage.

4.2.3 Bottom of Slab Strains

A wire strain gage was placed on the bottom of the slab to determine if measuring concrete surface strain in tension provided an acceptable means of estimating strain in the reinforcing bars. The gage was installed across a crack on

the bottom of the slab. Appendix A contains a description of the exact location. This gage yielded the highest strain values of all the instruments (Figure 4.10).

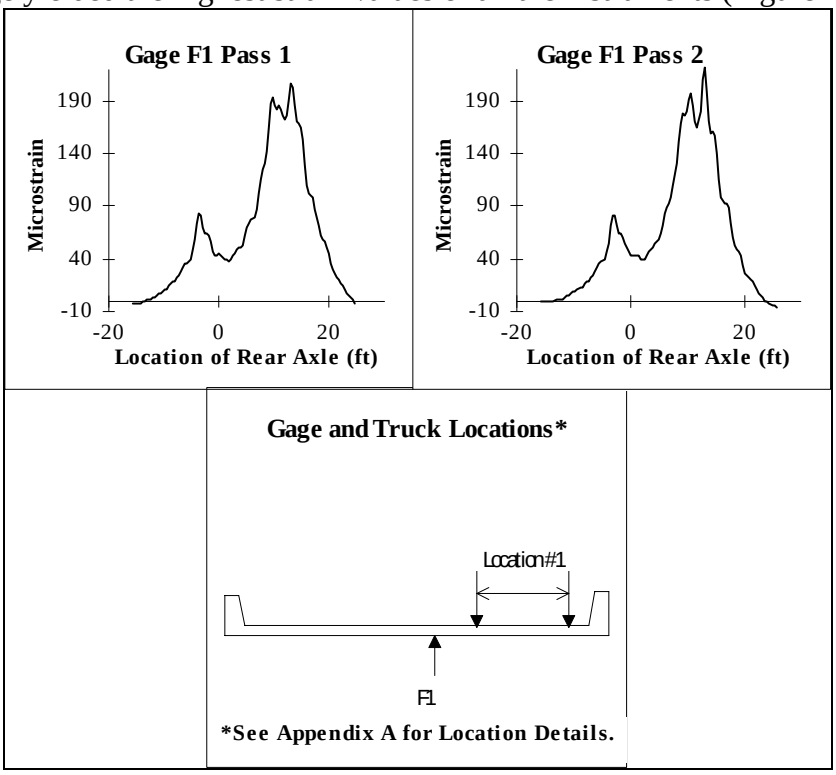

Figure 4.10 Strain Data for Test Series 3, Location 1, Pass 1 and Pass 2.

The general trend of the data is essentially the same as the gages mounted directly on the reinforcing bars. However, the maximum values are considerably higher and the peaks are sharper than the data recorded by the other gages. Appendix E contains all the plotted data for gage F1.

The maximum bottom strains are shown in Table 4.4. Figure 4.11 shows the comparison between passes 1 and 2. As shown in Table 4.4 and Figure 4.11, there were not enough data points to make a good evaluation of the sensitivity of the gages.

Table 4.4 Maximum Measured Strain Values for Bottom of Slab, microstrain.

Test Series	Truck Location	Pass	Gage # F1
3	1	1	208
	1	2	221
	2	1	257
	2	2	258

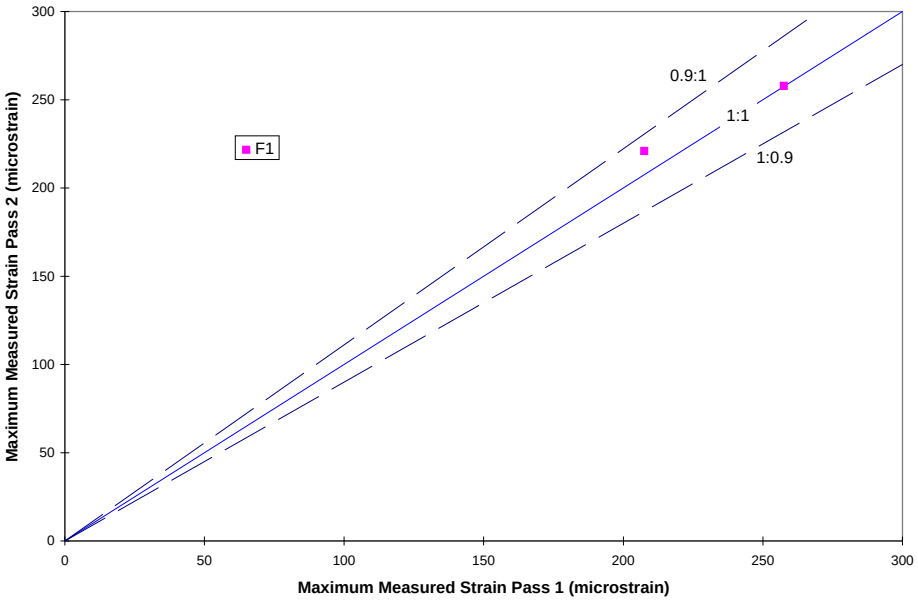

Figure 4.11 Comparison of Maximum Strain Values for the Bottom of Slab Gages.

4. 3 Measured Concrete Surface Strain using Strain Transducers

Mechanical strain transducers were also used to measure strain on the bottom of the slab. These gages are described in more detail in Appendix A.

Figure 4.12 shows the results recorded by the three transducers for truck location 1. The shape of the strain data is similar to the other gage types. The amplitude of the strain recorded by the transducers was higher than those measured by the reinforcing bar gages but not as high as the data from the wire gage mounted on the bottom of the slab.

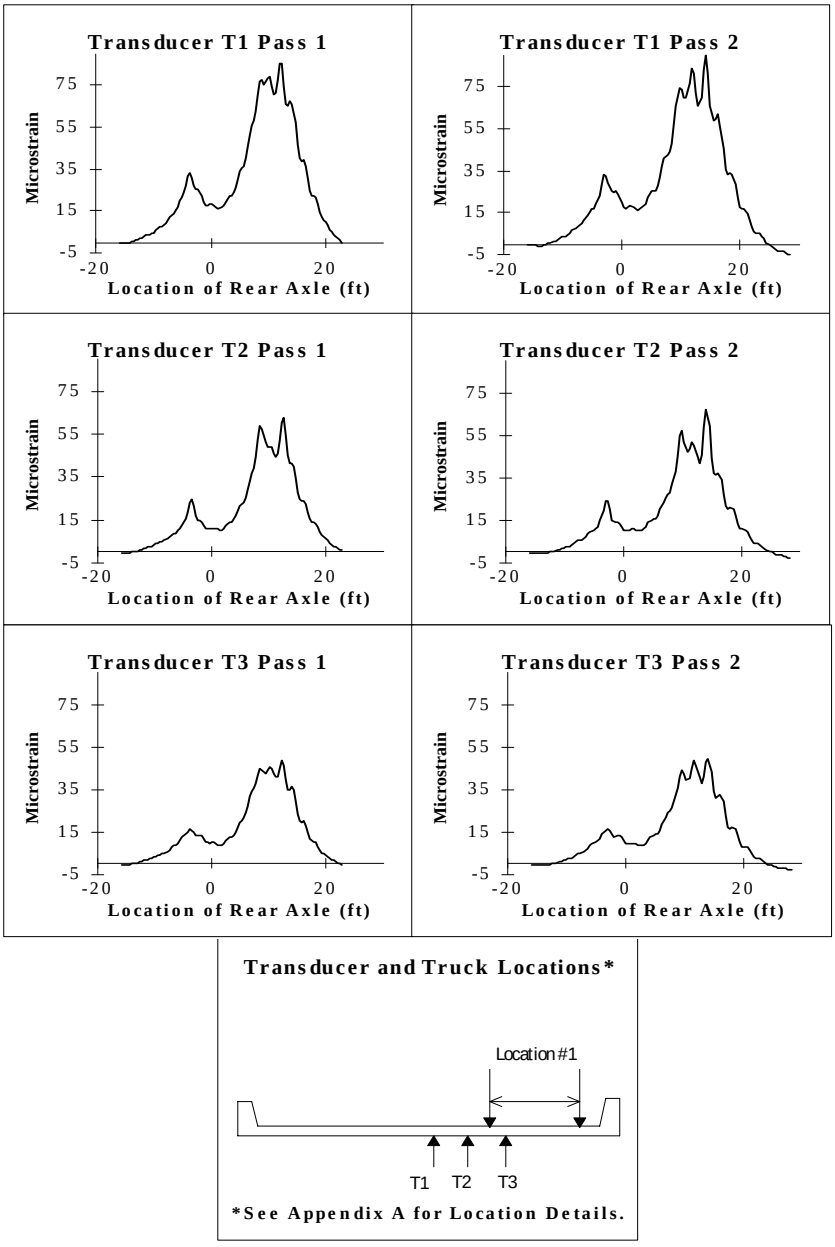

Figure 4.12 Strain Data for Test Series 2, Location 1, Pass 1 and Pass 2.

The maximum strains for each truck location and pass are shown in Table 4.5. The entire set of transducer data collected is shown in Appendix C. The

strains from T1 are larger than T2 and T3 by almost a factor of two. This significant difference is due to the fact that T1 spanned across a crack in the bottom of the slab. This crack is the same that the wire gage F1 crossed. Data from gages T1 and F1 will be discussed in Appendix H.

Table 4.5 Maximum Measured Strain Values for Transducers, microstrain.

Test Series	Truck Location	Pass	Gage #		
			T1	T2	T3
2	1	1	85	63	48
	1	2	90	67	50
	2	1	101	56	48
	2	2	110	58	50

The strain transducers performed similarly to the curb gages. The transducers had a sensitivity of ±2 microstrain. Again this value was determined by analyzing the transducer data before loading. Figure 4.13 shows the maximum strain data comparing pass 1 to pass 2. This comparison gives a measure of repeatability of the transducers.

There were no problems specific to the transducers during the test. The use of transducers for measuring tensile strains in concrete will be discussed further in Appendix H.

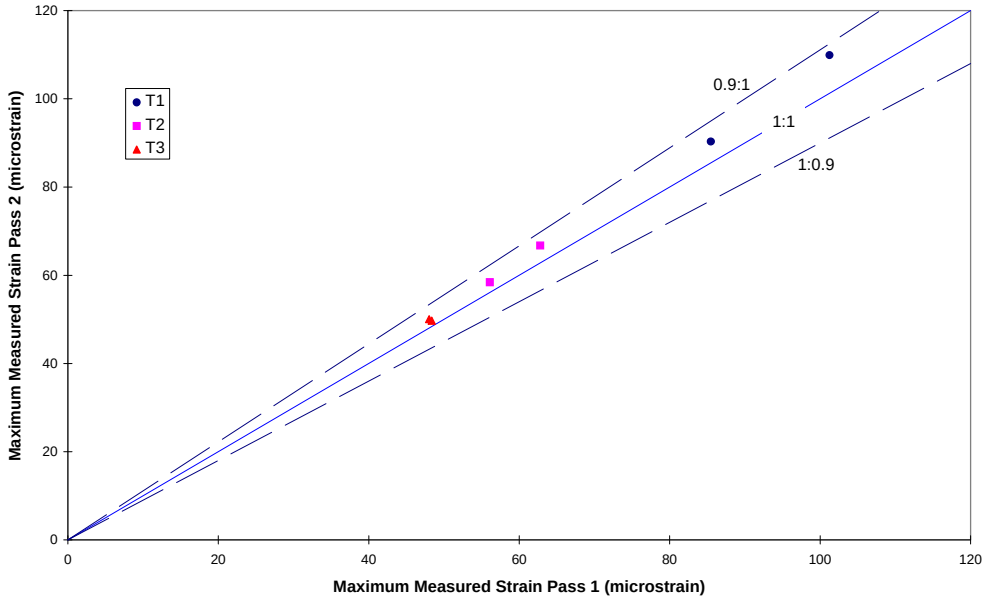

Figure 4.13 Comparison of Maximum Strain Values for Transducers.

4. 4 Measured Deflection of Bridge

Bridge deflections were measured using string potentiometers as described in Chapter 3. The locations and details of the instrumentation are discussed in Appendix A and a complete summary of the test results are presented in Appendix G. A sample of the deflection data is shown in Figure 4.14. Noticeable peaks occur in the deflection data only when the rear axles of the truck cross midspan. As shown in the figure, the greatest deflection occurs at gage SP4 for this particular truck location.

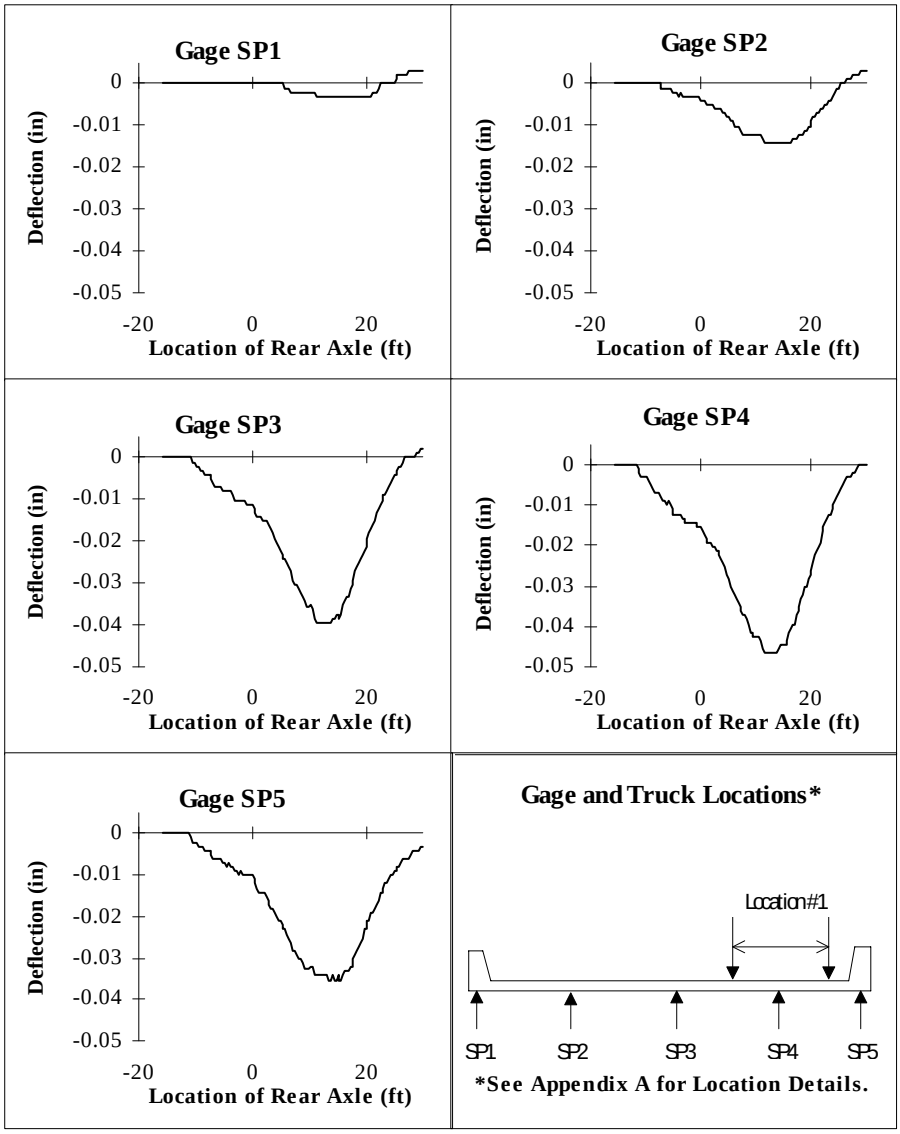

Figure 4.14 Deflection Data for Test Series 5, Location 1, Pass 1.

Figure 4.15 shows a comparison of the deflections across the bridge with each truck location. The behavior of the bridge is as expected, with the curbs deflecting less than the center of the slab. Notice in Figure 4.15 that the slab has significantly more deflection with the truck at location 2 than when the truck is at

location 3. This may be due to instrumentation error or the stiffness may be slightly different. The resolution of the data acquisition system was not small enough and resulted in the steps shown in the data in Figure 4.15.

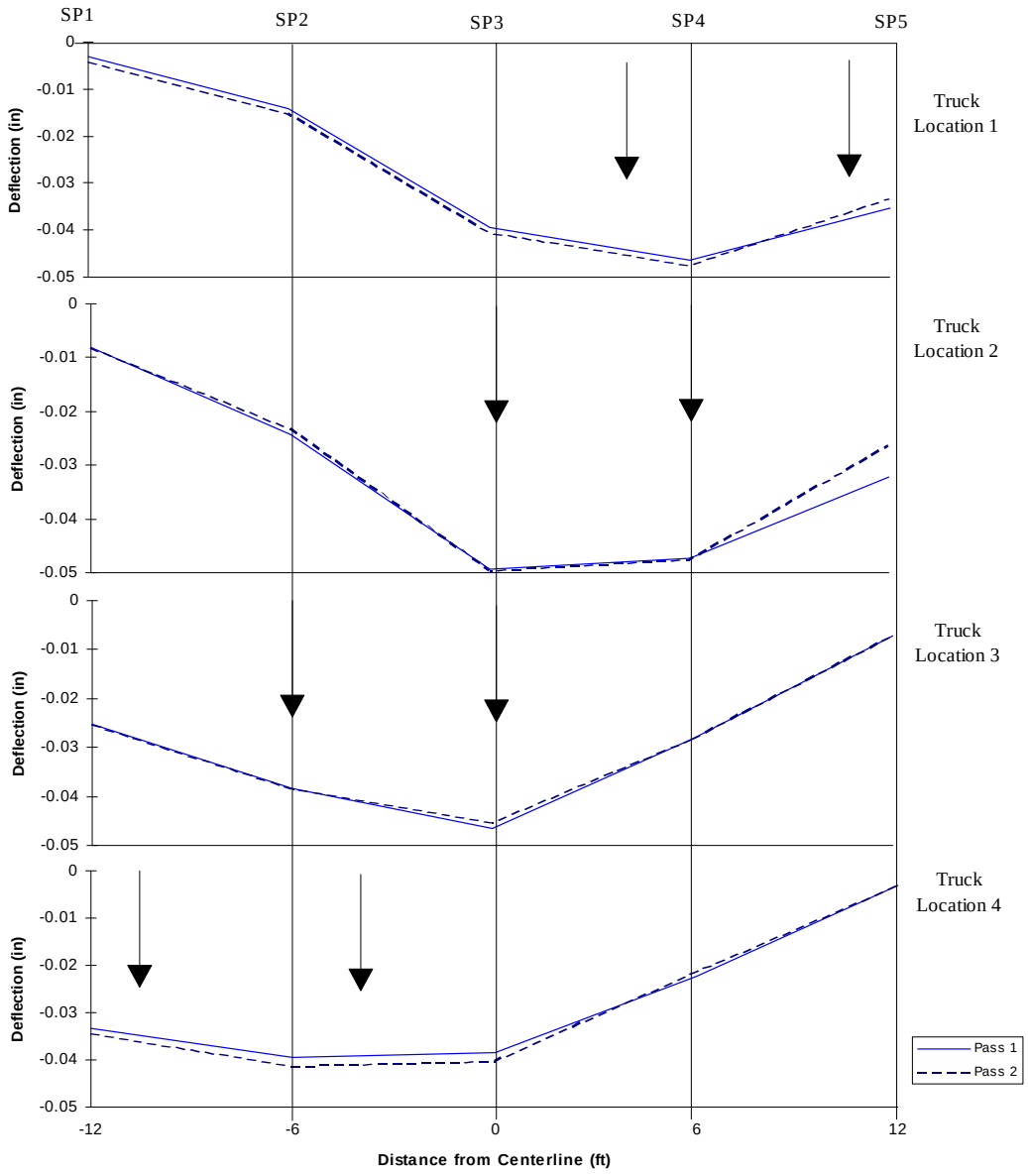

Figure 4.15 Deflection Comparisons based on Truck Location.

The maximum deflection for each truck location and pass is shown in Table 4.6.

Table 4.6 Maximum Measured Deflections, inches.

Test Series	Truck Location	Pass	Gage #				
			SP1	SP2	SP3	SP4	SP5
5	1	1	-0.003	-0.014	-0.039	-0.046	-0.035
	1	2	-0.004	-0.015	-0.040	-0.047	-0.033
	2	1	-0.008	-0.024	-0.049	-0.047	-0.032
	2	2	-0.008	-0.023	-0.049	-0.047	-0.026
	3	1	-0.025	-0.038	-0.046	-0.028	-0.007
	3	2	-0.025	-0.038	-0.045	-0.028	-0.007
	4	1	-0.033	-0.039	-0.038	-0.022	-0.003
	4	2	-0.034	-0.041	-0.040	-0.021	-0.003

Although there is concern about the accuracy of the deflection data, a check of the repeatability of the string potentiometers was done. Figure 4.16 shows the results of the comparison of pass 1 and pass 2 to check repeatability. There is some scatter of the data but not to the extent expected.

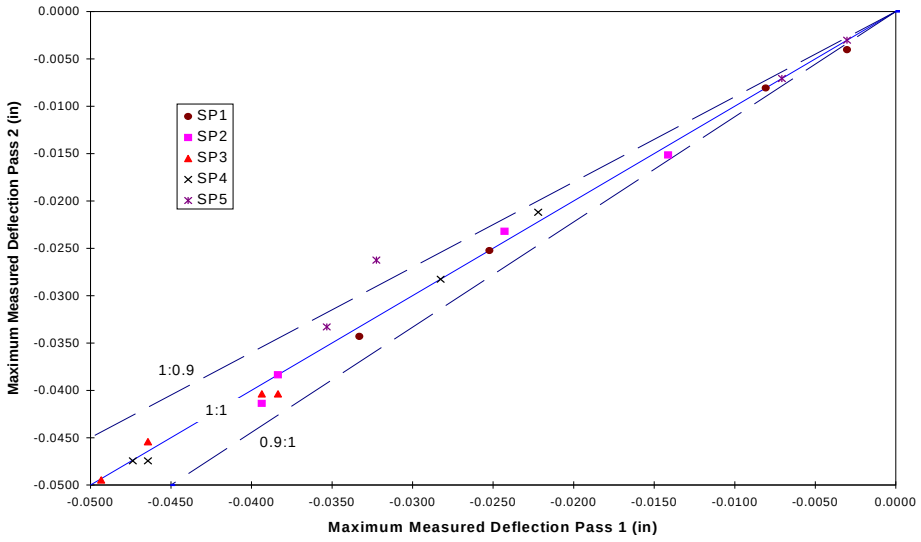

Figure 4.16 Comparison of Maximum Deflections for Pass 1 and Pass 2.

4.5 Summary

The strain gages provided reasonable, repeatable data with the exception of the concrete strain gages on the top of the slab. These gages had considerable noise and were adversely affected by the truck tires crossing the gage. The reinforcing bar gage RB4 provided consistently lower data than the two adjacent gages.

The curbs exhibited less strain and less deflection than the adjacent slab. The four gages attached to the curb provided data that verified a linear strain gradient along the height of the curb.

The bridge deflections require monitoring with a higher resolution. The data acquisition system should be adjusted in order to measure the necessary resolution.

Chapter 5. EVALUATION OF RESULTS

5.1 COMPARISON OF TEST RESULTS WITH ANALYSIS

5.1.1 Test Moments

The test truck shown in Chapter 3 is a three axle vehicle with a rear tandem axle. The design truck and the truck simulated in both the TxDOT Report [10] and the Illinois Bulletin 346 [5] were two axle trucks. Shown in Figure 5.1 is a comparison of the moment envelopes for the actual test truck and the ideal two axle truck with the same axle weights. There is approximately 20% difference in the maximum moment between the two truck configurations.

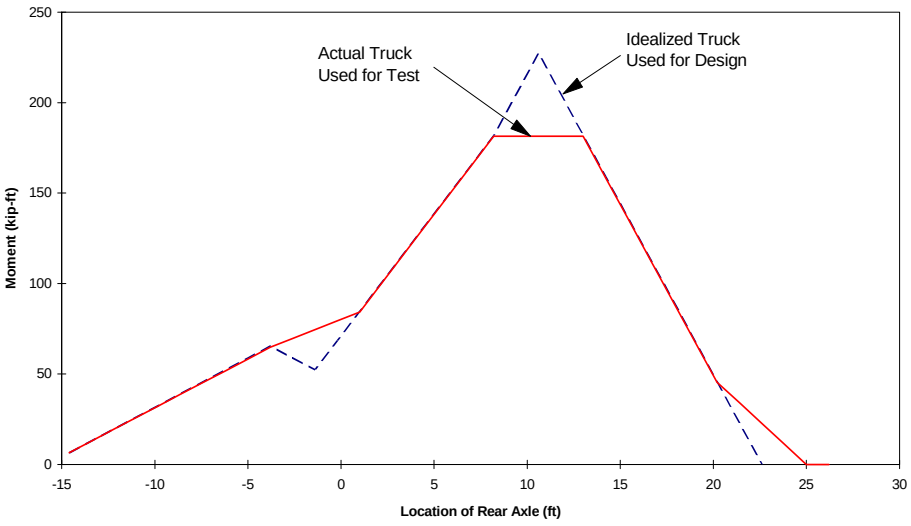

Figure 5.1 Moment Envelopes for Test Truck and Design Truck.

The methods shown in Chapter 2 to calculate moments distributed to the curb and to the slab are based on loading the bridge with two vehicles [5]. The formulas use given wheel weights to calculate moments based on two single axle trucks. The critical location for moment is when the rear axle is at midspan. A method had to be determined to reduce the moments based on the test truck.

The moments given by the equations [5] for live load moment in Chapter 2 are live load moment for a unit width of slab and live load moment for one curb. The total moment was calculated by summing the moments based on a slab width of 15.25 feet and two curbs. The formula for slab width is shown below.

$$Slab\,Width = Total\,Width - 2 \cdot (Curb\,Width + 4 \cdot (Slab\,Depth))$$

The percentage of moment to the slab and to the curb were then calculated by dividing the resulting moment from the live load moment equations [5] using the given axle weight by the total moment. The percentages of total moments are as follows:

M_{slab} = 2.4% per unit width of slab.

M_{curb} = 31.4% per curb.

These percentages were then applied to the moment envelope for the test truck shown in Figure 5.1 to give comparison moments for analysis. Strains were then calculated based on the moments and these were compared to the test results.

There was concern that there would be error in the distributed moments because the live load moment equations [5] are based on two trucks and there was only one test truck, therefore a second method of calculating distributed moments was used based on Illinois Bulletin 315 [18]. In Illinois Bulletin 315 [18] charts were developed in order to use wheel location, length to width ratios and relative

stiffness of the curb compared to the slab to determine a moment at midspan for a specific truck. The tandem axle loads were divided into two equivalent wheel loads and were used to calculate a moment based on the charts. The moment was then reduced 20% to account for the tandem axle. This moment was compared to the moment arrived at by the previous method. The comparison resulted in a 0.5% difference. Based on this small difference it was felt that the method used to distribute the moments was acceptable.

The moments used to determine the strain values were reduced based on a fixed end support because of the likelihood of bearing restraint. The use of fixed ends reduced the calculated moment by 44%. Although there may be some error in distribution by assuming fixed end supports this assumption will give a conservative value of strain for comparison.

5.1.2 Slab Evaluation

Although the slab and curb are integral each component was designed separately based on the methods outlined by the Illinois Bulletin 346 [5]. The slab was therefore analyzed separately based on a unit width and compared to the test results. The recommended portion of the bridge to be considered the slab is a width of 15.25 feet centered about the center line of the bridge. This value was arrived at based on the formula for slab width [5] shown above

Figure 5.2 shows a typical strain response based on the test truck. In addition to the test results, predicted strain values are plotted based on both cracked and uncracked section analysis. The test results are bounded by the calculated values.

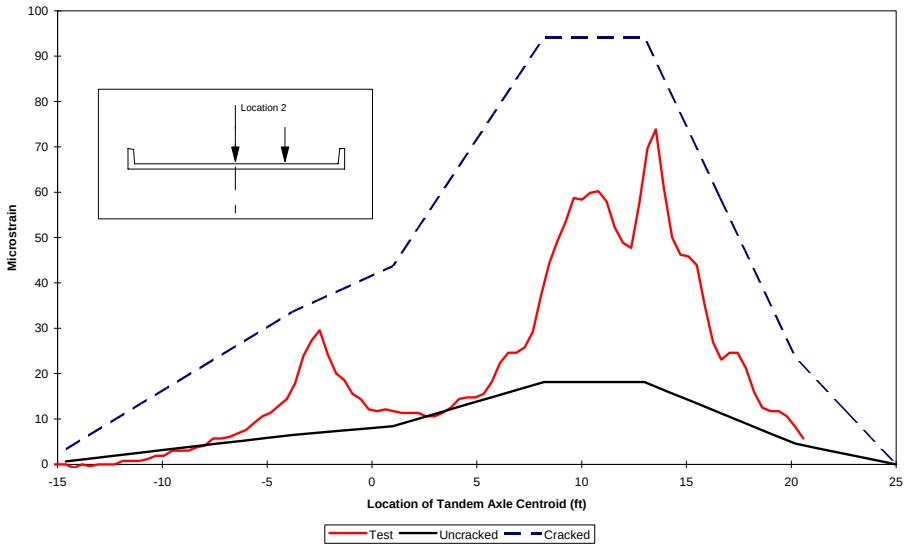

Figure 5.3 Comparison of Test Results to Analysis for RB1, Location 2.

The test results plotted in Figure 5.3 were the highest strain values observed in the slab portion. The peak strain value for RB1 was 74 microstrain compared with a maximum cracked strain of 94 microstrain and a maximum uncracked strain of 18 microstrain. From observing the test data the section appears to approach the behavior of a cracked section. This behavior will be discussed more later. As shown in the results in Appendix B, the strain values are less as the slab approaches the curb.

In addition to the reinforcing bar strains, the top of the slab was used to measure strains. As shown in Chapter 3, gages C1, C2 and C3 were used for this purpose. Figure 5.3 shows the plotted strain results with the strain values calculated based on the cracked and uncracked section. The peak strain value for C3 was -46 microstrain compared with a maximum cracked strain of -42 and a

maximum uncracked strain of -26. Although the test strain peaks exceed the cracked section values in several places, there is some doubt in the accuracy of the gages. As discussed in Chapter 3 and observing the results shown in Appendix D the gages on the top of the slab were inconsistent and unstable due to several factors. These factors were discussed in detail in Chapter 4. Based on these findings the C series gages were not used for calculating the final adjusted rating.

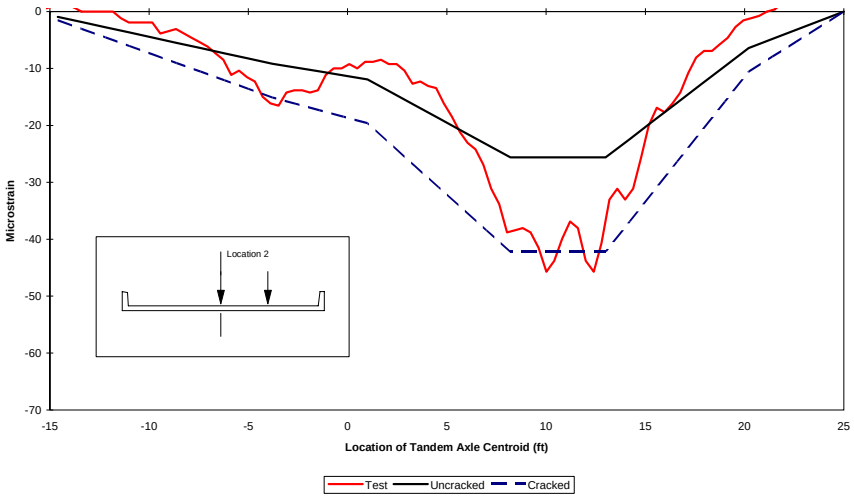

Figure 5.3 Comparison of Test Results with Analysis for C3, Location 1.

Although there was concern with the accuracy of the C series gages, the neutral axis was computed based on the values of paired RB gages and C gages. Gages RB1 and C1 and RB3 and C2 were used for calculating the neutral axis. Only the results from truck location 2 were used because of the erratic results with the truck in location 1. The results of this calculation are shown in Figure 5.4. Also shown on the graph are the centroid of the cracked section and the

centroid of the uncracked section. These two centroids bound the centroid based on the test results which leads to the assumption that the section may be behaving as a partially cracked section. As discussed earlier in observing the strain values of RB1, Figure 5.4 shows the section is likely behaving more like a cracked section because of the average centroid location.

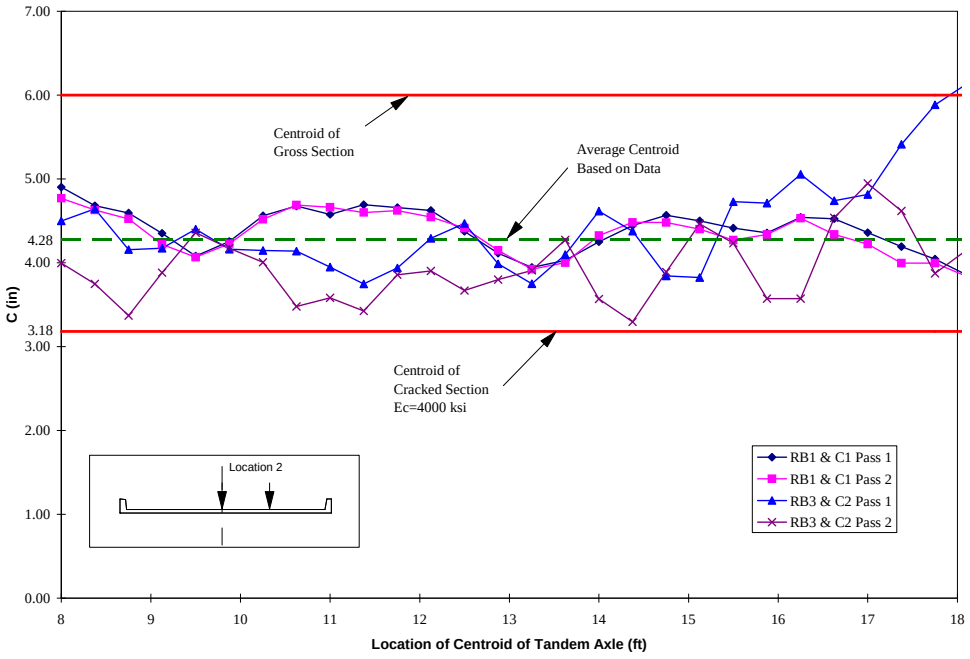

Figure 5.4 Centroid Locations for Slab.

Based on the questionable integrity of the top of the slab gages, the reinforcing steel gages were used exclusively for the slab load rating adjustment.

Because of the difficulty in predicting the nonlinear behavior of concrete, it was thought that the top of the slab gages would be required to gain insight on the true behavior of the slab section. But after evaluating the data, the gages were only used to determine that the centroid was indeed bounded by the centroids of

the cracked and uncracked sections. Based on the results of this test, the top of the slab gages were found to be unnecessary in most cases for future testing. By assuming a cracked section, a conservative estimate of the capacity of the slab can be determined. A careful examination of the underside of the slab may reveal extensive cracking caused by overloads. If there is some doubt in the load history of the bridge then top of the slab gages may be justified to verify the location of the neutral axis.

5.1.3 CURB EVALUATION

As discussed previously the moments distributed to the curb were 31.4% of the total moment. The curb was instrumented as shown in Appendix A. Gages R1 through R4 and RB7 were used to evaluate the curb.

Figure 5.5 shows the test strains compared with the cracked and uncracked strain values. The test value of 46 was the maximum strain value obtained during the test for this gage. This is compared with a maximum calculated strain values of 86 microstrain for the cracked section and 19 microstrain for the uncracked section.

As shown in Figure 5.5 the test strains are bounded by the calculated values but well below the expected cracked section strains. The section is likely only partially cracked resulting in the behavior shown. As discussed previously in Chapter 3, visible cracks were mapped out on the bottom of the slab. No cracks were visible approaching the curb as shown in Figure ??.

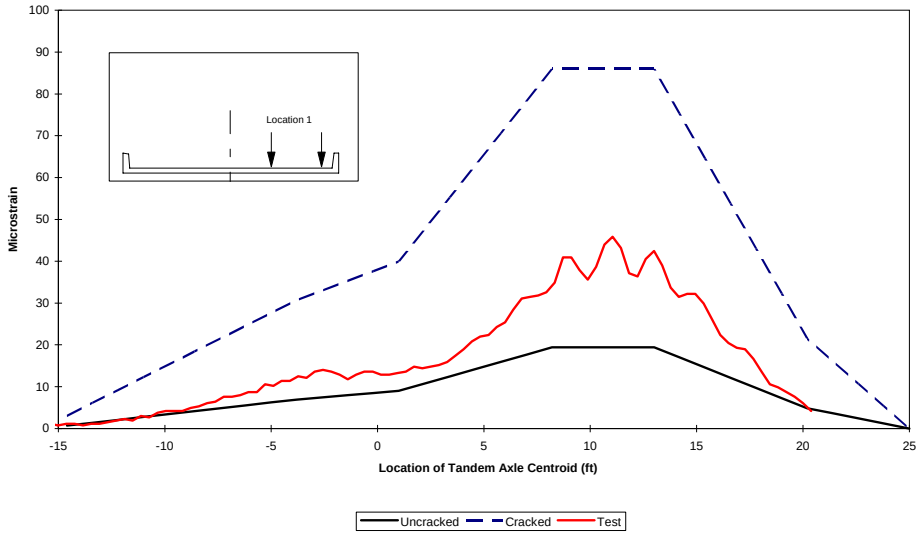

Figure 5.5 Comparison of Test Results and Analysis for RB7, Location 1.

As shown in Figure 5.5 the test strains are bounded by the calculated values but well below the expected cracked section strains. The section is likely only partially cracked resulting in the behavior shown. During the instrumentation, visible cracks were mapped out on the bottom of the slab. No visible cracks were approaching the curb as shown in Figure ??.

The top of the curb was instrumented in order to determine the neutral axis. This data was also plotted to compare the test results with the calculated strains. Figure 5.6 shows the results of this plot. The maximum measured value of strain for R2 was -70 microstrain. This value is compared with a calculated strain values of -65 microstrain for the cracked section and -57 microstrain for the uncracked section. This plot is similar to the top of the slab gage plot in that the gage performance is erratic. The peak values exceed the calculated cracked

section strains in several places. Because of the erratic behavior the data for the top of the curb gages was used only to determine the neutral axis.

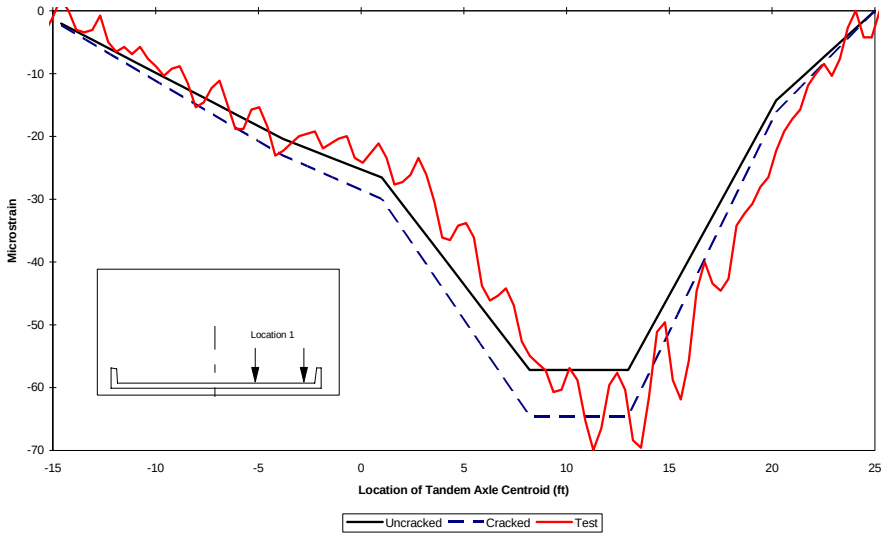

Figure 5.6 Comparison of Test Results and Analysis for R2, Location 1.

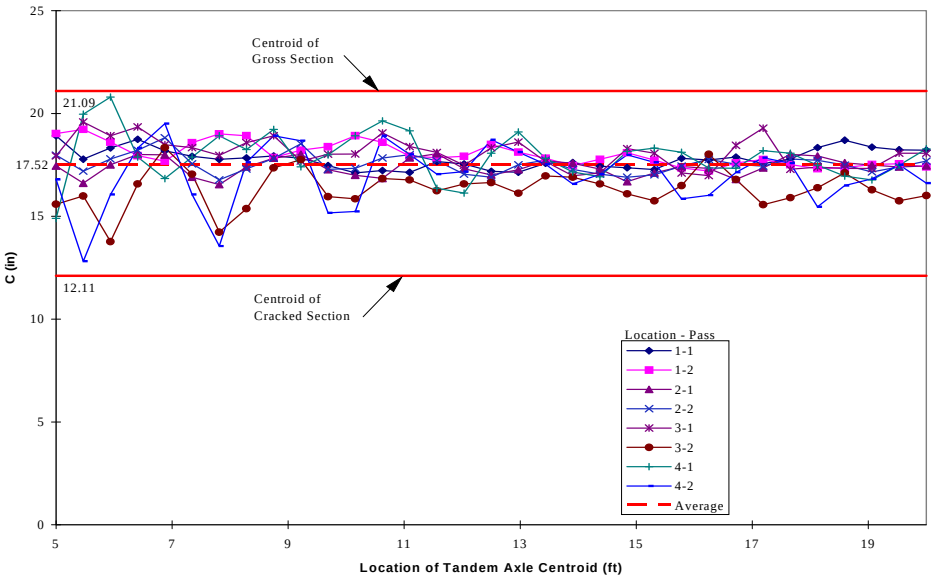

Figure 5.7 Centroid Locations for Curb.

Although the gages on the concrete were not as stable as the reinforcing steel gages, they worked well in predicting the neutral axis. Figure 5.7 shows the neutral axis based on the average values of the neutral axis from gages RB7 and R2.. In contrast to the slab centroid, the curb centroid leads to the assumption that the curb is behaving more as an uncracked section.

The data was also used to plot strain gradients of the curb. Figure 5.8 and Figure 5.9 show the strain gradients based on the four truck locations. Also plotted with the strain gradients are best fit lines based on the data. From observing these plots the gages appear to be performing adequately.

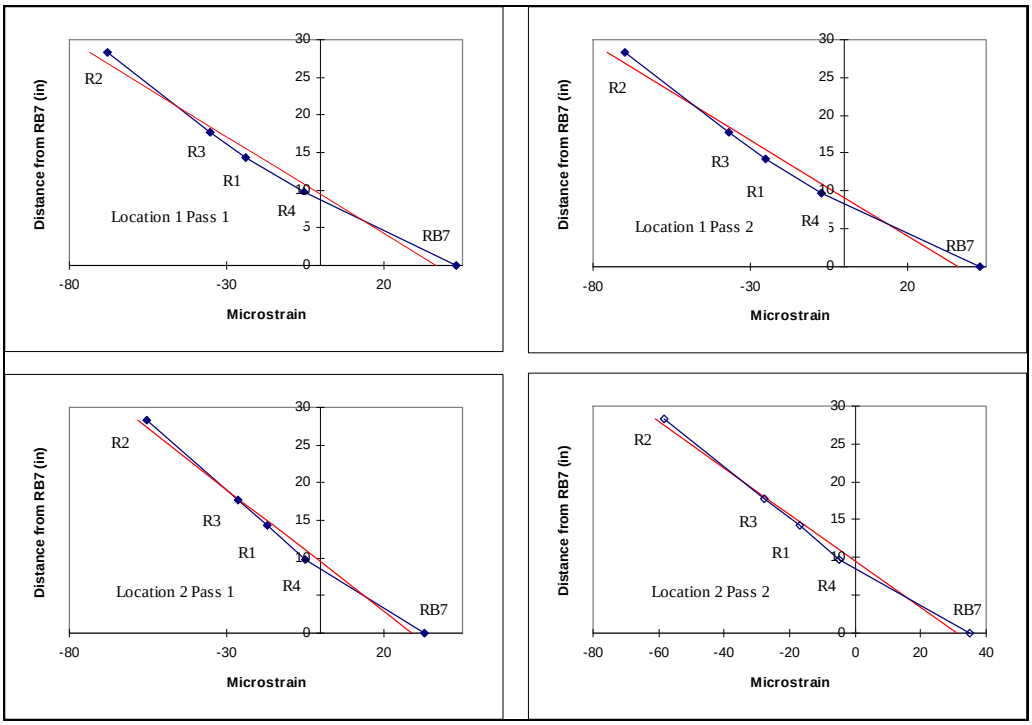

Figure 5.8 Strain Gradient for Curb, Locations 1 and 2.

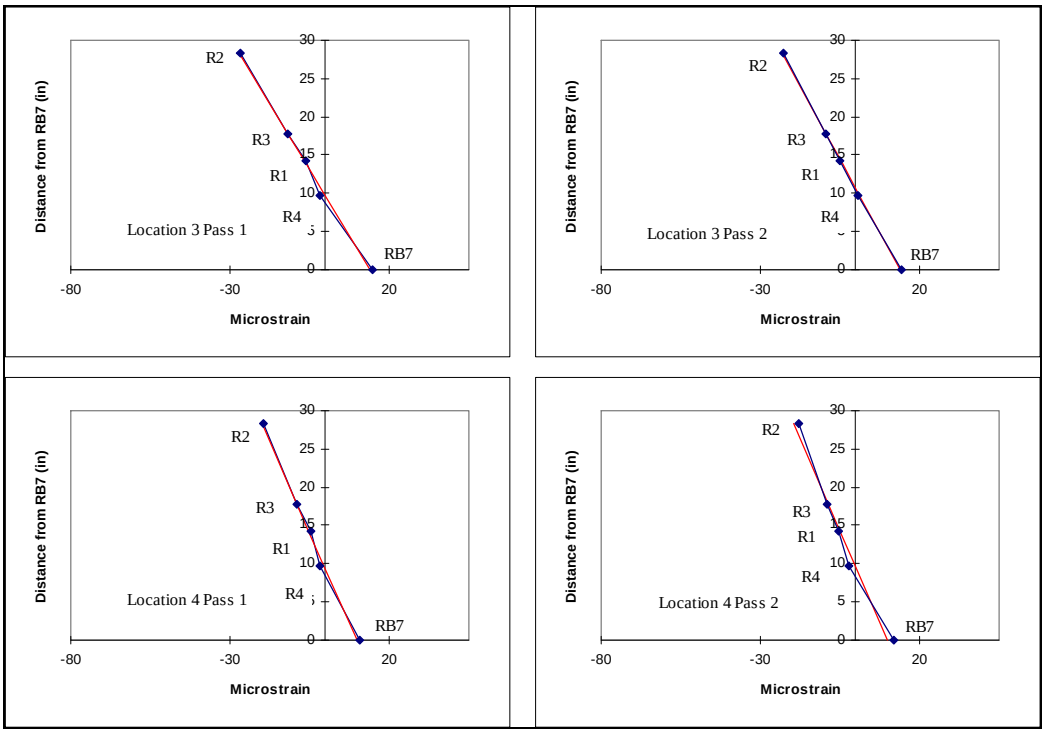

Figure 5.9 Strain Gradient for Curb, Locations 3 and 4.

Based on the linear strain behavior shown in Figures 5.8 and 5.9 only the top gage on the curb is required for future tests. As discussed previously in the slab evaluation section the gages on the concrete will not be used for rating purposes. But unlike the top of the slab gages, it is recommended that a gage be placed on the top of the curb for each test. This gage will verify the curb is behaving as expected. The reasoning behind using this gage as opposed to the top of the slab gages is that the curb is more accessible than the slab gages. To apply a gage to the top of the slab there are a number of factors that must be considered. Working in traffic is required which is both slow and dangerous, and the surface treatment must be removed from the top of the slab which is time consuming.

The gages must then be protected from traffic which is difficult if the test requires more than one day. The gages also require long leads which cause noise in the system.

The gage on the curb is easy to install and although not as precise as the reinforcing steel gages it will give insight to the curb behavior.

5.1.4 Deflection Evaluation

As discussed in Appendix A the validity of the deflection measurements is questionable. The string potentiometers were not sensitive enough to accurately measure the very small deflections occurring in the bridge. The data in Appendix G shows the discrete steps as the deflection changes indicating some question in the accuracy of the data.

Although there is doubt in the accuracy of the data, a comparison of the test results and calculated values was made. Figures 5.10 and 5.11 show the deflections for a truck at location 1 and location 2. In addition to the test data calculated deflections were plotted also. These deflections were based on both simple supports and fixed end supports. Based on the data from the plots the bridge is behaving somewhere between simple and fixed supports which is what was expected. The assumption discussed earlier of using fixed end supports is justified. The use of fixed supports will give conservative results for adjusting the load rating.

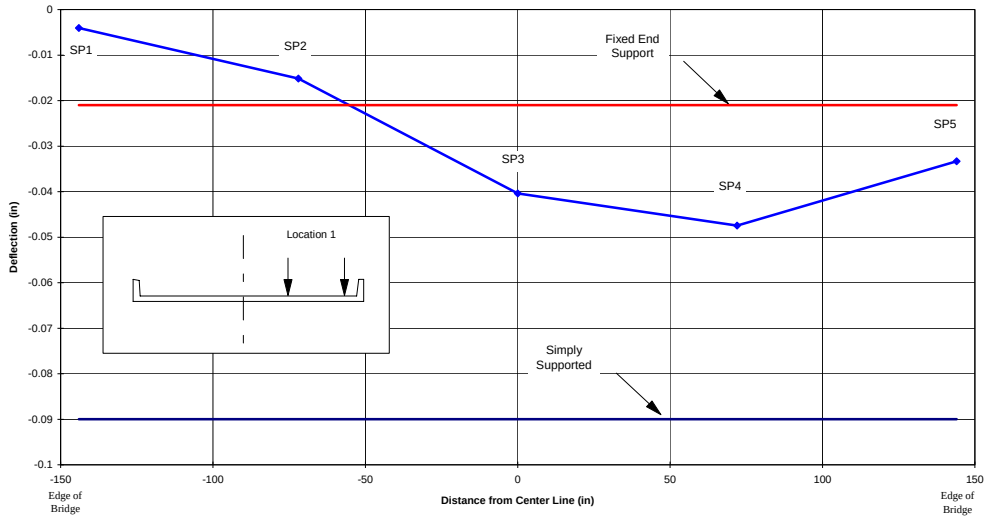

Figure 5.10 Comparison of Deflection Results with Analysis, Location 1.

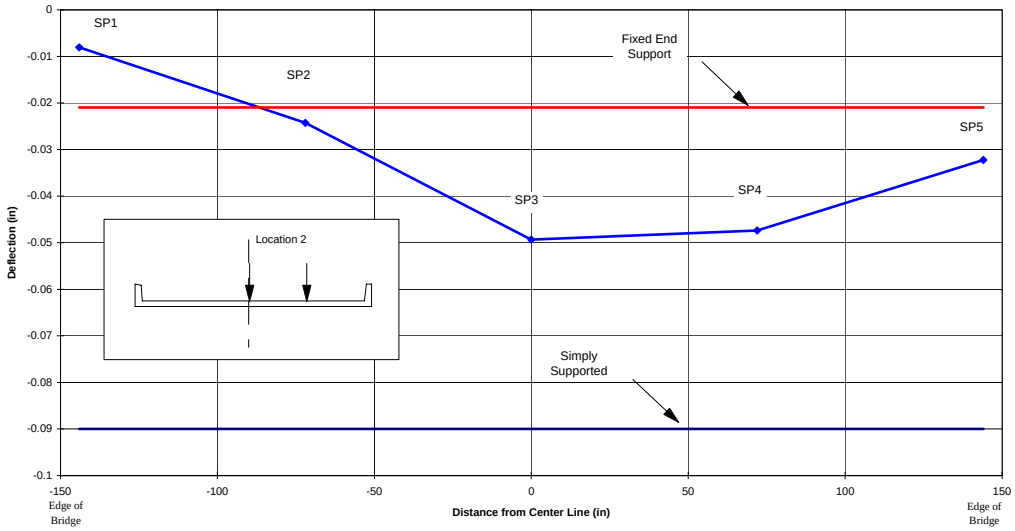

Figure 5.11 Comparison of Deflection Results with Analysis, Location 1.

5.1.5 Stress Comparison

Figure 5.12 shows the stress distribution across the bridge due to the truck in location 1 and in location 2. The stress distribution is higher at center line where the gages are located in partially cracked sections. Gage RB4 consistently gave readings less than expected therefore the data from this gage is questionable.

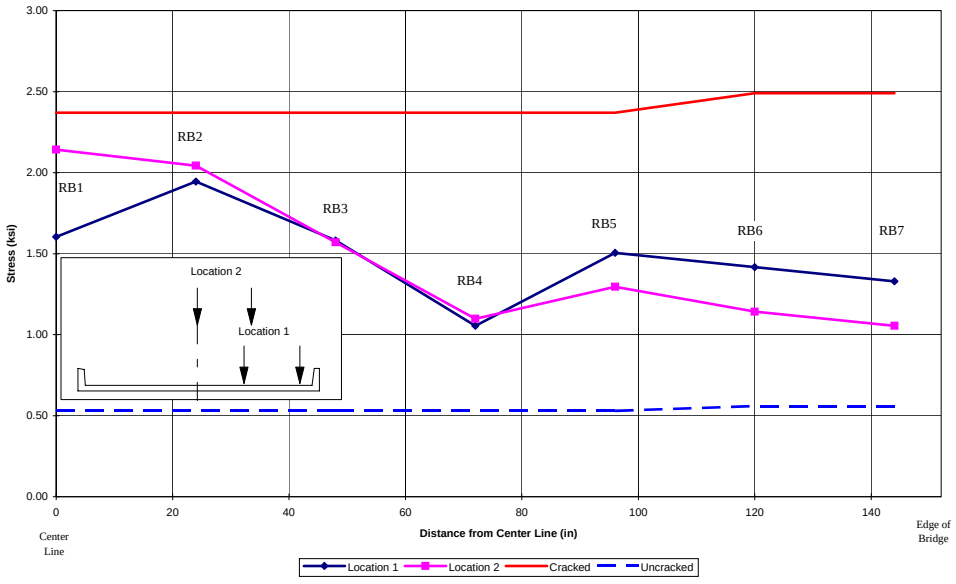

Figure 5.12 Stress Distribution in Reinforcing Steel.

The stress levels reached in the reinforcing bars are low compared to the design working stress. This bridge was designed using a working stress of 22 ksi as compared to the test stress level of approximately 2 ksi. These low levels of stress may justify a heavier test truck or possibly the use of two trucks during testing.

5.2 COMPARISON OF RESULTS WITH TXDOT TEST RESULTS

5.2.1 Strain Distribution Comparison

Strain distribution across one half of the bridge was compared with data from the slab test by TxDOT [10]. As shown in Figures 5.13 and 5.14 the TxDOT results were considerably higher than the test results.

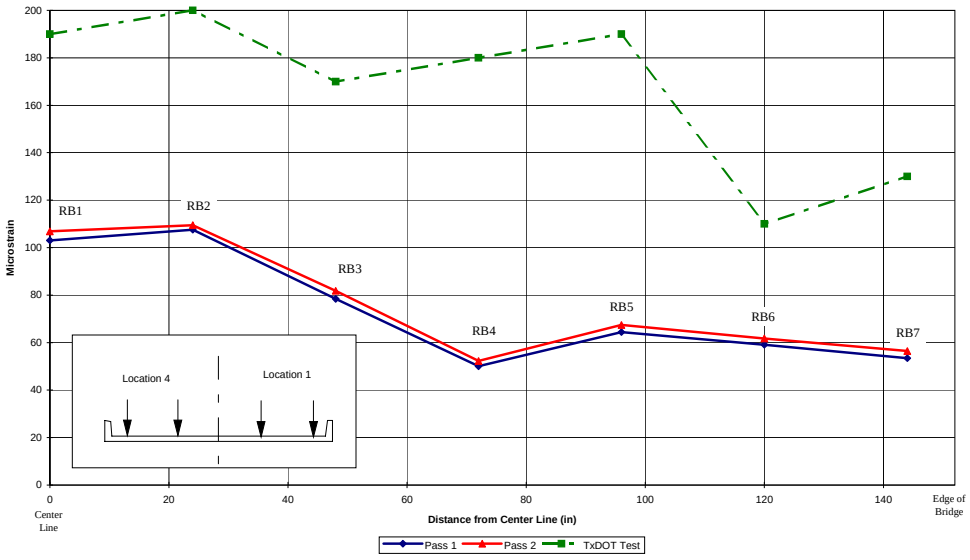

Figure 5.13 Comparison of Test Results and TxDOT Test, Locations 1 and 4.

For the comparison in Figure 5.13 the average difference in strain is 92 microstrain. For the comparison in Figure 5.14 the average difference in strain is 76 microstrain.

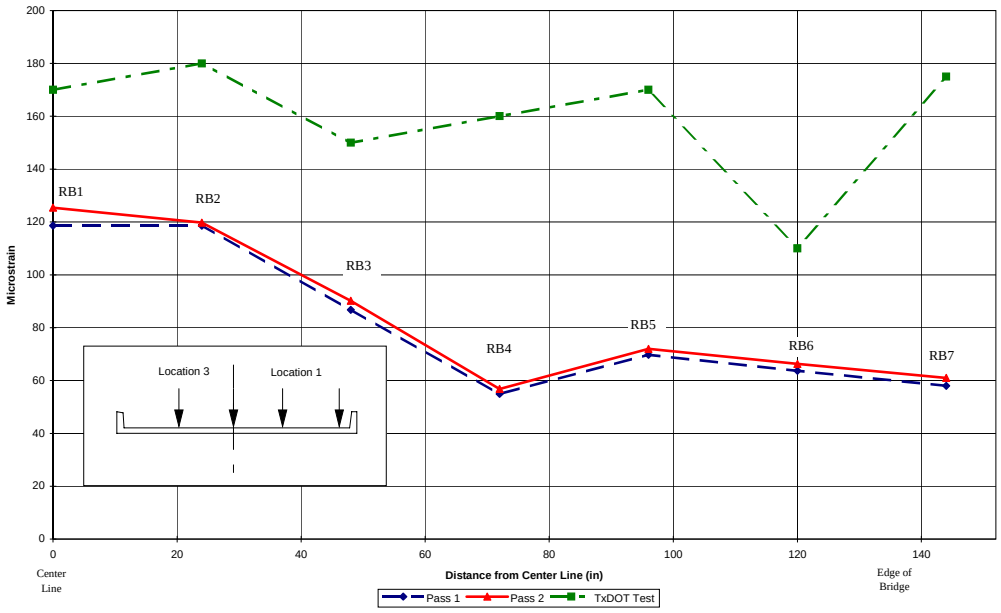

Figure 5.14 Comparison of Test Results and TxDOT Test, Locations 1 and 3.

There are several possible reasons for the discrepancies between the two tests. The TxDOT test loadings were done by using a frame system with rams to simulate 4 wheel loads at midspan [10]. This allowed for very accurate loading placement and increments. In order to compare with the TxDOT test, results were superimposed to simulate two trucks. The superpositioning of the loads would cause some difference because the truck positions were not exactly the same as the positions of the rams in the TxDOT test. The test truck also had a tandem axle where as the TxDOT test used rams to apply point loads. This was accounted for in the plots by applying a 20% reduction to the TxDOT results. In a future test two trucks configured similarly to the TxDOT test loads should be used to compare with the TxDOT test results.

The most probable cause of error is likely due to the fact that the loading method used by TxDOT led to full cracking of the curb and the slab. This would account for the difference because as discussed previously it is felt that this bridge may not be behaving like a fully cracked section.

5.2.2 Comparison of TxDOT Deflection Measurements

In addition to strain measurements, deflection data was also compared with the test results. As shown in Figure 5.15 the TxDOT deflections are greater than the test deflections. The average difference between the deflections is 0.03 inches or 48%. These differences are caused by the same reasons as were discussed for the differences in strain comparisons. The string potentiometers used to measure deflections were not precise enough to measure the very small deflections during the test. Because of these reasons the deflection comparison is of questionable value but included for completeness.

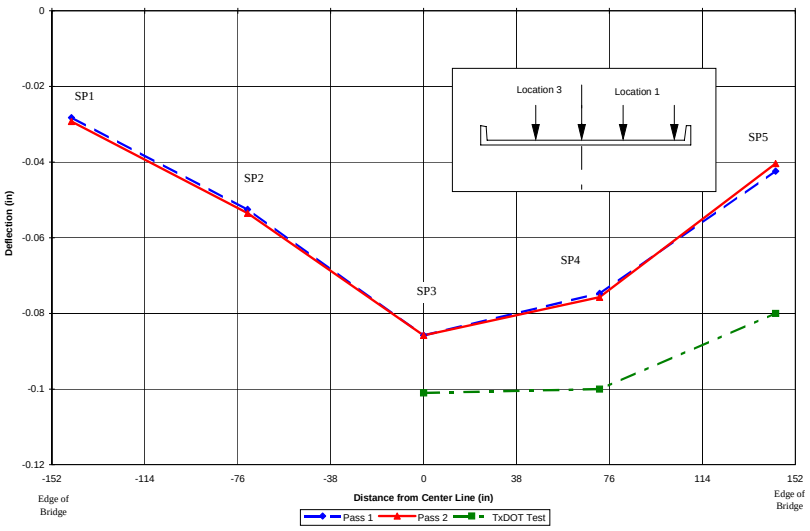

Figure 5.15 Comparison of Deflection Results and TxDOT Test.

5.3 SURFACE STRAIN MEASUREMENTS

5.3.1 Surface Strain Measurements with Mechanical Strain Transducers

As discussed in Chapter 3 and Appendix A, three mechanical strain transducers were attached to the bottom of the slab in an attempt to measure and correlate surface strain with the strain in the reinforcing bars. If a correlation could be determined then this method of measuring strain would be much easier and faster than attaching strain gages to the reinforcing bars.

One transducer (T1) was mounted across a visible crack in the concrete surface to observe the effects on surface strain. The two other transducers (T2 and T3) were mounted where no visible cracks were observed. Table 5.1 shows the comparison of T1 with the calculated strain at the bottom of the slab. As shown the calculated bottom strains are approximately 18% less than the surface strains.

Location 1 Pass 1				Location 1 Pass 2		
	Average	Std Dev			Average	Std Dev
T1	77	4.7		T1	77	7.6
Bottom	63	4.1		Bottom	64	6.4
% Diff	-18%			% Diff	-17%	
Location 2 Pass 1				Location 2 Pass 2		
	Average	Std Dev			Average	Std Dev
T1	91	7.3		T1	90	9.2
Bottom	75	5.5		Bottom	74	6.1
% Diff	-17%			% Diff	-18%	

Table 5.1 Comparison of Transducer T1 Data.

Figure 5.16 shows transducer T1 plotted with gages RB1 and RB2 which were on either side of T1 as shown in the instrumentation plan in Appendix A. Also plotted with the gage data is a projected bottom strain based on the cracked neutral axis location and the average strain of RB1 and RB2. The strain readings are consistently high throughout the entire loading spectrum. This shows no additional cracking occurred during the test loading.

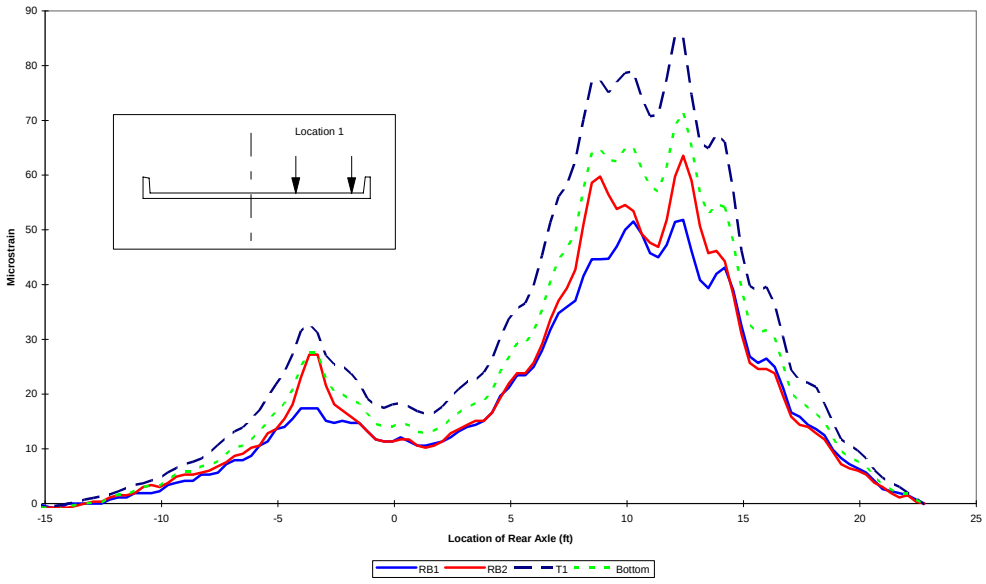

Figure 5.16 Transducer T1 compared with Expected Strains.

As stated earlier transducer T2 was placed in an area of no visible cracking. This placement was an attempt to compare the effects of the cracks on surface strain measurement. Table 5.2 shows that the expected bottom strain is approximately 40% higher than the transducer data.

Table 5.2 Comparison of Strain Transducer T2 Data.

Location 1 Pass 1				Location 1 Pass 2		
	Average	Std Dev			Average	Std Dev
T2	52	6.2		T2	51	7.1
Bottom	74	4.8		Bottom	67	7.5
% Diff	42%			% Diff	31%	
Location 2 Pass 1				Location 2 Pass 2		
	Average	Std Dev			Average	Std Dev
T2	54	1.7		T2	54	3.5
Bottom	76	3.7		Bottom	74	4.8
% Diff	39%			% Diff	39%	

The large difference in the expected strains and transducer data was thought due to the fact that the transducer gives average strain values based on the gage length. Figure 5.17 shows the transducer data bounded by the data from gages RB2 and RB3. The transducer data should be following the expected bottom strain line.

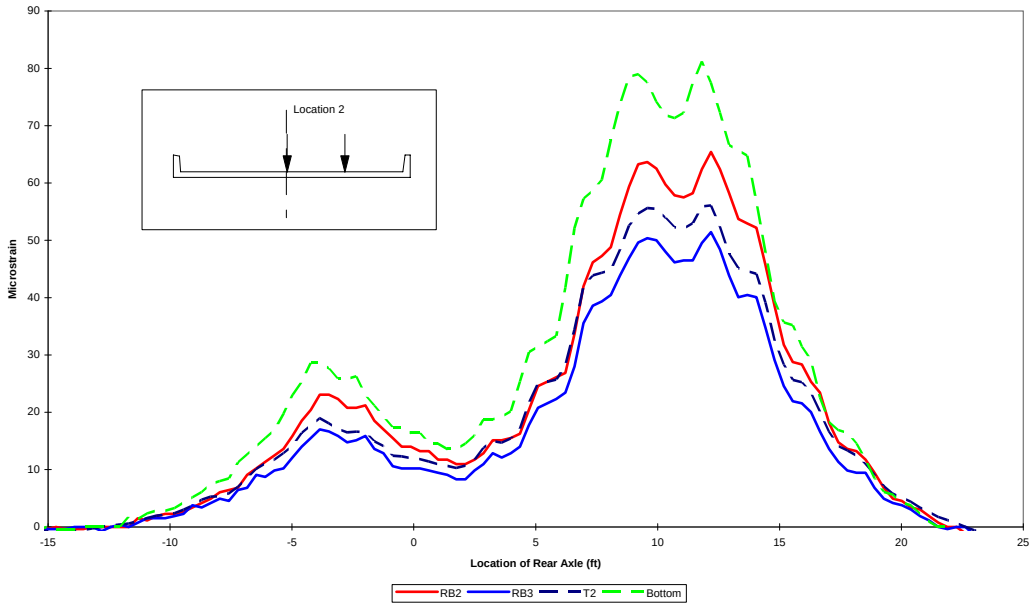

Figure 5.17 Transducer T2 compared with Expected Strains.

The results from transducer T3 were similar to T2. These results are not shown here because of the questionable quality of gage RB4. This gage gave consistently low readings and it was felt the data was unusable for this comparison.

5.3.2 Surface Strain Measurements with Concrete Foil Gage

In addition to mechanical strain transducers an attempt to measure surface strains was made using an electrical resistance (foil) strain gage with a 60mm gage length. The exact placement of the gage is shown in Appendix A. The gage was placed across the same crack as transducer T1 was placed. As shown in Table 5.3 the results of the foil gage F1 show extremely high values in

comparison with expected strain values. Figure 5.18 shows the magnitude of the differences in the strain.

Table 5.3 Comparison of Foil Gage F1 Data.

Location 1 Pass 1				Location 1 Pass 2		
	Average	Std Dev			Average	Std Dev
F1	185	10.3		F1	191	19.4
Bottom	60	1.9		Bottom	60	5.1
% Diff	-68%			% Diff	-69%	
Location 2 Pass 1				Location 2 Pass 2		
	Average	Std Dev			Average	Std Dev
F1	217	17.7		F1	218	18.3
Bottom	67	5.9		Bottom	67	5.6
% Diff	-69%			% Diff	-69%	

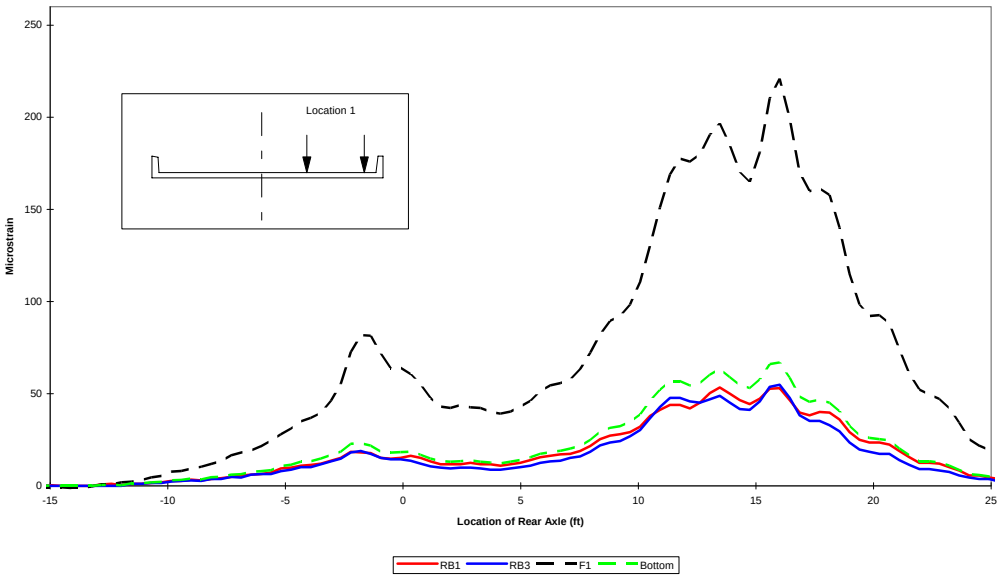

Figure 5.18 Strain Gage F1 compared with Expected Strains.

5.3.3 Summary of Surface Strain Measurements

As shown by the previous results, measuring tension surface strain on concrete is highly variable depending on the placement of the gage. There are several unknown variables that affect surface strain, such as the length of reinforcing bar debonding in the area of a crack, the exact number and location of microcracks and the load history of the structure. Based on the data obtained from this test, strain measurements cannot be used to determine strain in the tension reinforcing steel. Increased gage lengths to determine average strain values may be a viable option but further investigation is necessary.

5.4 LOAD RATING BASED ON LOAD TEST

5.4.1 Methodology of Load Rating Based on a Load Test

The method used to adjust the load rating of this bridge based on the load test results is outlined in Chapter 6 of the Manual for Bridge Rating through Load Testing [11]. The procedure outlined in the manual involves applying an adjustment factor (K factor) to the existing rating. This factor is based on the load test and may increase or decrease the load rating depending on the test results [11].

The K factor is defined as follows [11]:

$$K = 1 + K_a \times K_b$$

where:

$$K_a = \frac{\varepsilon_C}{\varepsilon_T} - 1$$

ε_T is the maximum test strain for a member.

ε_c is the calculated strain for a member based on the test load.

$K_b = K_{b1} \times K_{b2} \times K_{b3}$

In order to determine K_{b1}, K_{b2}, and K_{b3} the Manual [11] provides tables based on confidence in analysis, inspection frequencies, and critical structural features. These tables are repeated below for reference.

Table 5.4 Table to Determine K_{b1}. [11].

Can member behavior be extrapolated to 1.33W?		Magnitude of test load			K_{b1}
Yes	No	$\frac{T}{W} < 0.4$	$0.4 \le \frac{T}{W} \le 0.7$	$\frac{T}{W} > 0.7$	
√		√			0
√			√		0.8
√				√	1.0
	√	√			0
	√		√		0
	√			√	0.5

In Table 5.4 the variables W and T are defined as follows:

W = Rating Load Effect.

T = Test Vehicle Effect

Table 5.5 Table to Determine K_{b2}. [11].

INSPECTION		K_{b2}
Type	Frequency	
Routine	between 1 & 2 years	0.8
Routine	less than 1 year	0.9
In-Depth	between 1 & 2 years	0.9
In-Depth	less than 1 year	1.0

Table 5.6 Table to Determine K_{b3} [11].

Fatigue Controls?		Redundancy		K_{b3}
No	Yes	No	Yes	
	√	√		0.7
	√		√	0.8
√		√		0.9
√			√	1.0

5.4.2 Load Rating of the Test Bridge

As discussed in Chapter 2, the load rating of a bridge is based on the controlling member of the bridge. Therefore just as the rating in Chapter 2 considered both the curb and the slab this adjustment to the rating will consider both also. The highest peak values of strain are used to determine the K factor.

5.4.2.1 Slab Load Rating

The calculated value of strain for midspan based on the distributed moments from Section 5.1 is 94 microstrain. The peak value of strain during the test occurred at gage RB2, Location 2, Pass 2. This peak value was 74 microstrain. From the equation for K_a above:

$$K_a = \frac{94}{74} - 1 = 0.270$$

From Table 5.4 the value for K_{b1} can be determined. Based on weighted average of the contribution of the slab and curbs to the overall strength of the bridge, the behavior can be extrapolated to 1.33W. This method of weighted averages is currently used by TxDOT to determine the operating rating of a slab bridge. This method was not used in this study to determine the operating rating. In order to determine the magnitude of the test load the total moment for the test

truck was divided by the moment of the rating vehicle. This resulted in a ratio of 0.5. From Table 5.4 and the above factors,

$K_{b1} = 0.8$

From Table 5.5 and the current inspection report which shows an inspection frequency of 2 years,

$K_{b2} = 0.8.$

Because the bridge is reinforced concrete there is assumed redundancy and fatigue does not control therefore,

$K_{b3} = 1.0.$

Based on the values above,

$K_b = 0.8 \times 0.8 \times 1.0 = 0.64$

and

$K = 1 + 0.64 \times 0.270 = 1.17$

Based on the rating factor values from Chapter 2, the adjusted operating and inventory ratings are:

Operating Rating

$RF_{OR} = 1.17 \times 1.468 = 1.72 \times 20 \Rightarrow$ HS34

Inventory Rating

$RF_{IR} = 1.17 \times 0.879 = 1.03 \times 20 \Rightarrow$ HS21

Table 5.7 shows a comparison between the original load ratings based on analysis and the adjusted load ratings based on the load test.

Table 5.7 Comparison of Load Ratings.

Load Ratings			
	Original	Adjusted	% Increase
Operating	HS29	HS34	17%
Inventory	HS17	HS21	24%

Although the 24% increase is significant, the most important result of the load test is the inventory rating is now greater than HS20. This increase in rating means the bridge no longer has to be inspected on a less than two year frequency and may have even greater benefit if future TxDOT posting policy requires a bridge with less than an HS20 inventory rating to be posted.

Chapter 5. EVALUATION OF MEASURED DATA

The measured and calculated data are compared in this chapter. The methods used for distributing the moments to the slab and curb are discussed in section 5.1. An evaluation of the strain data for both the slab and curb is made in section 5.2. An evaluation of the neutral axis location is made in section 5.3, and deflection results are evaluated in section 5.4.

5.1 METHOD OF MOMENT DISTRIBUTION TO THE SLAB AND CURBS

5.1.1 Truck Moment Envelope Comparison

The test truck shown in Chapter 3 is a three-axle vehicle with a rear tandem axle. The design truck and the truck simulated in both the TxDOT Report [10] and the Illinois Bulletin 346 [5] were two axle trucks. Shown in Figure 5.1 is a comparison of the moment envelopes for the actual test truck and the ideal two axle truck with the same axle weights. There is approximately 20% difference in moment between the two truck configurations. The moment envelopes in Figure 5.1 are for a 24-foot, simple-span bridge.

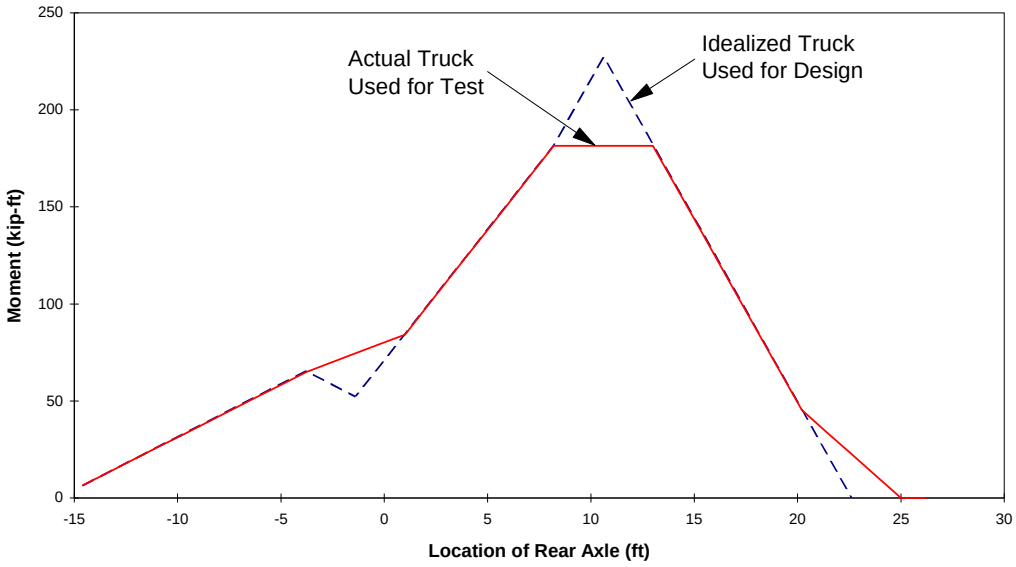

Figure 5.1 Moment Envelopes for Test Truck and Design Truck for Simple-Span.

Under actual conditions, bridge spans rarely behave in a simply-supported manner. Therefore, two types of end conditions were used in the evaluation of the measured data. A simple-span model was selected because it was assumed during design, and a fixed-end model was selected to represent the maximum amount of rotational restraint at the ends of the span. The moment envelopes for both the simple-span and fixed-end models are shown in Figure 5.2.

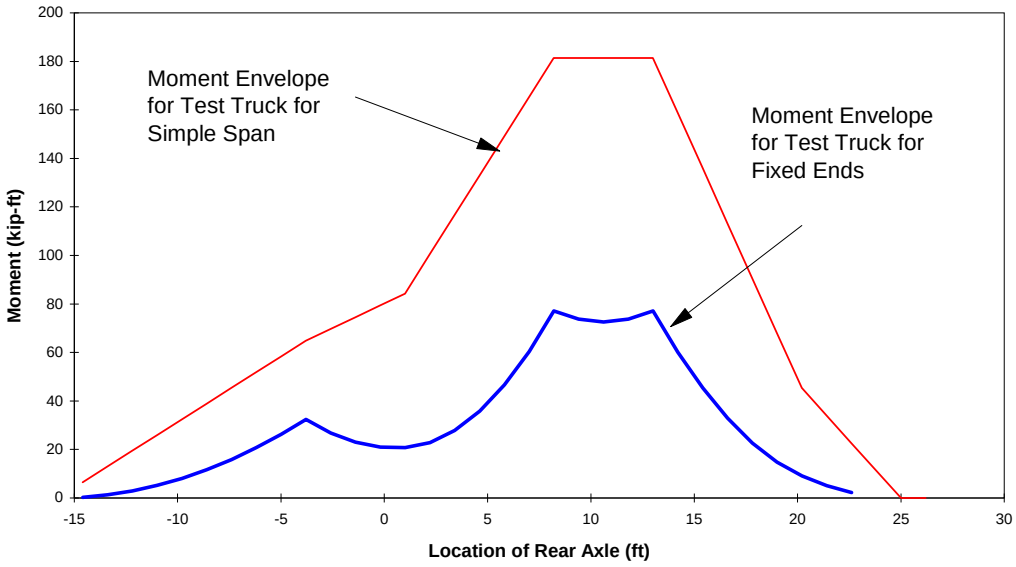

Figure 5.2 Comparison of Moment Envelopes based on End Condition.

There is a 55% reduction in maximum moment in the bridge when the ends of the span are assumed to be fixed. It is unlikely the bridge is behaving as an absolute fixed-end structure, but a fixed-end model provides a lower-bound to the moments developed in the span. Although there may be some error in distribution of the moments to the curb and slab by assuming fixed-end supports, this assumption should also give conservative values of strain.

5.1.2 Application of Illinois Bulletin 346 Method of Moment Distribution

The methods discussed in Chapter 2 to calculate the distribution of moments to the curb and to the slab are based on loading the bridge with two vehicles [5]. In addition, Equations 2.6 through 2.9 use the given wheel weights to calculate moments based on two single axle trucks. The critical location for

moment under this loading condition occurs when the rear axle is at midspan. A method had to be developed to relate the moments calculated using the design procedure to the moments induced in the bridge during the load test.

The moments given by Equations 2.6 and 2.8 correspond to the moment induced by live load per unit width of slab and per curb, respectively. The total moment for the bridge was calculated as shown below:

$$M_{TOTAL} = M_{LL}(slab) * w_E + 2 * M_{LL}(curb) \quad (5.1)$$

where:

$$w_E = Total\,Width - 2 \cdot (Curb\,Width + 4 \cdot (Slab\,Depth)) \quad (5.2)$$

The percentage of moment attributable to the slab and to the curb were then calculated by dividing $M_{LL}(slab)$ and $M_{LL}(curb)$ by M_{TOTAL}. The percentages of total moments are as follows:

M_{slab} = 2.4% per unit width of slab.

M_{curb} = 31.4% per curb.

These percentages were then applied to the moment envelope for the test truck shown in Figure 5.2.

There was concern that there would be error in the distributed moments because Equations 2.6 and 2.8 were developed for two trucks and only one truck was used during the test. Therefore a second method of calculating distributed moments was used based on the University of Illinois Engineering Experiment Station Bulletin 315 [18]. In Illinois Bulletin 315 [18] charts were developed in order to use wheel location, length to width ratios and relative stiffness of the curb compared with the slab to determine a moment at midspan for a specific truck. The tandem axle loads were divided into two equivalent wheel loads and a

moment was calculated for both the slab and the curb based on the charts [18]. The moment was then reduced 20% to account for the tandem axle. This moment was compared with the moment arrived at by the previous method, and differed by less than 0.5%. Based on this small difference, it was felt that the method used to distribute the moments was acceptable.

5.2 Evaluation of Strain Data

5.2.1 Method of Converting Moments to Strains

In order to compare the test results with the analysis, a method of converting moments to strains was derived. The moments assigned to the slab and the curb from section 5.1 were converted to strain by using the following relationship between curvature and strain.

$$\phi = \frac{M}{E_c \cdot I} \tag{5.3}$$

where:

ϕ = Curvature (1/in.)

M = Moment (kip-in)

E_c = Modulus of elasticity of concrete (ksi)

I = Effective moment of inertia (in.^{4}).

The modulus of elasticity of the concrete was calculated using the equation from the AASHTO Specifications [13] and f'c = 5,000 psi. The resulting modulus of elasticity for concrete was 4,000 ksi. The moment of inertia in equation 5.3 was calculated for fully cracked and gross section properties for both the curb and the slab.

Curvature was then related to strain by the following relationship.

$$\varepsilon_i = \phi y_i \qquad (5.4)$$

where:

ε_i = Strain in the desired location

y_i = Distance from the neutral axis to the desired strain location (in).

The values for y_i were calculated for the top of slab, the effective depth of the slab reinforcing bars and the bottom of slab. The y_i values were also calculated for the top of curb, the effective depth of the reinforcing bars in the curb and the bottom of curb. The calculated values for y_i and the moments of inertia are tabulated below in Table 5.1.

A strain envelope was then developed in order to compare with the test results. The strain envelope was developed by using equations 5.3 and 5.4, the appropriate values from Table 5.1 and the moment envelope from section 5.1.

Table 5.1 Calculated Values to Convert Moments to Strain.

		Cracked Section	Gross Section
Slab	I (in.^{4})	555	1,728
	y_t (top) (in.)	3.17	6.00
	y_s (rebar) (in.)	7.08	4.25
	y_b (bottom) (in.)	8.83	6.00
Curb	I (in.^{4})	22,085	43,400
	y_t (top) (in.)	12.11	21.09
	y_s (rebar) (in.)	16.14	7.16
	y_b (bottom) (in.)	17.89	8.91

5.2.2 Comparison of Strains for Simple-Span Model

5.2.2.1 Slab Comparisons

The strain envelope based on the simple-span moments was compared with the test results. Figures 5.3 through 5.8 show the comparisons for the reinforcing bars at the various locations. The test strains for each reinforcing bar are the highest values obtained during testing. The truck locations are shown on each figure.

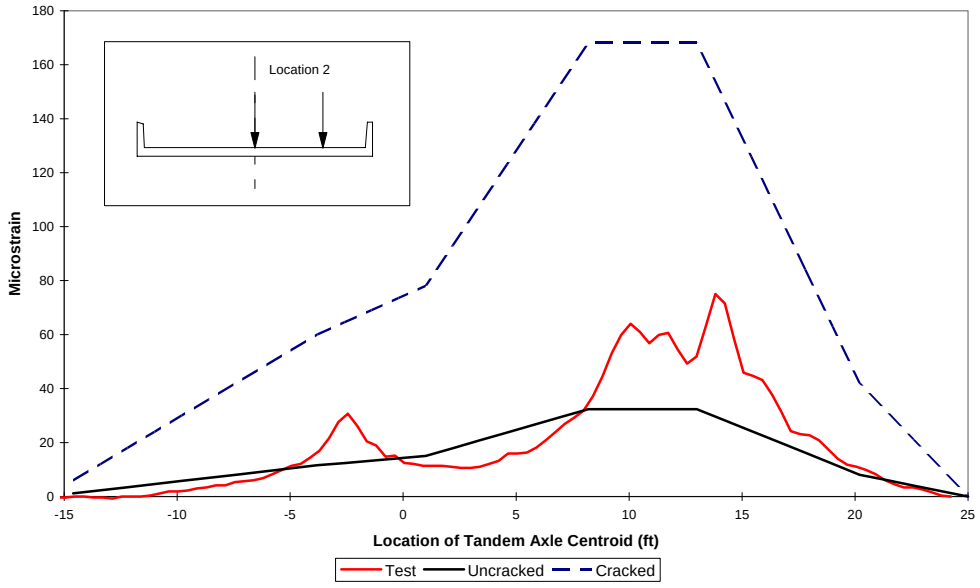

Figure 5.3 Comparison of Test Data and Simple-Span Analysis for RB1.

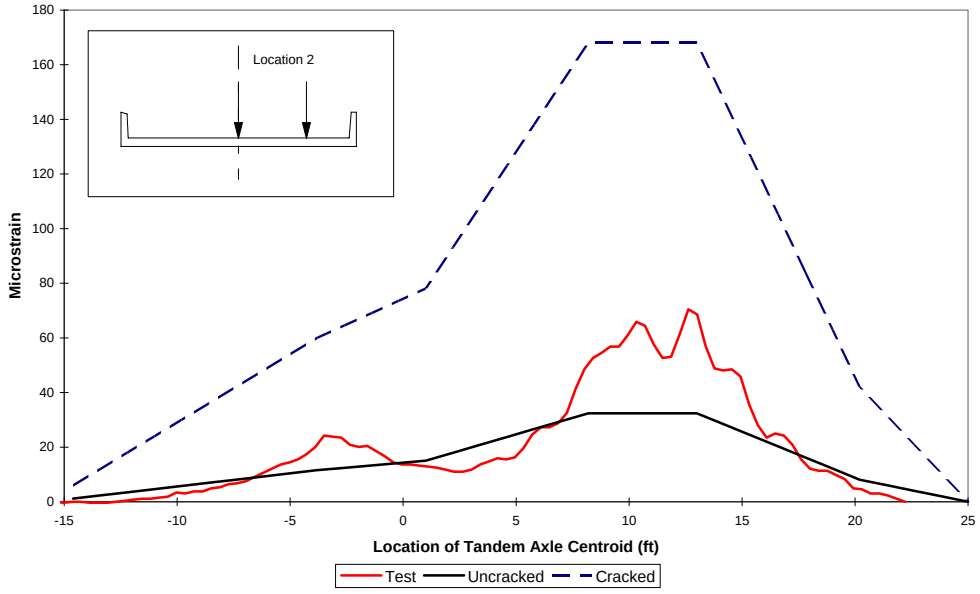

Figure 5.4 Comparison of Test Data and Simple-Span Analysis for RB2.

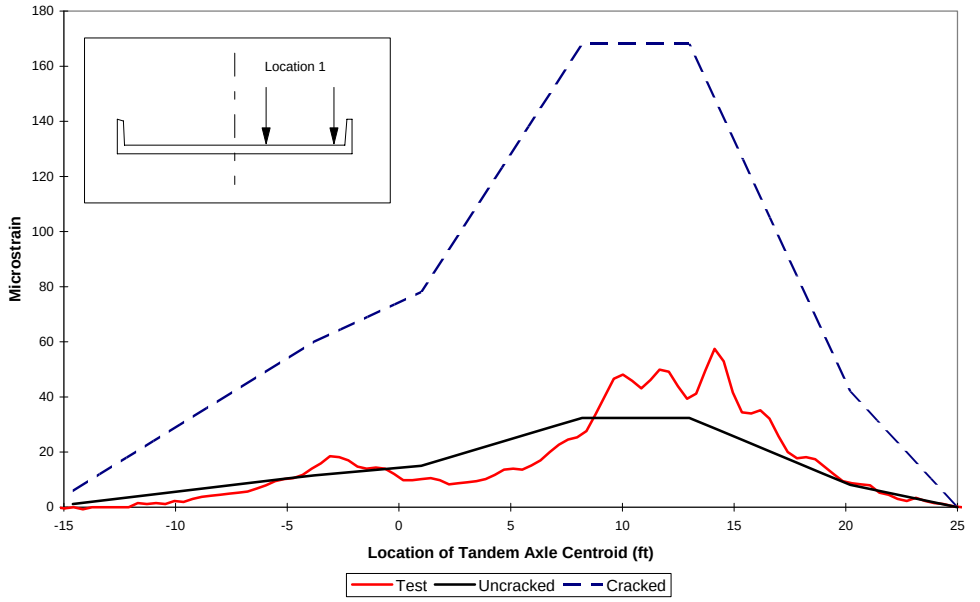

Figure 5.5 Comparison of Test Data and Simple-Span Analysis for RB3.

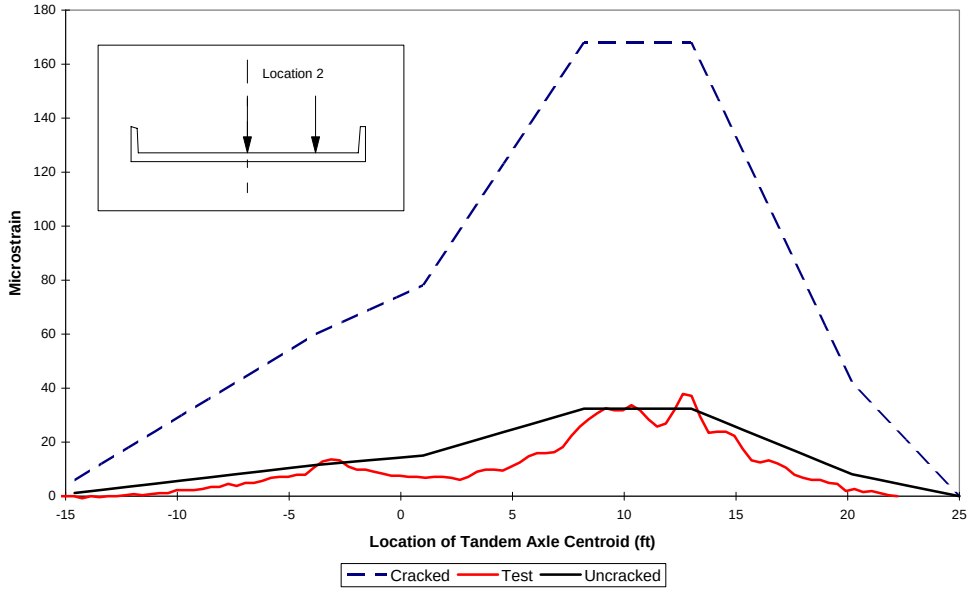

Figure 5.6 Comparison of Test Data and Simple-Span Analysis for RB4.

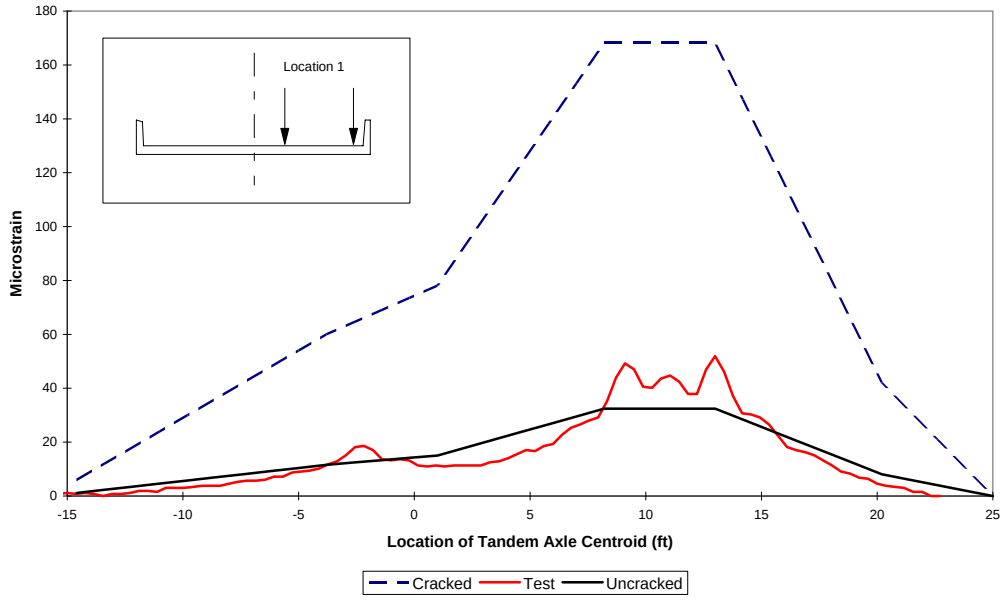

Figure 5.7 Comparison of Test Data and Simple-Span Analysis for RB5.

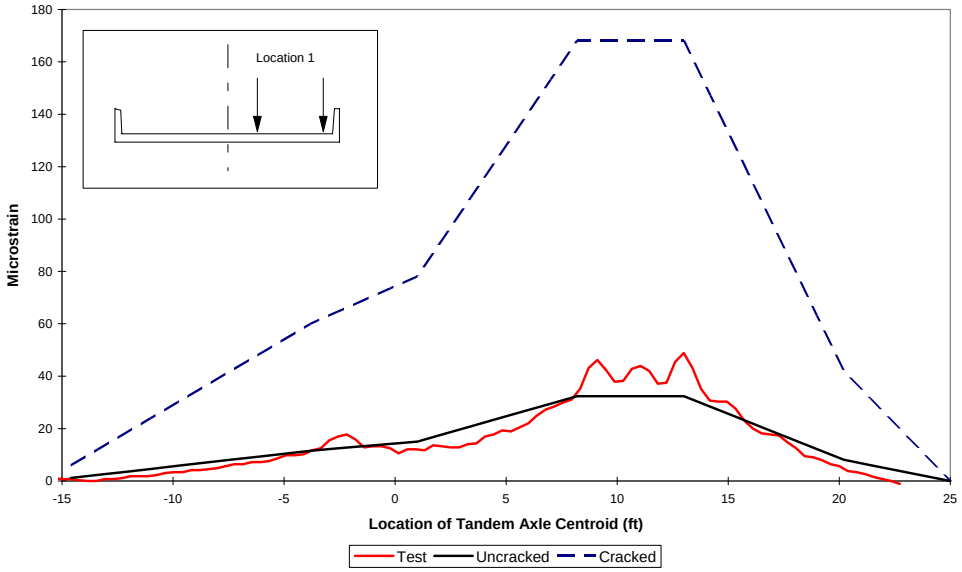

Figure 5.8 Comparison of Test Data and Simple-Span Analysis for RB6.

As shown by Figures 5.3 through 5.8, the simple-span model does not appear to be an accurate representation of the system. The test data match reasonably well with the gross section strain envelope, but the slab was known to be cracked. The problems with using the simple-span model will be discussed in the next section.

Figures 5.9 through 5.11 show strain comparisons at the top of the slab. Measured strains are compared with calculated stains corresponding to gross and cracked moments of inertia. The plotted test results are the highest values for that particular gage. The corresponding truck location for the data is shown on the figure.

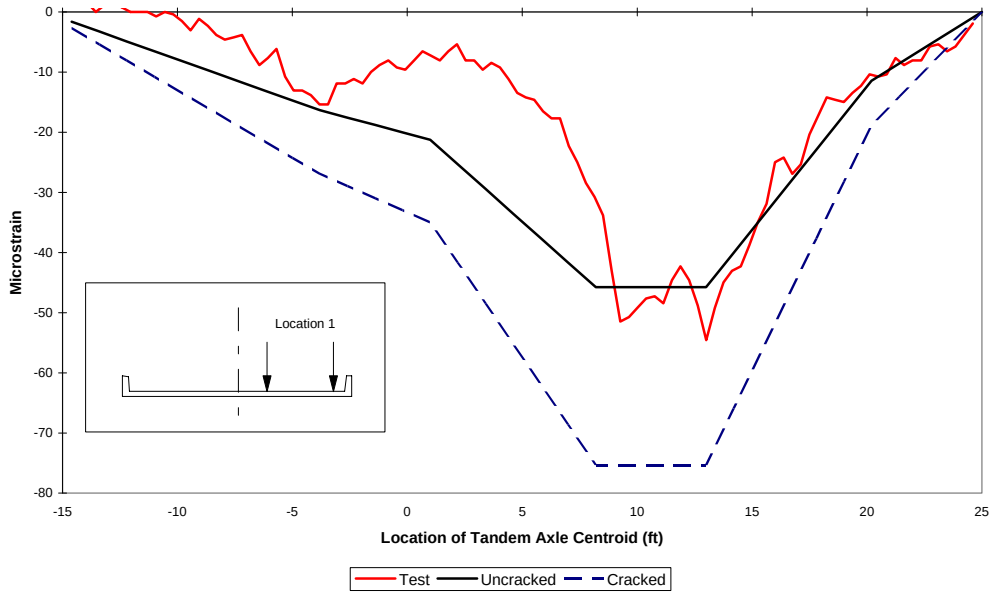

Figure 5.9 Comparison of Test Data and Simple-Span Analysis for C1.

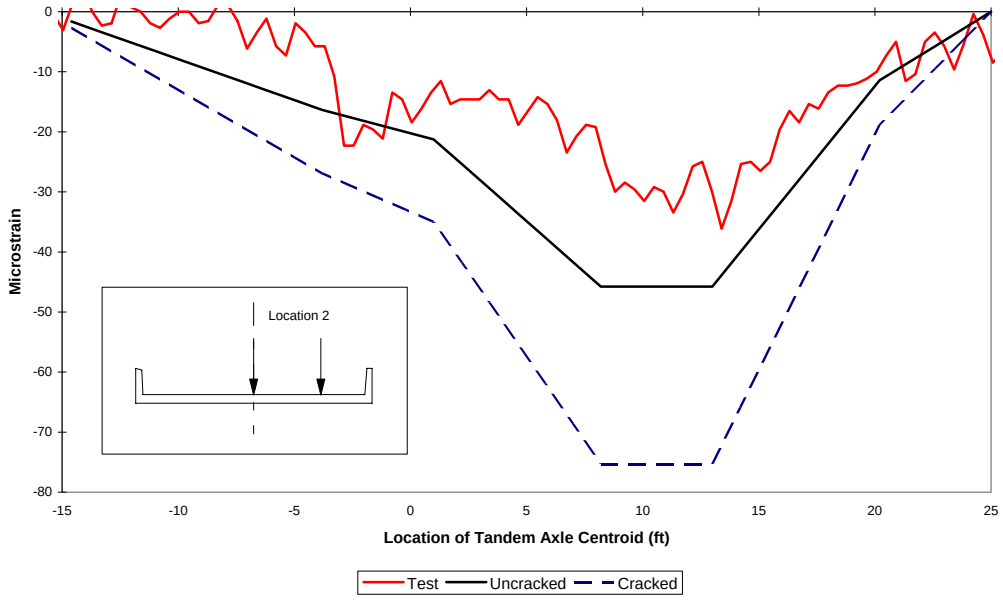

Figure 5.10 Comparison of Test Data and Simple-Span Analysis for C2.

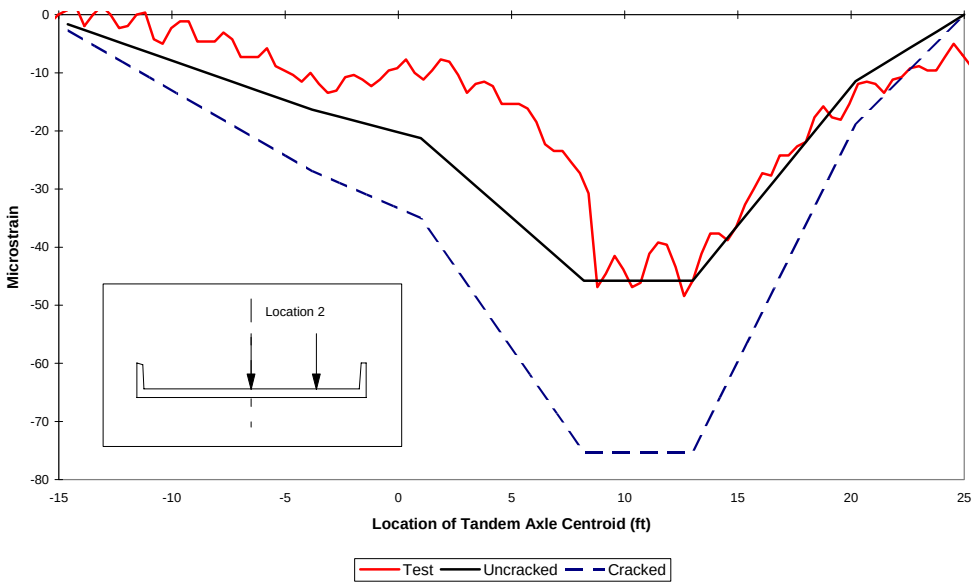

Figure 5.11 Comparison of Test Data and Simple-Span Analysis for C3.

As shown in Figures 5.9 through 5.11, the same general trend is occurring in the top of slab gages as is in the reinforcing bar gages. These figures reinforce the idea that the simple-span model is inappropriate for this system.

5.2.2.2 Curb Comparisons

Comparisons were made with the simple-span analysis for the curb and the test results for gages R2 and RB7. Gage R2 is attached to the top of the curb and RB7 is attached to the reinforcing bar within the curb.

Figures 5.12 and 5.13 show the results of the strain comparisons for the curb. The maximum strain envelope was used for each plot of the test data. The corresponding truck location for the strain envelope is shown on the figure.

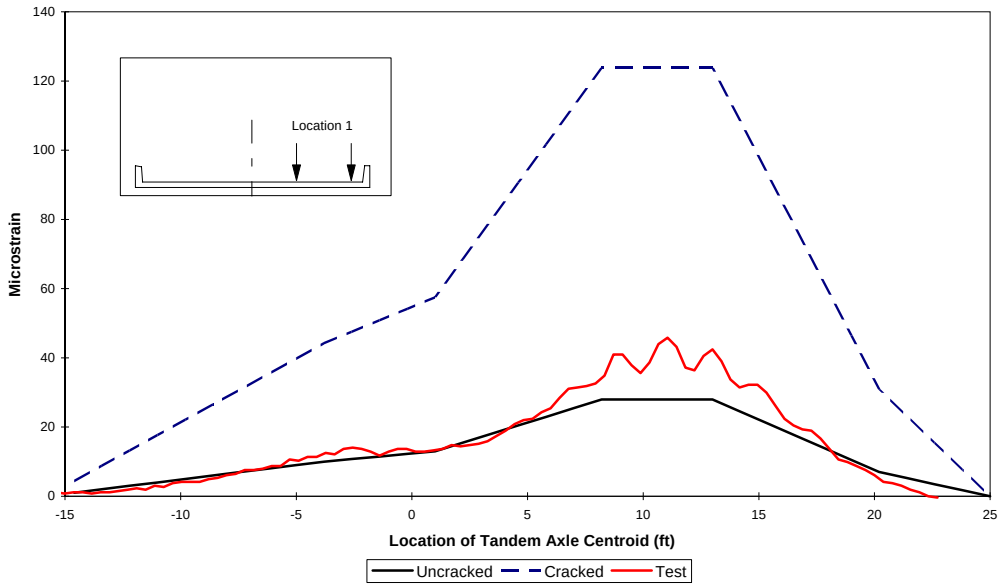

Figure 5.12 Comparison of Test Data and Simple-Span Analysis for RB7.

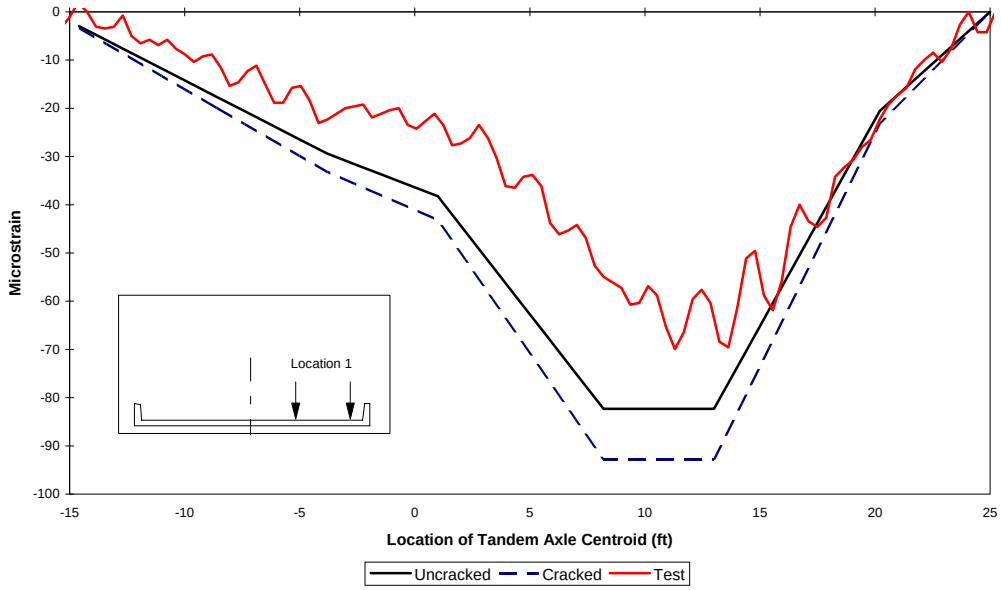

Figure 5.13 Comparison of Test Data and Simple-Span Analysis for R2.

As shown in Figures 5.12 and 5.13, the curb is behaving like the slab. The test results are lower than those calculated using cracked sections, and in the case of gage R2, the measured strains are lower than those calculated using gross sections.

There are three possibilities why the measured data do not match the expected response: (a) the modulus of elasticity of the concrete is higher than expected, (b) the moments are not distributed properly between the curb and slab and (c) the end conditions are not behaving as modeled.

The effects of the modulus of elasticity of the concrete on the behavior of the model were investigated in detail. A higher modulus of elasticity than the design value was used for the concrete in calculating the cracked section strains. This increase had very little effect on the calculated strains. The reason that the modulus had a minimal effect was because the relationship between the modulus and the neutral axis for the cracked section was proportional regardless of the value of the modulus.

There was also concern that improper distribution factors were used in distributing the moments to the slab and curbs, but as shown in the above figures this is not the case. The test results are consistently low for both the slab and the curbs, whereas, if the distribution of moments was wrong, then the curb or slab would have higher strains in relation to the calculated values.

The possibility of end restraint was investigated and the results are discussed in the next section.

5.2.3 Comparison of Strains for a Fixed-End Model

Because of the thickness of the slab and the height of the curbs, there was concern that the supports may not be behaving as expected. The bridge was originally designed a simple span. Details of the design end conditions are shown in Figure 5.14 and 5.15.

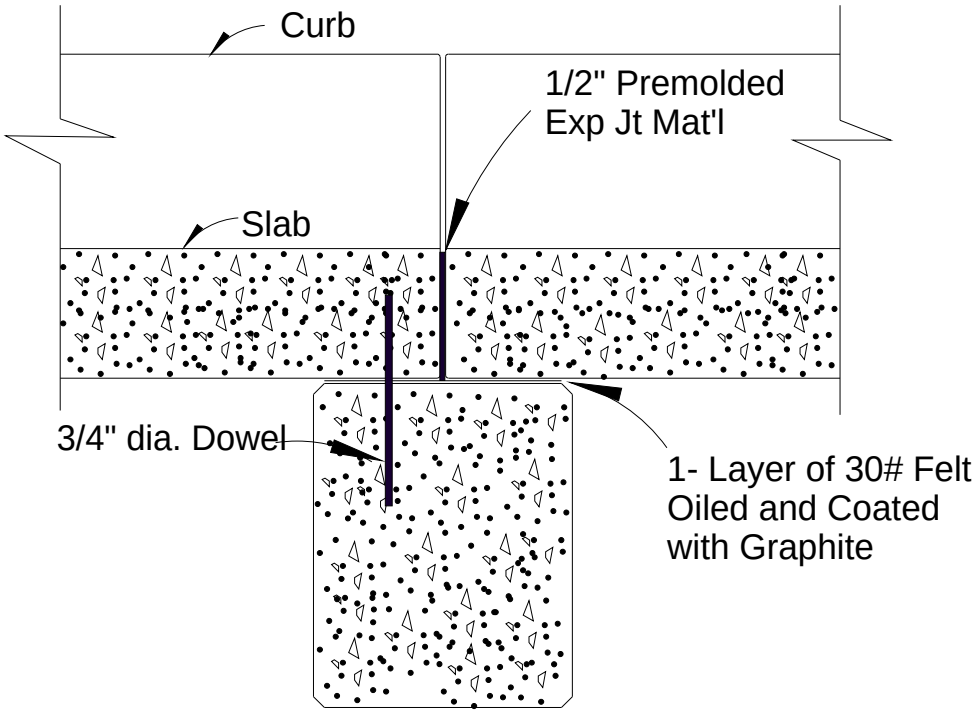

Figure 5.14 Details of Support at Interior Bent.

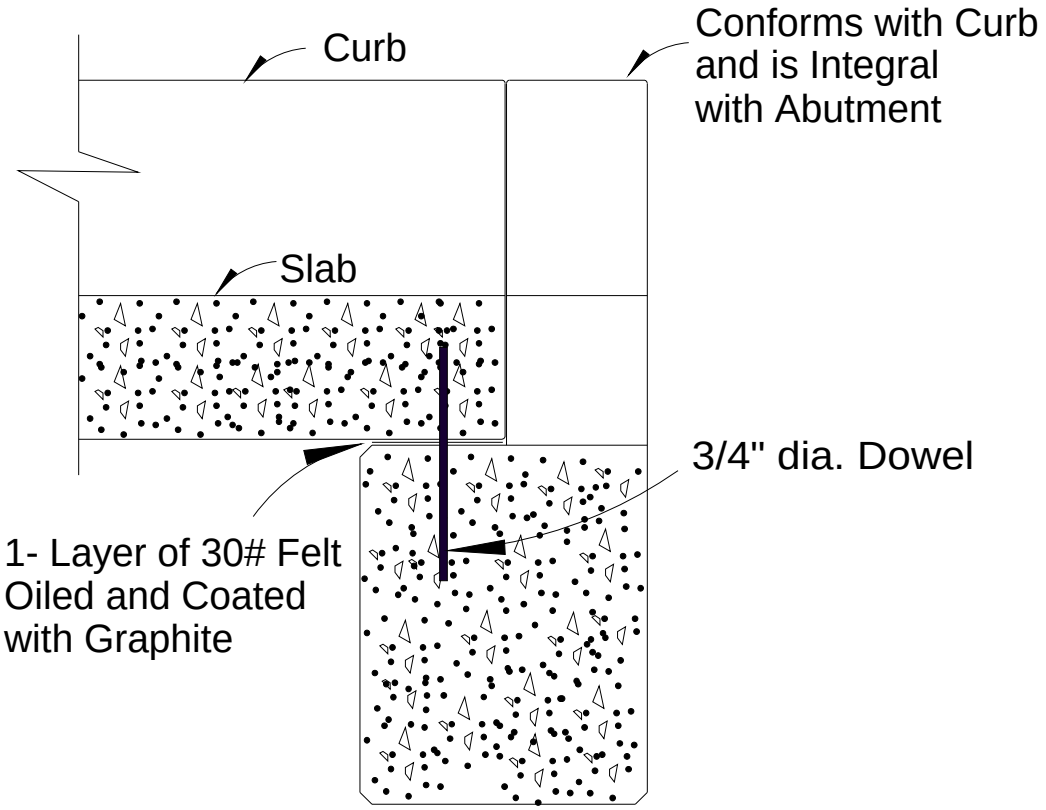

Figure 5.15 Details of Support at Abutment.

From field observations there was no indication that there was any felt remaining at the bearings. There was also cracking occurring in the curb extension on the abutment. The expansion joints at the interior support were completely closed.

Based on the comparison of the simple span analysis and the field observations of the support conditions, there appears to be considerable fixity at the supports. From this assumption the fixed-end moment envelope from Figure 5.2 was used to calculate a new strain envelope. This strain envelope was compared with the test results.

Figures 5.16 through 5.26 show a comparison of the test results with the fixed-end strains for both the curb and the slab. The slab reinforcing bar gage comparison is shown in Figures 5.16 through 5.21. The top of the slab gage comparison is shown in Figures 5. 22 through 5.24. The curb reinforcing bar gage comparison is shown in Figure 5.25 and the top of the curb gage comparison is shown in Figure 5.26. The same test results are shown in these figures as were shown in the simple-span model figures.

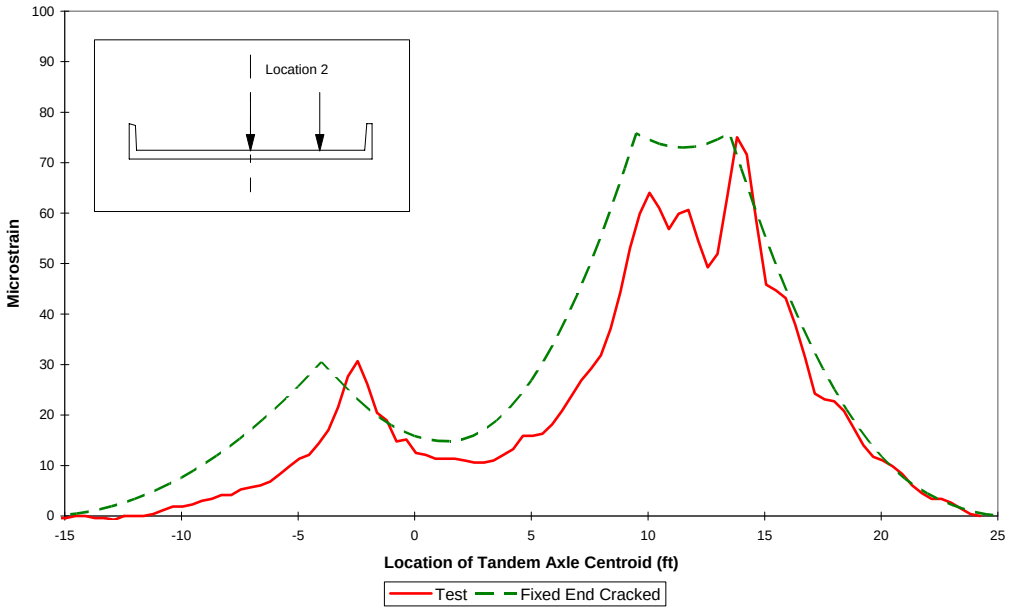

Figure 5.16 Comparison of Test Data and Fixed-End Analysis for RB1.

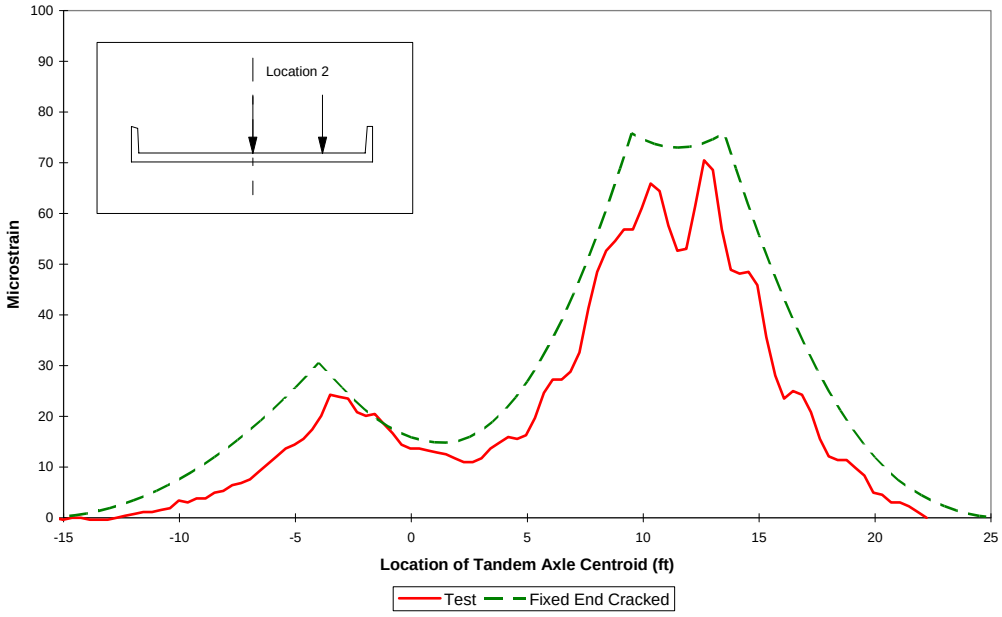

Figure 5.17 Comparison of Test Data and Fixed-End Analysis for RB2.

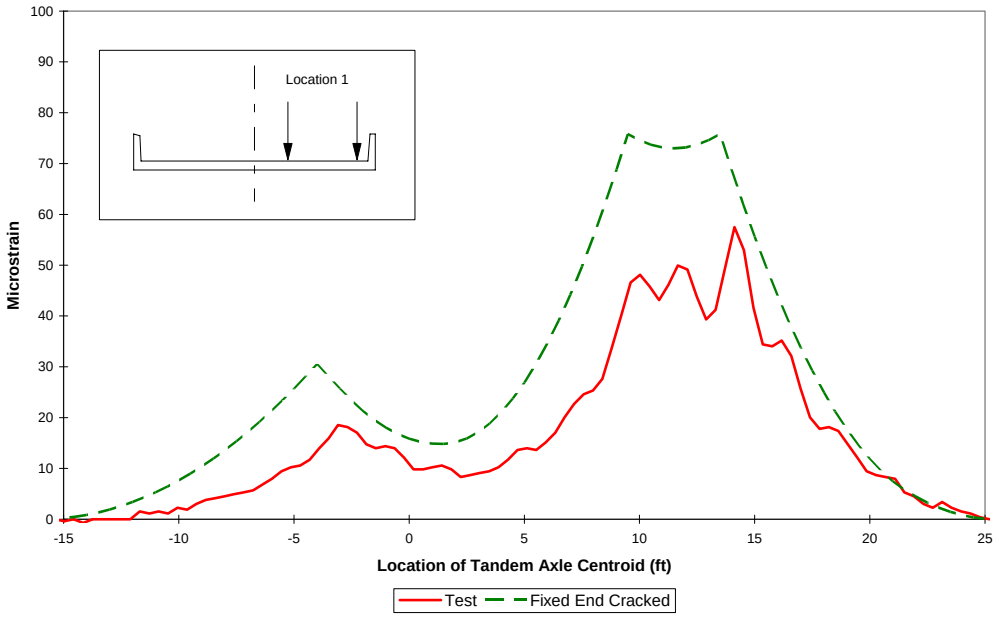

Figure 5.18 Comparison of Test Data and Fixed-End Analysis for RB3.

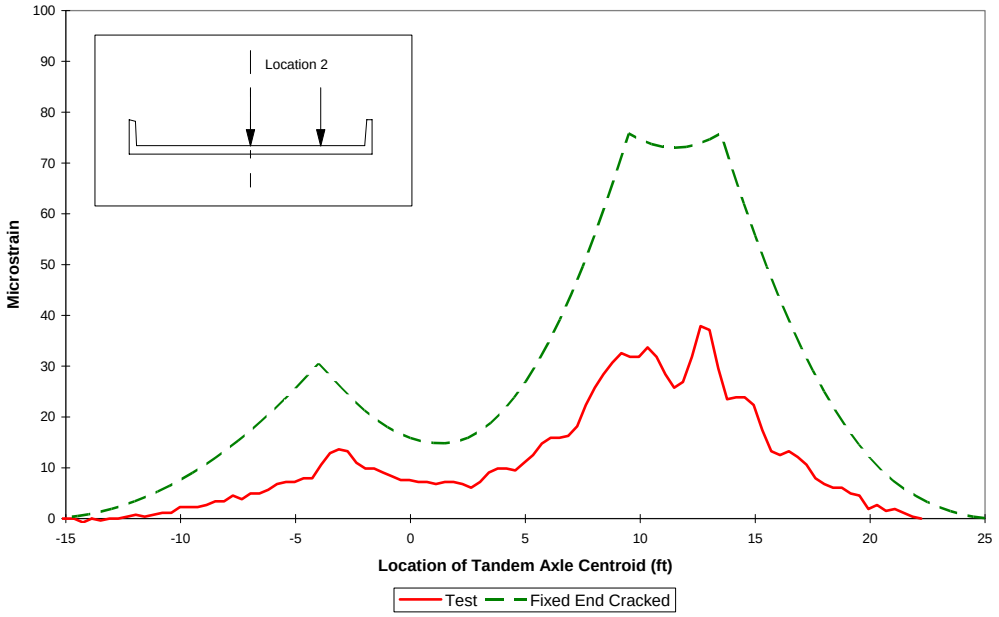

Figure 5.19 Comparison of Test Data and Fixed-End Analysis for RB4.

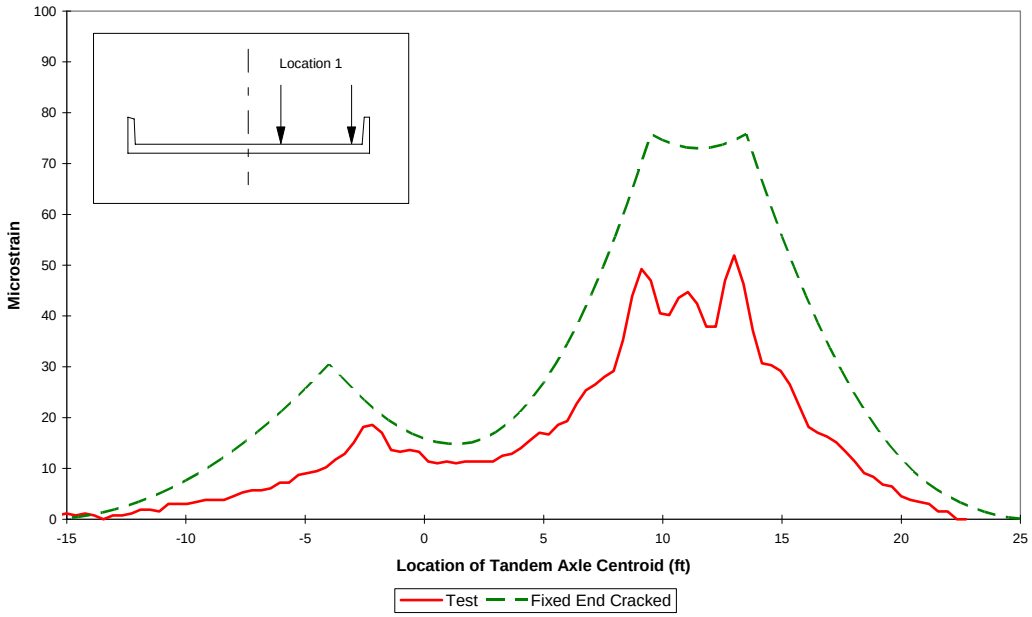

Figure 5.20 Comparison of Test Data and Fixed-End Analysis for RB5.

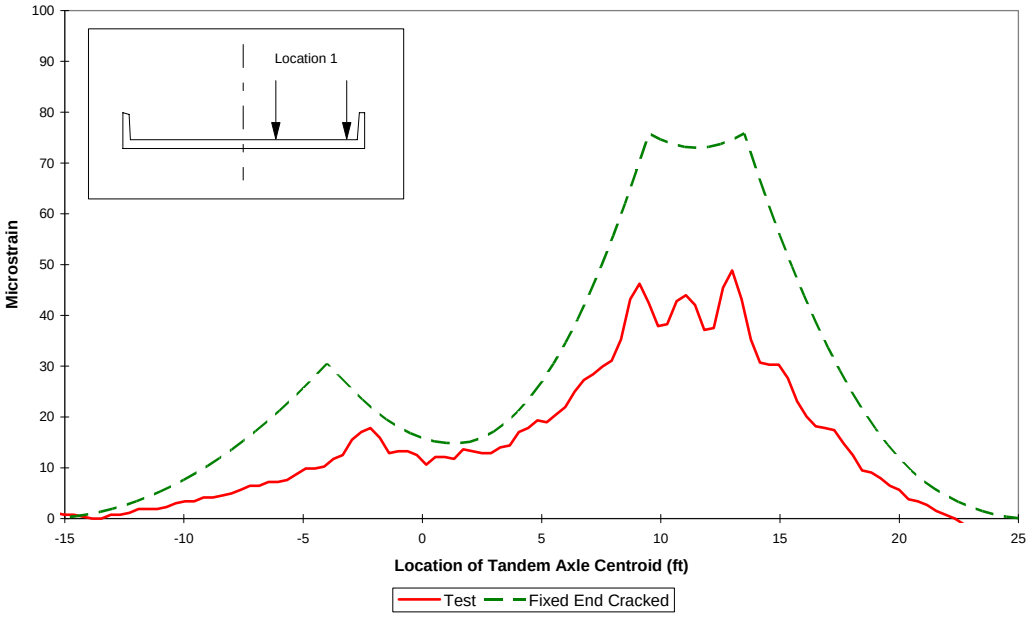

Figure 5.21 Comparison of Test Data and Fixed-End Analysis for RB6.

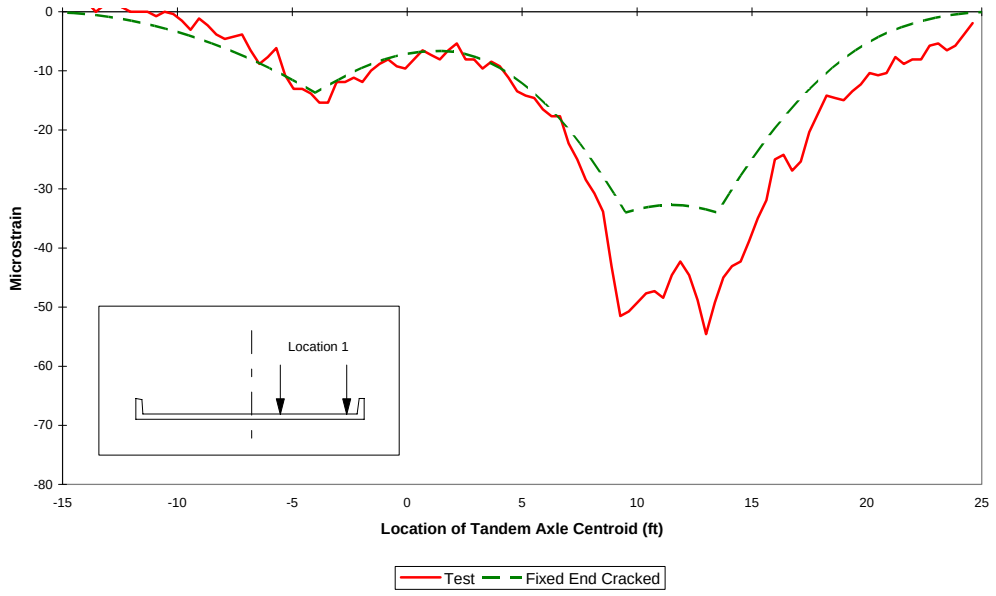

Figure 5.22 Comparison of Test Data and Fixed-End Analysis for C1.

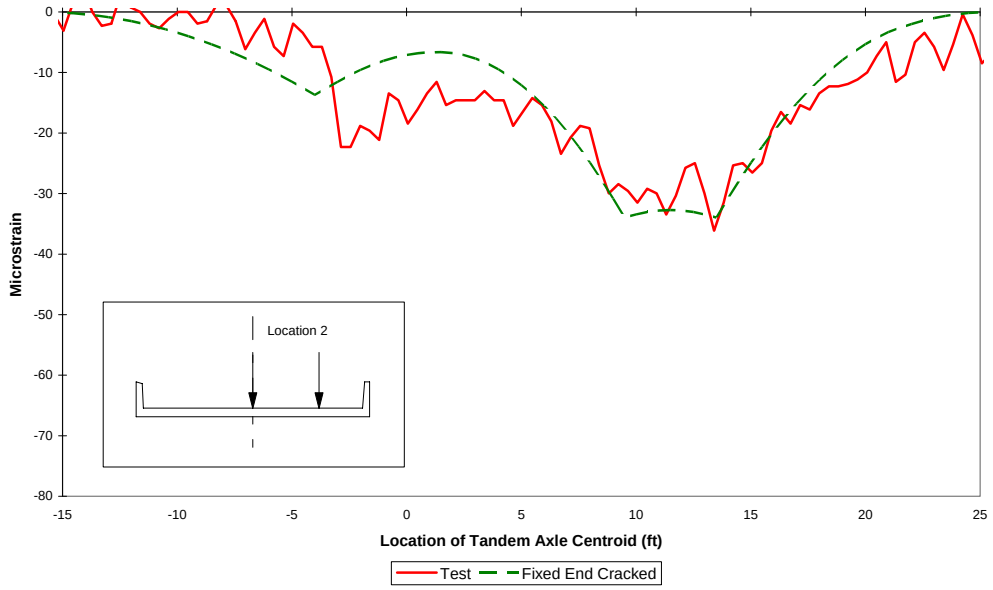

Figure 5.23 Comparison of Test Data and Fixed-End Analysis for C2.

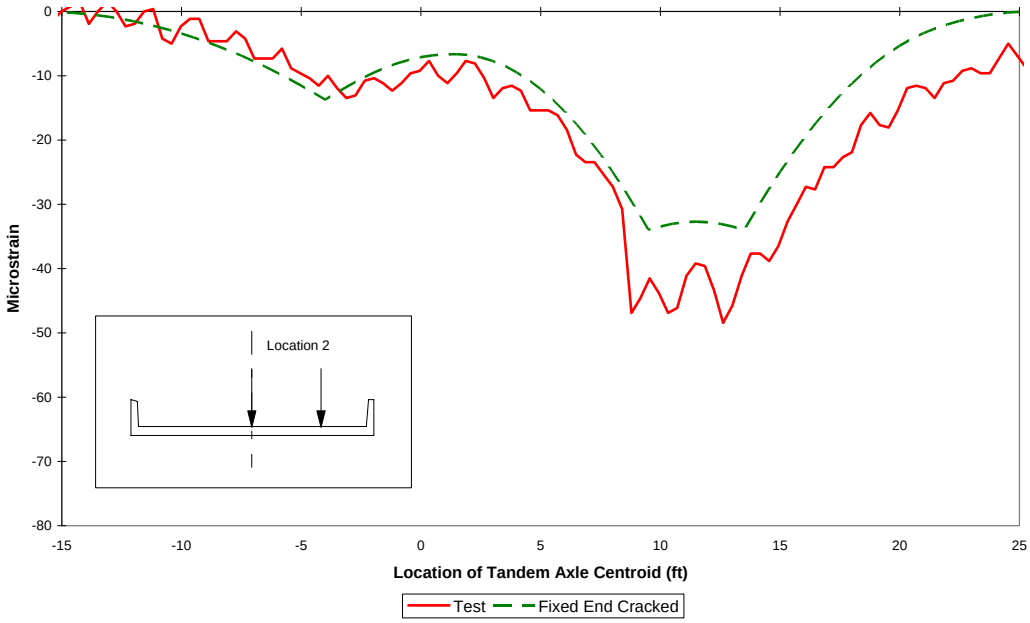

Figure 5.24 Comparison of Test Data and Fixed-End Analysis for C3.

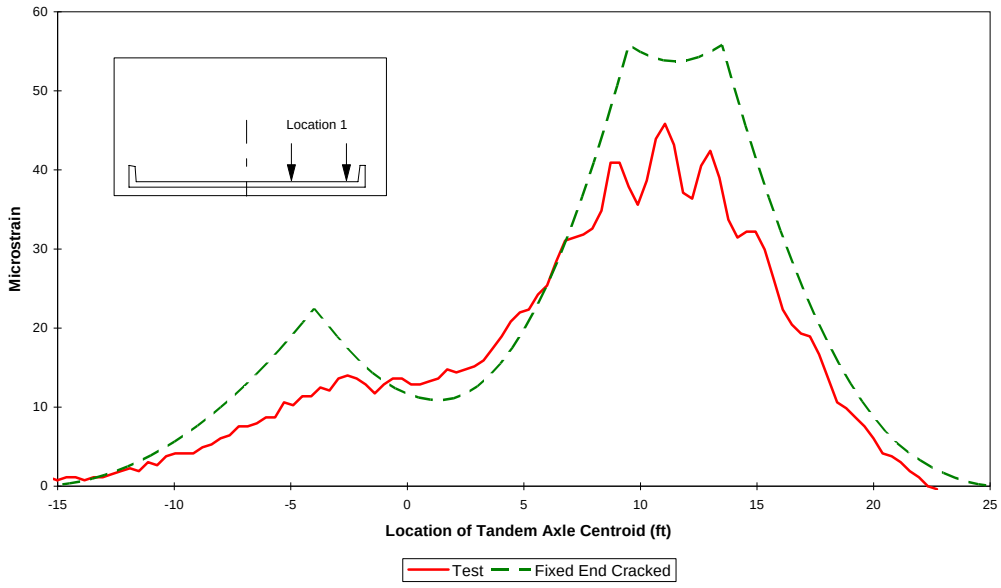

Figure 5.25 Comparison of Test Data and Fixed-End Analysis for RB7.

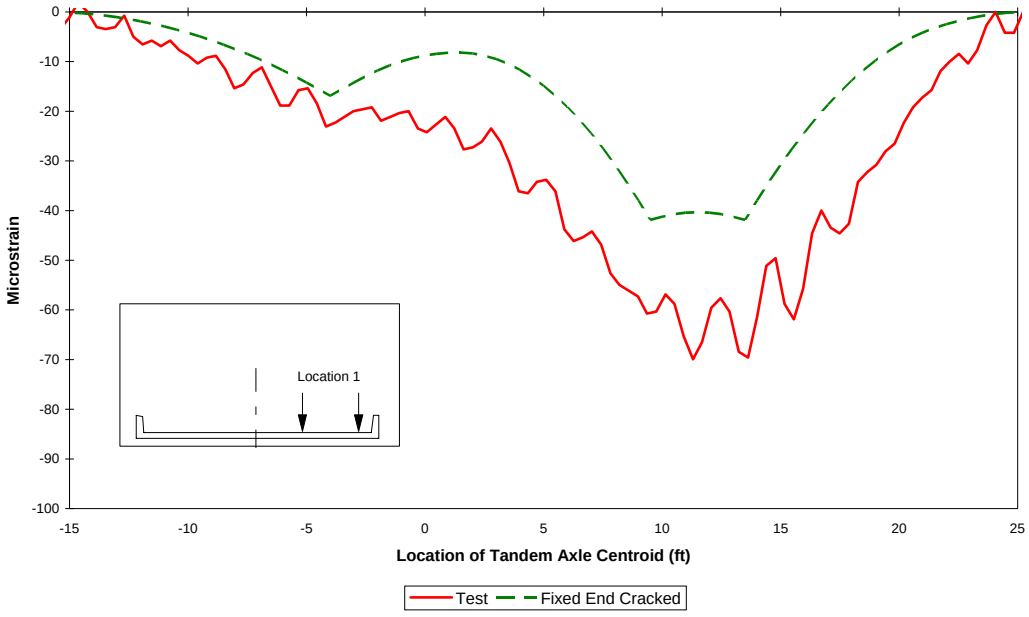

Figure 5.26 Comparison of Test Data and Fixed-End Analysis for R2.

As shown in Figures 5.16 through 5.26, the behavior of the bridge is much better modeled by assuming fixity at the ends. The general shape of the strain envelopes are similar with this model. By observing Figures 5.22, 5.24 and 5.26, the assumption of total fixity is not correct. From these figures it appears as though only partial fixity at the ends is occurring. Further testing should be performed to better model the actual behavior of the bridge.

5.3 Comparison of Neutral Axis Locations

The measured strain data from the top of the slab gages, C1 and C2, were compared with the corresponding reinforcing bar gages, RB1 and RB3, to determine the location of the neutral axis in the slab. Figure 5.27 shows the centroid from the test data of 4.28 inches, compared with the calculated centroids for both a fully cracked section and a gross section.

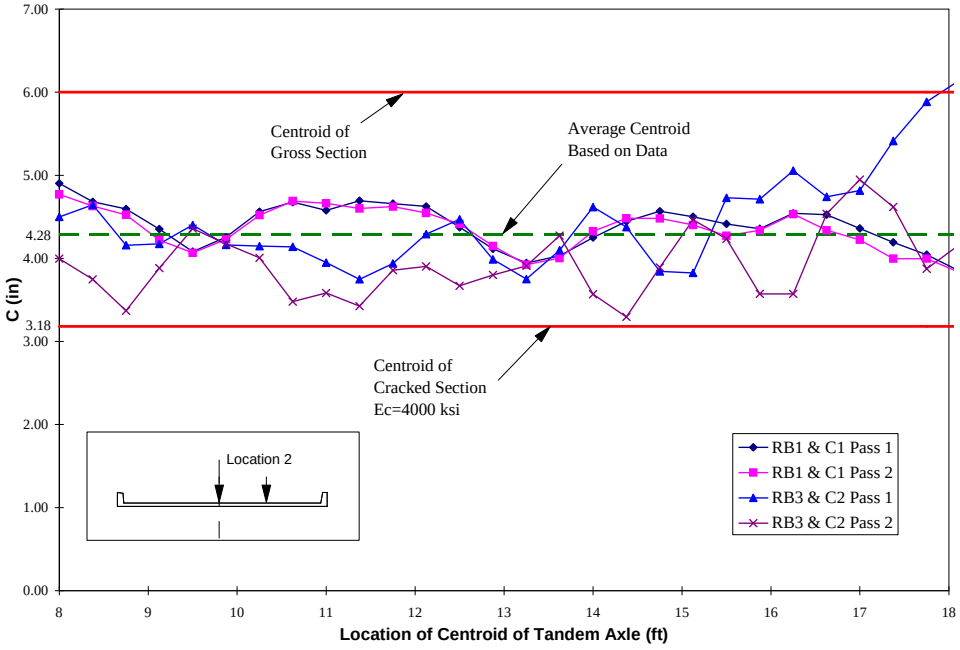

Figure 5.27 Comparison of Centroid Locations in the Slab.

From Figure 5.27, the slab appears to be behaving more like a cracked section because of the location of the average centroid.

A comparison of the neutral axis location was also made for the curb. The reinforcing bar gage RB7 and the top of the curb gage R2, were used to determine the location of the neutral axis in the curb. A mean value of 17.52 inches was calculated for the average centroid. Figure 5.28 shows the centroid based on the measured strain data compared with the centroid for both a fully cracked section and a gross section.

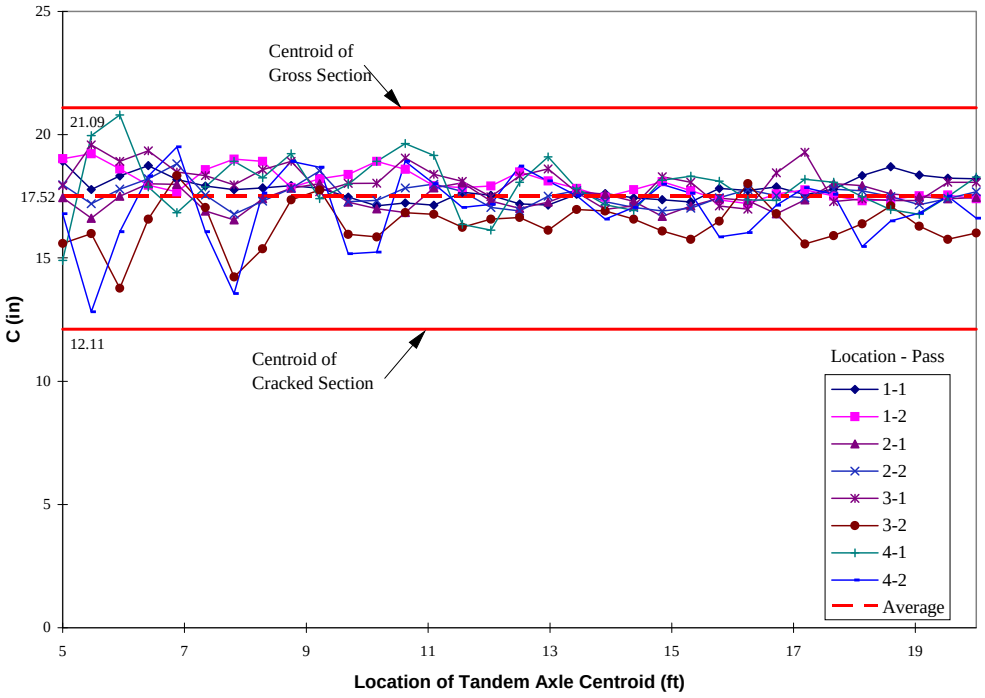

Figure 5.28 Comparison of Centroid Locations in the Curb.

The average centroid of the curb is closer to the calculated gross section centroid. The location of the average centroid reaffirms that the curb may not be behaving as a fully cracked section.

5.4 EVALUATION OF DEFLECTIONS

As discussed in Appendix A, the validity of the deflection measurements is questionable. The string potentiometers were not sensitive enough to accurately measure the very small deflections occurring in the bridge. The data in Appendix G shows the discrete steps as the deflection changes indicating some question in the accuracy of the data.

The deflections were calculated using an effective moment of inertia, I_e. The equation from the AASHTO Specifications [13] was used to calculate I_e. The effective moment of inertia was 1203 $in.^4$ for the slab and 34,300 $in.^4$ for the curbs. A structural analysis package was used to calculate the maximum deflections.

Although there is doubt in the accuracy of the data, a comparison of the test results and calculated values was made. Figures 5.29 and 5.30 show the deflections for a truck at location 1 and location 2. In addition to the test data, calculated deflections were plotted also. These deflections were based on both simple supports and fixed-end supports. Based on the data from the plots the bridge supports are behaving somewhere between simple and fixed, which is what was expected. The assumption discussed earlier of using fixed-end supports is justified. The use of fixed supports will give conservative results for adjusting the load rating.

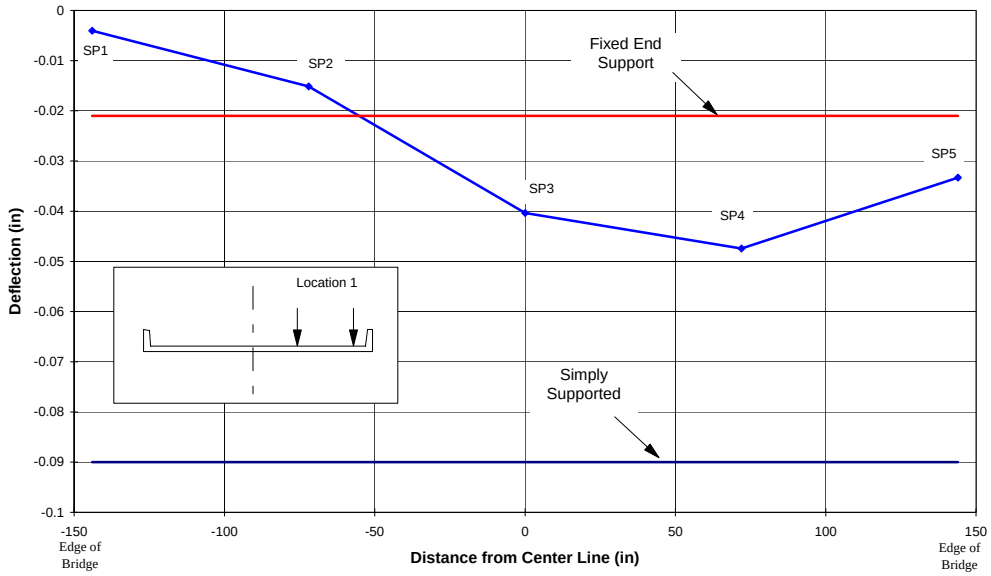

Figure 5.29 Comparison of Deflection Results with Analysis, Location 1.

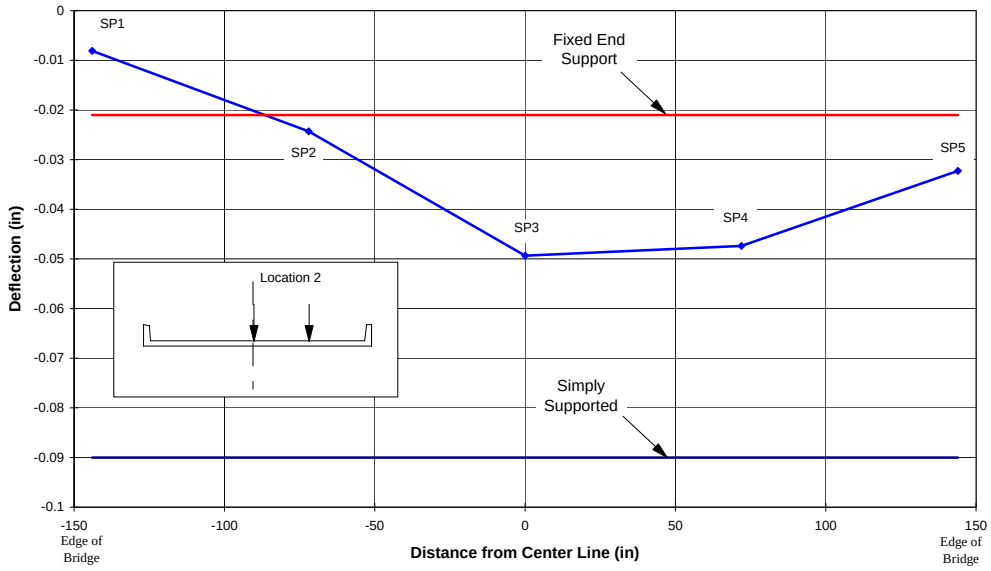

Figure 5.30 Comparison of Deflection Results with Analysis, Location 2.

5.5 SUMMARY

Although the bridge was designed as a simple span, it is proven from the discussion above that it is no longer behaving as a simple span. The supports may not be behaving as true fixed ends, but this model is giving reasonable results and these results will be conservative when applied to load rating adjustments. Further investigation in the behavior of the support conditions is necessary before a more accurate model can be used.

Chapter 6. CONCLUSIONS AND RECOMMENDATIONS

6.1 FEASIBILITY OF TESTING SLAB BRIDGES

Based solely on the improved load ratings shown by this test, the testing of slab bridges is economically feasible. Current TxDOT policy states that if a bridge has a inventory rating less than HS20 then the bridge will be posted or inspected more frequently [15]. Therefore if a slab bridge has an inventory rating less than HS20 then testing would be justified to reduce future inspections or to eliminate a posting.

The possible change in posting policy or an increase in the legal load should also be a consideration when deciding on a testing program. If the legal load is increased above the operating rating of a bridge then the bridge must be posted [15]. If this occurred it would be more economically feasible to test the bridges than to load post them.

6.2 CONCLUSIONS

The results of this research indicate the following:

1. Inspection of the bottom of the slab is important to determine crack location. The instruments should be placed at cracked locations if possible because these sections control.
2. Surface strain measurement of concrete in the tension areas is too dependent on placement to be reliable. The results may vary widely depending on whether a crack was crossed or not. Load history also

influences surface strain. Previous loadings that were very heavy may cause severe cracking.

3. Concrete compressive strengths were higher than design values. This will not affect the adjustment to the load rating but will increase the original load rating.
4. The load rating is controlled by the slab at centerline and midspan. The curb should be checked to verify this during the testing of each bridge.
5. The neutral axis of both the curb and the slab were higher than calculated. This was likely due to averaging across cracked and uncracked sections.
6. The string potentiometers used for deflection measurement were not sensitive enough for the very small deflections during this test. Instruments with greater sensitivity or heavier test trucks will be required to obtain good deflection data.

6.3 RECOMMENDATIONS FOR TESTING

The proper testing of a slab bridge requires planning, instrumentation and performing the actual test. Each of these steps are equally important and will be discussed in detail.

6.3.1 Planning

The planning of the test requires a thorough investigation of the bridge. The bridge should be checked to determine if it is actually a candidate for testing. This can be determined by checking the inspection record and verifying it is not structurally deficient. The bridge should then be analyzed and the controlling member should then be rated. At this point if the bridge is eligible for testing a

test plan should be developed. The plan should include detailed sketches and descriptions of gage locations, data acquisition setup, truck configuration, test speed and truck location. All members of the test team should be familiar with the plan during testing.

6.3.2 Instrumentation

The recommended instrumentation for a slab bridge should include gaging both the slab and curb. The bottom reinforcing bars should be exposed in three locations, centerline, curb and at the midpoint between the curb and centerline. These locations should be instrumented with strain gages as discussed in Appendix A. This type of instrumentation requires considerable effort but guarantees good tension strains. The top of the curb should be instrumented with a strain gage placed on the surface according to the procedure outlined in Appendix A. All gages should be installed with experienced personnel and according to manufacturer's instructions.

6.3.3 Testing

The actual testing requires proper planning in order to perform the test in a timely manner. The setup of the data acquisition system may require considerable time and this should be considered when planning for the test truck arrival time. Traffic control is a major consideration and should be planned for accordingly. This type of testing requires that traffic be stopped during the test. The recommended truck locations for testing are the same as location 1 and location 2 used in this test. These locations should give the worst case loadings to the curb and also to the slab at centerline.

With experience the complete testing of a slab bridge from first arriving at the site to the final clean up and repair should require an average of three days. This time will vary depending on the traffic and any problems during installation or testing.

6.3 FUTURE RESEARCH

Several areas should be investigated in the testing of slab bridges. These areas include:

1. Further investigation of surface strain measurements of concrete. If surface strain measurement could be accomplished this would greatly improve instrumentation time.
2. The method of measuring deflections should be studied. This bridge was ideal in that it was approximately 6 feet from the bottom of the slab to a stable surface. A method should be developed to measure deflections if the bridge spans something that cannot be anchored to, such as, water or a road carrying traffic.
3. The use of an electronic tape switch to mark the location of the truck should be studied. The use of this device would eliminate the need for a person to operate a triggering device and eliminate the human error involved in this operation.
4. The end restraint of this type of bridge should be studied. Fixed ends were assumed for this test. This should be investigated to determine if this assumption was valid.

5. Skewed bridges of this type should be analyzed and tested to determine if the testing procedure recommended here would apply to skewed bridges.
6. Bridges without curbs and bridges without structural curbs should both be tested to verify that the recommended method of testing would apply.

Chapter 6. COMPARISON WITH PREVIOUS TEST RESULTS

The test results from a 1946 test by TxDOT [10] on a bridge with identical design dimensions, will be compared with the measured response of the bridge near Austin. Because of the different loadings used for each test, a method of relating the tests had to be determined. In order to compare the results, superposition was used to simulate two loading vehicles. In addition, the strains from the TxDOT test were reduced by 20% to account for the difference between the point load and the tandem axle as shown in Figure 5.1.

6.1 STRAIN DISTRIBUTION COMPARISON

Measured reinforcing bar strains across one half of the bridge are compared with data from the slab test by TxDOT [10]. As shown in Figures 6.1 and 6.2, the TxDOT results were considerably higher than the strains measured in this test.

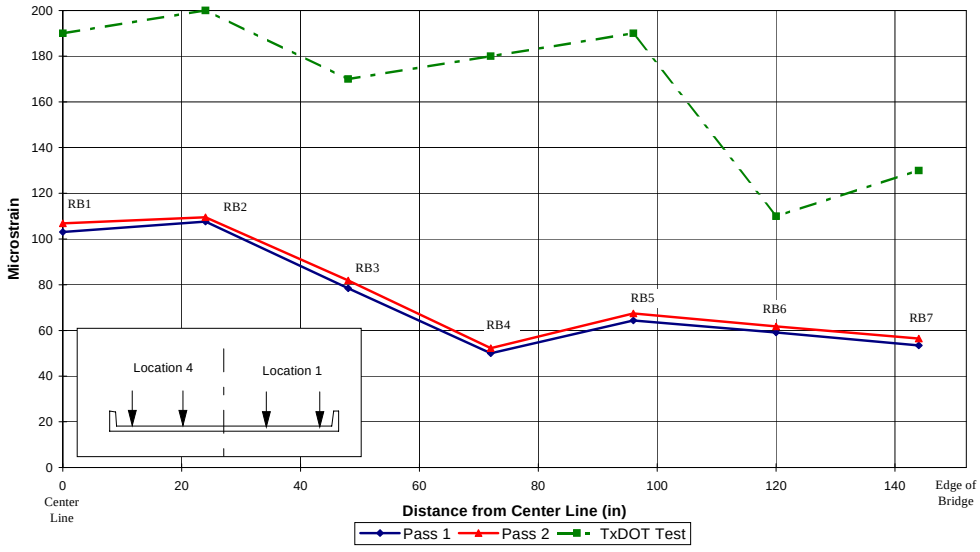

Figure 6.1 Comparison of Rebar Strains and TxDOT Test Strains, Location 1&4.

The average difference between the reinforcing bar strains is 92 microstrain for the data shown in Figure 6.1 and 76 microstrain for the data shown in Figure 6.2.

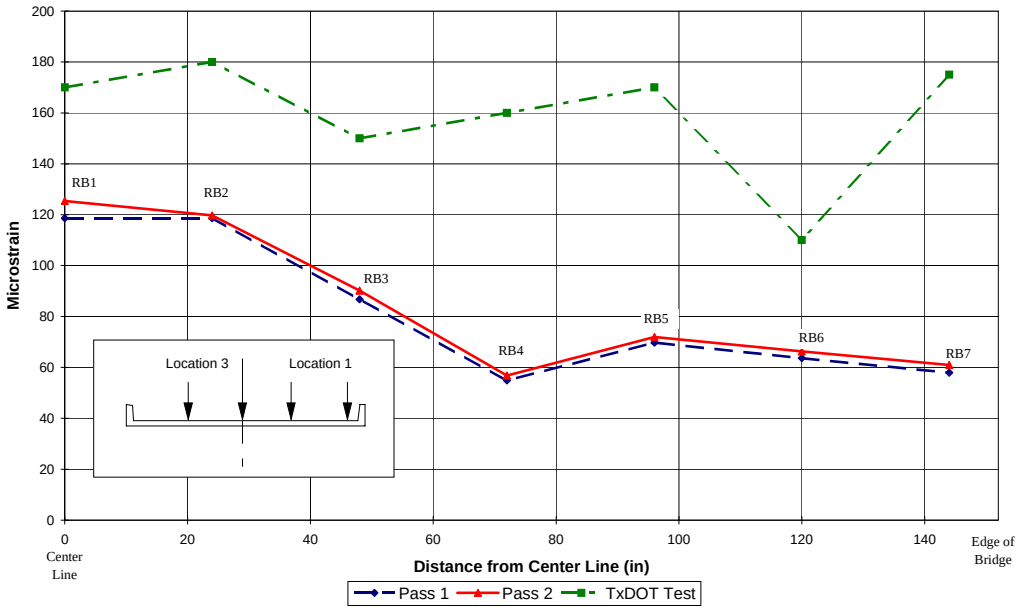

Figure 6.2 Comparison of Rebar Strains and TxDOT Test Strains, Location 1&3.

There are several possible reasons for the discrepancies between the two tests. The TxDOT test loadings were done by using a frame system with rams to simulate 4 wheel loads at midspan [10]. This allowed for very accurate load placement and loading increments.

In order to compare with the TxDOT test, results were superimposed to simulate two trucks. The superposition of the loads would cause some difference because the truck positions were not exactly the same as the positions of the rams

in the TxDOT test. There is also some error due to using superposition of a nonlinear system such as a concrete slab.

The test truck also had a tandem axle whereas the TxDOT test used rams to apply point loads. This difference was accounted for in the plots by applying a 20% reduction to the TxDOT results. In a future test, two trucks configured similarly to the TxDOT test loads should be used to compare with the TxDOT test results.

There is also some error due to the fact that the loading method used by TxDOT led to full cracking of the curb and the slab. Figure 6.3 shows the crack patterns observed during the TxDOT test. The patterns show a uniform crack across midspan. This cracking pattern is not apparent in this test bridge (Figure 3.3). This would account for some difference because as discussed previously it is felt that this bridge may not be behaving like a fully cracked section.

The most likely source of error is due to the support behavior. It was determined in Chapter 5 that the bridge is not behaving as a simple span. The fixed-end model shown in Chapter 5 resulted in a good comparison between the test results and the calculated strains.

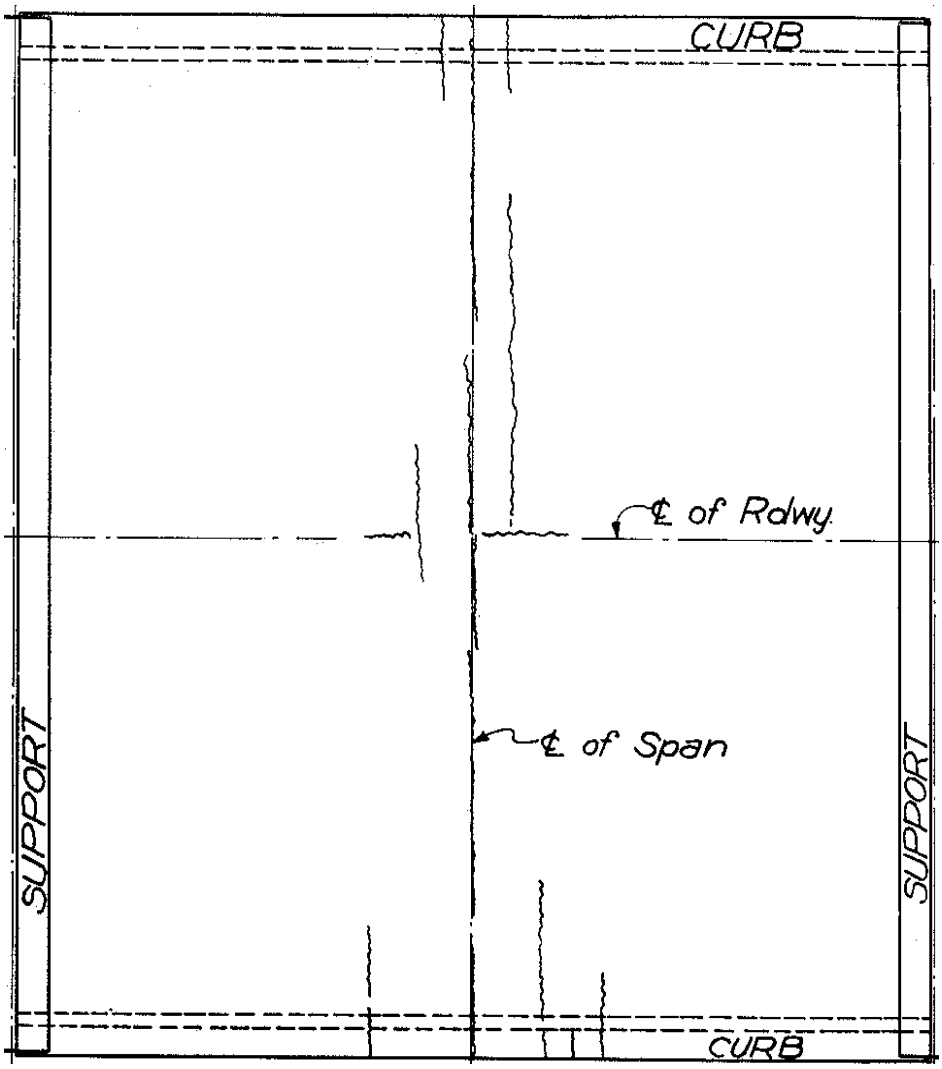

Figure 6.3 Crack Patterns for TxDOT Load Test [10].

6.2 Comparison of TxDOT Deflection Measurements

In addition to strain measurements, deflection data were also compared with the test results. As shown in Figure 6.4, the TxDOT deflections are greater than the test deflections. The average difference between the deflections is 0.03

inches or 48%. These differences are caused by the same reasons as were discussed for the differences in strain comparisons. In addition, the string potentiometers used to measure deflections were not precise enough to measure the very small deflections during the test. Because of these reasons the deflection comparison is of questionable value but included for completeness.

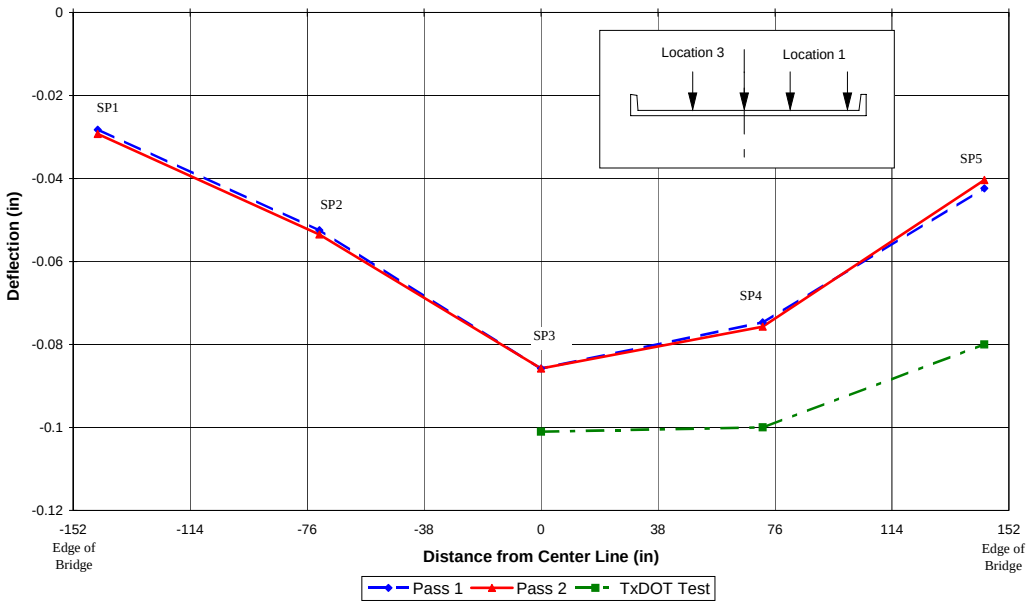

Figure 6.4 Comparison of Deflection Results and TxDOT Test.

6.3 Summary

The ability to match the previous test results [10] with future tests will be difficult because the original test was performed on a new bridge that had never been loaded. The end conditions were operating properly, the bridge was uncracked at the start of the test and the load was applied in a very precise manner.

Chapter 7. LOAD RATING BASED ON MEASURED DATA

7.1 METHODOLOGY OF LOAD RATING BASED ON A LOAD TEST

The method used to adjust the load rating of this bridge based on the load test results is outlined in Chapter 6 of the Manual for Bridge Rating through Load Testing [11]. The procedure outlined in the manual involves applying an adjustment factor (K factor) to the existing rating. This factor is based on the load test and may increase or decrease the load rating depending on the test results [11].

The K factor is defined as follows [11]:

$$K = 1 + K_a \times K_b \tag{7.1}$$

where:

$$K_a = \frac{\varepsilon_c}{\varepsilon_T} - 1 \tag{7.2}$$

ε_T is the maximum test strain for a member.

ε_c is the calculated strain for a member based on the test load.

$$K_b = K_{b1} \times K_{b2} \times K_{b3} \tag{7.3}$$

In order to determine K_{b1}, K_{b2}, and K_{b3}, the Manual [11] provides tables based on confidence in analysis, inspection frequencies, and critical structural features. These tables are repeated below for reference.

Table 7.1 Table to Determine K_{b1} [11].

Can member behavior be extrapolated to 1.33W?		Magnitude of test load			K_{b1}
Yes	No	$\frac{T}{W} < 0.4$	$0.4 \le \frac{T}{W} \le 0.7$	$\frac{T}{W} > 0.7$	
√		√			0
√			√		0.8
√				√	1.0
	√	√			0
	√		√		0
	√			√	0.5

In Table 7.1 the variables W and T are defined as follows:

W = Rating Load Effect.

T = Test Vehicle Effect

Table 7.2 Table to Determine K_{b2} [11].

INSPECTION		K_{b2}
Type	Frequency	
Routine	between 1 & 2 years	0.8
Routine	less than 1 year	0.9
In-Depth	between 1 & 2 years	0.9
In-Depth	less than 1 year	1.0

Table 7.3 Table to Determine K_{b3} [11].

Fatigue Controls?		Redundancy		K_{b3}
No	Yes	No	Yes	
	√	√		0.7
	√		√	0.8
√		√		0.9
√			√	1.0

7.2 LOAD RATING OF THE TEST BRIDGE

As discussed in Chapter 2, the load rating of a bridge is based on the controlling member of the bridge. Therefore just as the rating in Chapter 2 considered both the curb and the slab, this adjustment to the rating will consider both structural members also. The highest values of tensile strain measured from the reinforcing bars during the test are used to determine the K factor.

The ends of this bridge were partially restrained against rotation. As discussed in Chapter 5, this end restraint resulted in the development of two models of the bridge. The first model was a simple span and the second model was a span with fixed ends. Calculated strains from both models were compared with the test results and the fixed-end model compared favorably with the test data. Although the fixed-end model gave favorable results, the level of end fixity is still unknown. Therefore for the purpose of adjusting the load ratings based on test data, calculated strains from both the simple-span and fixed-end models will be used in an attempt to bound the actual load rating. Further testing of the end conditions will allow the load rating to be more reliably adjusted.

7.2.1 Slab Load Rating Adjustment Factor

The calculated values of strain for midspan based on the distributed moments from Section 5.1 are listed below. These values were based on a cracked section as discussed in Section 5.2.1.

Simple-span conditions: Maximum Strain = 168 με

Fixed-end conditions Maximum Strain = 76 με

The peak value of strain during the test occurred at gage RB1, Location 2, Pass 1 for test series 3 (Table 4.1). This peak value was 75 microstrain. From equation 7.2 for K_a:

Simple Span: $K_a = \frac{168}{75} - 1 = 1.24$

Fixed End: $K_a = \frac{76}{75} - 1 = 0.013$

These values will be used later to determine the adjustment to the load rating.

7.2.2 Curb Load Rating Adjustment Factor

The calculated values for strain in the curb for both simple and fixed-end conditions are shown below. These values are the maximum calculated values for the curb reinforcing bars.

Simple-span conditions: Maximum Strain = 137 με

Fixed-end conditions Maximum Strain = 56 με

The peak value of strain during the test occurred during test series 1, Location 1, Pass 2 (Table 4.1). This peak value was 46 microstrain. From equation 7.2 for K_a:

Simple Span: $K_a = \frac{137}{46} - 1 = 1.98$

Fixed End: $K_a = \frac{56}{46} - 1 = 0.217$

7.2.3 Determination of K_b

From Table 7.1 the value for K_{b1} can be determined. The bridge must behave linearly at 1.33 times the rating vehicle. From Chapter 2 the operating rating factor for the bridge was determined to be 1.47, therefore this shows that the bridge will behave linearly at 1.33W.

In order to determine the T/W ratio for Table 7.1, the total moment for the test truck was divided by the moment of the rating vehicle. This resulted in a ratio of 0.5. From Table 7.1 and the above factors,

$K_{b1} = 0.8$

From Table 7.2 and the current inspection report which shows an inspection frequency of 2 years,

$K_{b2} = 0.8.$

Because the bridge is reinforced concrete, it is assumed to have redundancy and is not susceptible to fracture or fatigue failures. Therefore,

$K_{b3} = 1.0.$

The calculated K_b factor based on equation 7.3 is shown below.

$K_b = 0.8 \times 0.8 \times 1.0 = 0.64$

7.2.4 Adjusted Load Rating

Based on the values discussed above and equation 7.1, the calculated results for the adjustment factor K are shown in Table 7.4

Table 7.4 K Factors for Slab and Curb

	End Conditions	
	Simple	Fixed
Slab	1.79	1.01
Curb	2.27	1.14

The K factors from Table 7.4 were applied to the original rating factors from Chapter 2 and the resulting adjusted load ratings are shown in Table 7.5 and 7.6. The original load ratings in Table 7.5 and Table 7.6 are based on simple span analysis only. The percent increase is based on the increase from the original load rating. The controlling factors for the bridge are slab ratings in all cases.

Table 7.5 Comparison of Load Ratings for the Curb.

Load Ratings				
End Conditions		Original	Adjusted	% Increase
Simple	Operating	HS41.2	HS93.5	127%
	Inventory	HS24.6	HS55.8	127%
Fixed	Operating		HS47.0	14%
	Inventory		HS28.0	14%

Table 7.6 Comparison of Load Ratings for the Slab.

Load Ratings				
End Conditions		Original	Adjusted	% Increase
Simple	Operating	HS29.4	HS52.6	79%
	Inventory	HS17.6	HS31.5	79%
Fixed	Operating		HS29.7	1%
	Inventory		HS17.8	1%

7.3 SUMMARY

From observing the results in Tables 7.5 and 7.6, it is obvious that a very unconservative rating could be obtained if the improper choice is made for the in-situ end conditions of the bridge. From these results, no significant increase in load rating is achieved, but the model used is based on totally fixed ends which is not the case with this bridge. Therefore it could be proven with further testing for end restraint, that a more appropriate and higher load rating may be used.

Chapter 8. CONCLUSIONS AND RECOMMENDATIONS

8.1 FEASIBILITY OF TESTING SLAB BRIDGES

Based solely on the improved load ratings shown by this test, the testing of slab bridges is economically feasible. Current TxDOT policy states that if a bridge has a inventory rating less than HS20 then the bridge will be posted or inspected more frequently [15]. Therefore if a slab bridge has an inventory rating less than HS20 then testing would be justified to reduce future inspections or to eliminate a posting.

The possible change in posting policy or an increase in the legal load should also be a consideration when deciding on a testing program. If the legal load is increased above the operating rating of a bridge then the bridge must be posted [15]. If this occurred it would be more economically feasible to test the bridges than to load post them.

8.2 CONCLUSIONS

The results of this research indicate the following:

1. Inspection of the bottom of the slab is important to determine crack location. The instruments should be placed at cracked locations if possible because these sections control.
2. Surface strain measurement of concrete in the tension areas is too dependent on placement to be reliable. The results may vary widely depending on whether a crack was crossed or not. Load history also

influences surface strain. Previous loadings that were very heavy may cause severe cracking.

3. Concrete compressive strengths were higher than design values. This will not affect the adjustment to the load rating but will increase the original load rating.
4. The load rating is controlled by the slab at centerline and midspan. The curb should be checked to verify this during the testing of each bridge.
5. The neutral axis of both the curb and the slab were higher than calculated. This was likely due to averaging across cracked and uncracked sections.
6. The string potentiometers used for deflection measurement were not sensitive enough for the very small deflections during this test. Instruments with greater sensitivity or heavier test trucks will be required to obtain good deflection data.

8.3 RECOMMENDATIONS FOR TESTING

The proper testing of a slab bridge requires planning, instrumentation and performing the actual test. Each of these steps are equally important and will be discussed in detail.

8.3.1 Planning

The planning of the test requires a thorough investigation of the bridge. The bridge should be checked to determine if it is actually a candidate for testing. This can be determined by checking the inspection record and verifying it is not structurally deficient. The bridge should then be analyzed and the controlling member should then be rated. At this point if the bridge is eligible for testing a

test plan should be developed. The plan should include detailed sketches and descriptions of gage locations, data acquisition setup, truck configuration, test speed and truck location. All members of the test team should be familiar with the plan during testing.

8.3.2 Instrumentation

The recommended instrumentation for a slab bridge should include gaging both the slab and curb. The bottom reinforcing bars should be exposed in three locations, centerline, curb and at the midpoint between the curb and centerline. These locations should be instrumented with strain gages as discussed in Appendix A. This type of instrumentation requires considerable effort but guarantees good tension strains. The top of the curb should be instrumented with a strain gage placed on the surface according to the procedure outlined in Appendix A. All gages should be installed with experienced personnel and according to manufacturer's instructions.

8.3.3 Testing

The actual testing requires proper planning in order to perform the test in a timely manner. The setup of the data acquisition system may require considerable time and this should be considered when planning for the test truck arrival time. Traffic control is a major consideration and should be planned for accordingly. This type of testing requires that traffic be stopped during the test. The recommended truck locations for testing are the same as location 1 and location 2 used in this test. These locations should give the worst case loadings to the curb and also to the slab at centerline.

With experience the complete testing of a slab bridge from first arriving at the site to the final clean up and repair should require an average of three days. This time will vary depending on the traffic and any problems during installation or testing.

8.3 FUTURE RESEARCH

Several areas should be investigated in the testing of slab bridges. These areas include:

1. Further investigation of surface strain measurements of concrete. If surface strain measurement could be accomplished this would greatly improve instrumentation time.
2. The method of measuring deflections should be studied. This bridge was ideal in that it was approximately 6 feet from the bottom of the slab to a stable surface. A method should be developed to measure deflections if the bridge spans something that cannot be anchored to, such as, water or a road carrying traffic.
3. The use of an electronic tape switch to mark the location of the truck should be studied. The use of this device would eliminate the need for a person to operate a triggering device and eliminate the human error involved in this operation.
4. The end restraint of this type of bridge should be studied. Fixed ends were assumed for this test. This should be investigated to determine if this assumption was valid.

5. Skewed bridges of this type should be analyzed and tested to determine if the testing procedure recommended here would apply to skewed bridges.
6. Bridges without curbs and bridges without structural curbs should both be tested to verify that the recommended method of testing would apply.

Chapter 8. CONCLUSIONS AND RECOMMENDATIONS

8.1 FEASIBILITY OF LOAD TESTING SLAB BRIDGES

The results of this test are inconclusive in determining the feasibility of load testing slab bridges. The end conditions of the slab bridge must be evaluated before an improved load rating can be determined. If the load rating is adjusted based on simply supported condition (design assumption), then the results are likely to be very unconservative.

8.2 CONCLUSIONS

The results of this research indicate the following:

1. All measurements were very sensitive to the extent of cracking. The extent of cracking is difficult to determine because the load history of the bridge is unknown and the traffic loads were not applied in a monotonic manner. A detailed evaluation of the bridge is necessary before testing to locate and measure all existing cracks.
2. The method for load testing was reliable and repeatable. Slight differences in truck location influenced peak measured strains by less than ±10%.
3. The instruments should be placed across existing cracks or in regions of distributed cracks. Strains measured by instruments that crossed cracks were significantly higher than strains measured by instruments attached to sound concrete.

4. The most reliable results were obtained by instrumenting the reinforcing bars. Although this requires considerable effort, the quality of the test results justifies the effort.
5. Reliable results were also obtained using wire strain gages attached to the surface of the concrete in the compression areas. However, gages installed on the top surface of the slab malfunctioned when subjected to traffic. An improved procedure should be developed to protect these gages.
6. Surface strain measurement of concrete in the tension areas using wire strain gages or strain transducers is too dependent on placement of the gage to be reliable. The results vary widely depending on the gage location in relation to the cracks.
7. For this bridge, the load rating was controlled by the slab at centerline and midspan. However, the ends of the span should be instrumented to determine rotational restraint. The curb should be checked to verify end rotation and to verify the slab controls during the testing of each bridge.
8. The neutral axis of both the curb and the slab were bounded by the cracked section neutral axis and the gross section neutral axis. This was likely due to averaging across cracked and uncracked sections.
9. Concrete compressive strengths were considerably higher than design values based on the results of nondestructive tests. The increased strength leads to an increase in the original load rating because the member capacity is increased, but has essentially no effect on the calculated strains for comparison with test results.

10. The string potentiometers used for deflection measurement were not sensitive enough for the very small deflections during this test. Instruments with greater sensitivity or heavier test trucks will be required to obtain good deflection data.

8.3 RECOMMENDATIONS FOR TESTING

The proper testing of a slab bridge requires planning, instrumentation and performing the actual test. Each of these steps is equally important and will be discussed in detail.

8.3.1 Planning

The planning of the test requires a thorough investigation of the bridge. The bridge should be checked to determine if it is actually a candidate for testing. This can be determined by checking the inspection record and verifying it is not structurally deficient. At this point the bridge is eligible for testing. The bridge should then be analyzed and the controlling member should then be rated. A test plan should be developed for each specific bridge. The plan should include detailed sketches and descriptions of gage locations, data acquisition setup, truck configuration, test speed and truck location. All members of the test team should be familiar with the plan during testing.

8.3.2 Instrumentation

The recommended instrumentation for a slab bridge should include gaging both the slab and curb. The bottom reinforcing bars should be exposed in three locations, centerline, curb and at the midpoint between the curb and centerline. These locations should be instrumented with strain gages as discussed in

Appendix A. This type of instrumentation requires considerable effort but guarantees good tensile strains. The top of the curb should be instrumented with a strain gage placed on the surface according to the procedure outlined in Appendix A. The ends of the bridge should be gaged to determine rotational restraint. Deflection gages should be installed at three locations, centerline and at each curb line. All gages should be installed with experienced personnel and according to manufacturer's instructions.

A data acquisition system with faster sampling rates and more available channels is highly recommended. The actual testing time would be reduced considerably if such a system is used. The effects of dynamic impact could also be measured with a faster sampling system.

8.3.3 Testing

The actual testing requires proper planning in order to perform the test in a timely manner. The setup of the data acquisition system may require considerable time and this should be considered when planning for the test truck arrival time. Traffic control is a major consideration and should be planned for accordingly. This type of testing requires that traffic be stopped during the test. The recommended truck locations for testing are the same as location 1 and location 2 used in this test. These locations should give the worst case loadings to the curb and also to the slab at centerline.

With experience the complete testing of a slab bridge from first arriving at the site, to the final clean up and repair, should require an average of three days.

This time will vary depending on the traffic and any problems during installation or testing.

8.4 FUTURE RESEARCH

Several areas should be investigated in the testing of slab bridges. These areas include:

1. Further investigation of surface strain measurements of concrete is necessary. If surface strain measurement could be accomplished this would greatly reduce instrumentation time.
2. The method of measuring deflections should be studied. This bridge was ideal in that it was approximately 6 feet from the bottom of the slab to a stable surface. A method should be developed to measure deflections if the bridge spans something that makes anchoring difficult, such as water or a road carrying traffic.
3. The use of an electronic tape switch to mark the location of the truck should be studied. The use of this device would eliminate the need for a person to operate a triggering device and eliminate the human error involved in this operation.
4. The end restraint of this type of bridge should be studied. The measured data were bounded by simple-support conditions and fixed-end conditions. The evaluation of rotational restraint would lead to better estimates of capacity.
5. Skewed bridges of this type should be analyzed and tested to determine if the testing procedure recommended here would apply to skewed bridges.

6. Bridges without curbs and bridges without structural curbs should both be tested to verify that the recommended method of testing would apply.

Appendix A. TEST INSTRUMENTATION AND PROCEDURE

A.1. INSTRUMENTATION

A.1.1 Strain Gages

Two types of electrical resistance strain gages were used to measure strain during this load test. The first type was a strain gage commonly identified as a foil gage. These gages had a gage length of 6mm, a resistance of 119.5 (±0.5) ohms and a gage factor of 2.12 (±1%). These gages had three wire leads of approximately 3 feet. The second type of strain gage has a long gage length of 60 mm and is usually used on concrete. These gages are sometimes referred to as wire gages. The gages had two wire leads of approximately 3 feet. The gages had a resistance of 120.3 (±0.5) ohms and a gage factor of 2.09 (±1%).

A.1.2 Strain Transducers

The strain transducers used in this series of tests were borrowed from the Texas Department of Transportation (TxDOT). The transducers were originally developed during a previous research project to measure fatigue stresses in steel girder bridges [17]. They are 1.5 inches by 8 inches by 0.25 inches in size and have a gage length of 7 inches. The gages provide a mechanical amplification of about 7.5 [17]. The transducers may be mounted on the bridge with C clamps or by bolting to previously mounted tabs.

A.1.3 Deflection Measurement Devices

String potentiometers were used to measure deflections for this test. They have approximately 5 inches of range which was more than sufficient for this test.

A.1.4 Data Acquisition System

A Campbell Scientific, Inc. 21X Micrologger was used to sample the data. This system was also borrowed from TxDOT. The system was limited to eight channels and one channel was used for measuring external excitation. This resulted in only seven channels available to gather data. This channel limitation was due to the slow sampling rate of the system. The sampling rate was limited to 16 Hz. An IBM compatible laptop computer was used to control the system.

A.1.5 Number and Location of Gages

The number and general location of the strain gages used for this test are shown in Table A.1 and in Figure A.1. The strain gages and transducers were all placed at midspan of the bridge. Figures A.2 through A.4 show the location of the various gages.

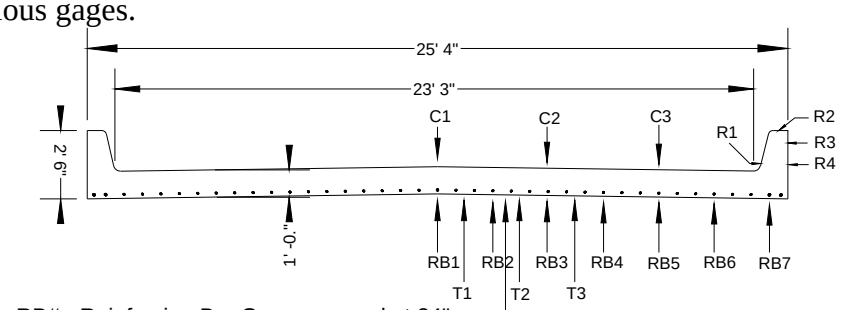

RB# - Reinforcing Bar Gages spaced at 24"
T# - Strain Transducers spaced at 24"
F# - Wire Strain Gages placed in tension
C# - Wire Strain Gages placed on top of slab
R# - Wire Strain Gages placed on structural curb
represents gage number

Note: All gages are placed at midspan of the bridge.

Figure A.1 General Location and Type of Instrumentation Used for Bridge Test.

Table A.1 Instrumentation Details for Each Test Series.

	Test Series	1	2	3	4	5
	Truck Location	1, 2, 3, 4	1, 2	1, 2	1, 2, 3, 4	1, 2, 3, 4
Gage Type	Gage Number					
Resistance Gage (Foil Gage) Placed on Exposed Tension Rebar	RB1	X	X	X		
	RB2	X	X			
	RB3	X	X	X		
	RB4	X	X			
	RB5	X		X	X	X
	RB6	X				
	RB7	X			X	
Resistance Gage (Wire Gage) Placed on Surface of Curb	R1				X	
	R2				X	
	R3				X	
	R4				X	
Resistance Gage (Wire Gage) Placed on Top of Slab	C1			X		
	C2			X		
	C3			X	X	X
Resistance Gage (Wire Gage) Placed on Bottom Surface of Slab	F1			X		
Strain Transducers Mounted on Bottom Surface of Slab	T1		X			
	T2		X			
	T3		X			
String Potentiometers Mounted on Bottom Surface of Slab	SP1					X
	SP2					X
	SP3					X
	SP4					X
	SP5					X

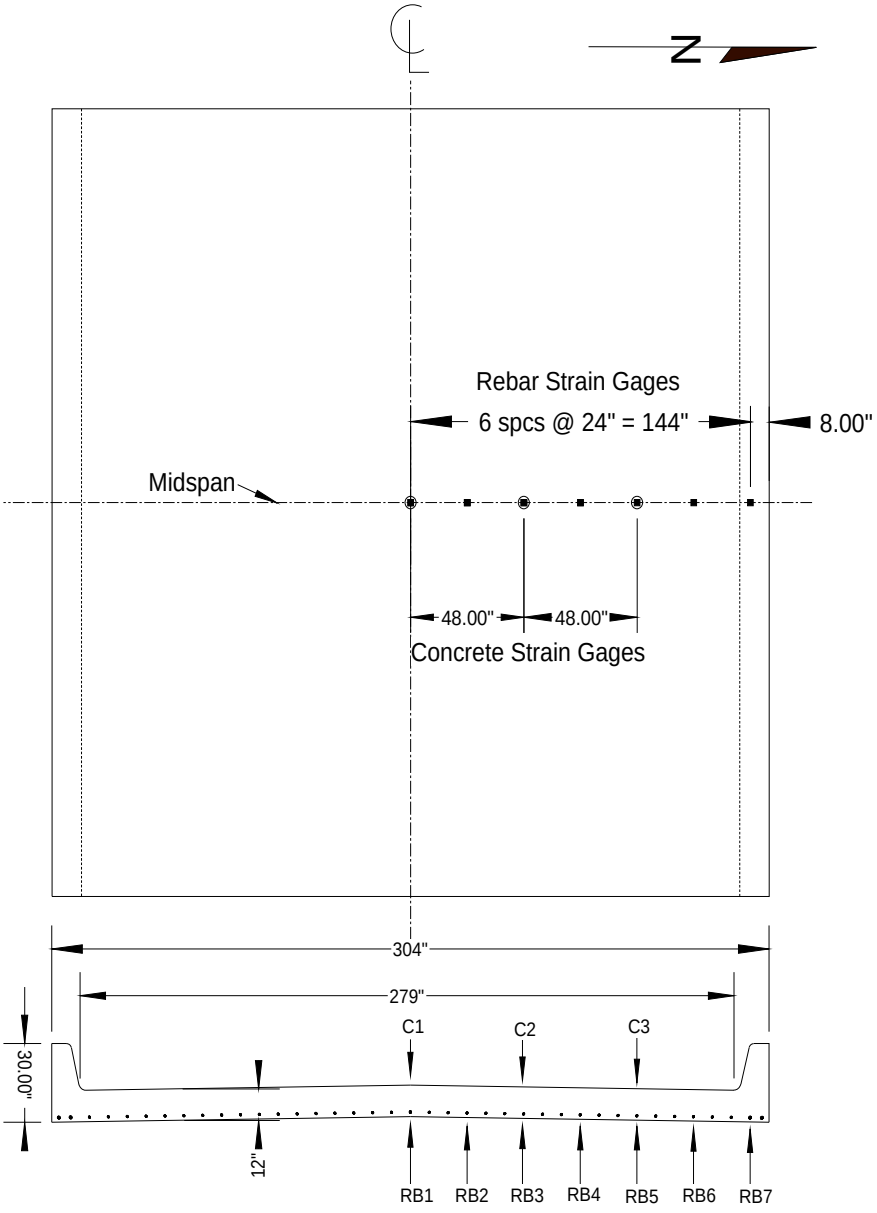

Figure A.2 Detailed Locations of Rebar Gages and Slab Gages.

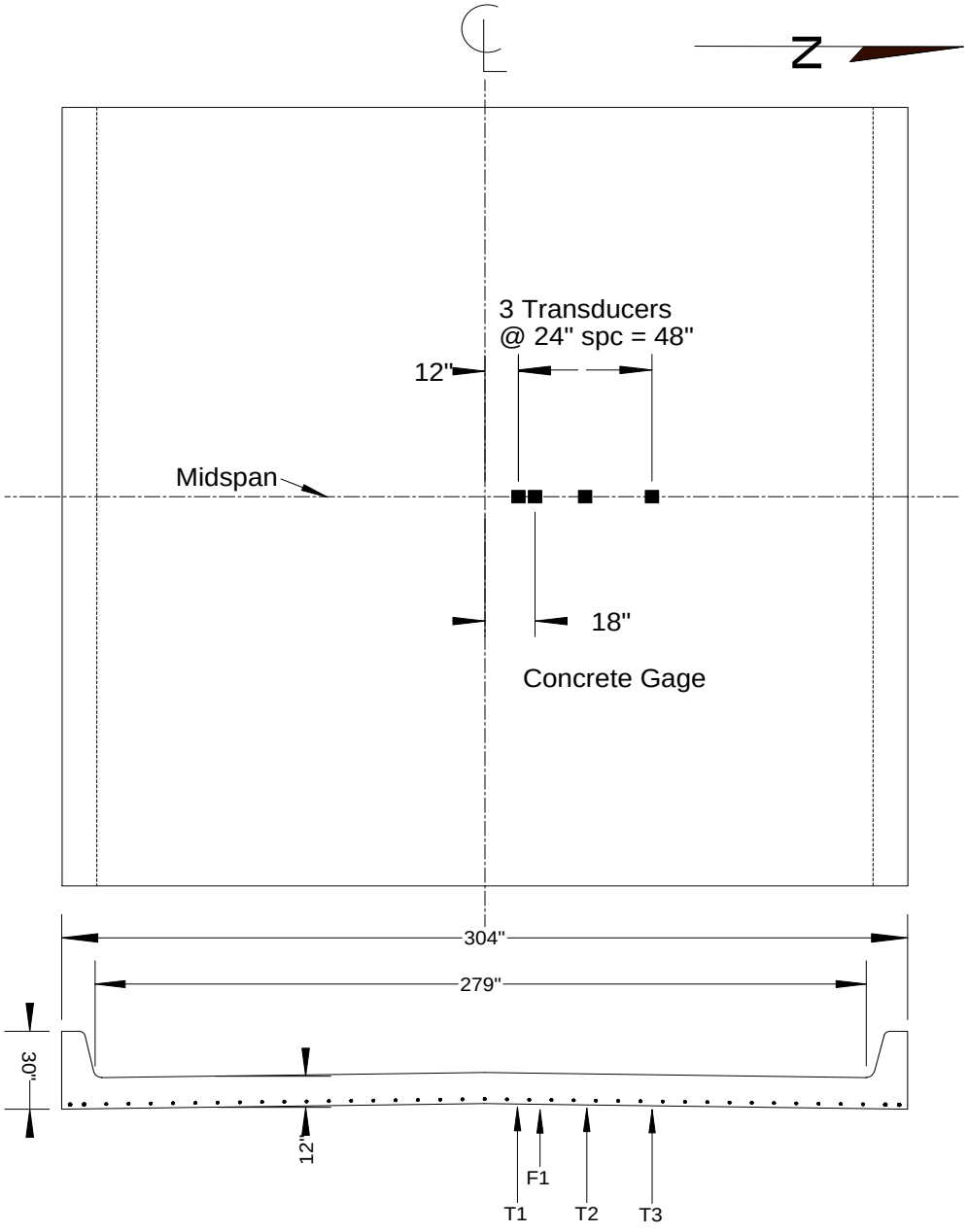

Figure A.3 Detailed Locations of Transducers and Bottom of Slab Gage.

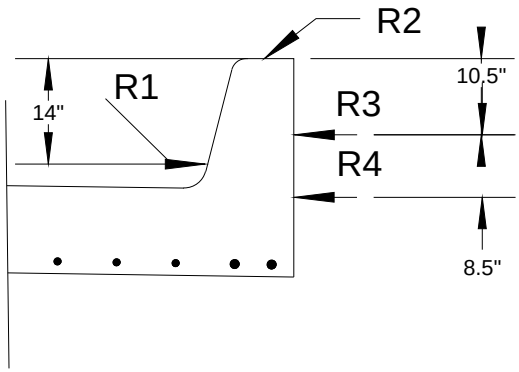

Figure A.4 Detailed Locations of the Concrete Gages on the Rail.

The locations of the gages were limited to one side of the bridge because the bridge is symmetrical about centerline. The locations were chosen to determine load distribution, rail behavior and to compare surface strain measurements with strains measured on the surface of the reinforcing bars.

A.2 LOADING

A.2.1 Loading Vehicle

The loading vehicle used for this test was a 10 cubic yard dump truck. The vehicle and driver were furnished by TxDOT. Figure A.5 shows the truck used during the test. The truck was weighed using scales at a local feed mill. The truck was loaded with roadway base material and the gross weight was 48,740 pounds. The truck had a single front axle weighing 10,850 pounds and a tandem rear axle weighing 37,890 pounds. Figure A.6 shows a sketch of the axle weights and the axle spacing.

Figure A.5 Side View of Truck Used for the Load Test.

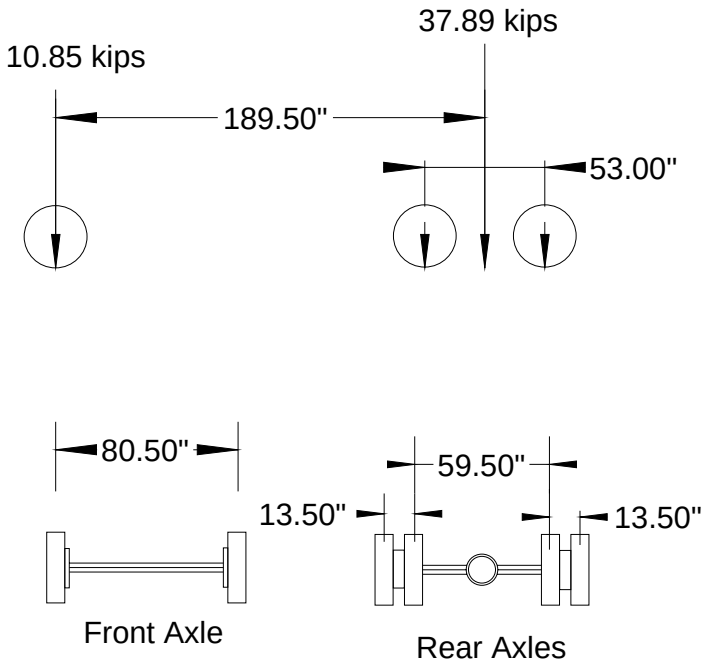

Figure A.6 Sketch of the Truck Configuration.

A.2.2 Loading Procedure

The truck was driven across the bridge at approximately 5 miles per hour for most of the tests and at approximately 30 miles per hour for one test series. The 30 mph truck speed was an attempt to measure impact, but because of the limitations of the data acquisition system, adequate data could not be obtained. A moving load was used to minimize the time required to test. The negative effect on the traveling public was lessened by minimizing test times. The behavior of the bridge could also be observed as the load was moved across the bridge. The slow speed was used in order to minimize dynamic impact and maximize the data obtained.

A.2.3 Location of Loads

The locations of the loads are shown in Figure A.7. These locations were chosen based on previous tests [10].

A location indicator was used to mark the longitudinal location of the truck in the data sample. This was done by a member of the test team triggering the device as the front axle passed over each bearing. The device was a manually operated electronic device, physically connected to the data acquisition system. The cable limited movement and made it difficult to get accurate markings for this test.

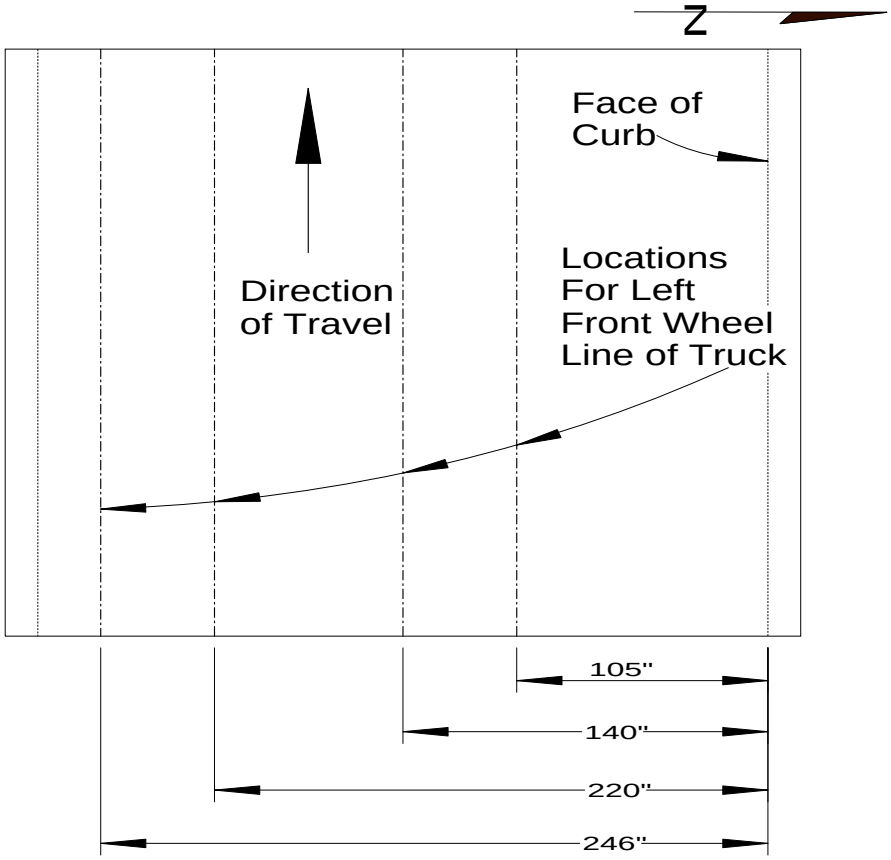

Figure A.7 Test Truck Locations for Bridge.

A.3 LOAD TEST

A.3.1 Test Plan

In preparation for the test, a detailed test plan was developed that covered the following items:

- Gage Type
- Gage Location
- Loading Vehicle

- Load Locations
- Truck Speed
- Number of Passes
- Channel Configurations

These items are considered to be the most important when planning a test. It is assumed that all necessary analyses have been performed and expected stresses and strains are known for the particular loading vehicle. The test plan should include sketches of the truck locations and the gage locations for each test. This test was limited by the data acquisition system which was capable of recording only seven gages per test. This limitation makes it very important to know which channels are connected to which gages. It is also very important that everyone involved in the test be familiar with the test plan. The plan will likely change as the test proceeds, but it is essential to have a good plan.

A.3.2 Instrumentation Installation

For this test, strain gages for both concrete and steel, mechanical strain transducers and string potentiometers were used. Each of these instruments required specific installation procedure. All gages were checked with an ohm meter and strain indicator after installation to insure proper operation.

Before installation of the instrumentation, the bottom of the slab at midspan was marked off in a 6 in. x 6 in. grid. This grid aided in locating and marking the existing cracks in the slab. Because the cracked section controls during analysis, an effort was made to place the gages as near to cracks as possible.

A.3.2.1 Rebar Strain Gages

The strain gages attached to the reinforcing bars were standard 6-mm gage length, electrical resistance strain gages. The #8 reinforcing bars were instrumented in the bottom of the slab and a #11 reinforcing bar was instrumented in the bottom of the curb.

To prepare for installation the reinforcing bars must first be exposed. The reinforcing bar can be located using a rebar locator, such as the HILTI FerroScan, or by observing crack patterns and checking the crack locations with the as built plans. The reinforcing bar was then exposed using a hammer drill and chipping hammers. A hole of approximately 6 inches in diameter was broken out to expose the rebar. This size of hole will allow adequate room to apply the gage. The reinforcing bar must then have a flat area ground on the surface. The grinding was done with a small tool grinder. Once the flat surface has been ground, the remainder of the procedure is just a standard strain gage installation on steel. Wet sand paper was used to smooth the finish, acetone was used to clean the surface and a cyanoacrilate adhesive, M-Bond 200 from Measurements Group, was used to attach the gage. A small piece of butyl rubber was used to insulate the lead wires from the reinforcing bar. The gages were then protected by a layer of white acrylic and a layer of gray silicone sealant. Terminals were soldered to the leads and terminal blocks were mounted to the underside of the slab to ease connections during test setups.

A.3.2.2 Concrete Strain Gages

The procedure for attaching concrete strain gages was relatively easy for the curbs, but much more difficult for the top of the slab. The gage locations were marked on the surface of the concrete. The gages on the top of the slab required removing the asphalt wearing surface. The concrete was then prepared by sanding and cleaning. The sanding was done using standard 150 grit wet sandpaper. The concrete was then cleaned thoroughly with acetone. A thin layer of two part epoxy was then applied to the concrete and allowed to cure. The epoxy was then sanded and cleaned with water. The gage was then attached using M-Bond AE-10 Epoxy from Measurements Group, Inc. A clamping apparatus was constructed in order to clamp the gage and apply steady pressure for curing. After curing overnight, the gages were then protected in the same manner as the reinforcing bar gages. Again terminals and terminal blocks were used to simplify connections.

A possible improved method of installation that should be investigated uses the cyanoacrilate adhesive to attach the gage to the epoxy. This method would eliminate the need for a clamping apparatus and reduce installation time considerably.

A.3.2.3 Strain Transducers

The strain transducers were attached by mounting a tab to the concrete and then bolting the transducer to the tab. Figure A.8 shows details of the mounting tabs used.

The tabs were attached to concrete by a combination of adhesive and epoxies. The surface was first prepared as discussed previously for installing concrete strain gages. A thin layer of two-part epoxy was applied to the surface and allowed to cure. The epoxy was sanded and then cleaned with water to remove any dust. The tabs were then bolted on the transducers. A mixture of PC-7, a two-part epoxy, was prepared and a thin layer was applied to all but the center of the bottom surface of the tabs. A small amount of cyanoacrilate adhesive (super glue) was applied in this clear area. The transducer and tabs were then pressed into place and held for one minute. The super glue held the tabs in place while the epoxy cured. The transducers were then removed and additional epoxy was applied along the edges of the tabs. The epoxy was then allowed to cure for 24 hours before reattaching the transducers and tightening the bolts.

Based on problems experienced during this test, the use of all epoxies and adhesives should be limited to when the temperatures are above 60° F.

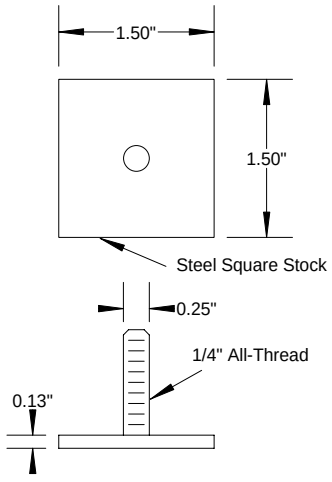

Figure A.8 Strain Transducer Mounting Tab Details.

A.3.2.4 String Potentiometers

The string potentiometers were mounted on the underside of the bridge to measure deflection. The instruments were screwed to a 6 inch by 8 inch piece of 1/2 inch plywood. The locations were marked on the underside of the slab and holes were drilled into the concrete. Anchor bolts were inserted into the concrete and the string potentiometers and plywood were bolted to the slab using the anchor bolts.

Holes were drilled in the concrete riprap directly below the string potentiometers. Lead anchors and eye bolts were inserted into the holes and coated fishing line was attached to the eye bolts and then to the string potentiometer.

A.4 METHOD OF DATA REDUCTION

The strain gage setup was based on the quarter wheatstone bridge circuit. The raw data were in the form of input voltage (E_I)and output in millivolts (E_O). The following formula was used to convert the data to microstrain:

$$\mu\varepsilon = \frac{4000}{G_F} \cdot \frac{E_O}{E_I} \qquad \text{(A.1)}$$

where:

$\mu\varepsilon$ = microstrain

G_F = Gage Factor

The strain transducer data were in the same form as the strain gage data although the transducers contained a full wheatstone bridge circuit. The data were converted to microstrain by the following formula:

$$\mu\varepsilon = \frac{1}{G_F} \cdot \frac{E_O}{E_I} \qquad \text{(A.2)}$$

The string potentiometer data was converted to inches of deflection by a similar formula:

$$\Delta = \frac{1}{G_F} \cdot \frac{E_O}{E_I} \qquad \text{(A.3)}$$

Appendix B. REINFORCING BAR STRAIN DATA

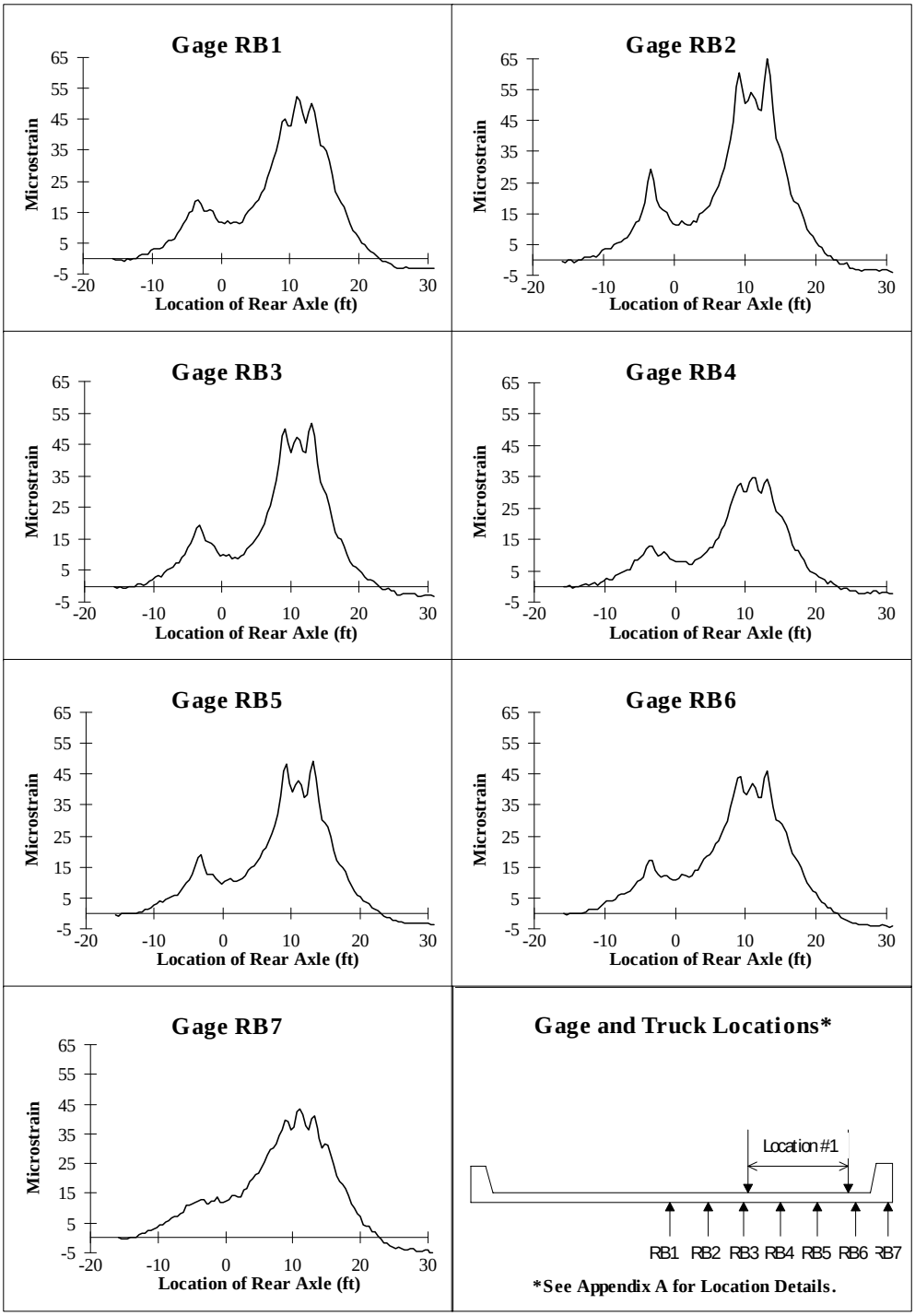

Figure B.1 Strain Data for Test Series 1, Location 1, Pass 1.

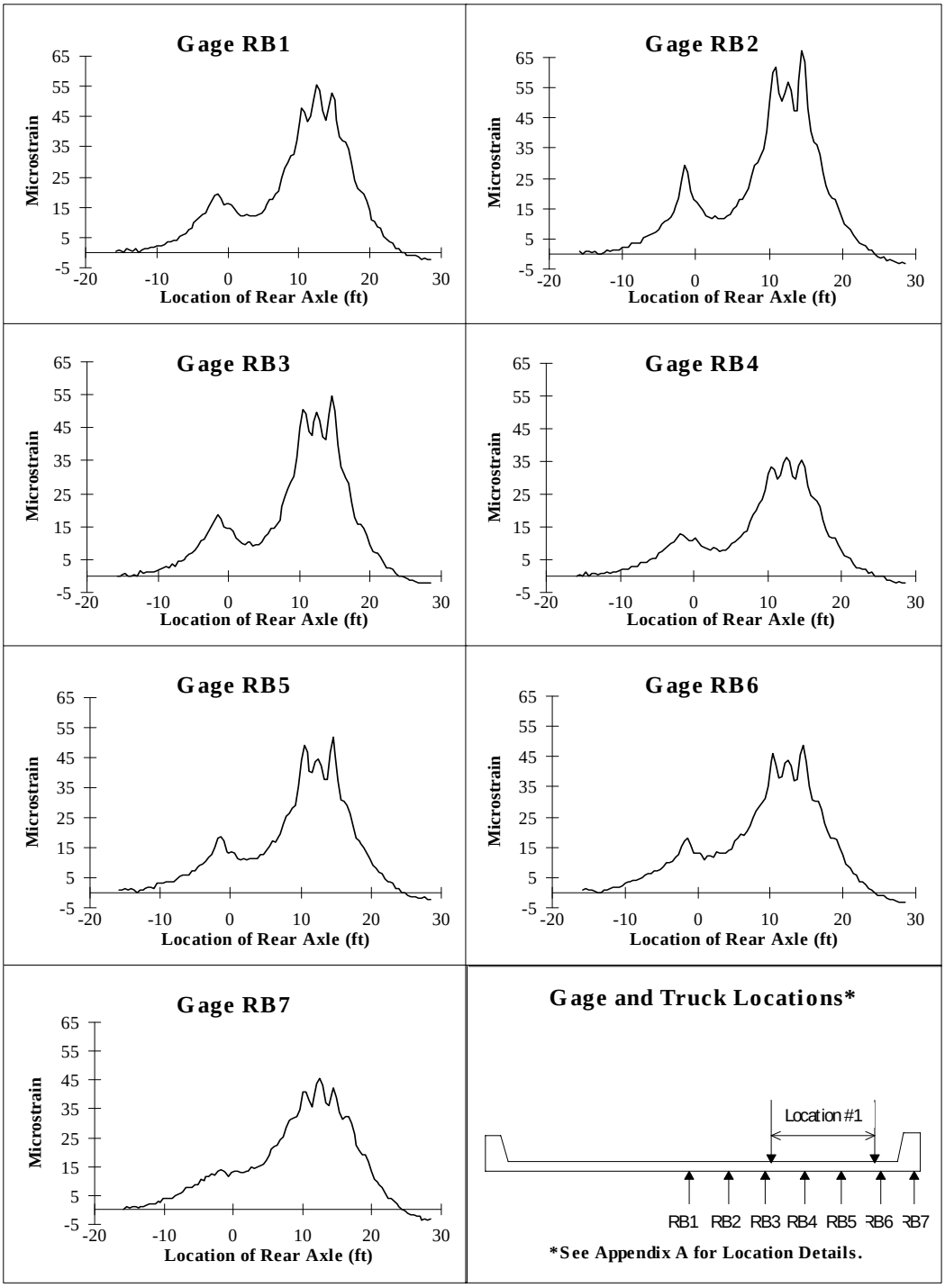

Figure B.2 Strain Data for Test Series 1, Location 1, Pass 2.

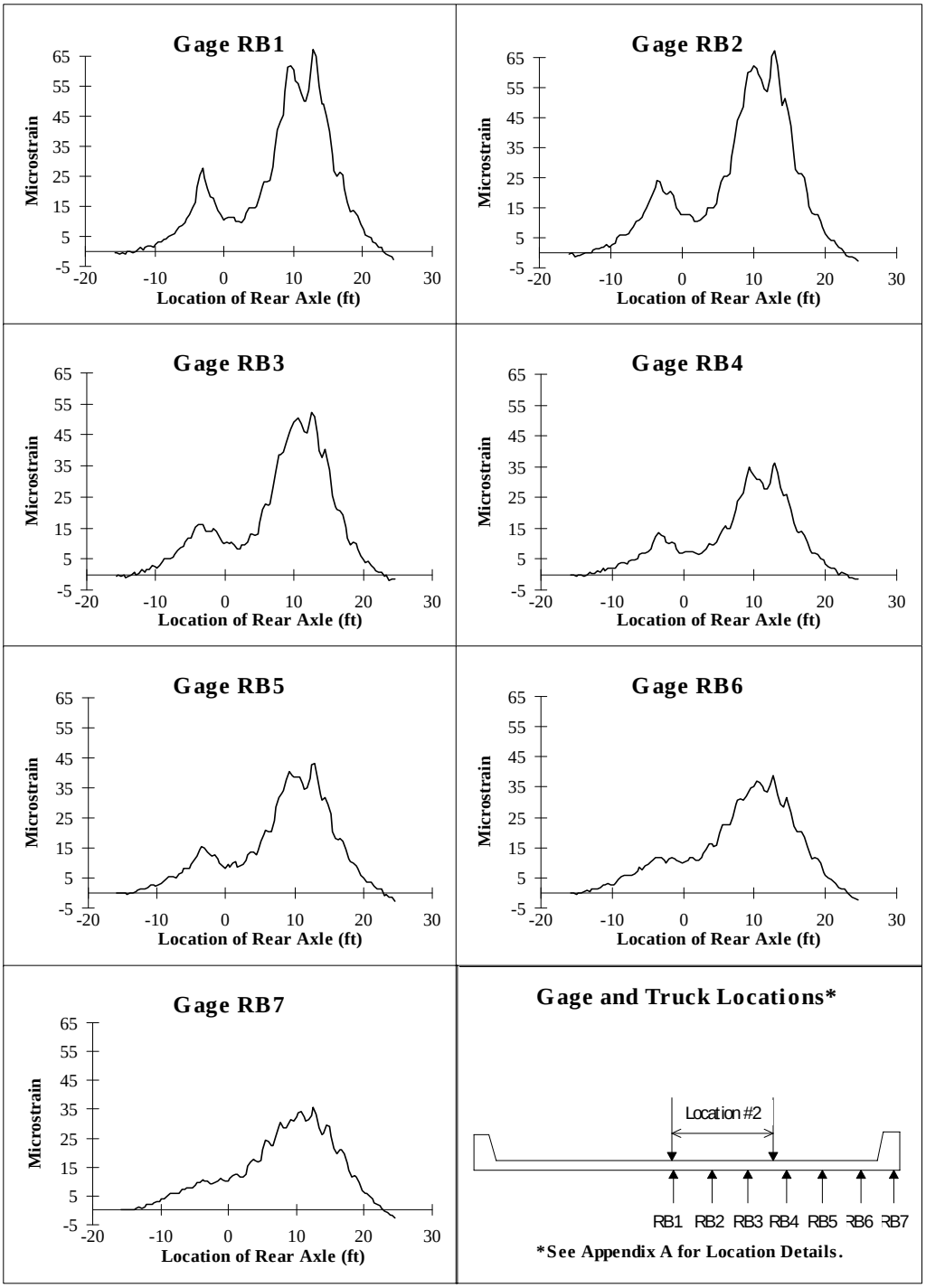

Figure B.3 Strain Data for Test Series 1, Location 2, Pass 1.

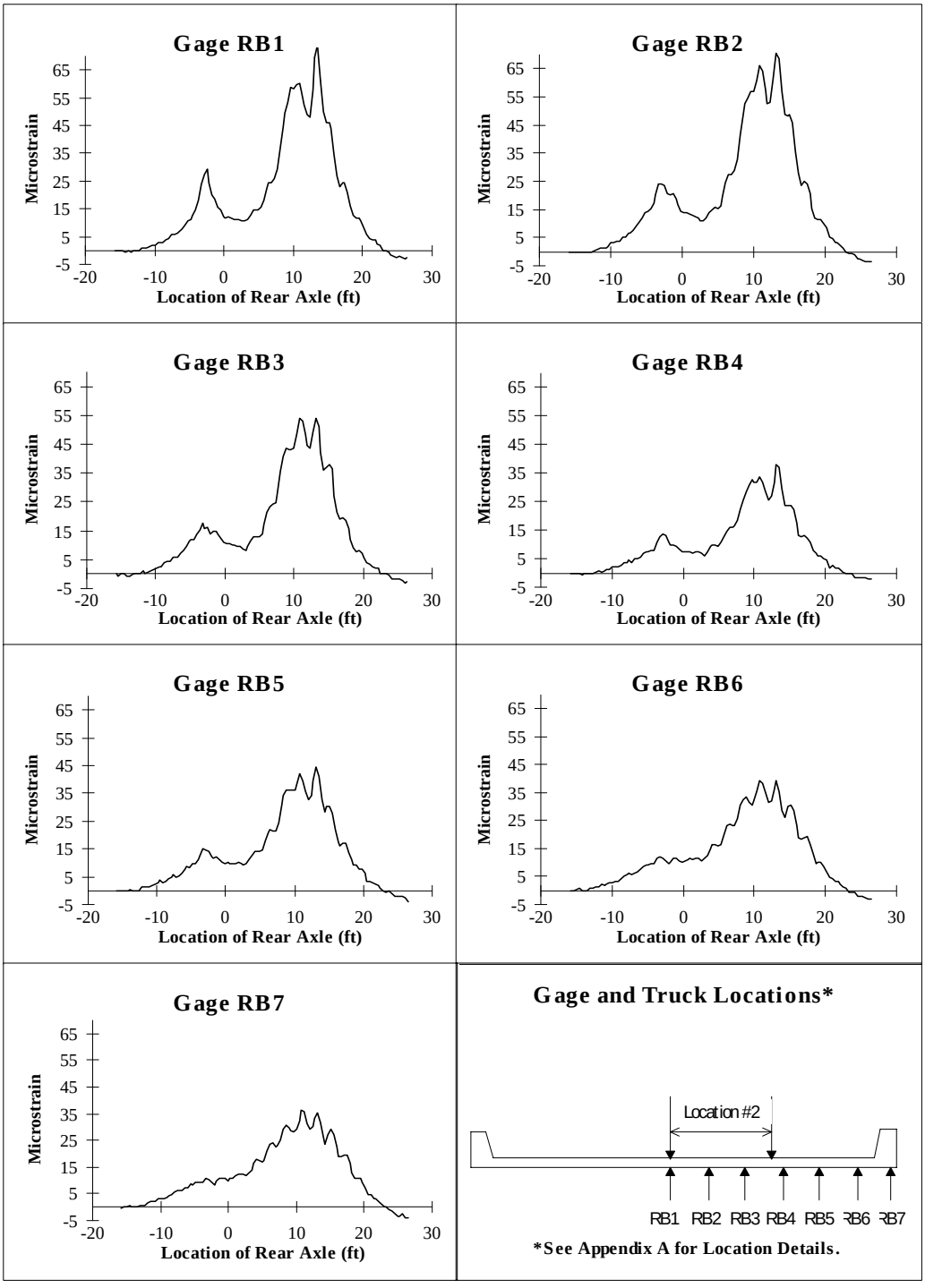

Figure B.4 Strain Data for Test Series 1, Location 2, Pass 2.

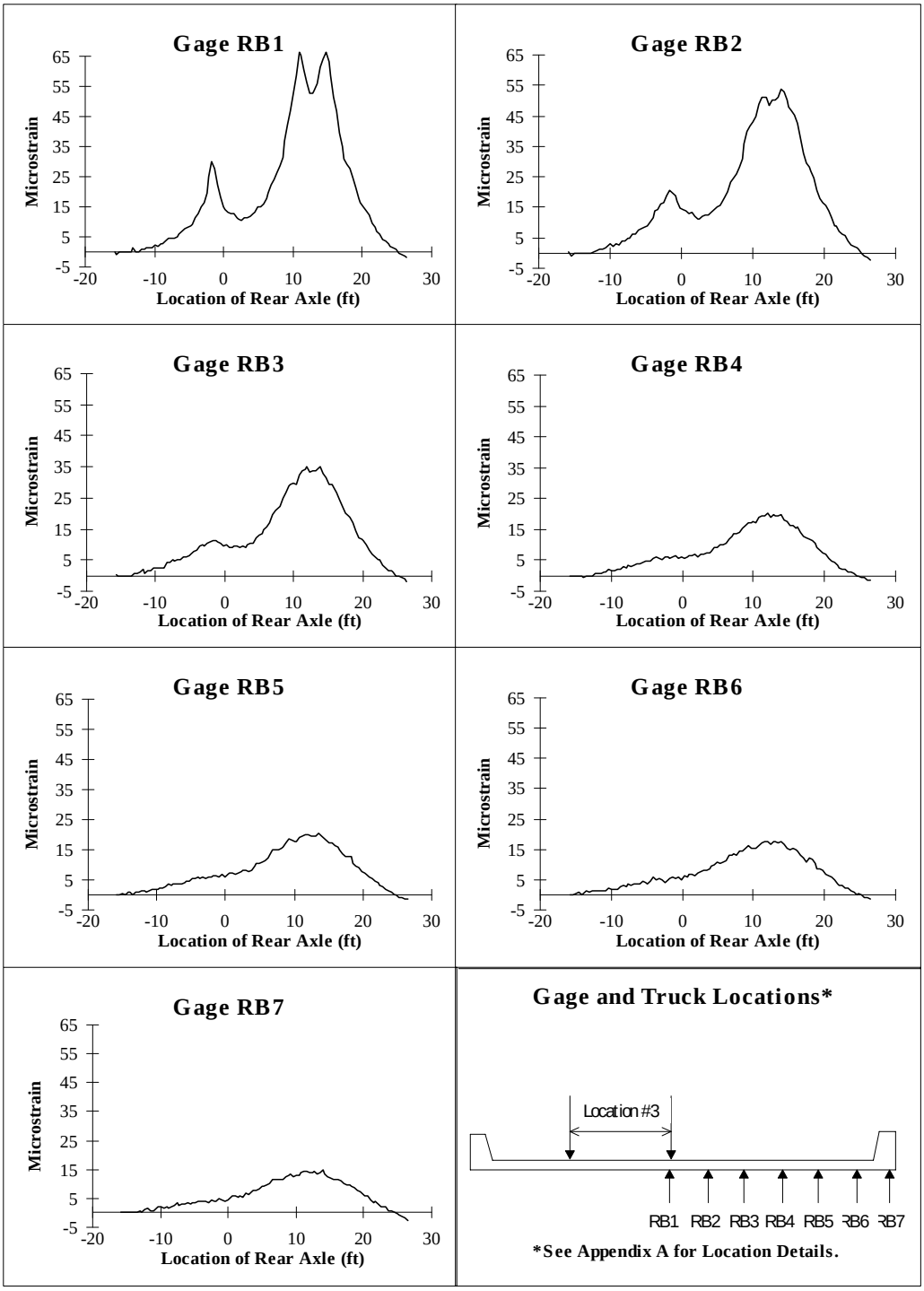

Figure B.5 Stain Data for Test Series 1, Location 3, Pass 1.

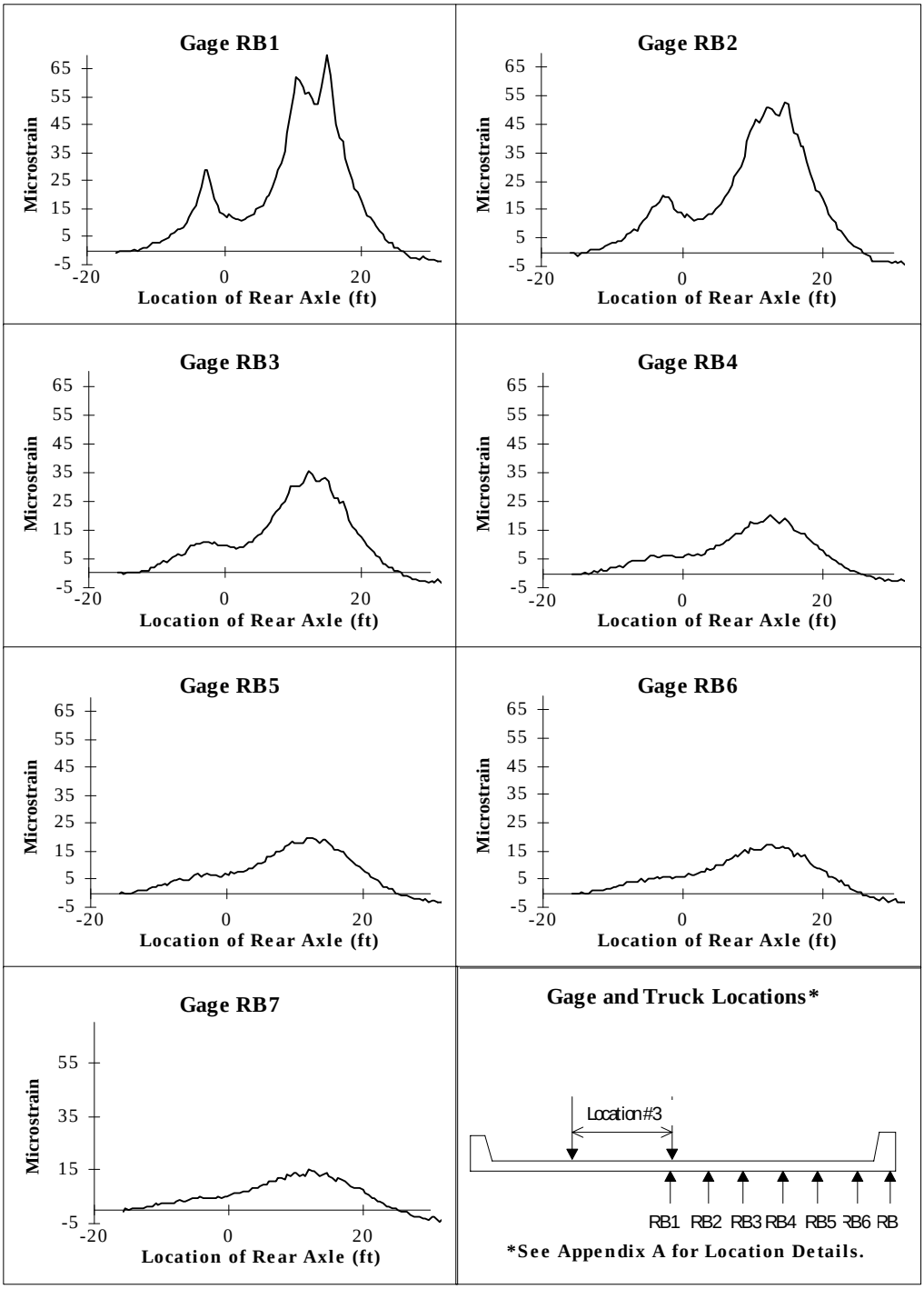

Figure B.6 Strain Data for Test Series 1, Lccation 3, Pass 2.

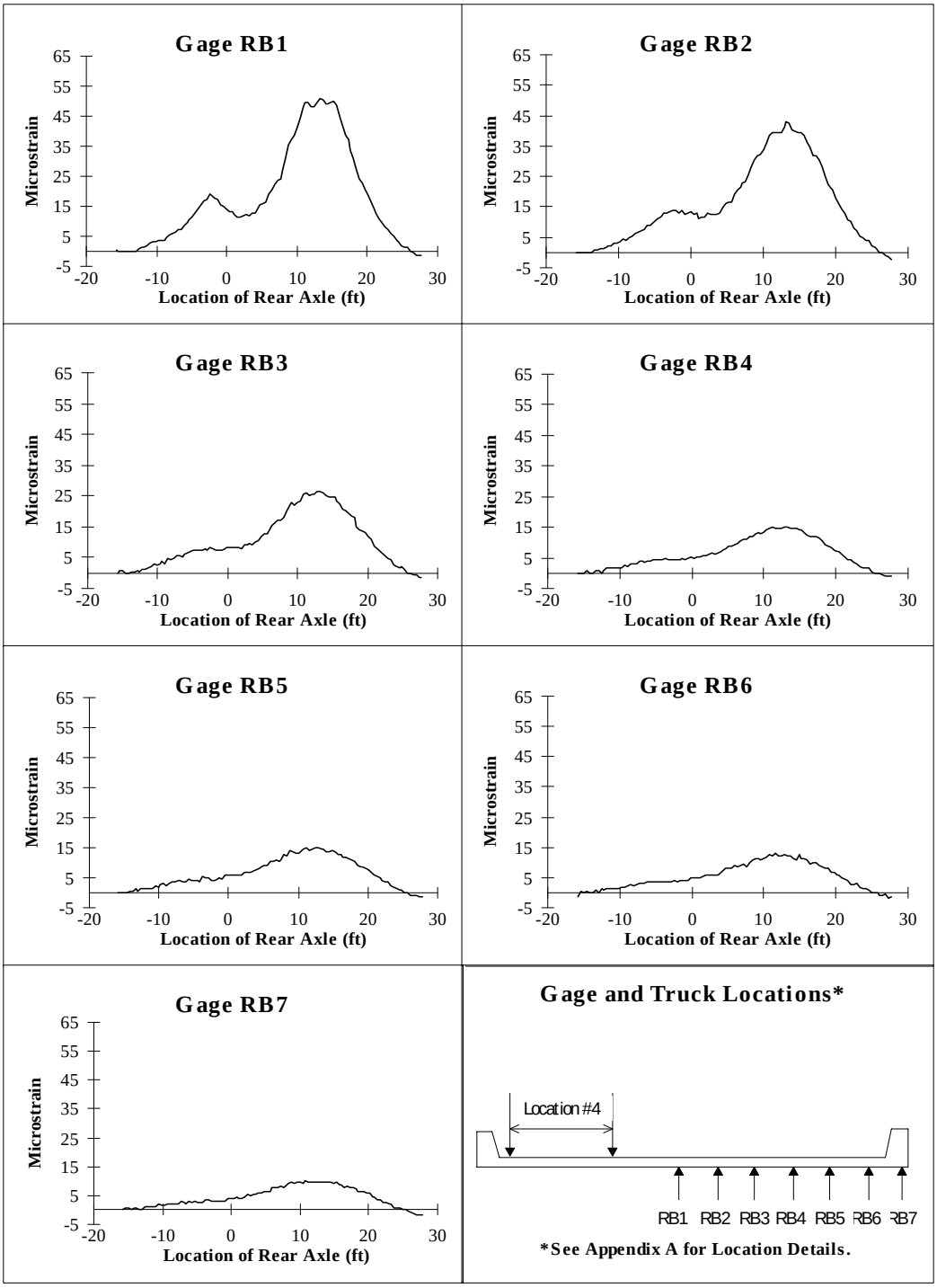

Figure B.7 Stain Data for Test Series 1, Location 4, Pass 1.

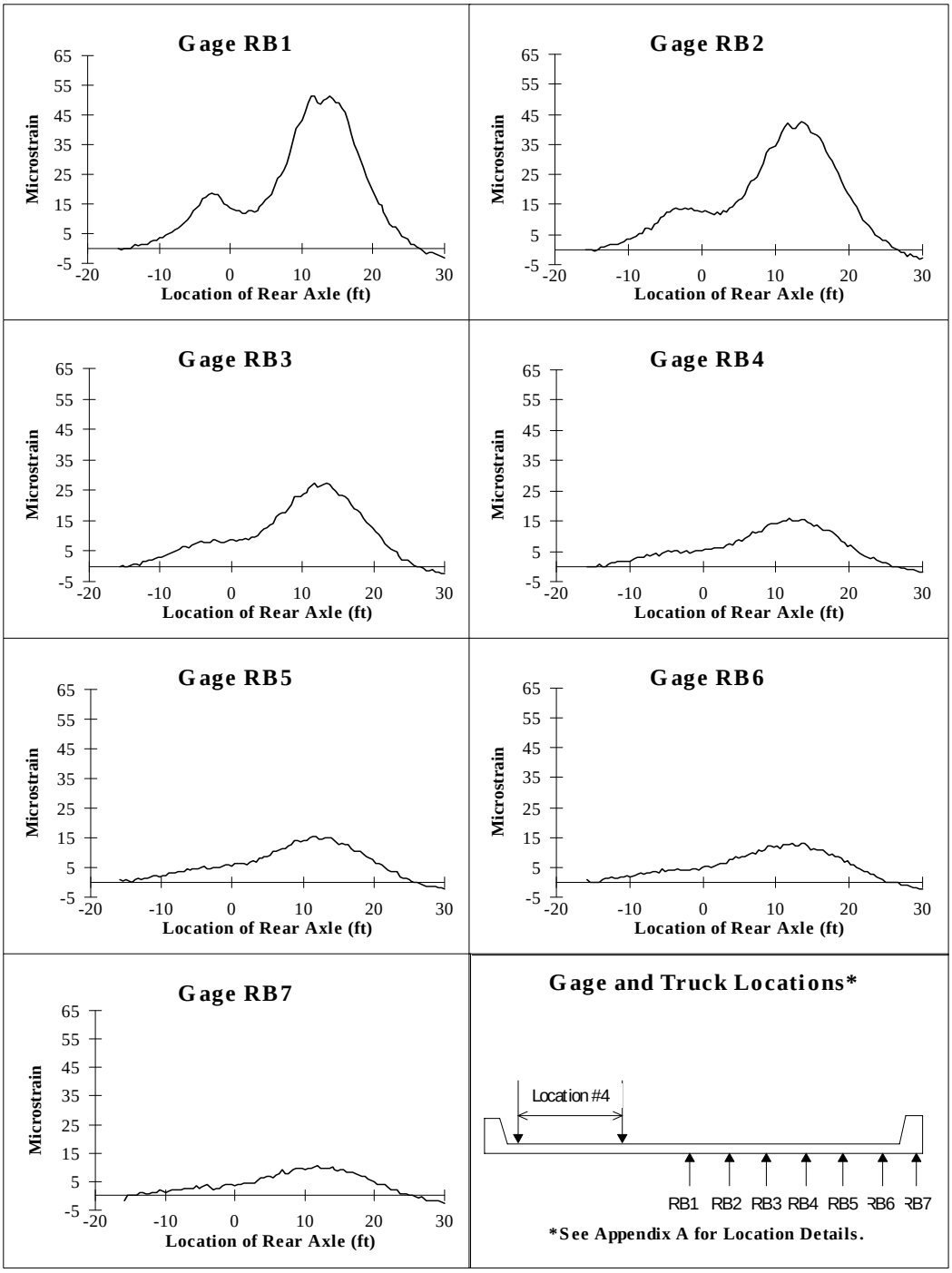

Figure B.8 Strain Data for Test Series 1, Location 4, Pass 2.

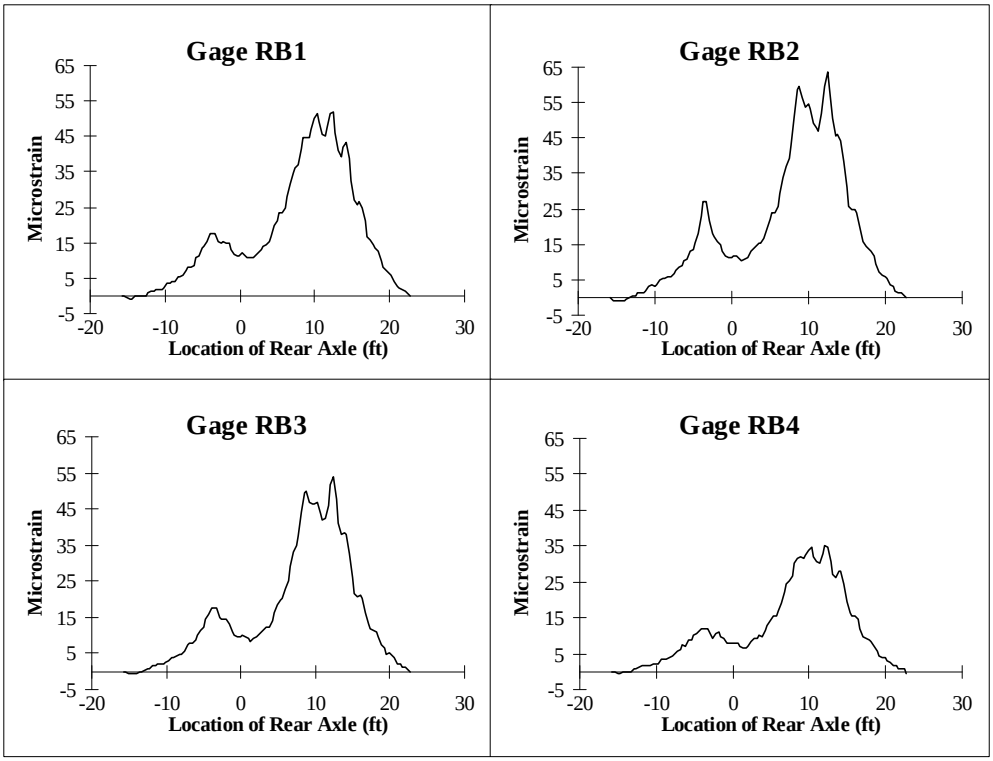

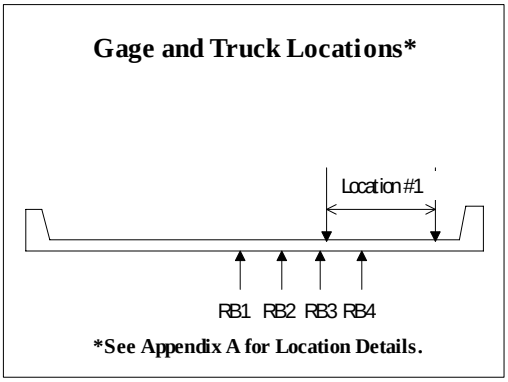

Figure B.9 Strain Data for Test Series 2, Location 1, Pass 1.

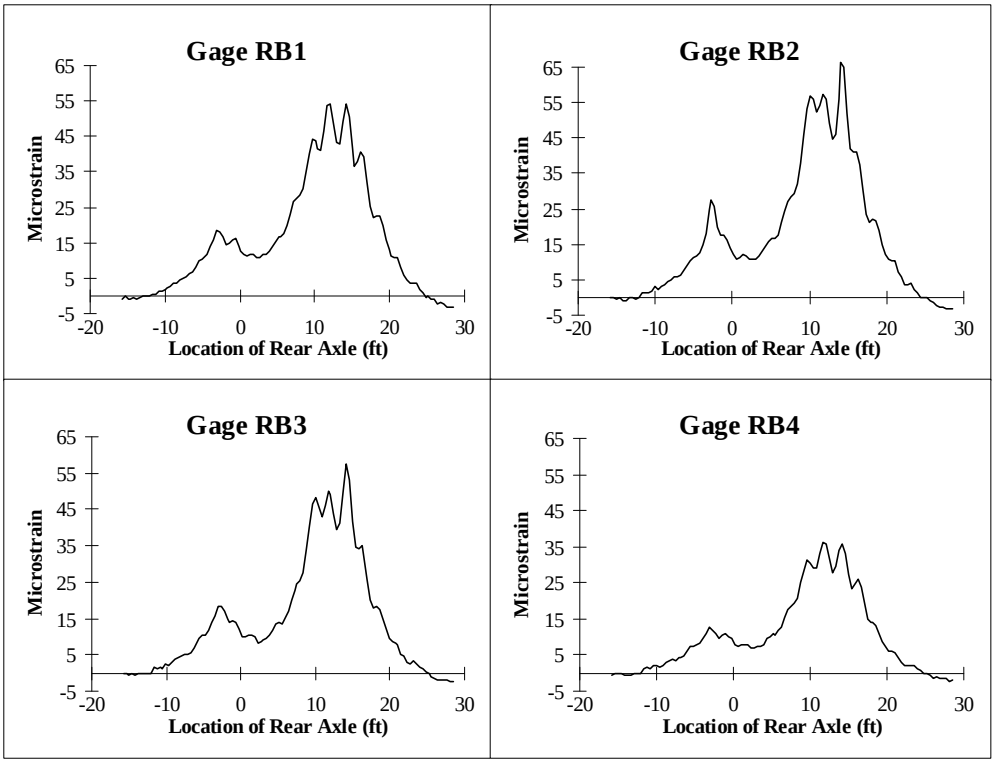

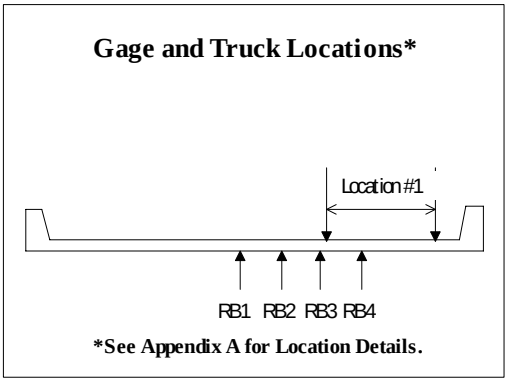

Figure B.10 Strain Data for Test Series 2, Location 1, Pass 2.

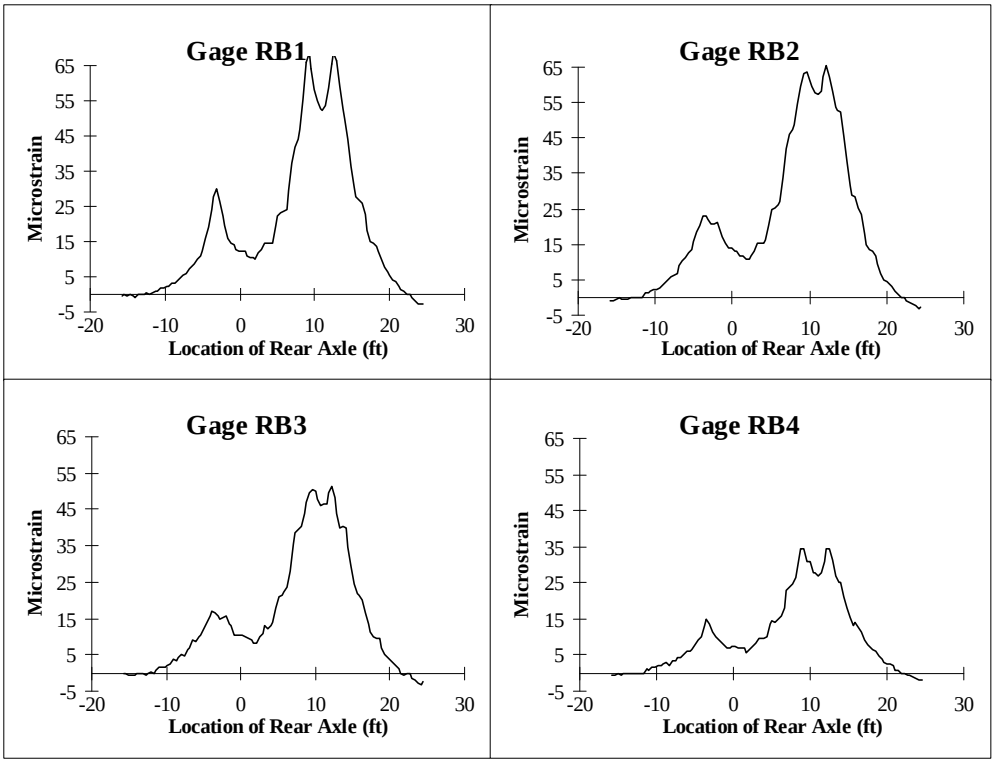

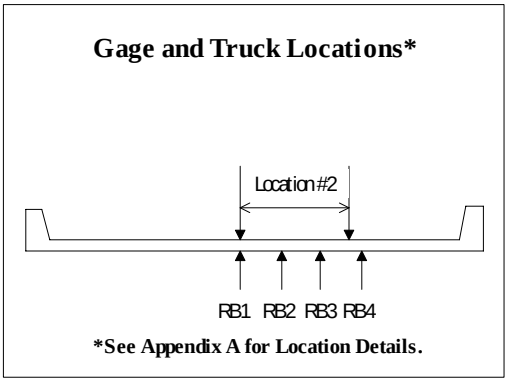

Figure B.11 Strain Data for Test Series 2, Location 2, Pass 1.

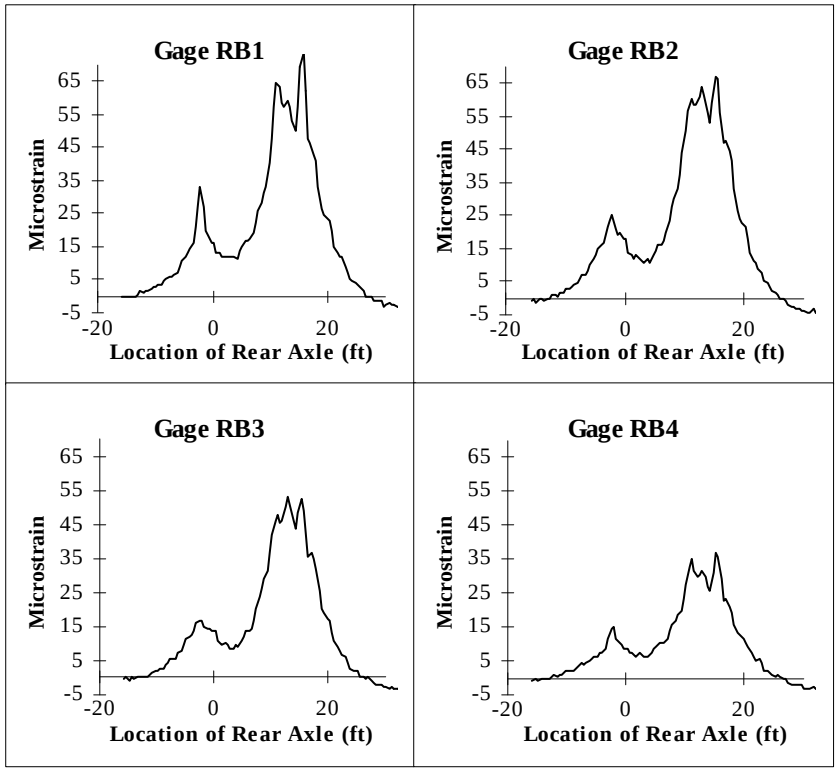

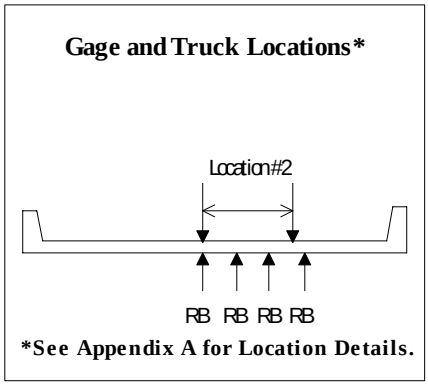

Figure B.12 Strain Data for Test Series 2, Location 2, Pass 2.

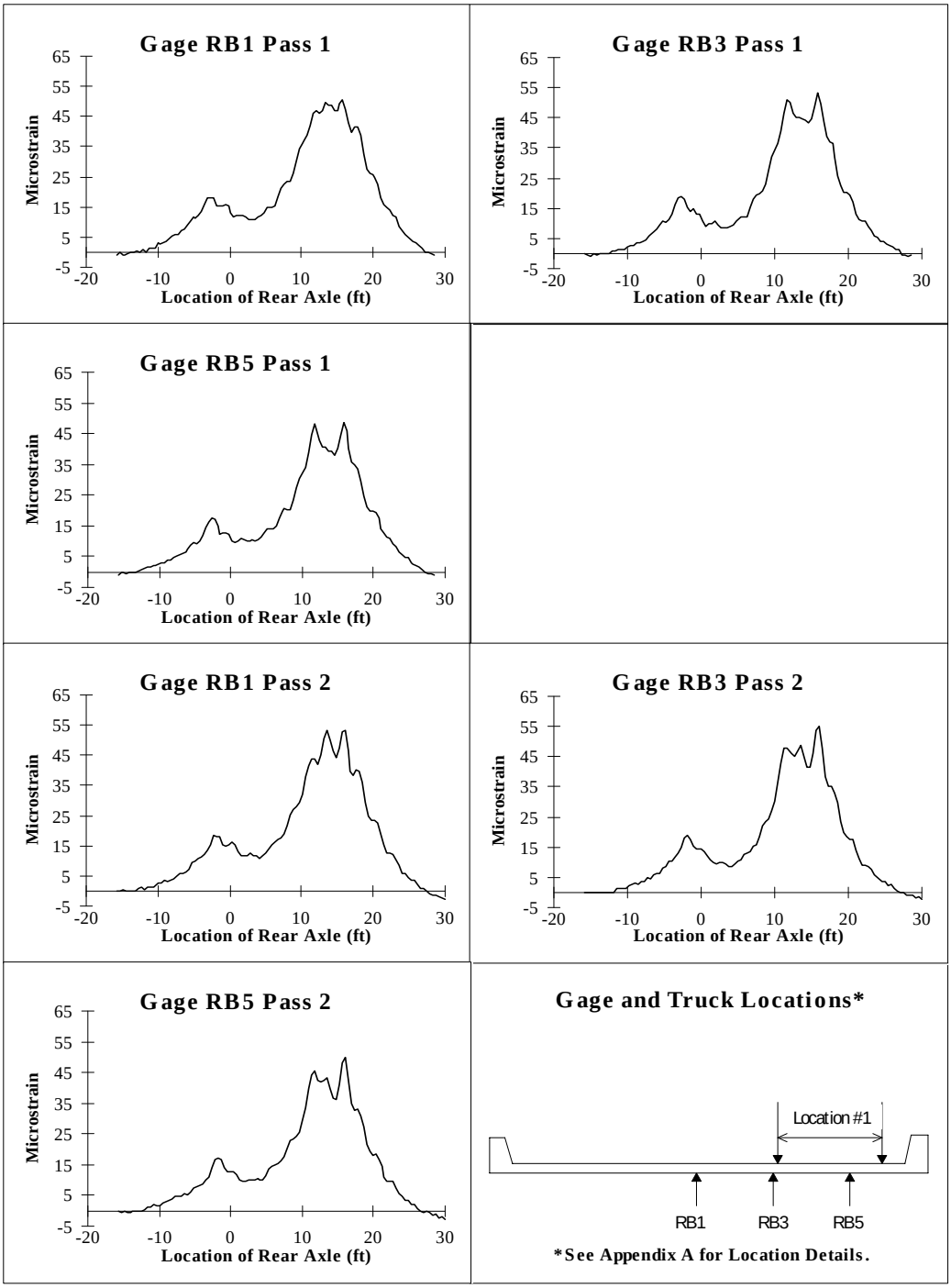

Figure B.13 Strain Data for Test Series 3, Location 1, Passes 1 & 2.

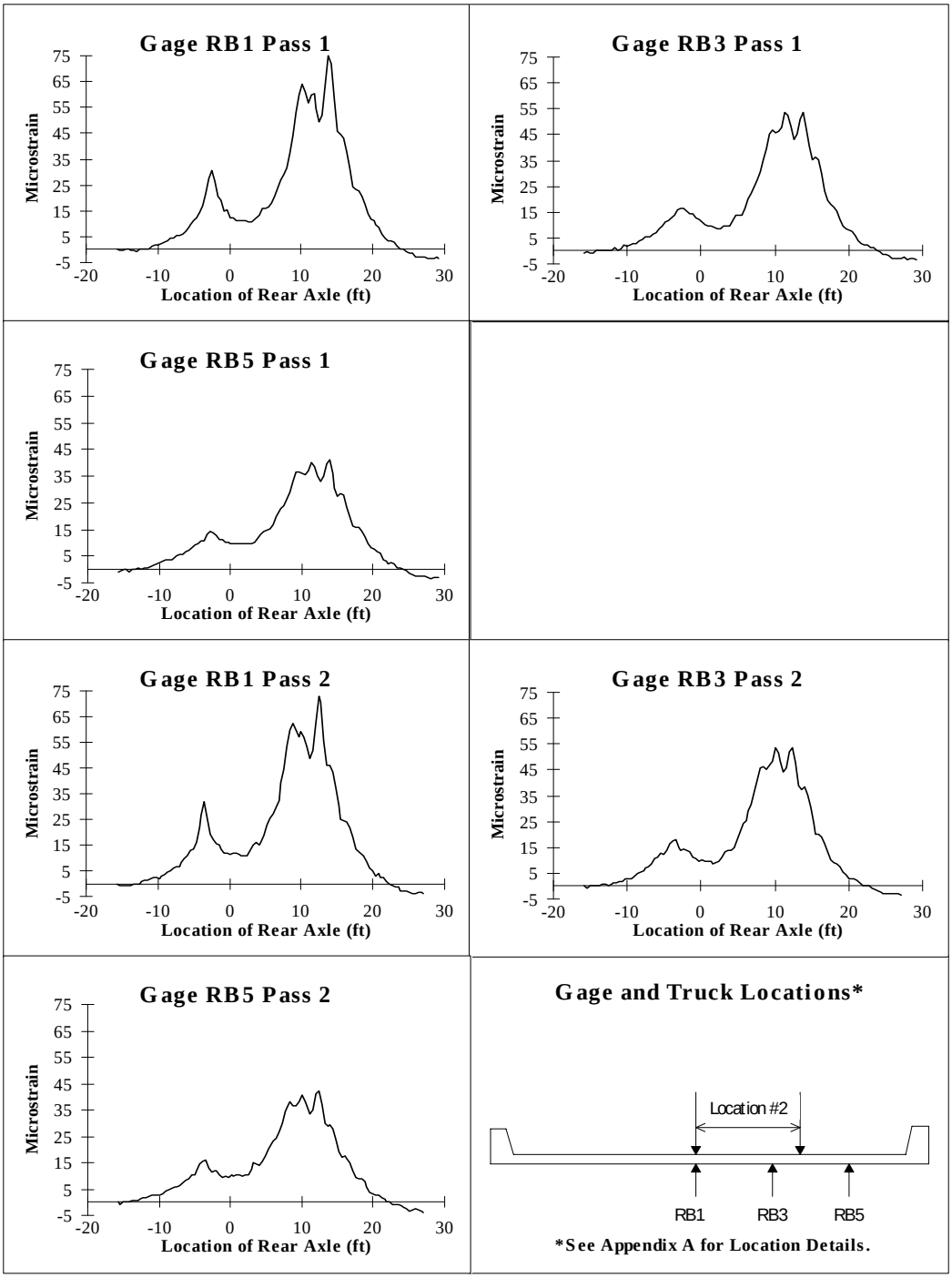

Figure B.14 Strain Data for Test Series 3, Location 2, Passes 1 & 2.

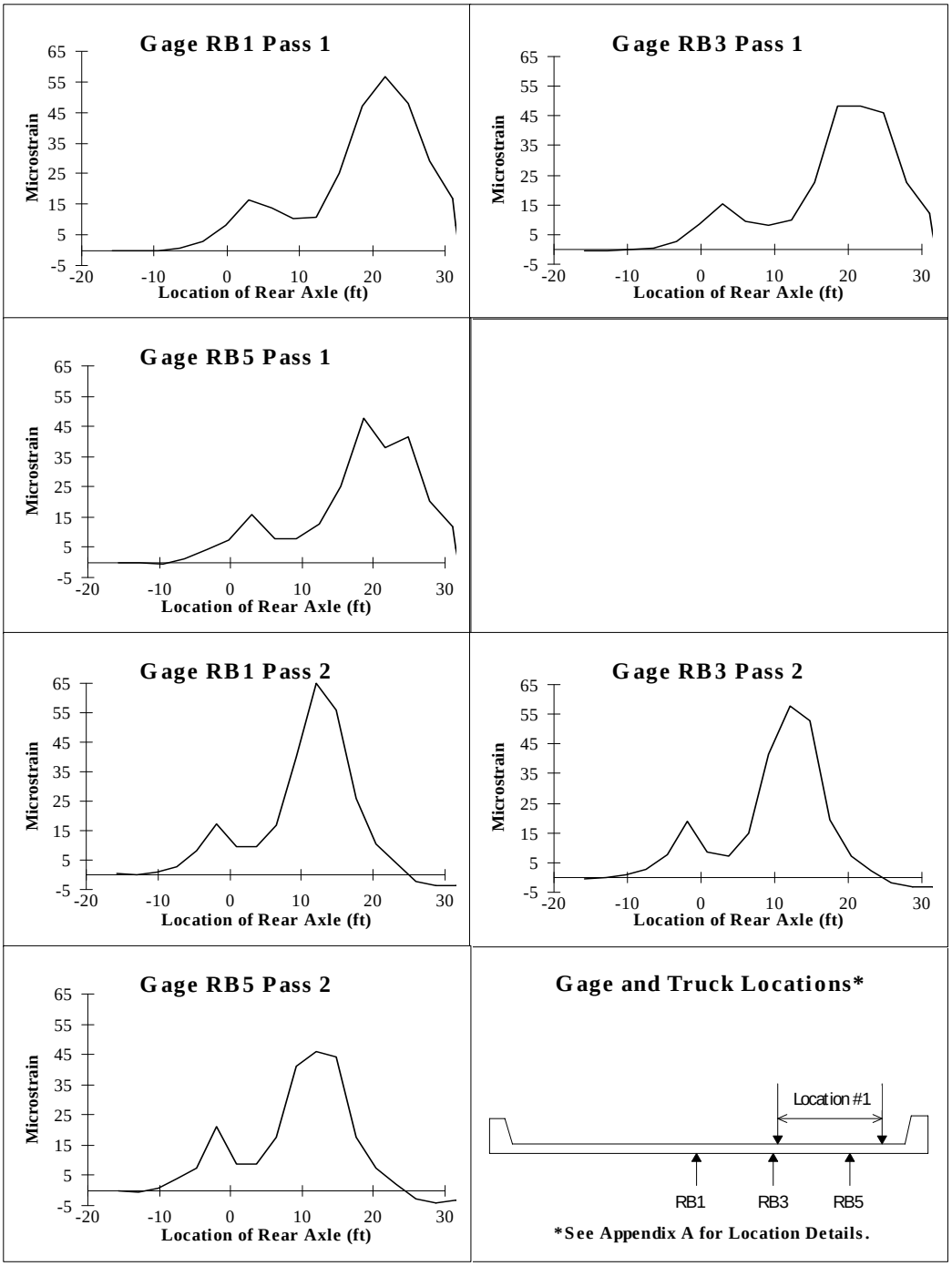

Figure B.15 Strain Data for Test Series 3A, Location 1, Passes 1 & 2.

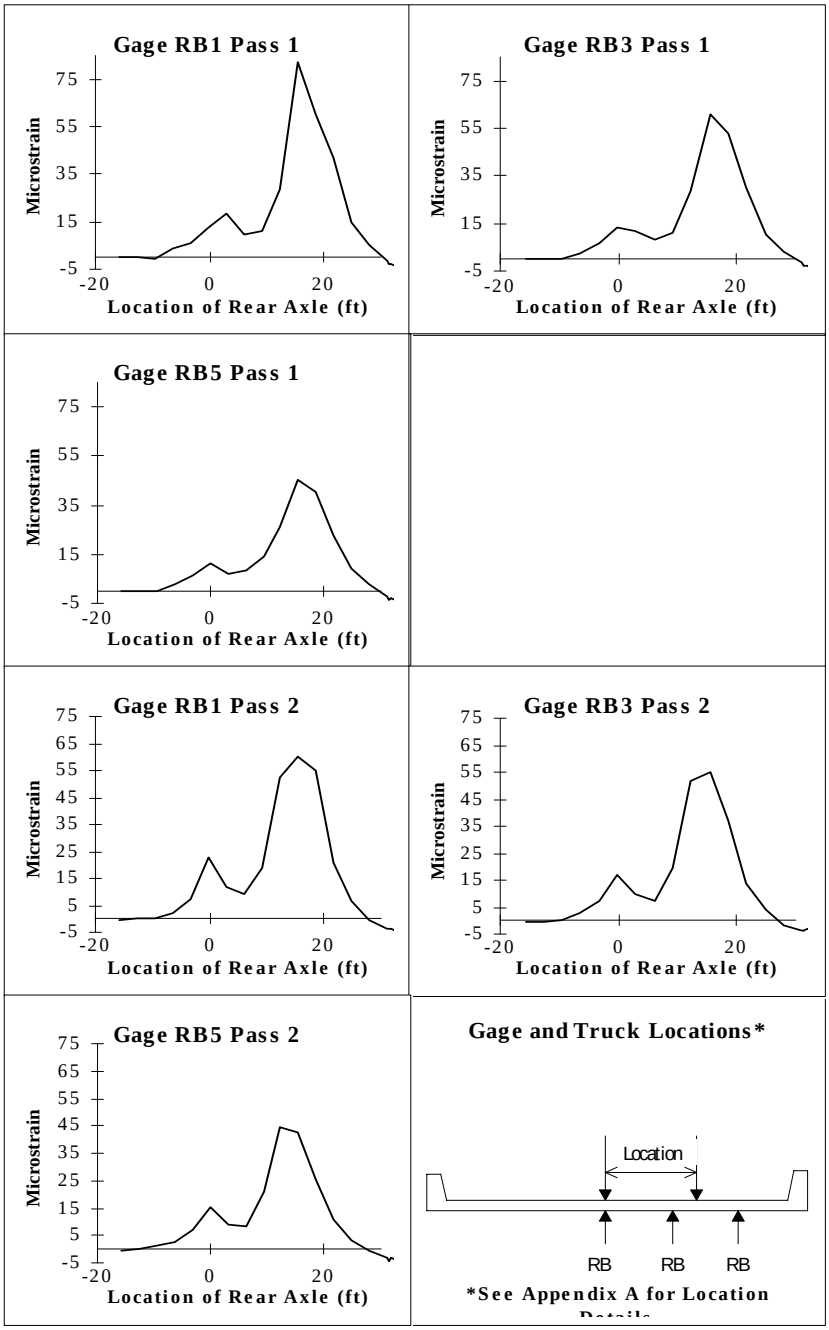

Figure B.16 Strain Data for Test Series 3A, Location 2, Passes 1 & 2.

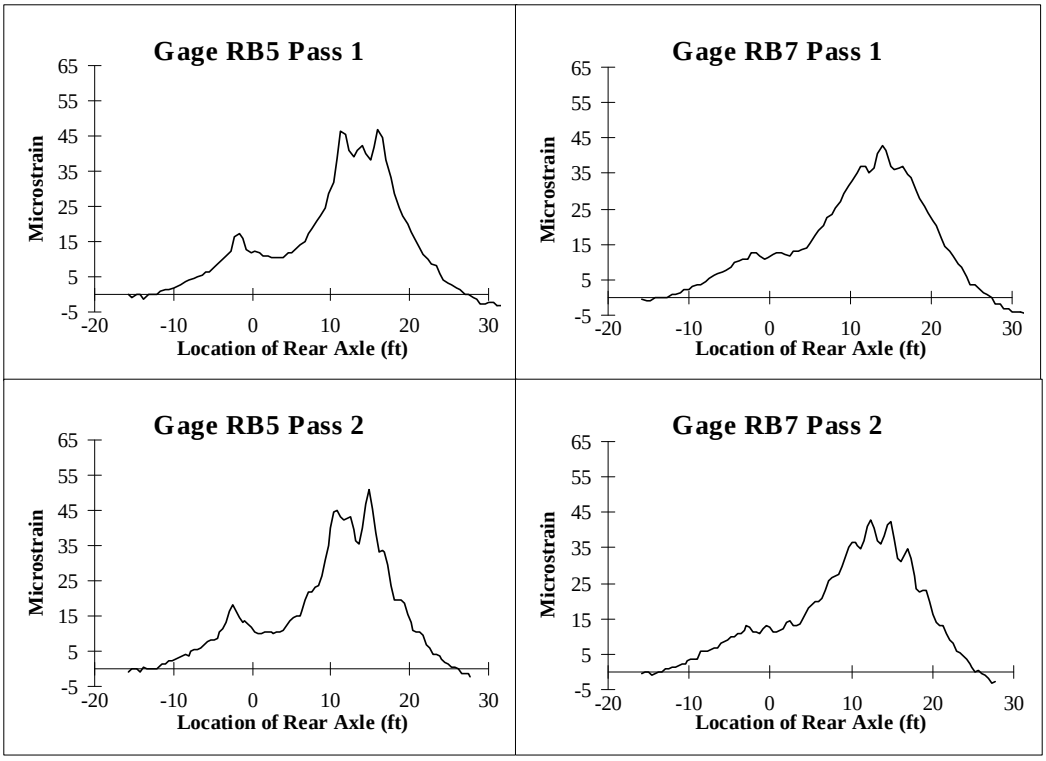

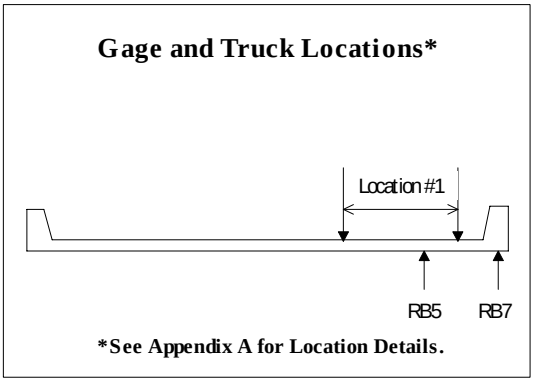

Figure B.17 Strain Data for Test Series 4, Location 1, Passes 1 & 2.

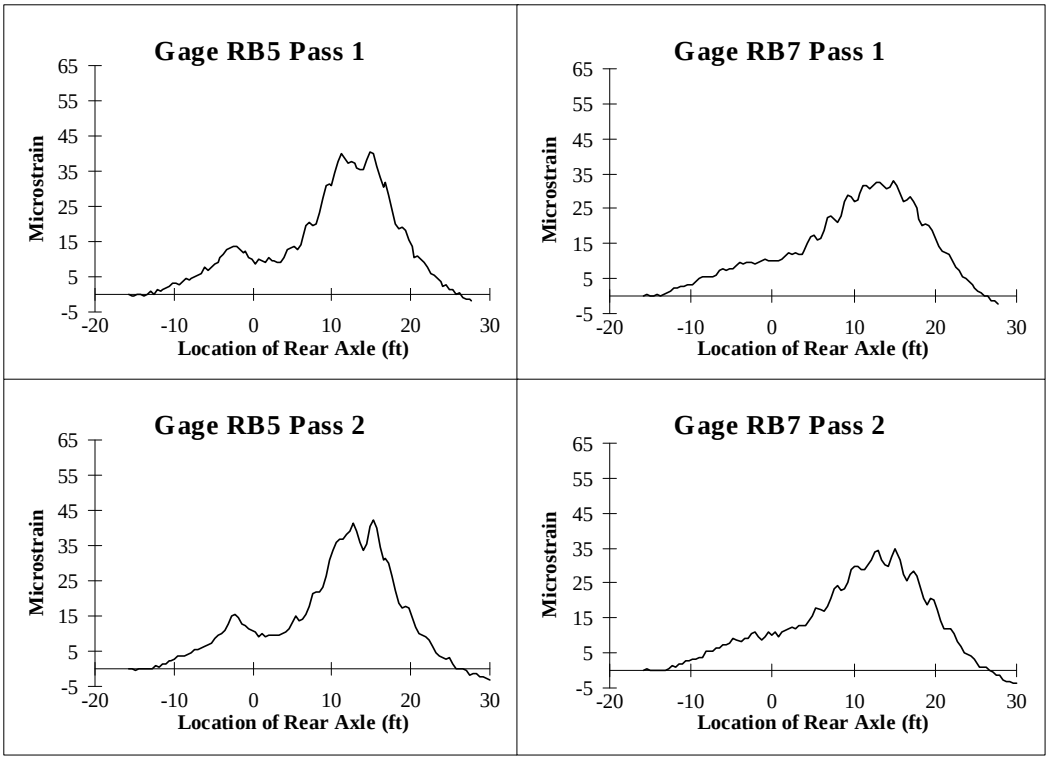

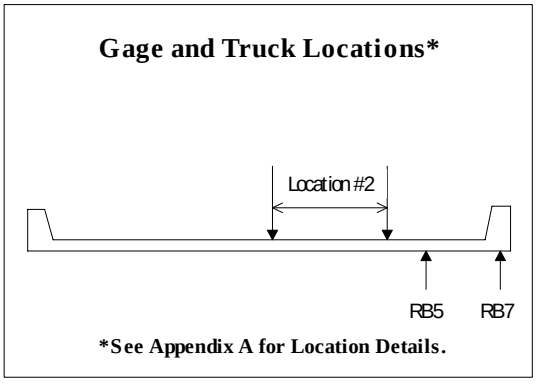

Figure B.18 Strain Data for Test Series 4, Location 2, Passes 1 & 2.

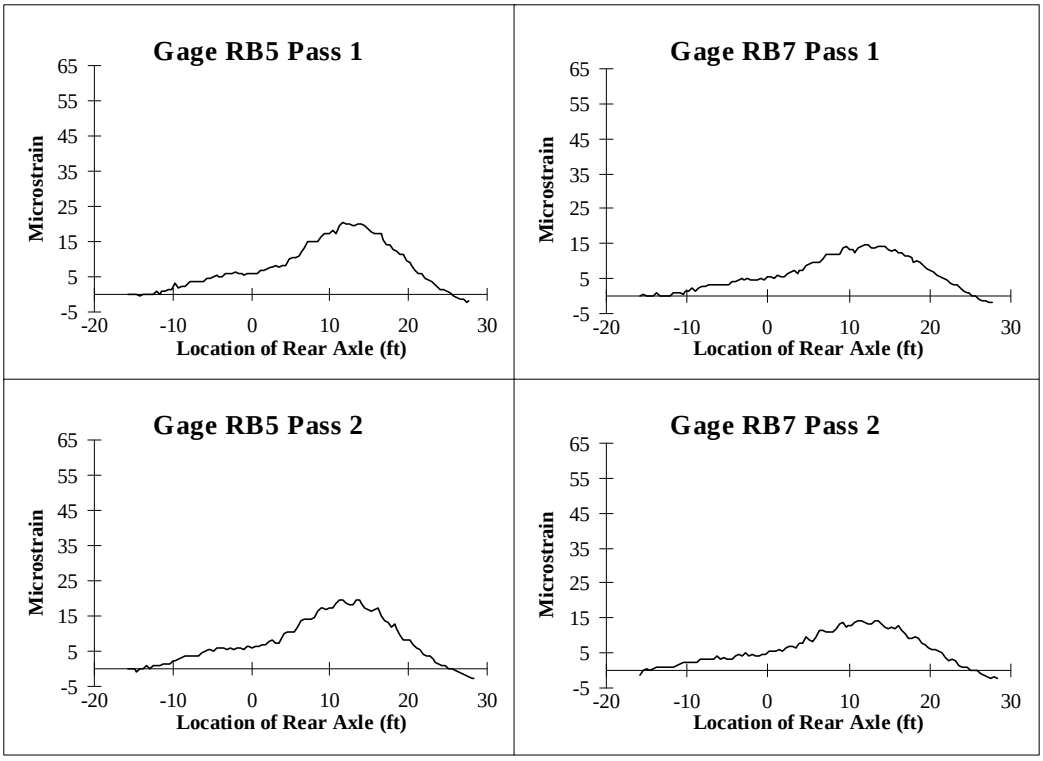

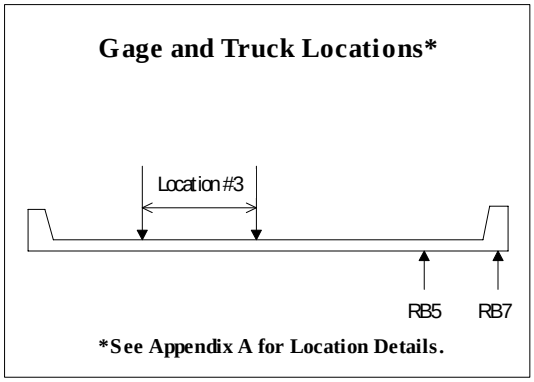

Figure B.19 Strain Data for Test Series 4, Location 3, Passes 1 & 2.

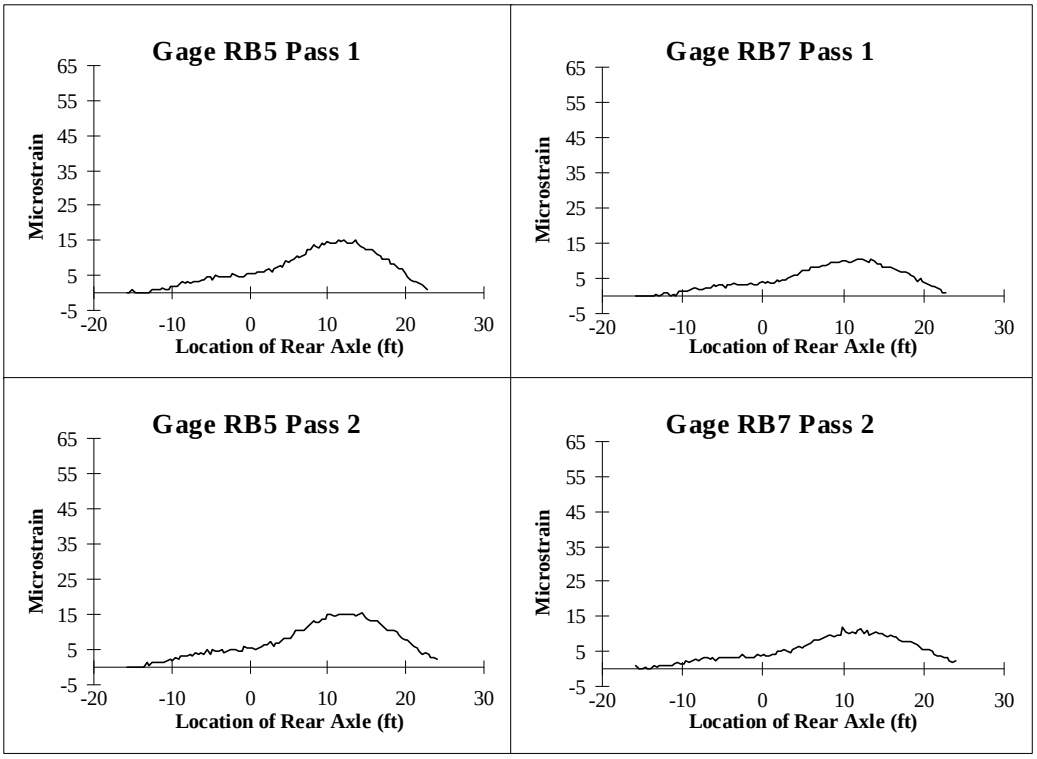

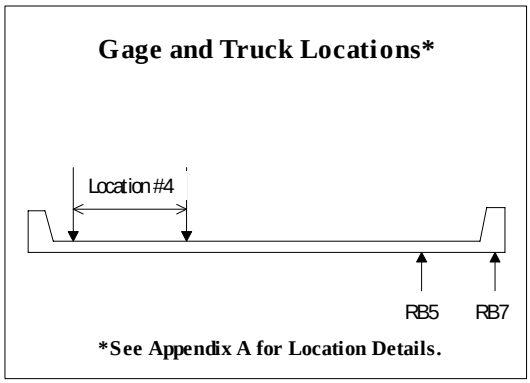

Figure B.20 Strain Data for Test Series 4, Location 4, Passes 1 & 2.

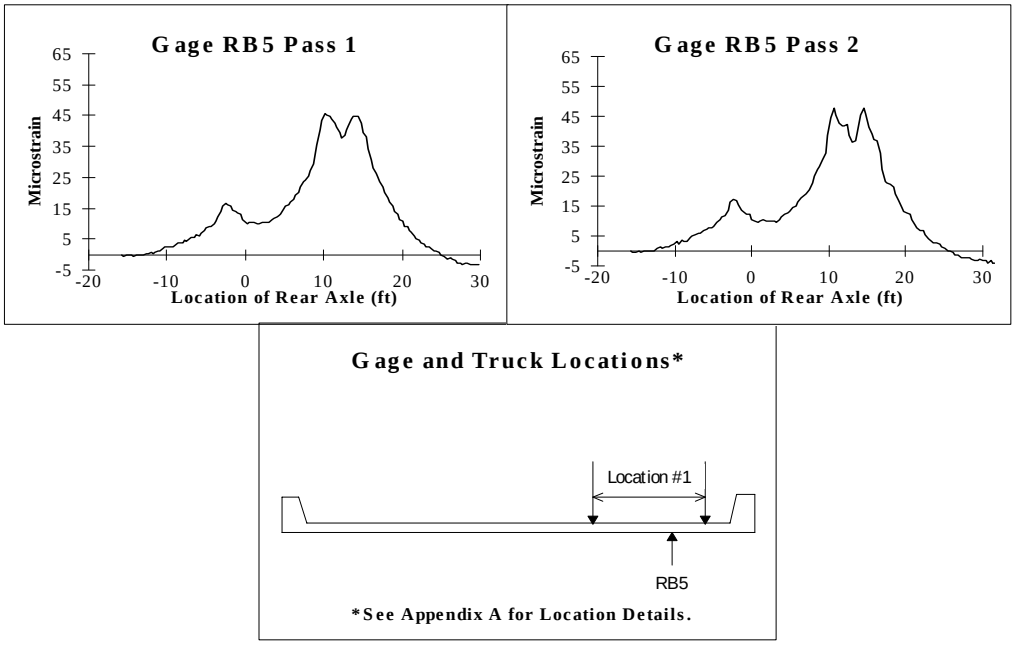

Figure B.21. Strain Data for Test Series 5, Location 1, Passes 1 & 2.

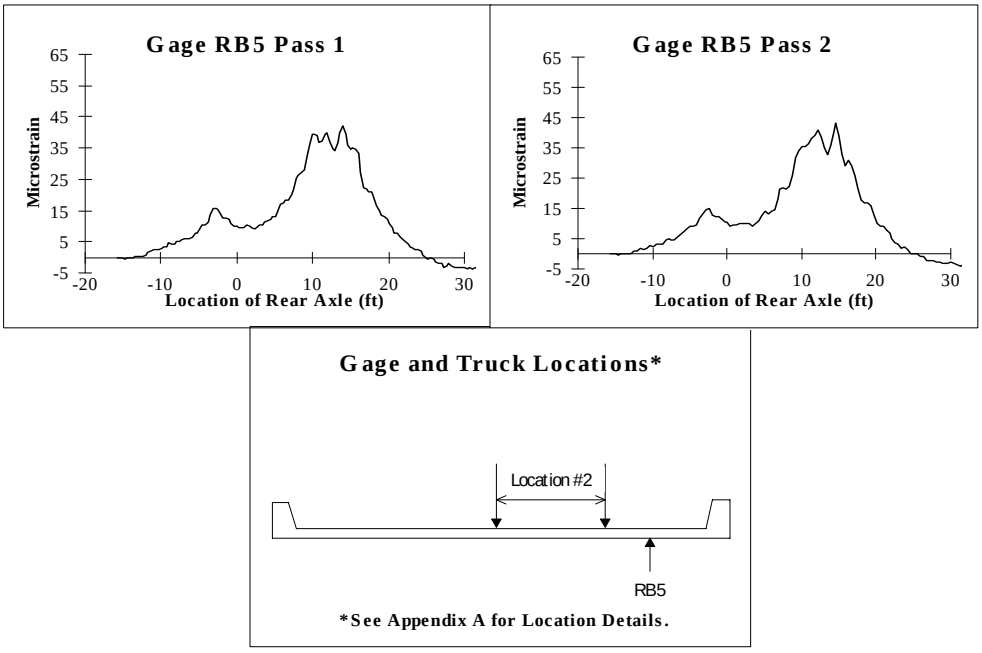

Figure B.22 Strain Data for Test Series 5, Location 2, Passes 1 & 2.

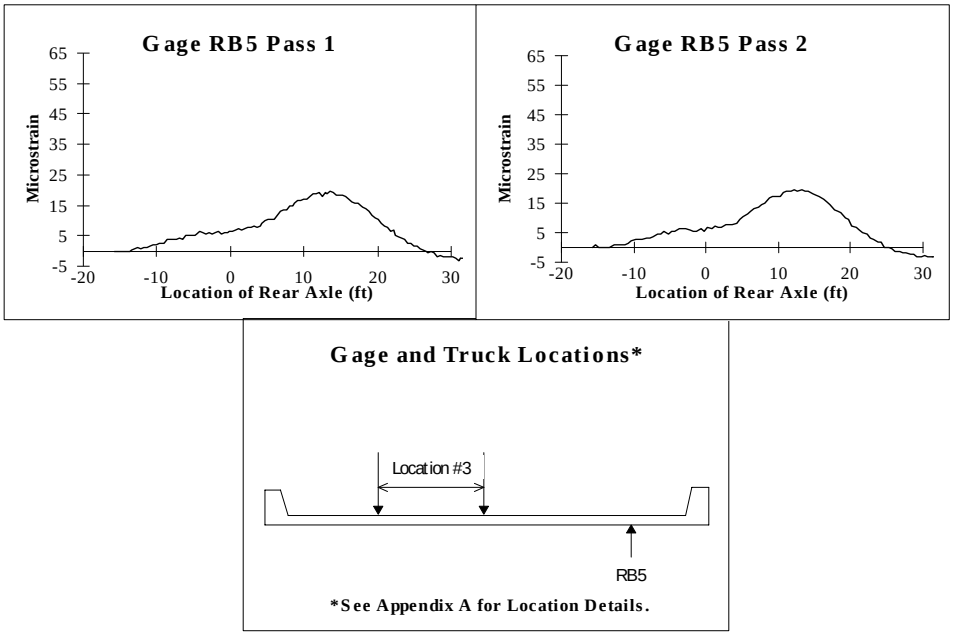

Figure B.23 Strain Data for Test Series 5, Location 3, Passes 1 & 2.

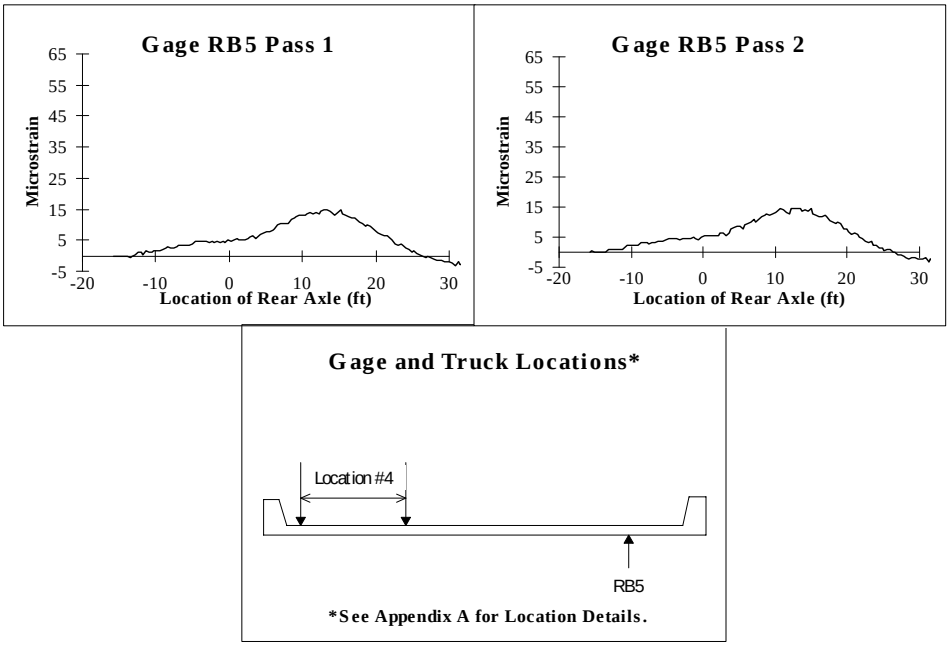

Figure B.24 Strain Data for Test Series 5, Location 4, Passes 1 & 2.

Appendix C. TRANSDUCER STRAIN DATA

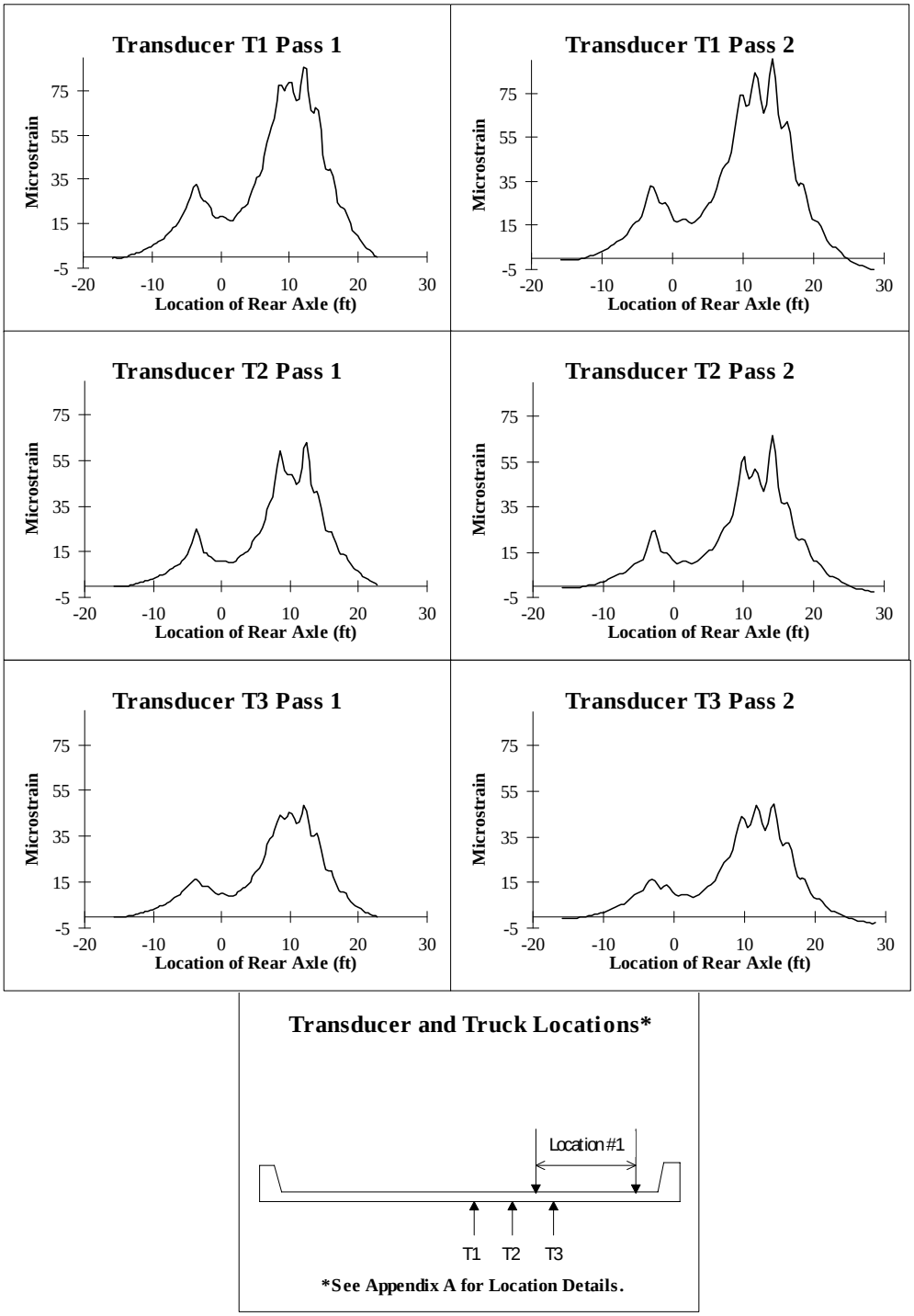

Figure C.1. Strain Data for Test Series 2, Location 1, Passes 1 & 2.

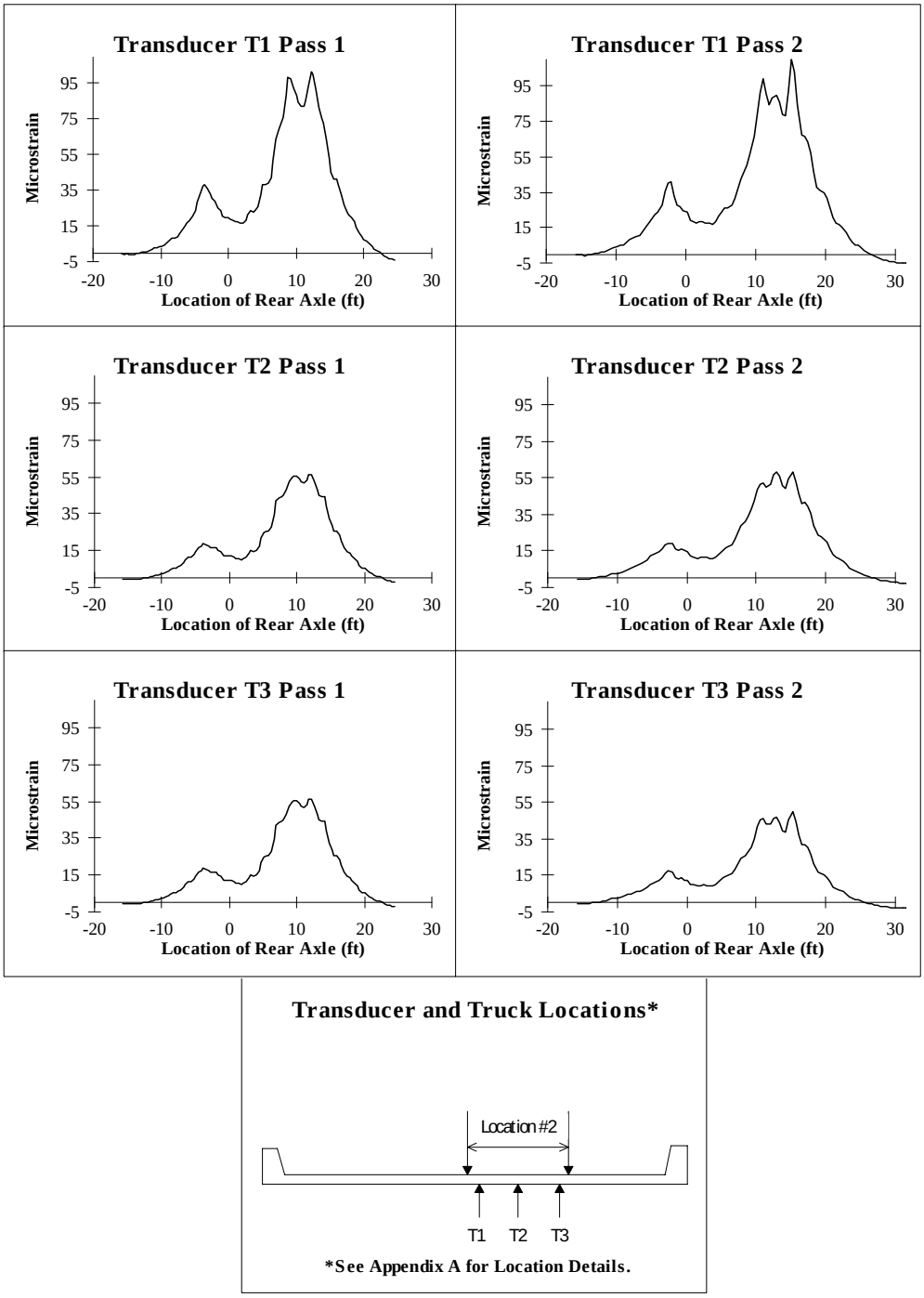

Figure C.2. Strain Data for Test Series 2, Location 2, Passes 1 & 2.

Appendix D. TOP OF SLAB STRAIN DATA

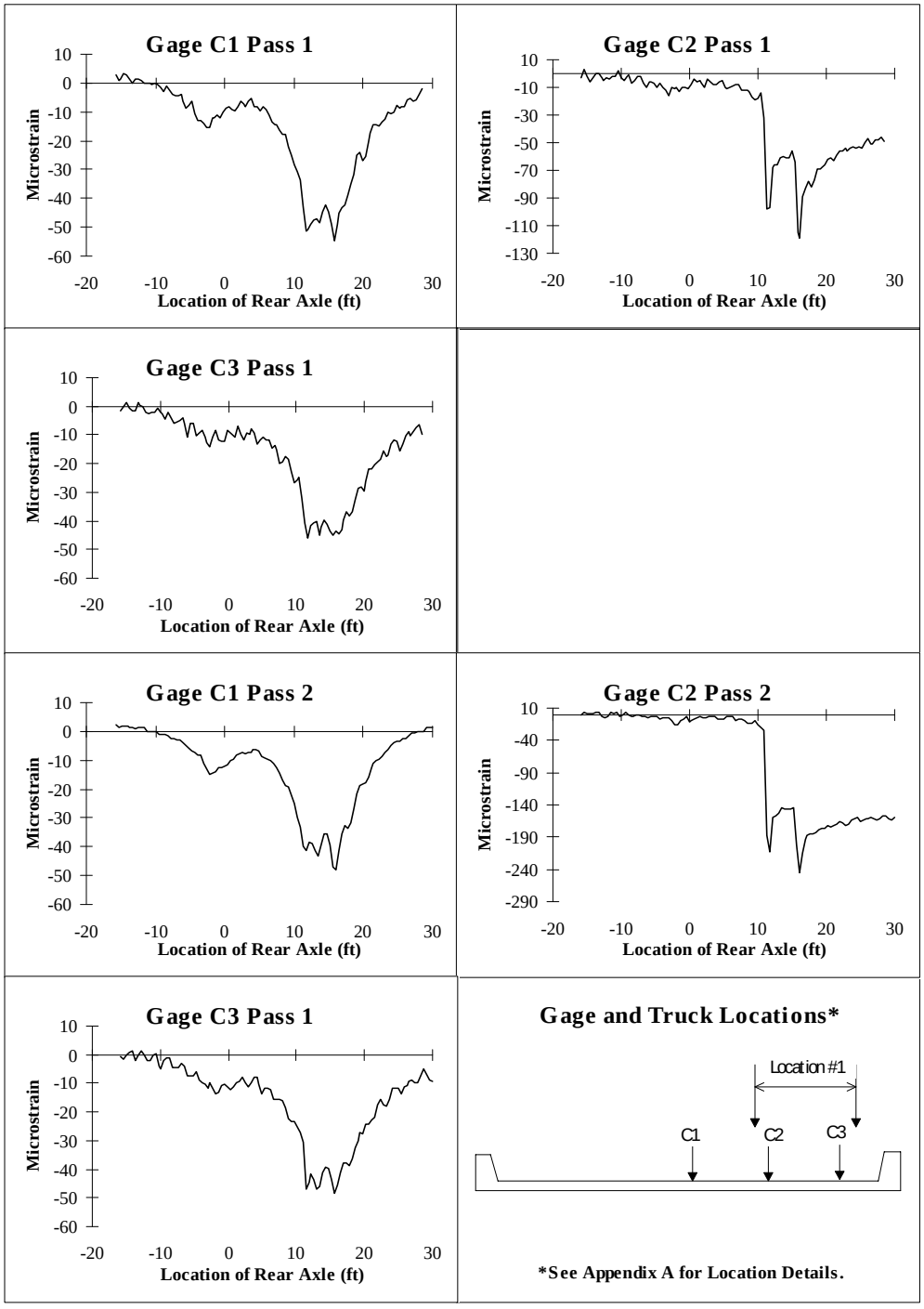

Figure D.1. Strain Data for Test Series 3, Location 1, Passes 1 & 2.

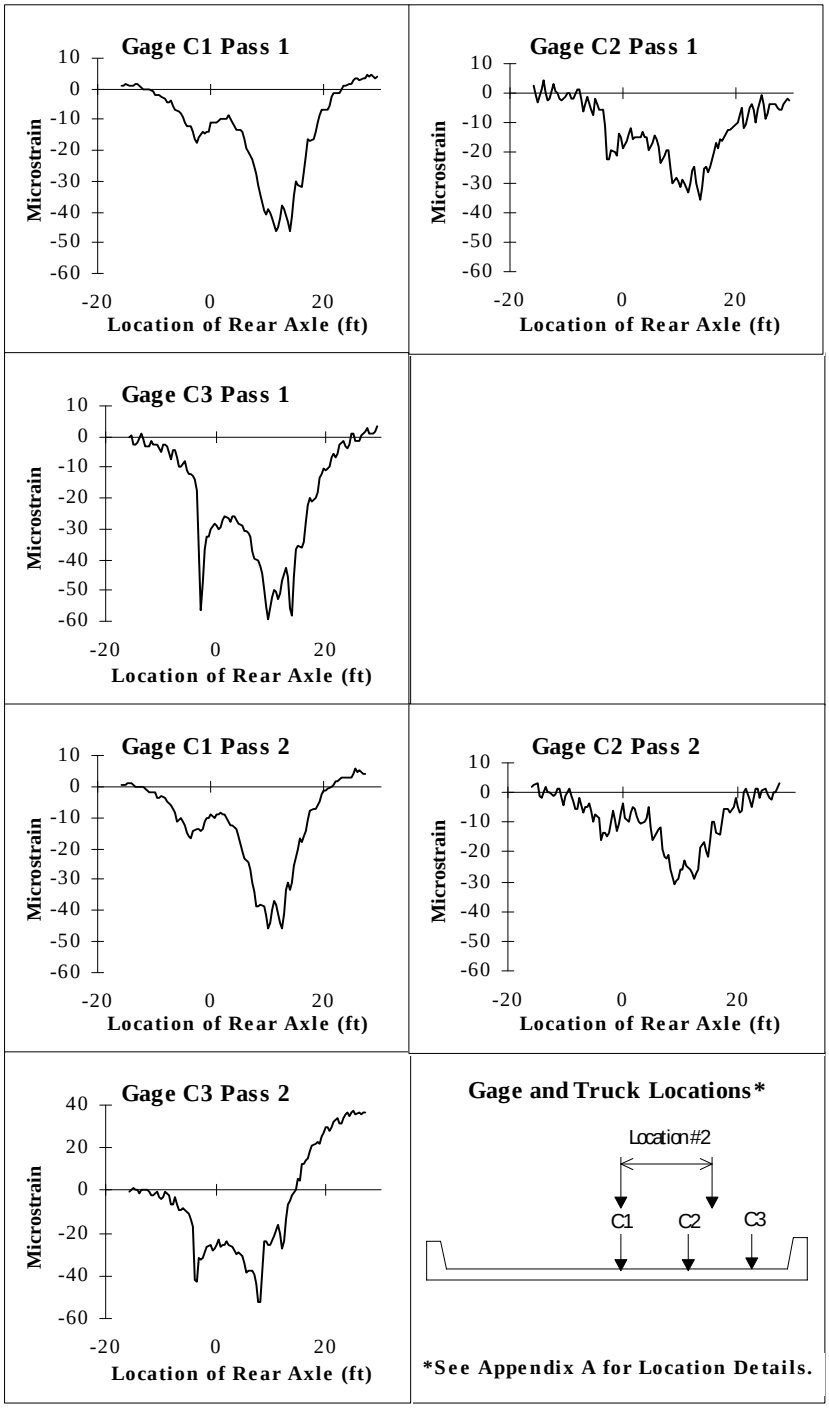

Figure D.2. Strain Data for Test Series 3, Location 2, Passes 1 & 2.

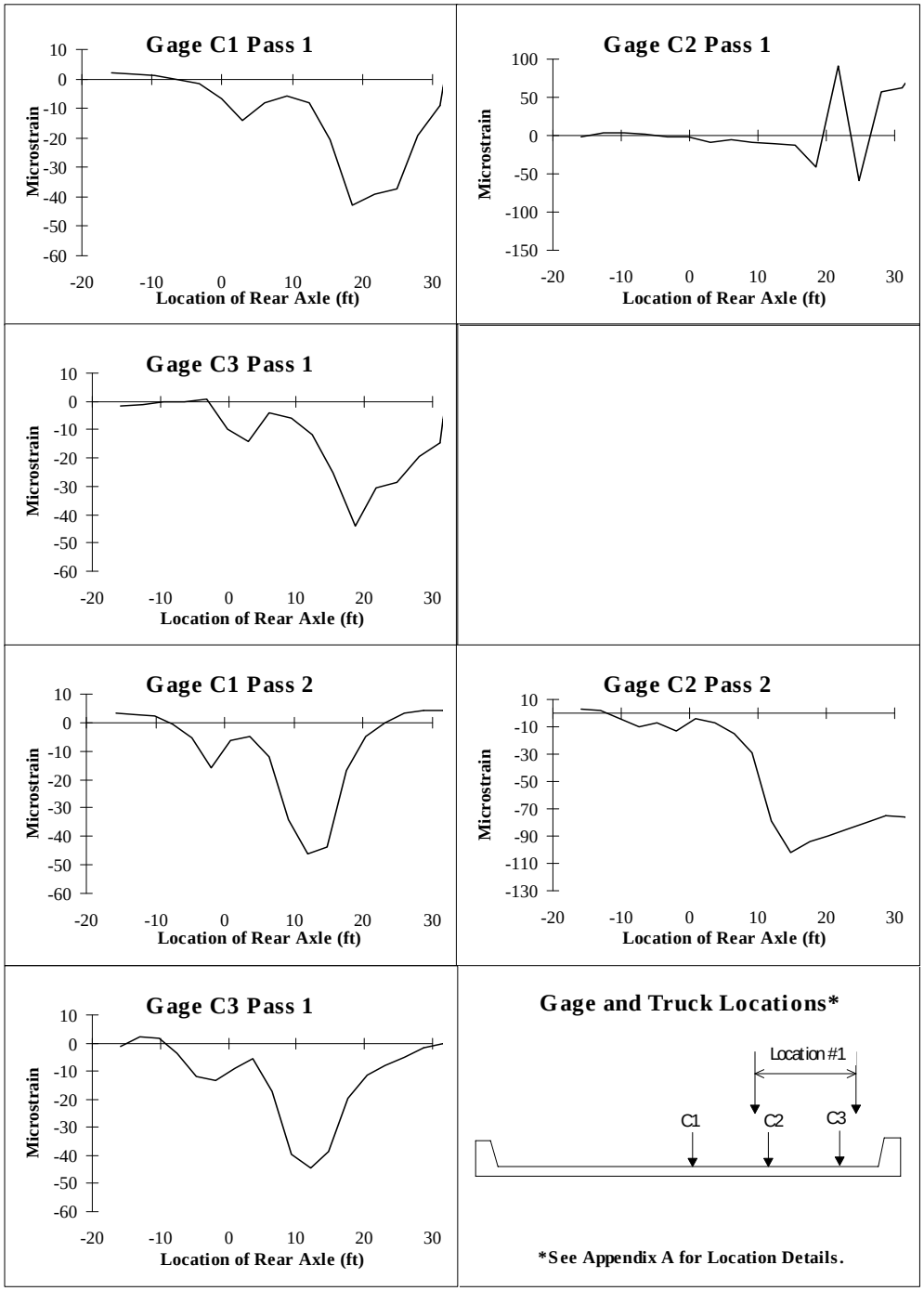

Figure D.3. Strain Data for Test Series 3A, Location 1, Passes 1 & 2.

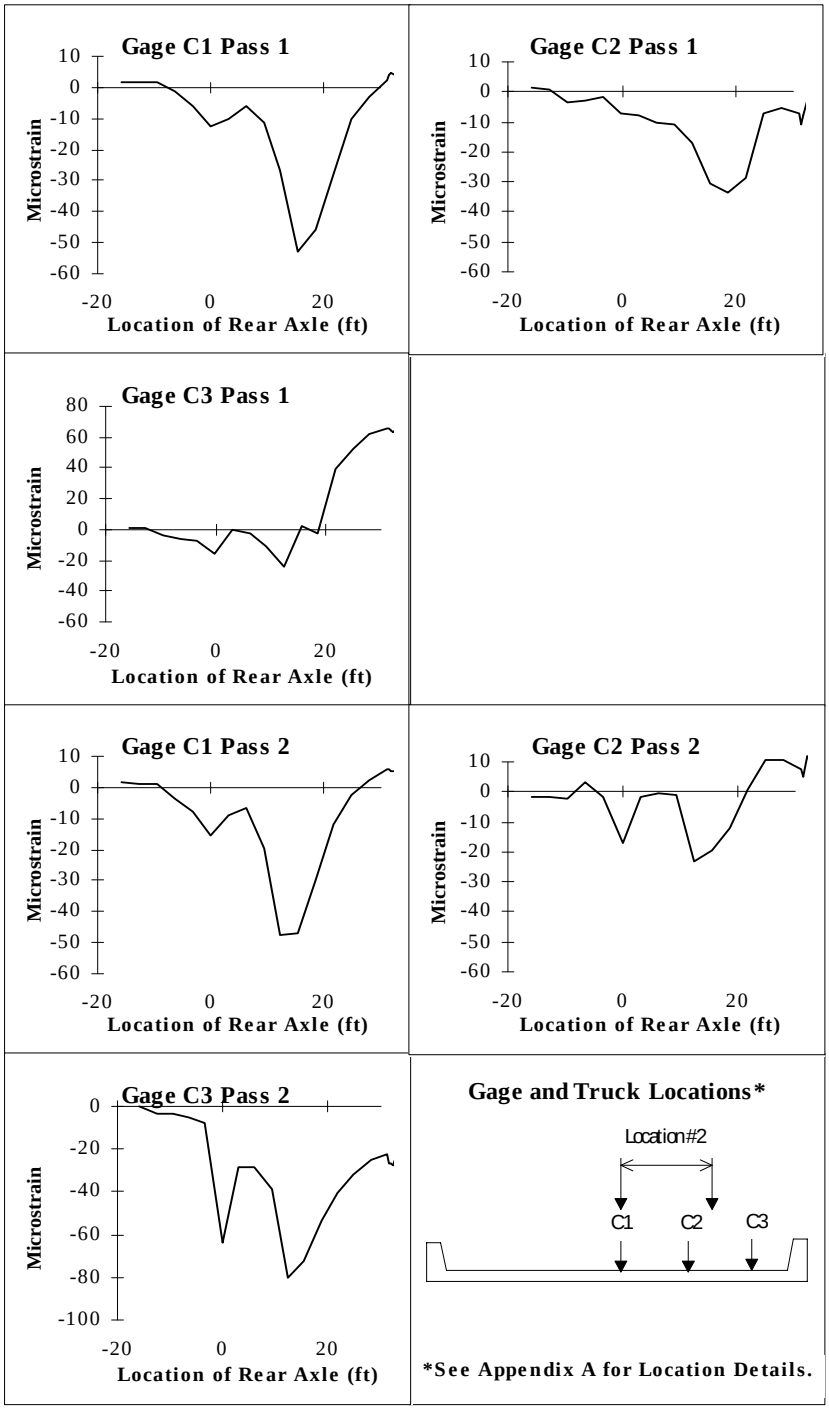

Figure D.4. Strain Data for Test Series 3A, Location 2, Passes 1 & 2.

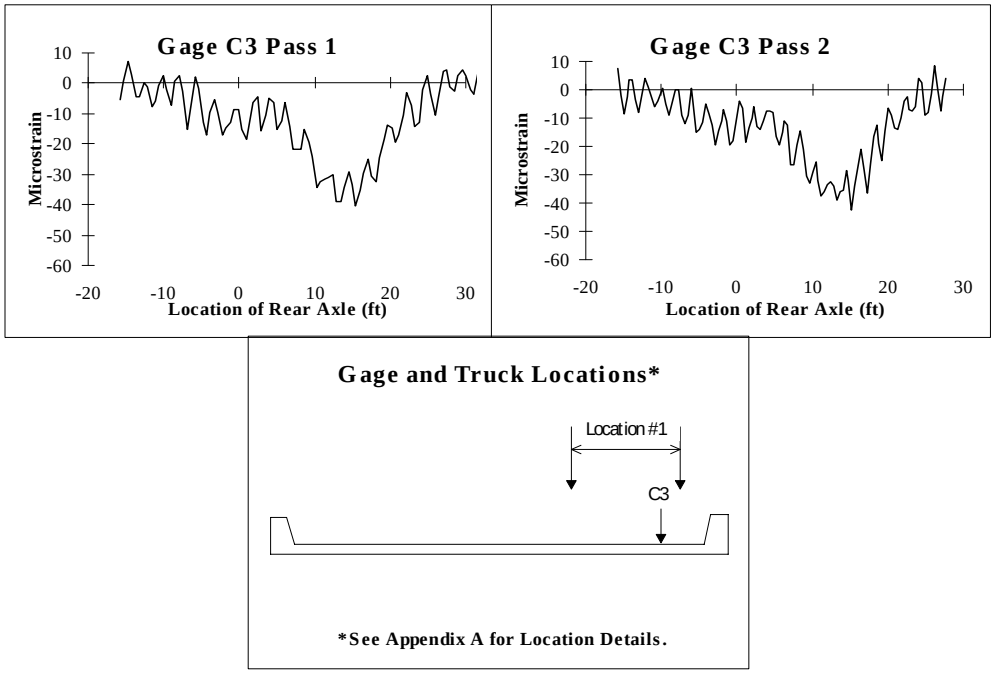

Figure D.5. Strain Data for Test Series 4, Location 1, Passes 1 & 2.

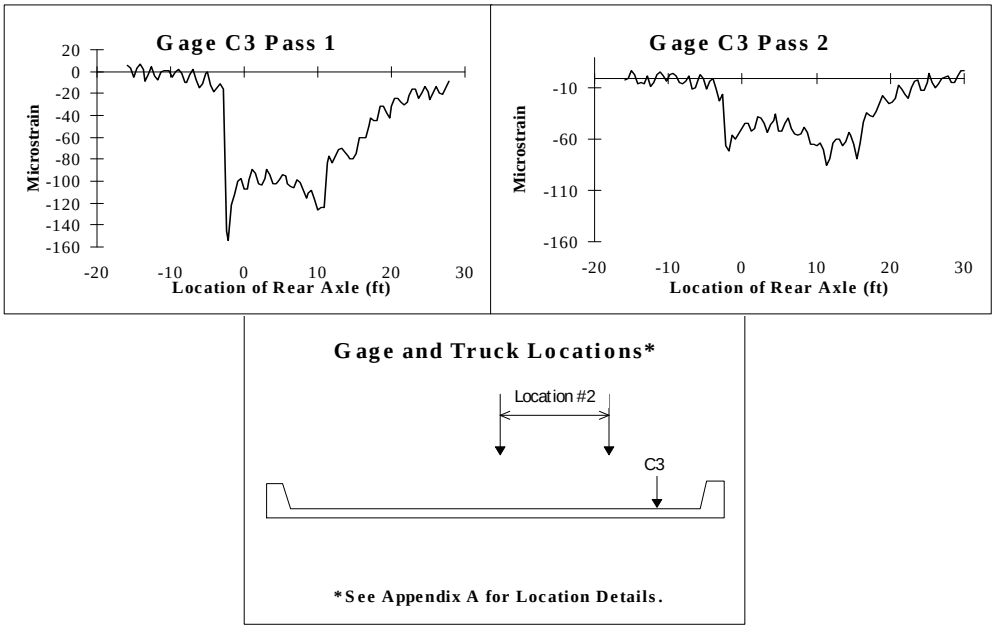

Figure D.6. Strain Data for Test Series 4, Location 2, Passes 1 & 2.

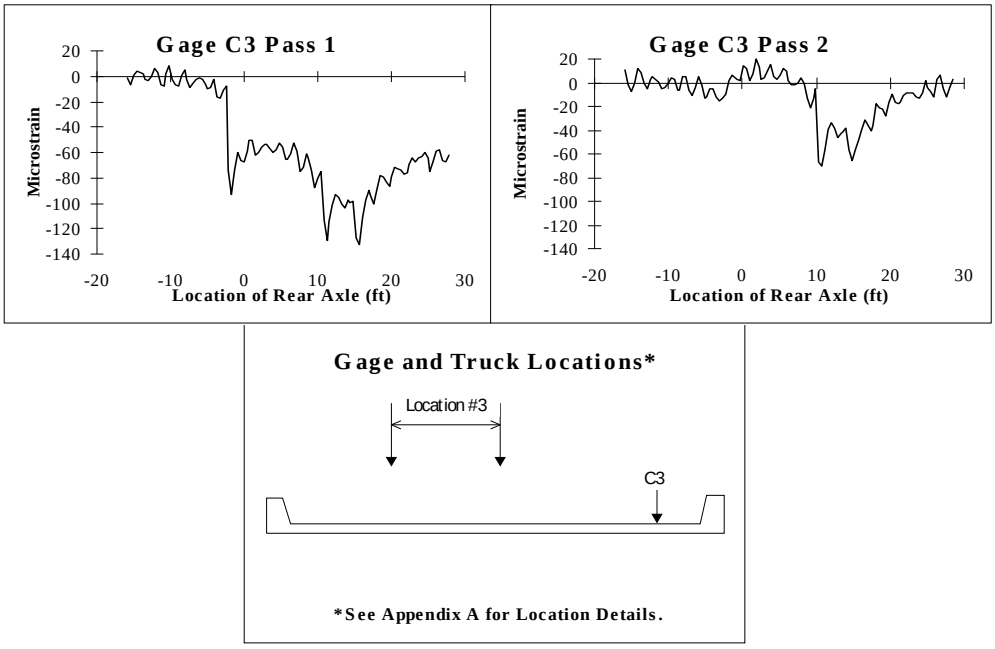

Figure D.7. Strain Data for Test Series 4, Location 3, Passes 1 & 2.

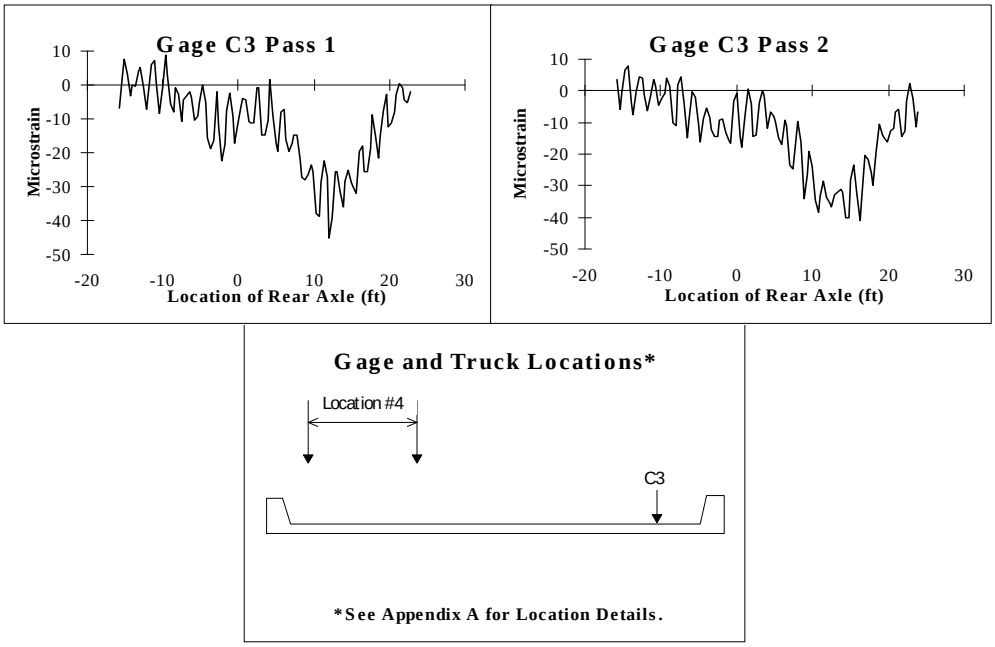

Figure D.8. Strain Data for Test Series 4, Location 4, Passes 1 & 2.

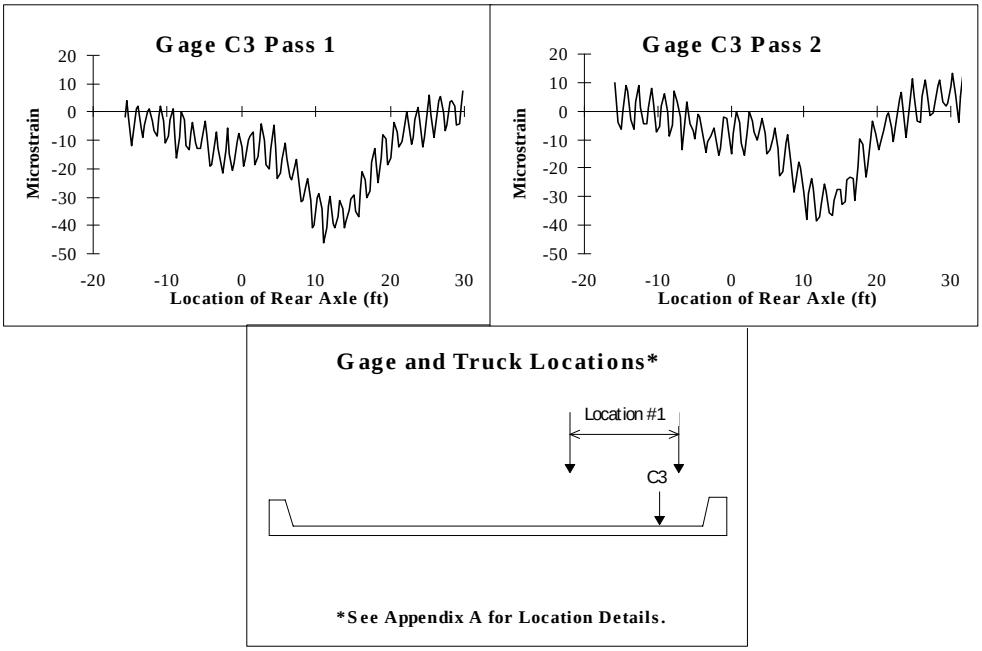

Figure D.9. Strain Data for Test Series 5, Location 1, Passes 1 & 2.

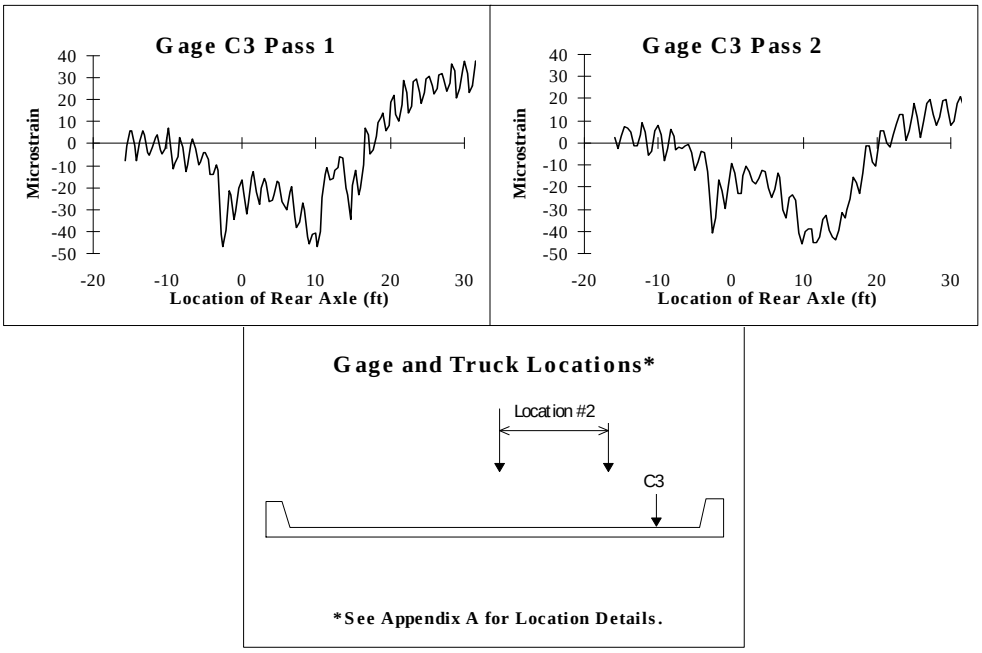

Figure D.10. Strain Data for Test Series 5, Location 2, Passes 1 & 2.

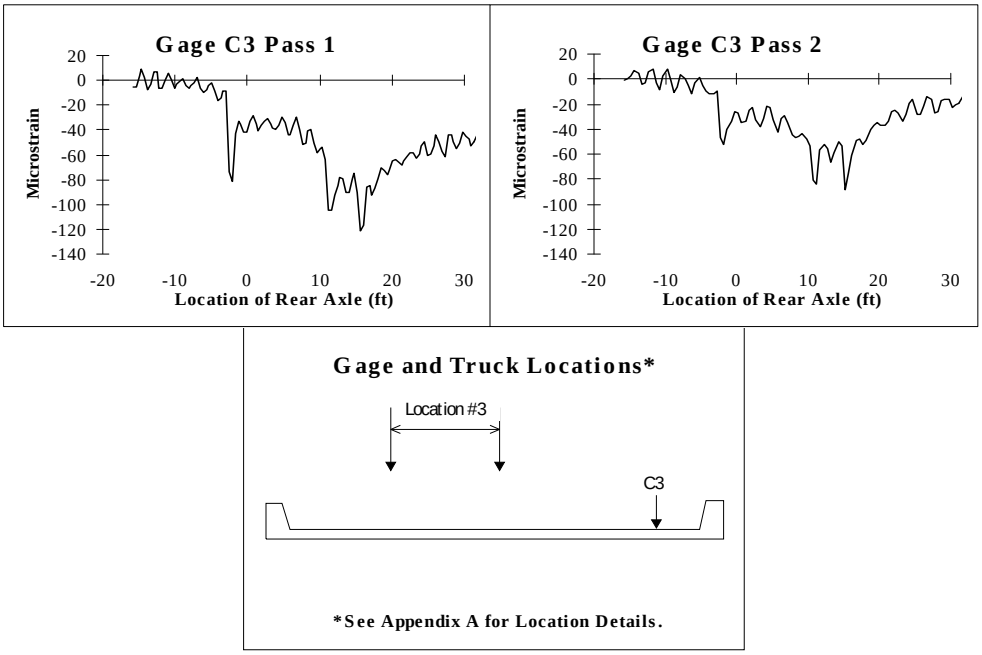

Figure D.11. Strain Data for Test Series 5, Location 3, Passes 1 & 2.

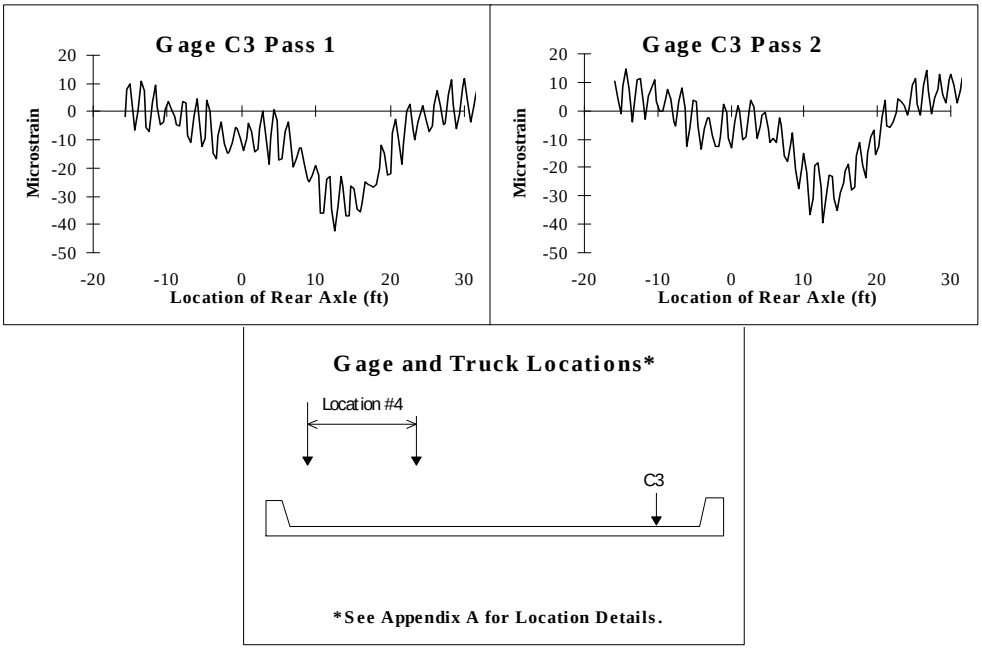

Figure D.12. Strain Data for Test Series 5, Location 4, Passes 1 & 2.

Appendix E. BOTTOM OF SLAB STRAIN DATA

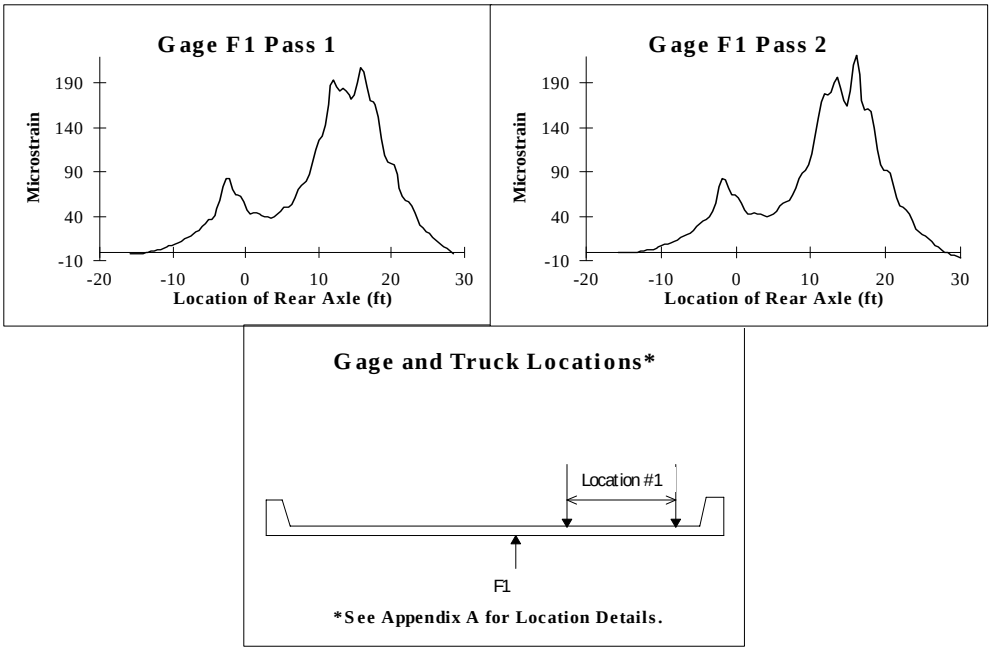

Figure E.1. Strain Data for Test Series 3, Location 1, Passes 1 & 2.

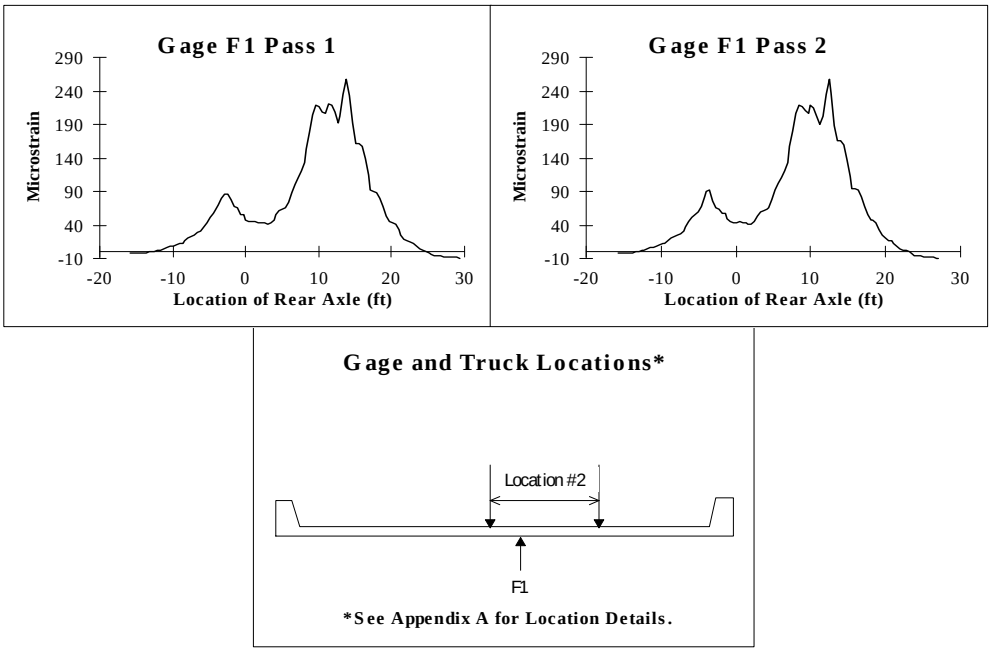

Figure E.2. Strain Data for Test Series 3, Location 2, Passes 1 & 2.

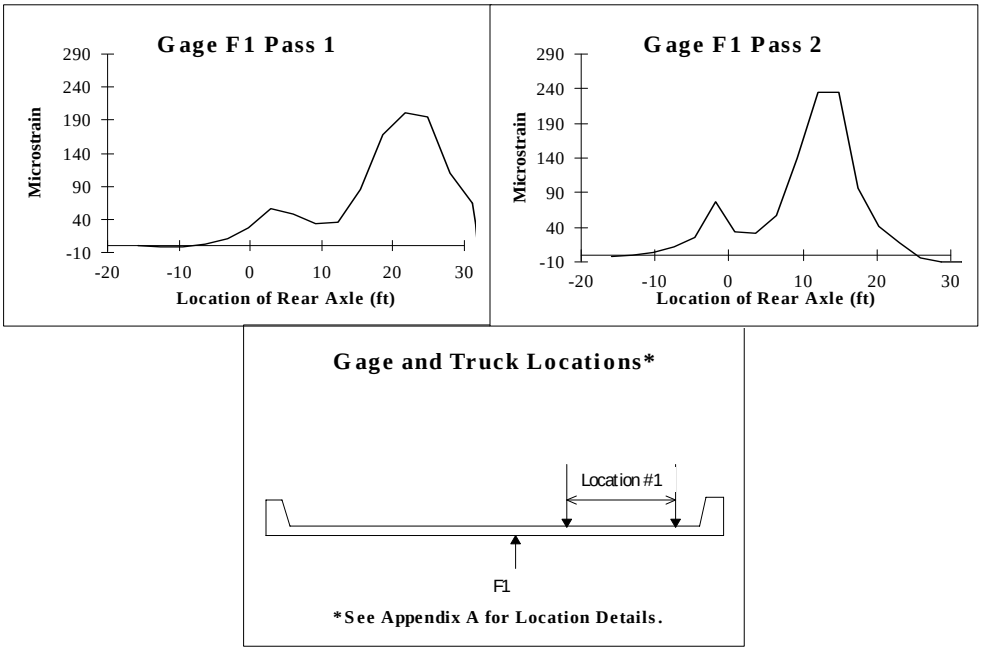

Figure E.3. Strain Data for Test Series 3A, Location 1, Passes 1 & 2.

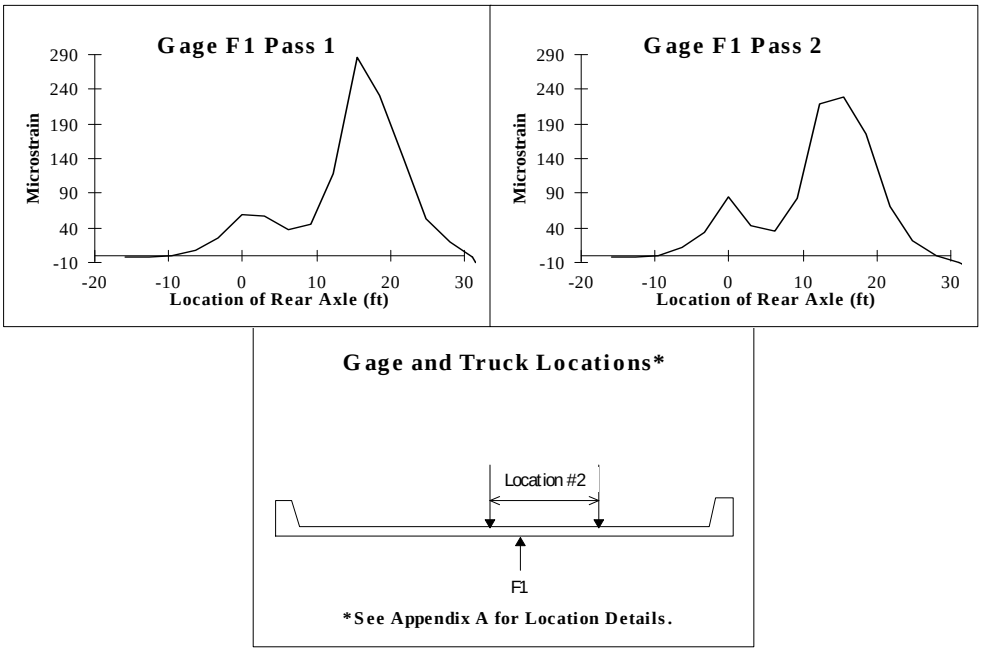

Figure E.4. Strain Data for Test Series 3A, Location 2, Passes 1 & 2.

Appendix F. CURB STRAIN DATA

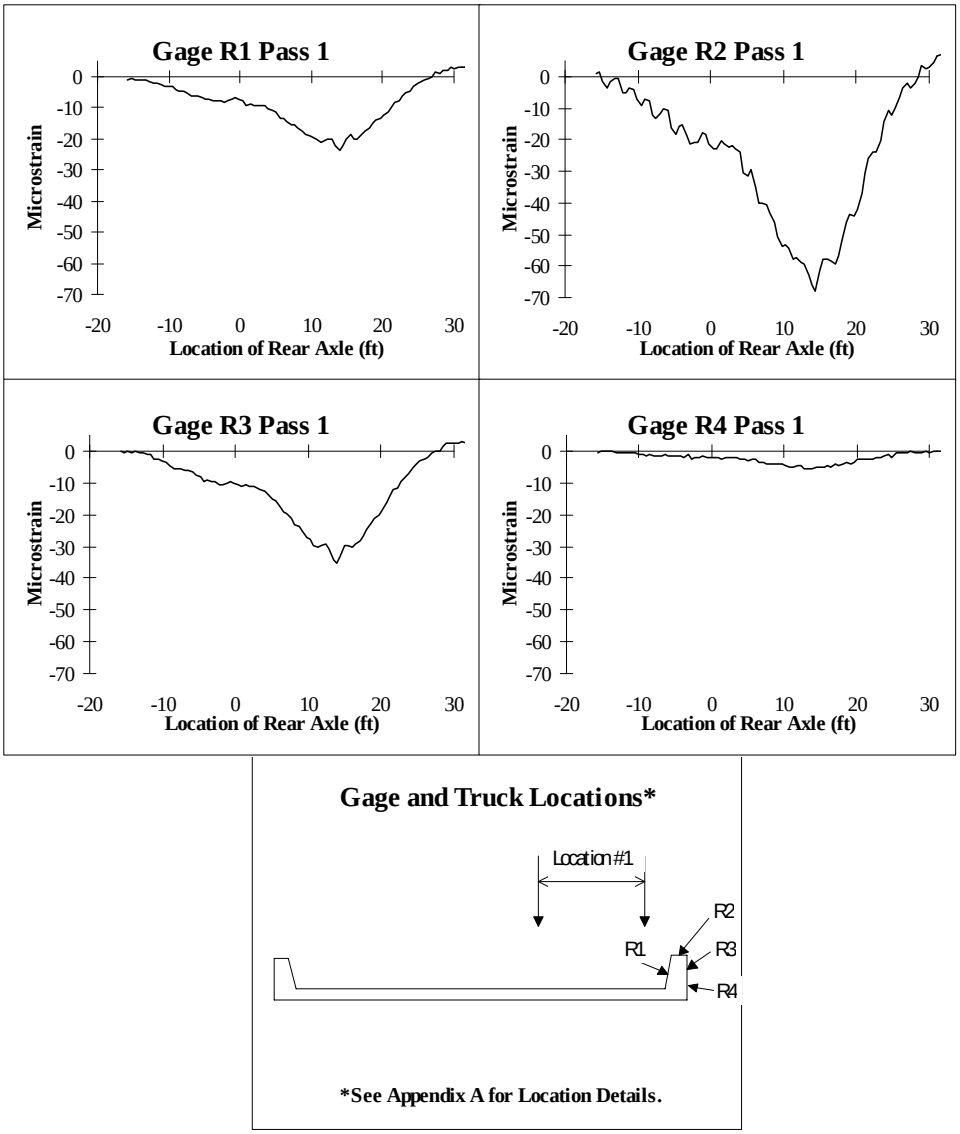

Figure F.1 Strain Data for Test Series 4, Location 1, Pass 1.

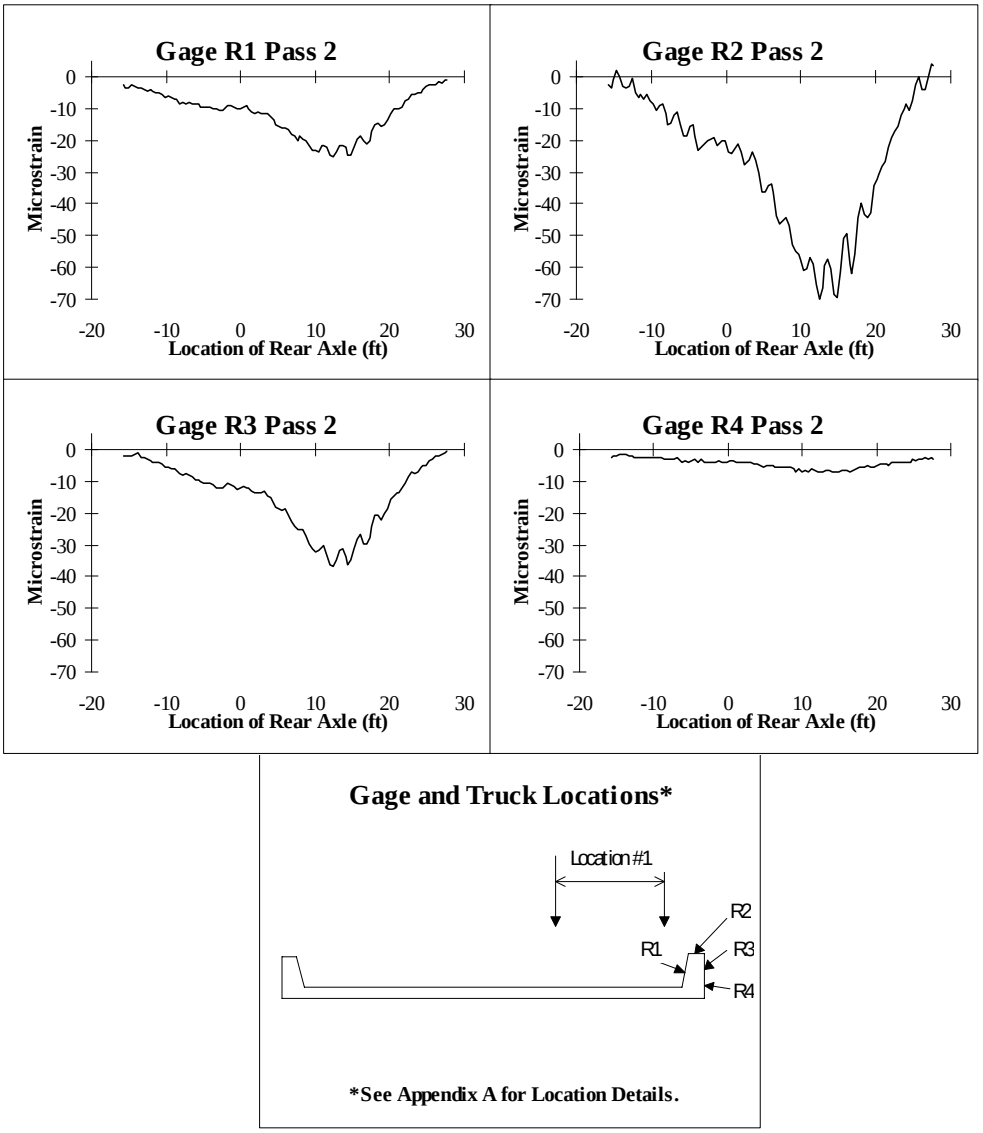

Figure F.2 Strain Data for Test Series 4, Location 1, Pass 2.

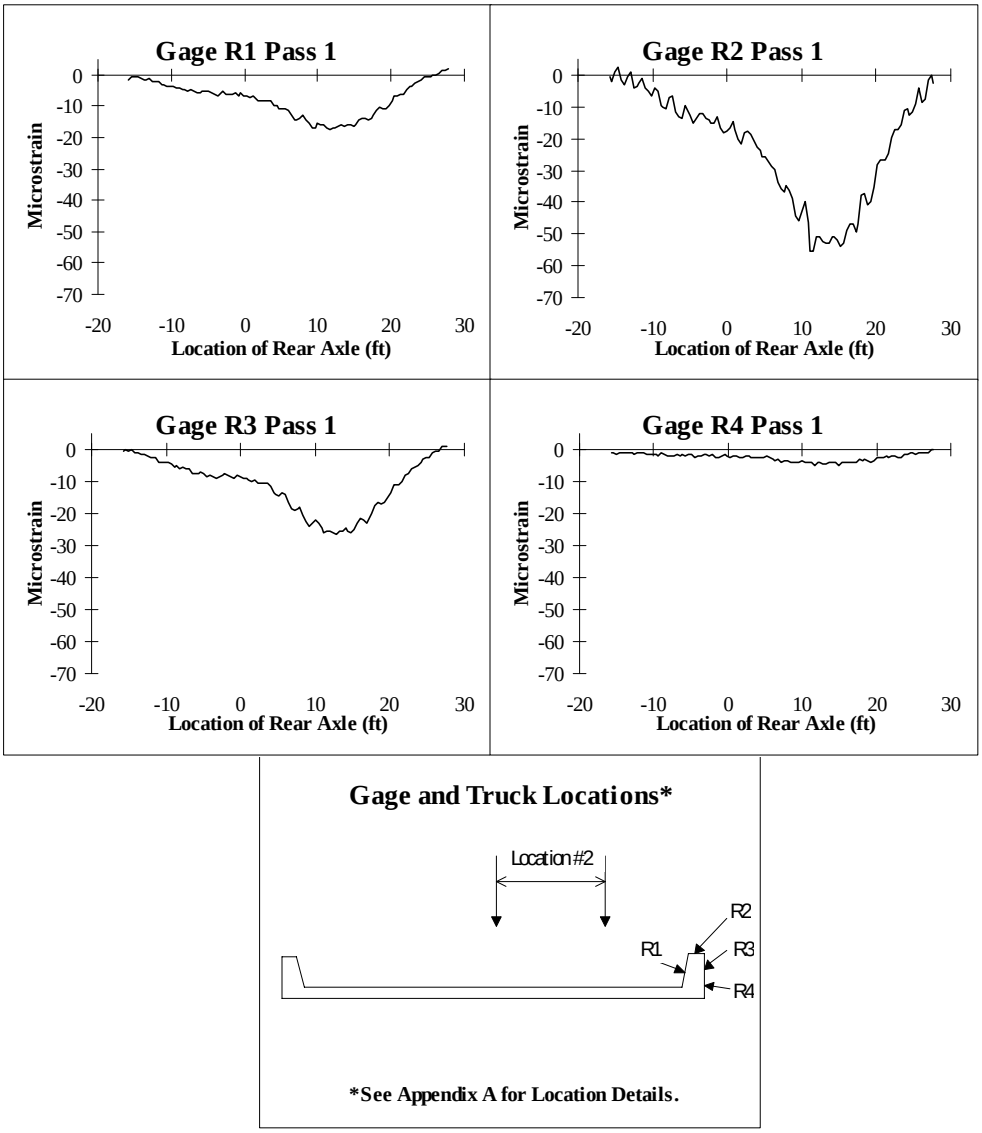

Figure F.3 Strain Data for Test Series 4, Location 2, Pass 1.

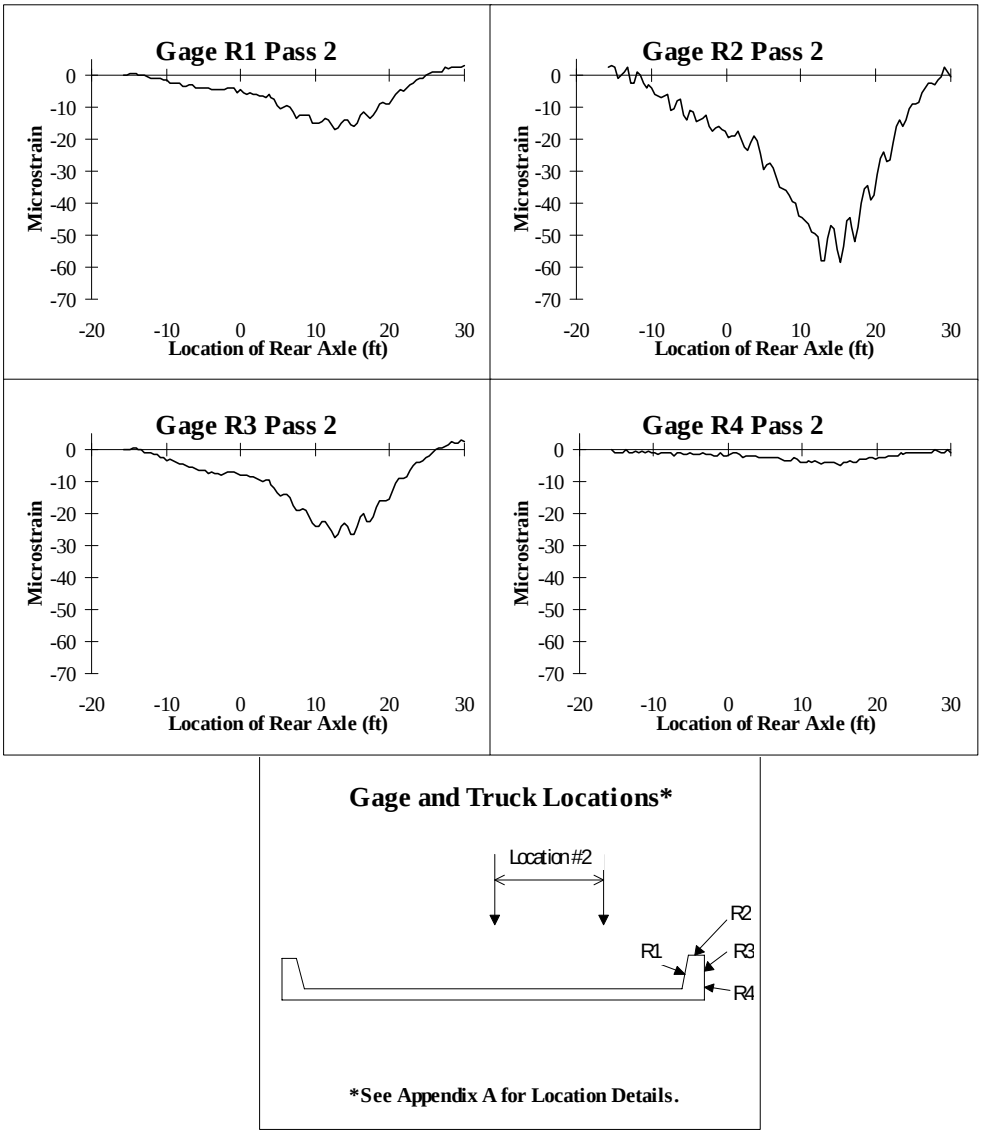

Figure F.4 Strain Data for Test Series 4, Location 2, Pass 2.

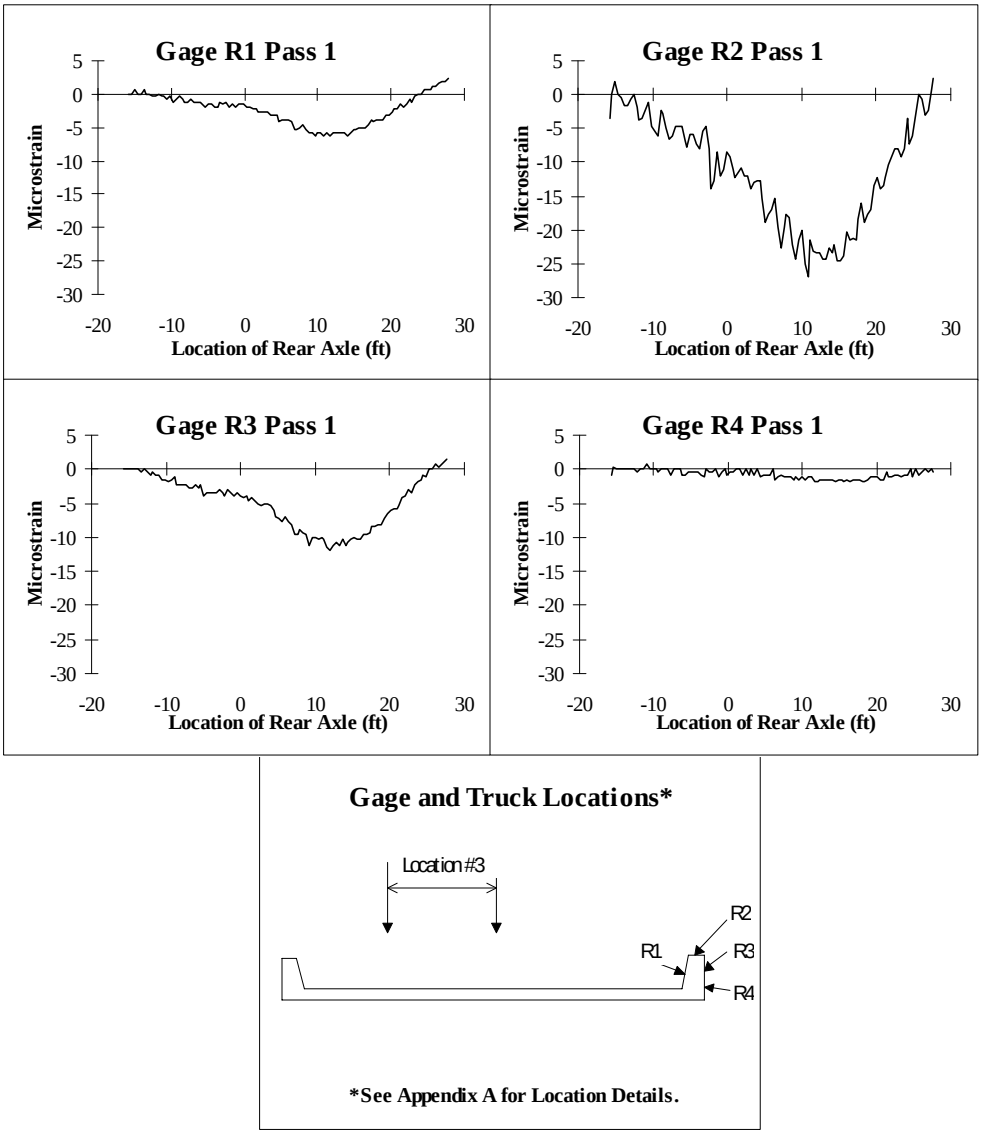

Figure F.5 Strain Data for Test Series 4, Location 3, Pass 1.

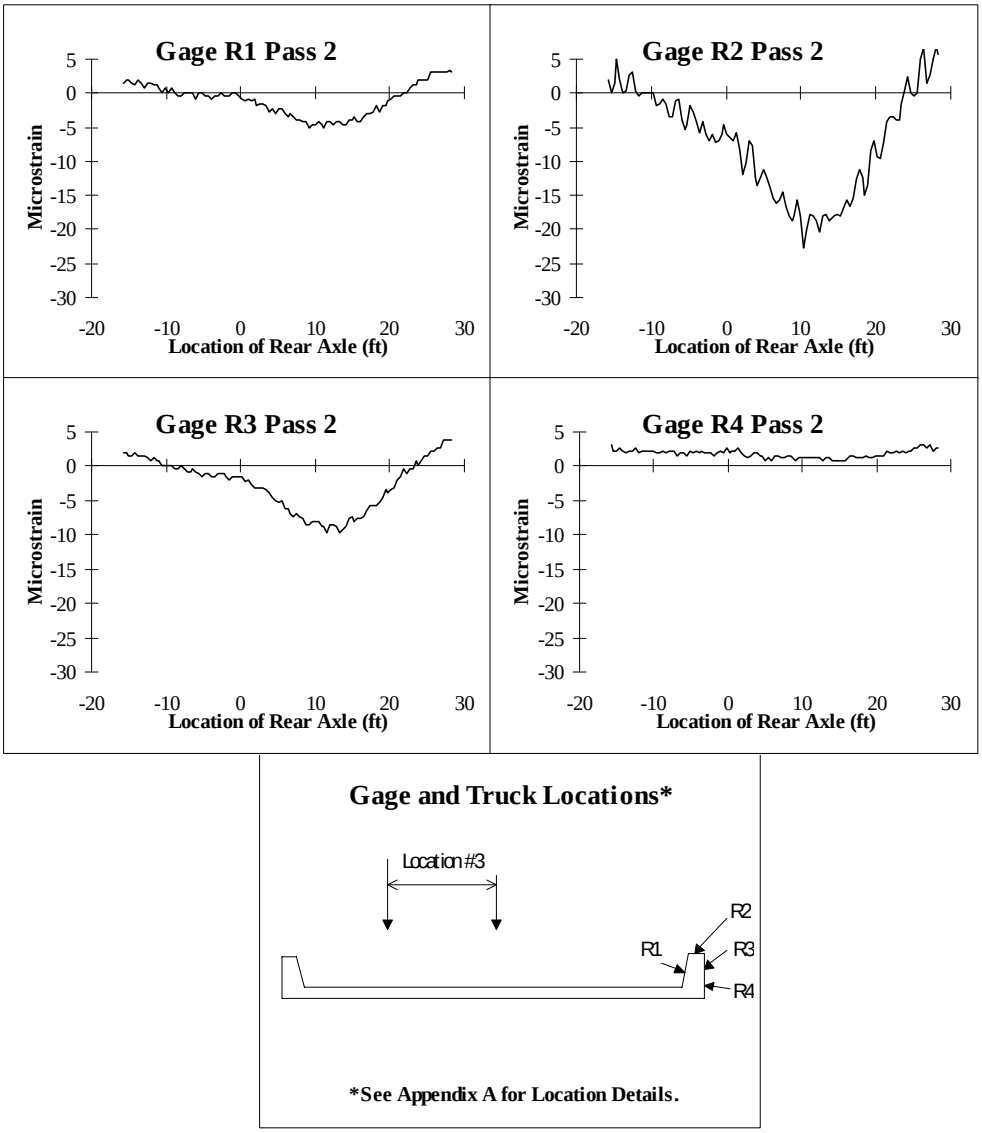

Figure F.6 Strain Data for Test Series 4, Location 3, Pass 2.

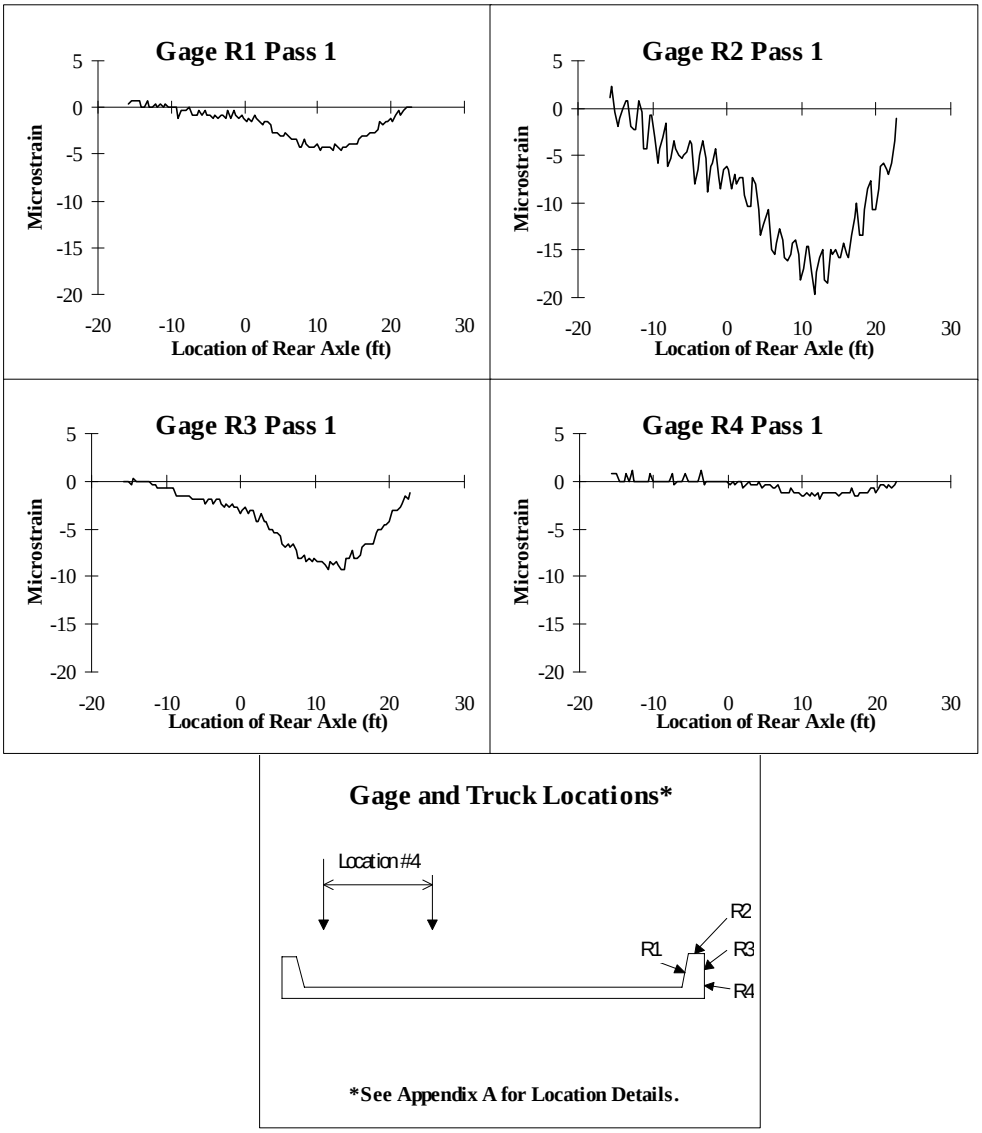

Figure F.7 Strain Data for Test Series 4, Location 4, Pass 1.

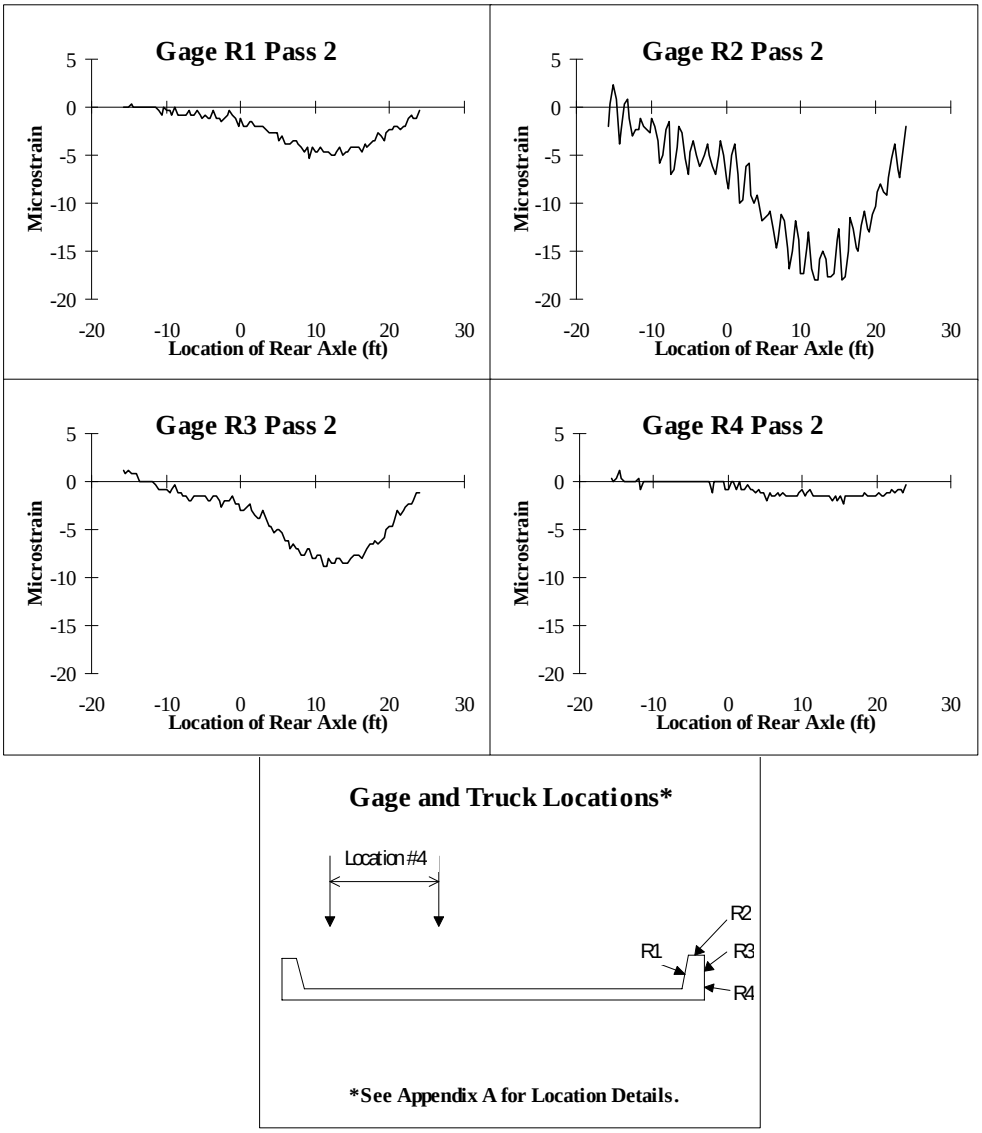

Figure F.8 Strain Data for Test Series 4, Location 4, Pass 2.

Appendix G. DEFLECTION DATA

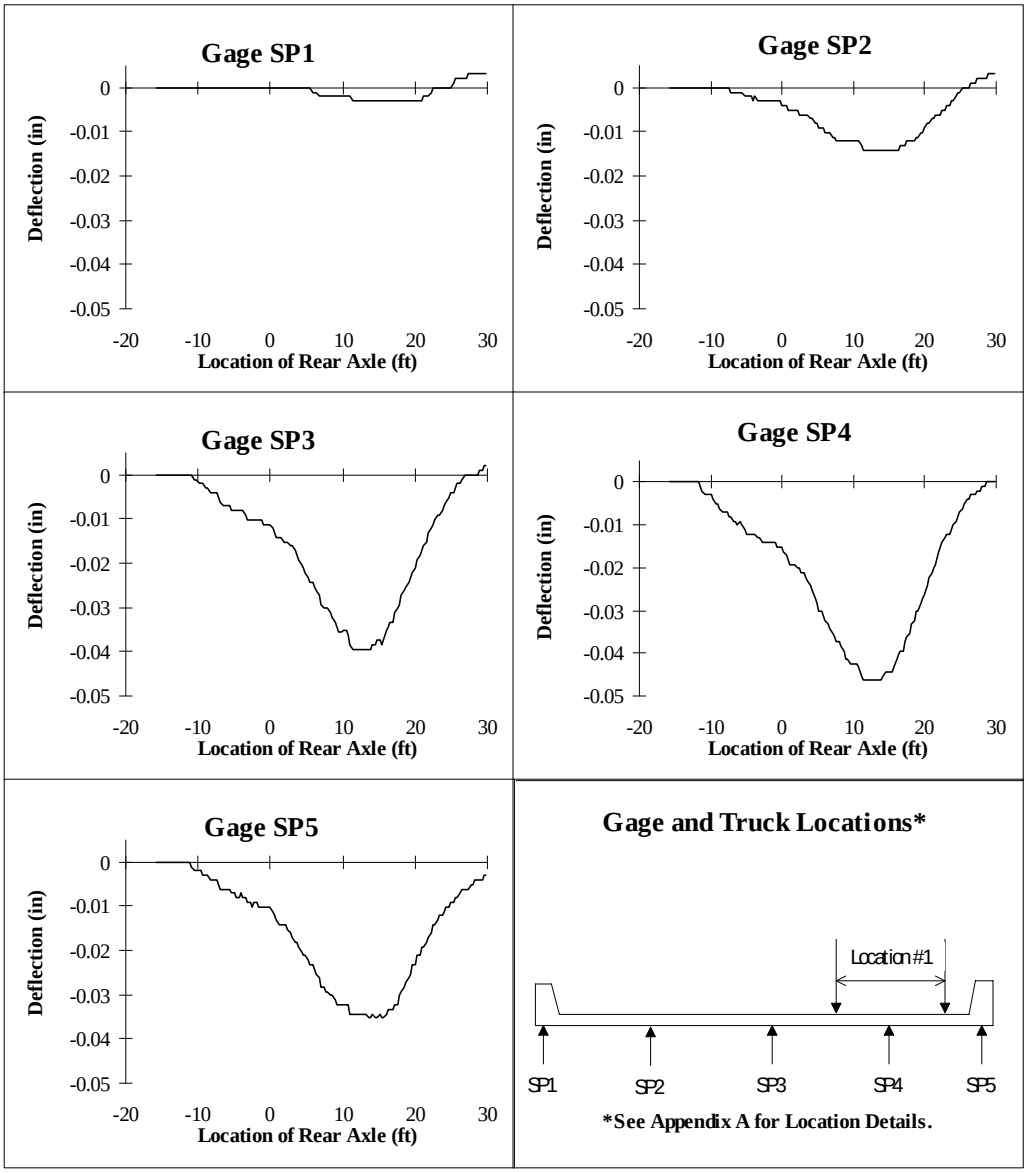

Figure G.1. Deflection Data for Test Series 5, Location 1, Pass 1.

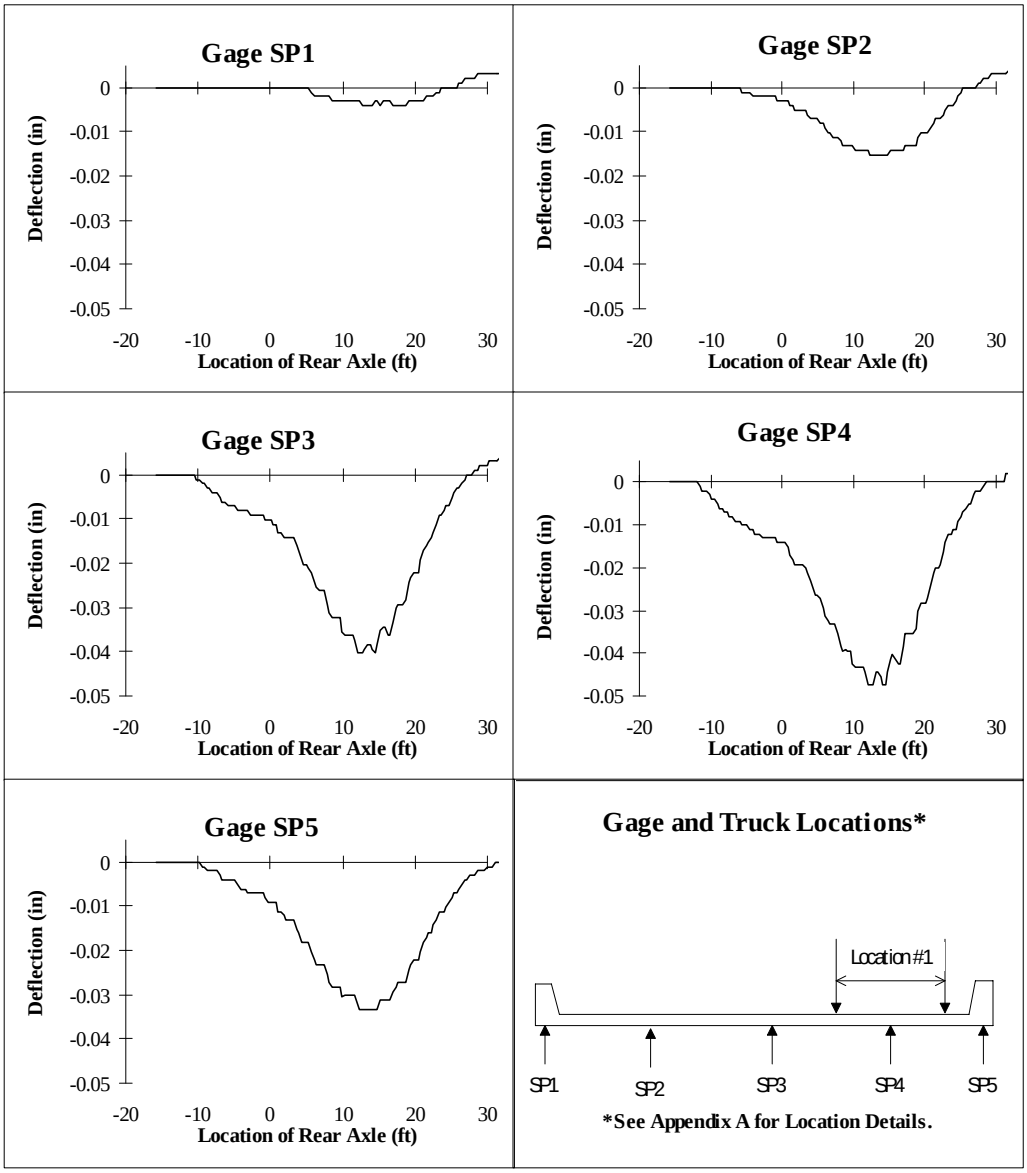

Figure G.2. Deflection Data for Test Series 5, Location 1, Pass 2.

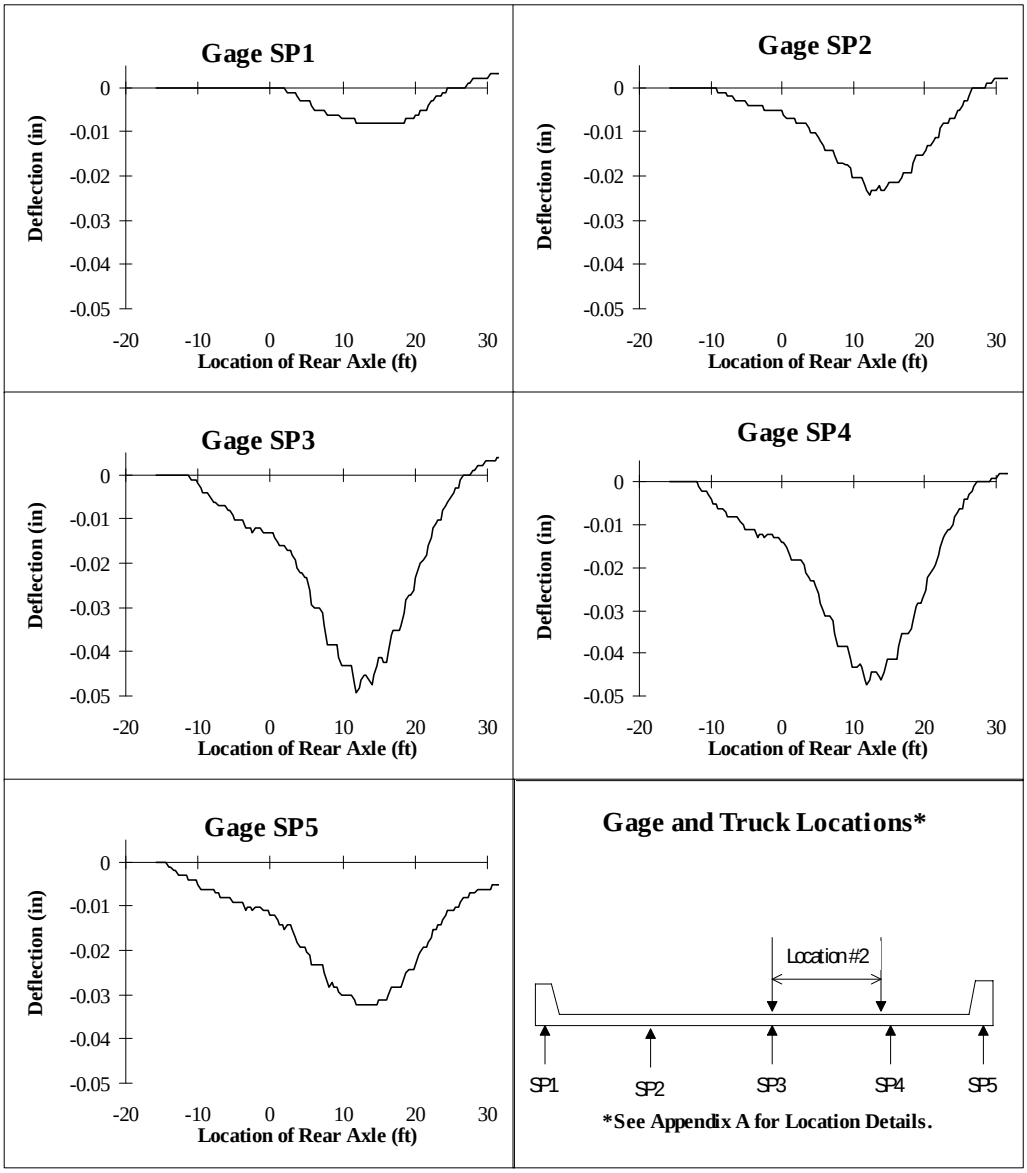

Figure G.3. Deflection Data for Test Series 5, Location 2, Pass 1.

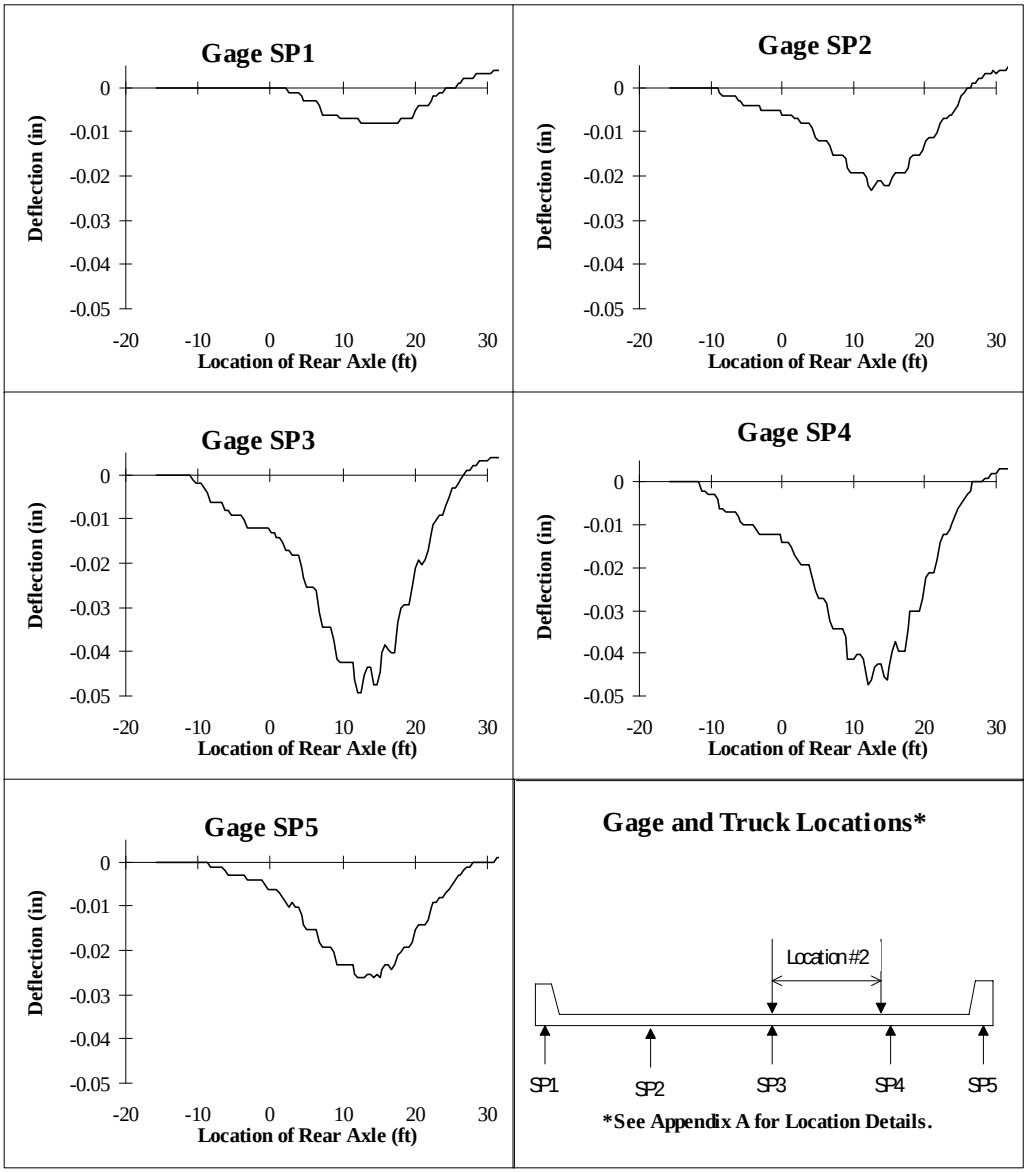

Figure G.4. Deflection Data for Test Series 5, Location 2, Pass 2.

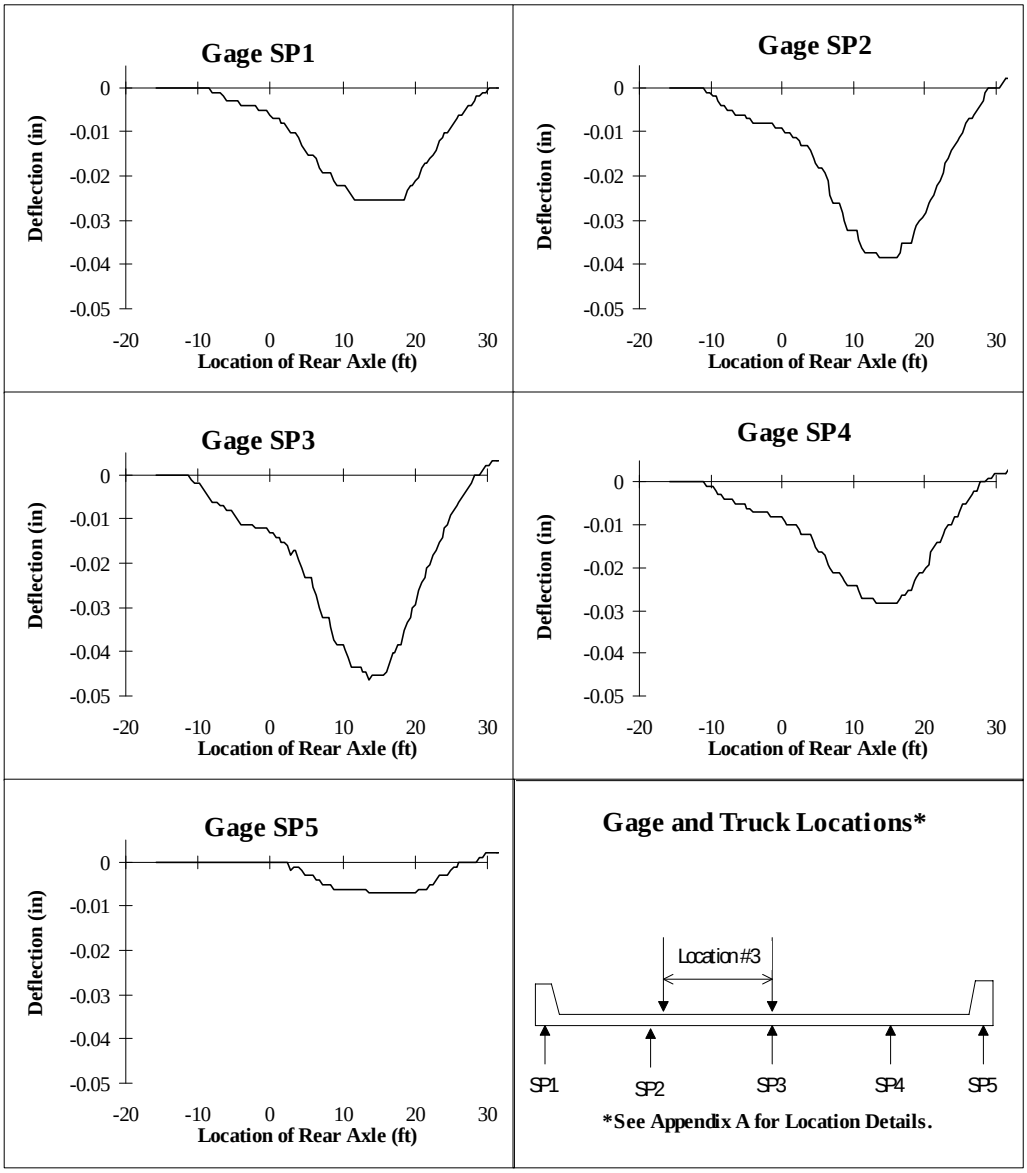

Figure G.5. Deflection Data for Test Series 5, Location 3, Pass 1.

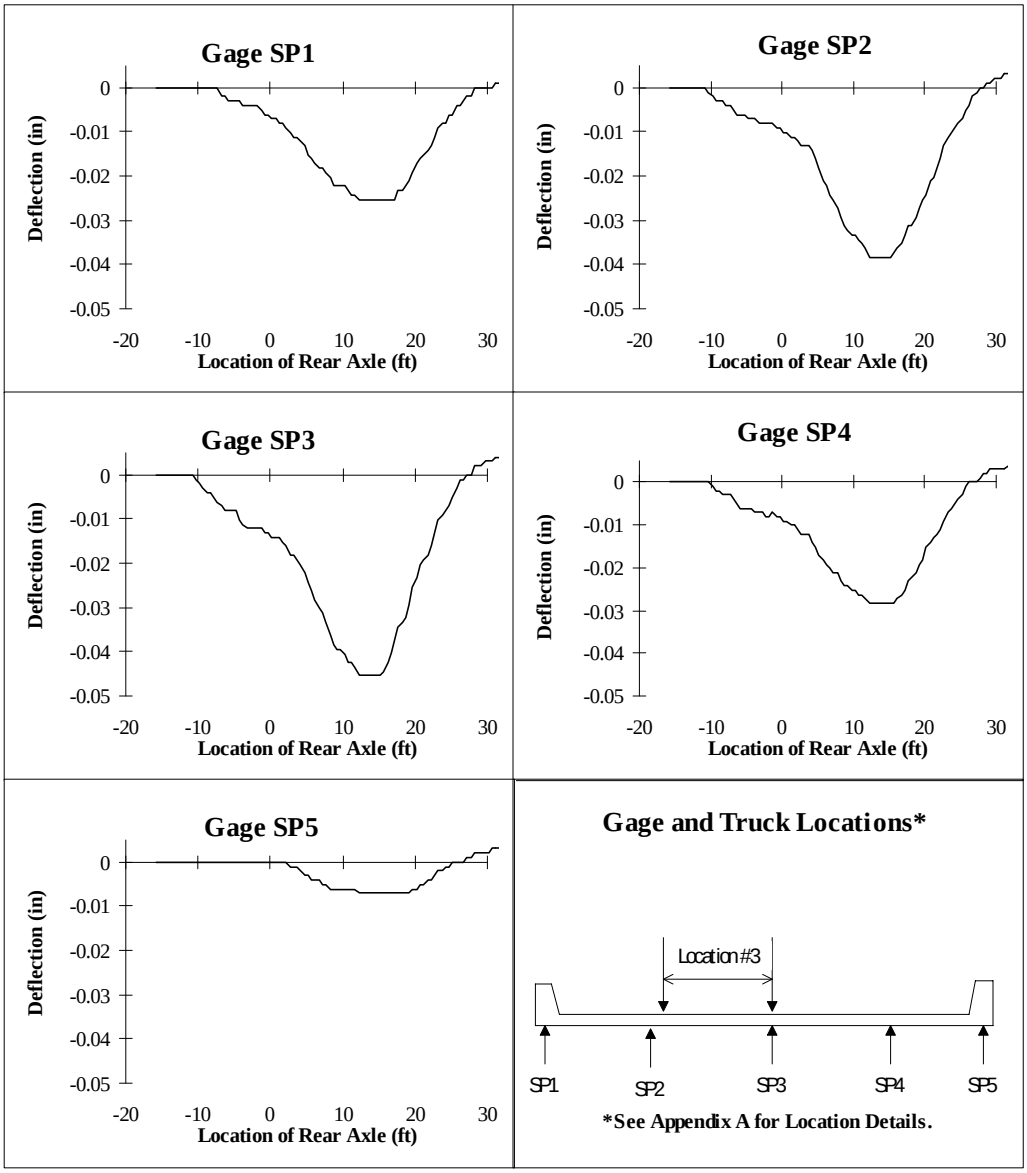

Figure G.6. Deflection Data for Test Series 5, Location 3, Pass 2.

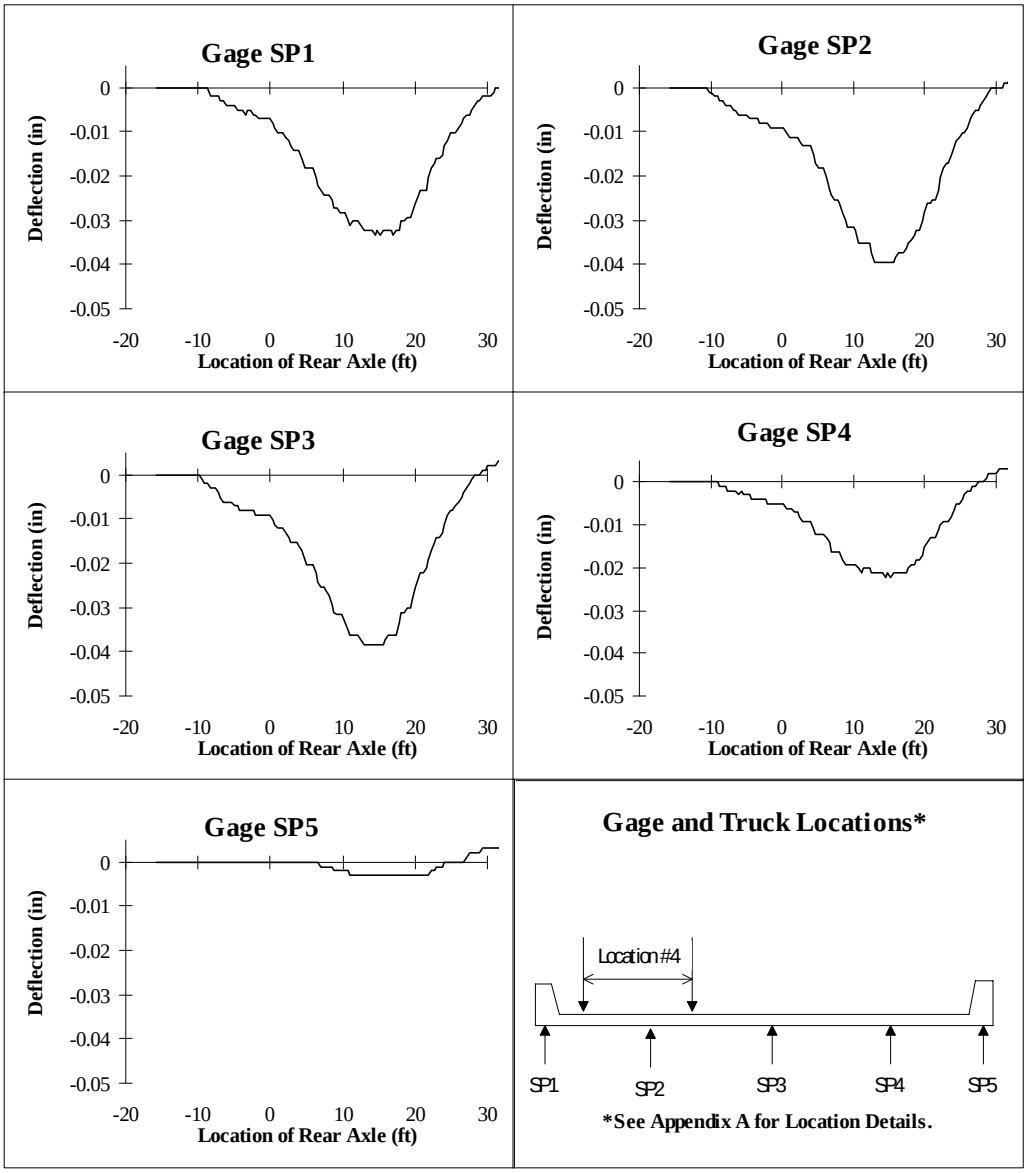

Figure G.7. Deflection Data for Test Series 5, Location 4, Pass 1.

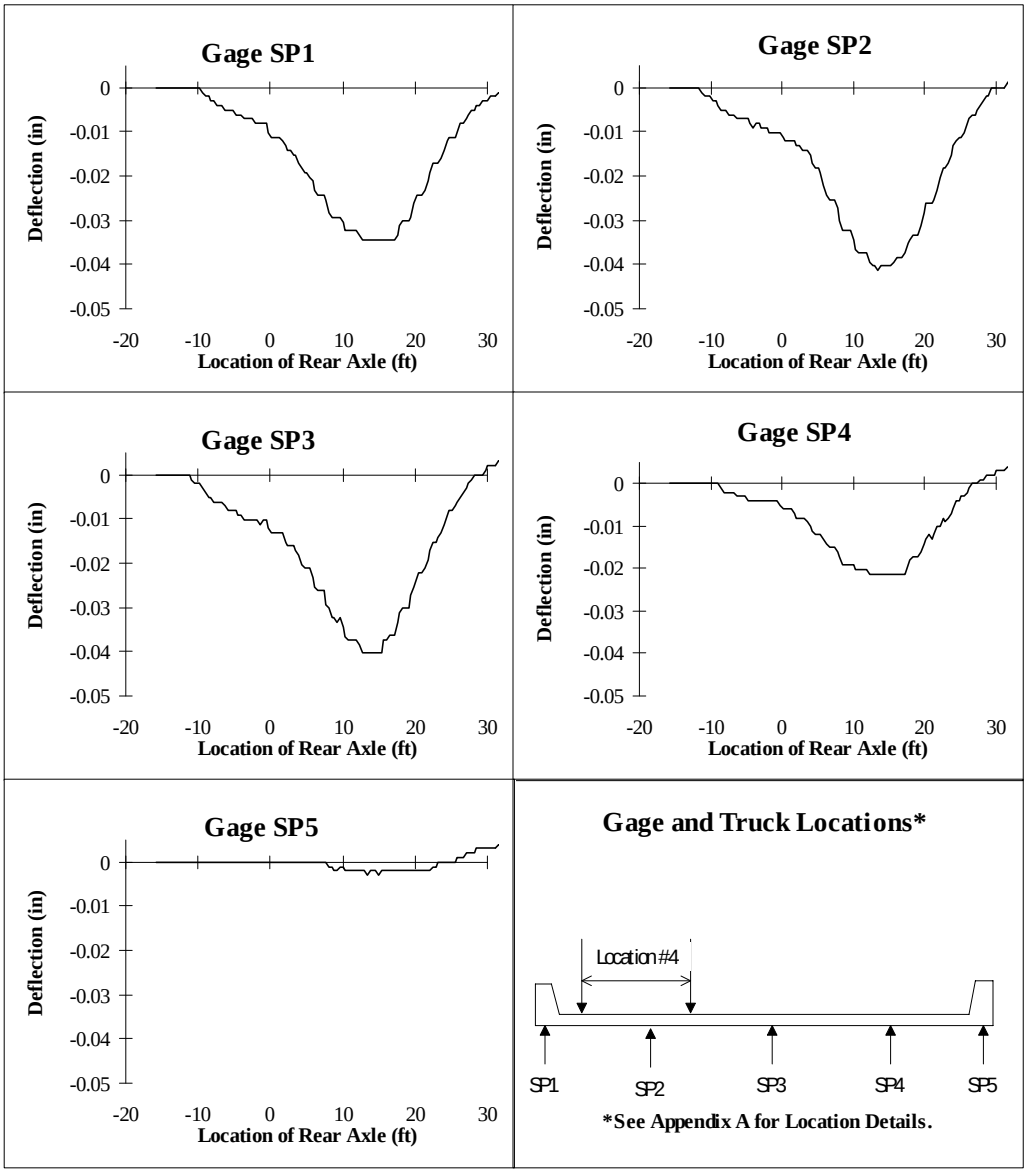

Figure G.8. Deflection Data for Test Series 5, Location 4, Pass 2.

Appendix H. COMPARISON OF CONCRETE SURFACE STRAIN MEASUREMENTS

H.1 Comparison of Strain Transducers and Wire Strain Gages

Both strain transducer T1 and strain gage F1 were placed on the tension surface of the slab. In order to compare the results, the gages both spanned across the same crack in the bottom of the slab. Figure H.1 shows the comparison of strains measured by these two gages. The measured strains from T1 were corrected for the 1/4 in. offset from the bottom of the slab. The large difference between the two strain readings is due to the fact that the strain is averaged over the length of the gage and the transducer has more than twice the gage length of the strain gage. The shift in the location of maximum value is due to the varying speed of the truck between the two tests and is not pertinent to this discussion.

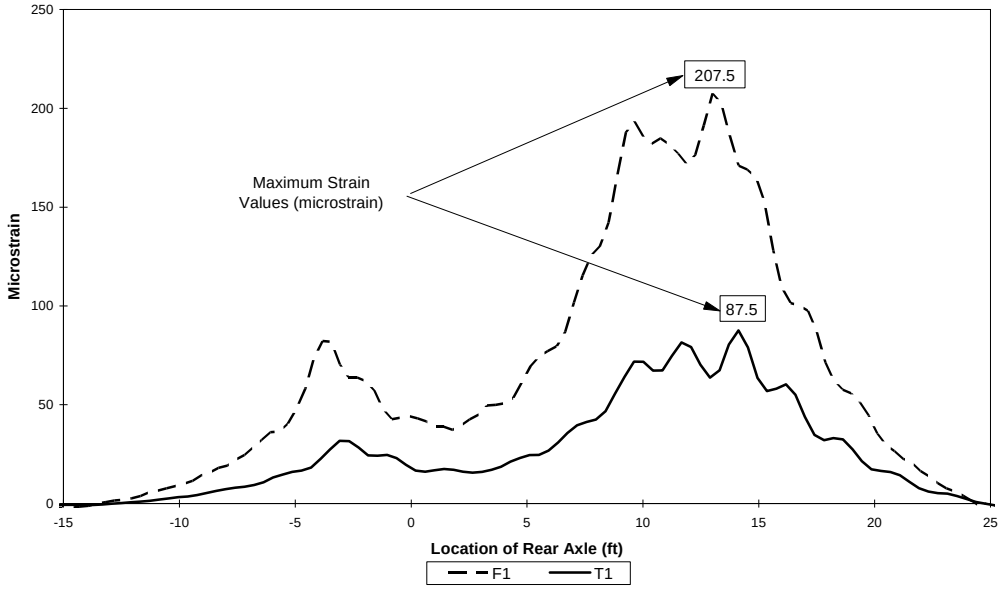

Figure H.1 Comparison of Strain for Transducers and Strain Gages.

By taking the strain values and multiplying by the gage lengths, a change in length can be determined. As shown in Table H.1 the difference in the measured elongation is within an average of 15%. The lesser values of elongation of the strain gage are expected because of the shorter gage length.

Table H.1 Comparison of Strain Transducers and Strain Gages.

Truck	Pass	Transducer T1*		Strain Gage F1**		% Difference
Location		strain, με	elongation, in.	strain, με	elongation, in.	in Elongation
1	1	82.8	0.00058	207.5	0.00049	15.5%
1	2	87.5	0.00061	221.0	0.00052	14.9%
2	1	98.1	0.00069	257.5	0.00061	11.5%
2	2	106.5	0.00075	257.9	0.00061	18.4%
				Average % Difference		15.1%

* Gage Length for T1 = 7 in.
**Gage Length for F1 = 60 mm.

Although the difference in elongation is 15%, the difference in gage length is 66%. This shows that the majority of the strain occurred at the crack. This confirms that regardless of the type of gage used, the cracks in a cracked section must be crossed with the gage.

H.2 Surface Strain Measurements with Mechanical Strain Transducers

As discussed in Chapter 3 and Appendix A, three mechanical strain transducers were attached to the bottom of the slab in an attempt to measure and correlate surface strain with the strain in the reinforcing bars. If a correlation could be determined, then this method of measuring strain would be much easier and faster than attaching strain gages to the reinforcing bars.

One transducer (T1) was mounted across a visible crack in the concrete surface to observe the effects on surface strain. The two other transducers (T2 and T3) were mounted where no visible cracks were observed. Table H.2 shows

the comparison of T1 with the strain at the bottom of the slab calculated by the methods outlined in Chapter 5. As shown the calculated bottom strains are approximately 18% less than the surface strains measured with T1.

Table H.2 Comparison of Transducer T1 Data.

Location 1 Pass 1				Location 1 Pass 2		
	Average	Std Dev			Average	Std Dev
T1	77	4.7		T1	77	7.6
Bottom	63	4.1		Bottom	64	6.4
% Diff	-18%			% Diff	-17%	
Location 2 Pass 1				Location 2 Pass 2		
	Average	Std Dev			Average	Std Dev
T1	91	7.3		T1	90	9.2
Bottom	75	5.5		Bottom	74	6.1
% Diff	-17%			% Diff	-18%	

Figure H.2 shows transducer T1 plotted with gages RB1 and RB2 which were on either side of T1 as shown in the instrumentation plan in Appendix A. Also plotted with the gage data is a projected bottom strain based on the cracked neutral axis location and the average strain of RB1 and RB2. The strain readings are consistently high throughout the entire loading spectrum. This shows no additional cracking occurred during the test loading.

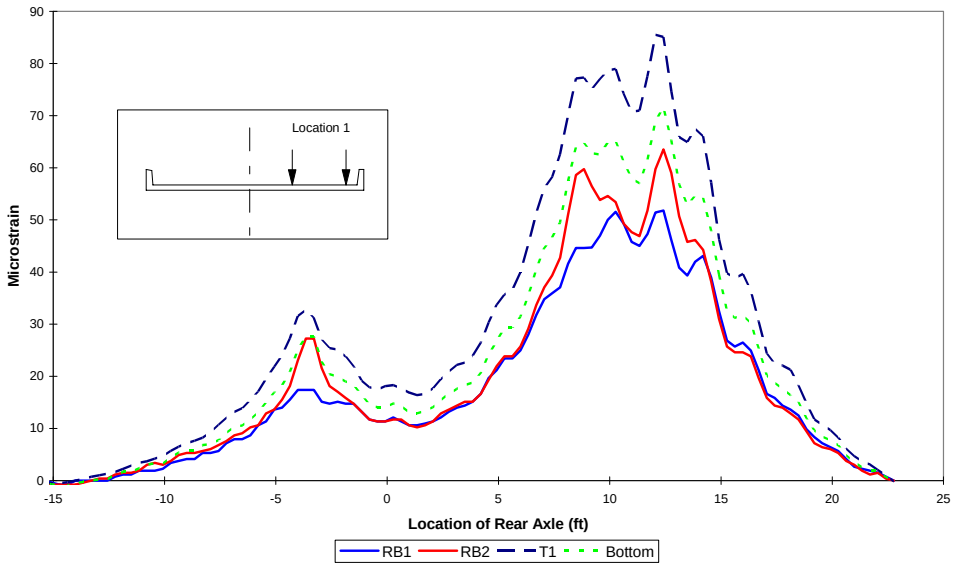

Figure H.2 Transducer T1 compared with Expected Strains.

As stated earlier transducer T2 was placed in an area of no visible cracking. This placement was an attempt to compare the effects of the cracks on surface strain measurement. Table H.3 shows that the expected bottom strain is approximately 40% higher than the transducer data.

Table H.3 Comparison of Strain Transducer T2 Data.

Location 1 Pass 1				Location 1 Pass 2		
	Average	Std Dev			Average	Std Dev
T2	52	6.2		T2	51	7.1
Bottom	74	4.8		Bottom	67	7.5
% Diff	42%			% Diff	31%	
Location 2 Pass 1				Location 2 Pass 2		
	Average	Std Dev			Average	Std Dev
T2	54	1.7		T2	54	3.5
Bottom	76	3.7		Bottom	74	4.8
% Diff	39%			% Diff	39%	

The large difference in the expected strains and transducer data was thought due to the fact that the transducer gives average strain values based on the gage length. Figure H.3 shows the transducer data bounded by the data from gages RB2 and RB3. The transducer data should be following the expected bottom strain line.

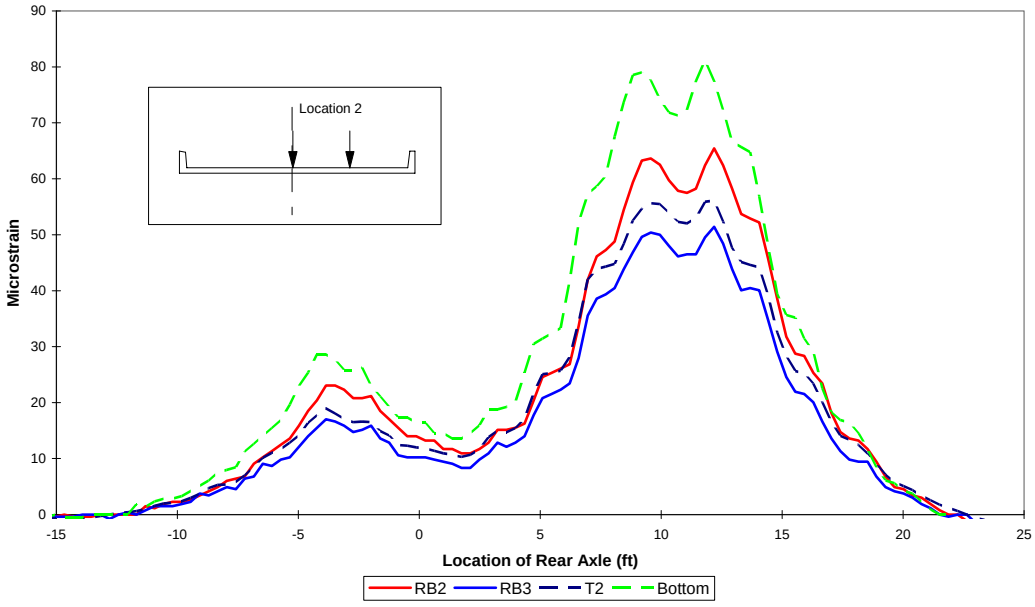

Figure H.3 Transducer T2 compared with Expected Strains.

The results from transducer T3 were similar to T2. These results are not shown here because of the questionable quality of gage RB4. This gage gave consistently low readings and it was felt the data was unusable for this comparison.

H.3 Surface Strain Measurements with Concrete Foil Gage

In addition to mechanical strain transducers an attempt to measure surface strains was made using an electrical resistance (foil) strain gage with a 60-mm gage length. The exact placement of the gage is shown in Appendix A. The gage was placed across the same crack as transducer T1 was placed. As shown in Table H.4 the results of the foil gage F1 show extremely high values in comparison with expected strain values. Figure H.4 shows the magnitude of the differences in the strain.

Table H.4 Comparison of Foil Gage F1 Data.

Location 1 Pass 1				Location 1 Pass 2		
	Average	Std Dev			Average	Std Dev
F1	185	10.3		F1	191	19.4
Bottom	60	1.9		Bottom	60	5.1
% Diff	-68%			% Diff	-69%	
Location 2 Pass 1				Location 2 Pass 2		
	Average	Std Dev			Average	Std Dev
F1	217	17.7		F1	218	18.3
Bottom	67	5.9		Bottom	67	5.6
% Diff	-69%			% Diff	-69%	

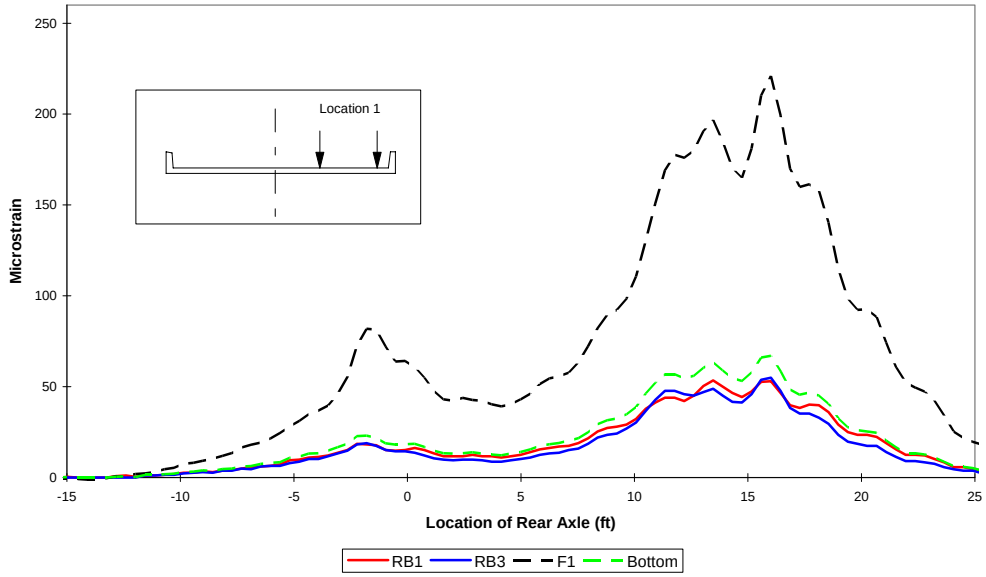

Figure H.4 Strain Gage F1 compared with Expected Strains.

H.4 Summary of Surface Strain Measurements

As shown by the previous results, measuring tension surface strain on concrete is highly variable depending on the placement of the gage. There are several unknown variables that affect surface strain, such as the length of reinforcing bar debonding in the area of a crack, the exact number and location of microcracks and the load history of the structure. Based on the data obtained from this test, surface strain measurements cannot be used to determine strain in the tension reinforcing bars. Increased gage lengths to determine average strain values may be a viable option but further investigation is necessary.

References

1. AASHTO, Manual for Condition Evaluation of Bridges, Washington, D.C., 1994.

2. Azizinamini, A., Shekar, Y., Barnhill, G. and Boothby, T.E., "Old Concrete Slab Bridges: Can They Carry Modern Traffic Loads?", Concrete International, February 1994, Vol. 16, No. 2, pp 64-69.

3. Azizinamini, A, Boothby, T.E., Shekar, Y., Barnhill, G., "Old Concrete Slab Bridges. I: Experimental Investigation", ASCE Journal of Structural Engineering, 1994, Vol 120, No. 11, pp. 3284-3304.

4. Azizinamini, A, Boothby, T.E., Shekar, Y., Barnhill, G., "Old Concrete Slab Bridges. II: Analysis", ASCE Journal of Structural Engineering, 1994, Vol 120, No. 11, pp. 3305-3319.

5. Jensen, V.P., Kluge, R.W. and Williams, C.B., "Highway Slab-Bridges with Curbs: Laboratory Tests and Proposed Design Method", University of Illinois Engineering Experiment Station Bulletin, July 6, 1943, Vol. 40, No. 46.

6. Aktan, A.E., Zwick, M., Miller, R., Shahrooz, B., "Nondestructive and Destructive Testing of a Decommissioned R.C. Slab Highway Bridge and Associated Analytical Studies.", Transportation Research Record, 1992, Transportation Research Board, Washington, D.C., pp. 142-153.

7. Miller, R.A., Aktan, A.E., Shahrooz, B.M., "Destructive Testing of Decommissioned Concrete Slab Bridge", ASCE Journal of Structural Engineering, 1994, Vol. 120, No. 7, pp. 2176-2198.

8. Hrinko, W., Miller, R., Aktan, A., Shahrooz, B. and Young, C., "Instrumentation Considerations for Nondestructive and Destructive Testing of Reinforced Concrete Slab Bridges", Proceedings of the Symposium on Structural Engineering in Natural Hazards Mitigation, 1993, pp. 1557-1562.

9. Huria, V., Lee, K. and Aktan, A., "Different Approaches to Rating Slab Bridges", ASCE Journal of Structural Engineering, 1994, Vol. 120 No. 10, pp. 3056-3062.

10. Clark, P.W., "Loading Tests of a Reinforced Concrete Slab Bridge of 25 Foot Span", Austin, Texas: Texas Highway Department, Bridge Division, November, 1946.

11. Lichtenstein, A.G., "Manual for Bridge Rating Through Load Testing", Final Draft, NCHRP 12-28(13)A, June, 1993.

12. Texas Department of Transportation, Bridge Design Guide, First Edition, 1990.

13. AASHTO, Standard Specifications for Highway Bridges, Washington, D.C., 1994.

14. Texas Department of Transportation, Bridge Inventory, Inspection and Appraisal Program (BRINSAP) Database, August 1996.

15. Texas Department of Transportation, Bridge Inventory , Inspection and Appraisal Program (BRINSAP) Manual of Procedures, September 1984.

18. Jenson, V.P., "Moments in Simple Span Bridge Slabs with Stiffened Edges", University of Illinois Engineering Experiment Station Bulletin No. 315, August 1, 1939, Vol. 36, No. 97.

17. G. Jeff Post, Karl H. Frank and Bahram Tahmassebi, "Estimating Residual Fatigue Life of Bridge", Center for Transportation Research, Report 464-1F, March 1988.

18. Conner, G.H., Stallings, J.M., McDuffie, T.L., Campbell, J.R., Fulton, R.Y., Shelton, B.A. and Mullins, R.B., "Bridge Load Testing in Alabama", July, 1996, Unpublished Paper.

19. Wood, Sharon L., "Evaluation of the Long-Term Properties of Concrete", ACI Materials Journal, Novermber/December 1991, Vol. 88, No. 6, pp. 630-643.

20. Jenson, V.P, “Solutions for Certain Rectangular Slabs Continuous over Flexible Supports”, University of Illinois Engineering Experiment Station Bulletin No. 303, June 7, 1938, Vol. 35, No. 81.